Understanding a High Resolution Regional Climate Model's Ability in Simulating Tropical East Africa Climate Variability and Change

Sarah Emerald Osima

Thesis Presented for the degree of

DOCTOR OF PHILOSOPHY
In the Department of Environmental and Geographical Science
UNIVERSITY OF CAPE TOWN
June 2014

DEDICATION

To my beloved

Husband Elisaria J Mosha &

Daughters:

Faith, Jewel, Agape & Righteous

Understanding a High Resolution Regional Climate Model's Ability in Simulating Tropical East Africa Climate Variability and Change

Sarah Emerald Osima

June 2014

Abstract

The main aim of this thesis is to investigate the potential benefits of increasing resolution in regional climate models in the simulation of climate variability and change over East Africa. This study is based on two high resolution regional climate simulations with a horizontal resolution of 50km and 10km, respectively. These represent present day climate and a projection of future climate change over East Africa. The regional climate model (RCM) used here is HIRHAM5, which is driven by the global circulation model (ECHAM5). Downscaled ECHAM5 output is used to drive the 50km HIRHAM5 simulation for the period 1950-2100, and output from this simulation is used to drive the 10km simulation for three time slices: 1980-1999, representative for present-day climate and two time slices for near future (2046-2065) and far future (2080–2099), respectively.

HIRHAM5 is evaluated with respect to the observed mean climatologies of rainfall, surface temperature and surface winds over East Africa, and representations of the observed annual cycles and inter-annual variability of rainfall and surface temperature. This study utilizes reanalysis and observational datasets: a hindcast of HIRHAM5 forced with ERA Interim, as well as two observation datasets for temperature and rainfall. Since reanalyses aim to make "best use" of all available observations by making a physically consistent representation continuous in time and space, and since there is a paucity of observations over many parts of Africa, the ERAI reanalysis is also used as a best estimate for model evaluation. Additionally, for evaluation of the bimodal nature of East Africa's rainfall, especially over Tanzania, three stations run by the Tanzania Meteorological Agency were used. The model data used in this evaluation ranges from 1980 to 2006.

HIRHAM5 demonstrates reasonable skill in the reproduction of observed patterns of mean climatology of rainfall, surface temperature and winds over East Africa. Moreover, the patterns of annual cycles of rainfall and surface temperature in the bimodal nature of East Africa are well represented. Furthermore, the model showed reasonable skill in the representation of the inter-annual variability and ENSO signals as suggested by the observation. Despite these strengths, HIRHAM5 shows some shortcomings. One weakness of the model is the simulation of the magnitude of a given variable over a specific region. For example, HIRHAM5 driven by ERAI underestimates rainfall and overestimates surface temperature over the entire domain of East Africa. The higher resolution HIRHAM5 (10km resolution) overestimates rainfall over high ground.

The model bias could be due in part to the inadequacy of the observation networks in East Africa, represented in this thesis by the CRU and FEWS datasets. However, these two datasets draw on some different sources and neither do they have the same resolution. FEWS is a high resolution data (0.1^{o}) gridded satellite-derived precipitation estimate covering the entire African continent while CRU datasets is a relatively low resolution (0.5^{o}) dataset based on rain gauge monthly precipitation only; in addition, near surface temperature is also available. As no reliable wind observations exist, wind data was taken from the ERA-Interim reanalysis.

The different observational datasets do not agree particularly well, which impedes evaluating the quality of the HIRHAM5 simulations, in particular the high resolution one. So while the higher resolution HIRHAM5 appears to be generally reliable, caution must be exercised in formulating conclusions from the results, especially over high ground and remote areas without adequate observation data. Under these constraints, the results suggest HIRHAM5 may be useful for assessing climate variability and change over East Africa. A weakness of the analysis presented here is that only one combination of GCM and RCM could be investigated in depth due to computer and time constraints. Therefore the results presented here, if used in application for climate change adaptation, should be considered in conjunction with a broader suite of data, such from the CORDEX programme.| This has potential to increase the reliability of information about climate variability and change at a regional to local level necessary for impact assessment.

ACKNOWLEDGMENTS

First and foremost, I want to address my sincerest thanks to my husband and daughters who never failed to encourage me in spite of the fact that I had to be away from home for a long period. Without their understanding and their continuous support I never would have accomplished this dream.

I am very grateful to my supervisors, Prof. Bruce Hewitson and Dr. Martin Stendel (Danish Meteorological Institute). Indeed, I am indebted to my supervisors because I feel privileged to have had such friendly support, encouragement and constructive criticism and suggestions that have enhanced this work. Dr. Martin, I thank you so much; your commitment and endless support are highly appreciated. God bless you.

This study was funded by the Danish International Development Agency (Danida) through the CLIVET Project in Tanzania in collaboration with the Geological Survey for Denmark and Greenland (GEUS), the Danish Meteorological Institute (DMI), the Tanzania Meteorological Agency (TMA) and the University of Dar es Salaam (IRA). I thank you all for your financial support. I also thank you so much Prof. Bruce Hewitson of the University of Cape Town for paying my last year's school fees.

My special thanks go to all CSAGers for your smiles; they were always my encouragement. I cannot forget my officemates especially Mr. Lawal and Mr. Arlindo. I call them brothers and they call me sister. This made my life so easy and I never got bored. I also thank you Dr. Abiodun Babatunde for your encouragement and support.

Table of Contents

Chapter 1

Introduction

Global climate has changed and is expected to continue to change according to the future projections. Recent studies and reports (IPCC 2007, 2013) have confirmed this with evidence (Stott et al. 2010). For example, in East Africa the extreme heavy rainfall (1997/98, 2006), prolonged drought conditions (1999 to 2005), increase in malaria epidemic over the highlands and glacier retreat atop Mount Kilimanjaro already been witnessed (Kabanda et al. 1999, Hastenrath et al. 2007; Kijazi & Reason 2009; Williams & Funk 2011; Wolff et al. 2011). All of these events have threatened human life, the economy and eco-systems. It is therefore necessary to continuously conduct climate change assessments which will provide reliable information for policy decisions, awareness and strategic development planning. Studies have shown that high resolution RCMs simulations present more detailed information necessary for impact assessments at a regional and local level in comparison to low resolution RCM (Denis et al. 2002, Giorgi 2006). High resolution RCMs, provide meaningful small–scale features over a limited region at affordable computational cost compared to a high resolution GCM. Moreover, high resolution regional climate models (RCMs) were found to simulate plausible information at a regional/local scale, as they are able to resolve details of topography compared to the coarse resolution global climate models (GCMs). Despite the importance of regional climate model projections at a regional/local level, very limited information is available on climate variability and change in East Africa. Regional climate model simulations at reasonably high resolution, apart from the very recent CORDEX approach (Coordinated Regional climate Downscaling Experiment (Kim et al. 2013)) are currently limited. The current CORDEX data has a horizontal resolution of 50km; there is obviously room for further downscaling in using RCMs at a higher resolution. This study therefore aims to contribute to a broader understanding of the significance of increasing resolution in the RCMs in simulating East African climate variability and change.

The understanding of climate variability and change in East Africa is very important due to its direct impact on socio-economic development. Available information collected by instruments

and through proxy indicators such as tree rings suggests that the frequency and magnitude of variability and change is increasing in East Africa. Observed temperature changes over the last century indicate a similar trend both globally (Jones et al. 1998; Thompson et al. 2005; Moberg et al. 2005; Mann et al. 2008; Kemp et al. 2011) and specifically for East Africa (New et al. 2006; Wolff et al. 2011). These changes have contributed to an increase in extreme events especially floods, seasonal shift of rainfall, drought, glacier retreat atop Mount Kilimanjaro, coral morbidity and mortality, and sea level rise (Barker 2007; Thompson et al. 2005; IPCC 2007; Mölg et al. 2010; Thompson et al. 2009; Thompson et al. 2010; Shongwe et al. 2011). For example, it is suggested that the glacier retreat atop Mount Kilimanjaro is caused by different climatological drivers which needs to be taken into consideration (Thompson et al. 2009).

East Africa, as part of the developing world, mainly relies on rain-fed agriculture with the result that it has a low capacity to adapt to climate changes (Funk et al. 2008; Mongi et al. 2010; Cooper et al. 2008; Tumbo et al. 2012). Future climate change projections, based on anthropogenic greenhouse gas emission scenarios show that the rate of change of future warming will be higher than the current warming and will thus increase pressure on developing countries, especially on the East African economy (Ruosteenoja et al. 2003; IPCC, 2007; Murray & Ebi 2012).

This thesis aims at understanding the importance of increasing resolution in regional climate models in the simulation of climate variability and change over East Africa. It postulates that increasing model resolution will improve simulation of climate variability and change over East Africa.

1.1 Thesis Outline

This thesis is composed of seven chapters outlined as follows. The introductory chapter provides a rationale for this thesis by first giving an overview of drivers and challenges of climate variability and change; secondly by exploring the previous climate models used in monitoring the physical processes that determine climate variability and change and their challenges in East

Africa. Furthermore, the espousal literature review, offers a description of climate variability, circulation patterns and climate models and their application. Chapter 2 discusses the models, field work conducted over the Great Ruaha River sub basin and observation data used in this research. Chapter 3 explores the results which compare the observations from CRU and FEWS datasets, and meteorological stations from TMA, as well as the reanalysis data from ERA-Interim with the model output, showing how well the models represent annual cycles of rainfall and temperature over Tanzania and East Africa in general. This chapter also presents the model simulation of extreme rainfall and temperature by comparing the two high resolutions and one ECHAM5 (GCM) for present day and future climate. Chapter 4 continues to assess how skillful the model is in capturing inter-annual variability over East Africa during ENSO years. This chapter will also discuss the limitations and strengths of the two resolutions as found in the results. Chapter 5 discusses model simulations of present day and future climate change projection. It then presents the dynamic and thermodynamic of the projected changes of climate variables. Chapter 6 presents the synthesis of the study, conclusions and recommendation for future studies.

The following sections represent a rationale for this thesis by giving an overview of East African climatology, followed by a discussion of the drivers behind climate variability and change which will also introduce a map of the study domain. Furthermore, the role of Indian Ocean, which may be a key factor, will be discussed separately. This will be followed by the discussion of the impacts of climate variability and change on the community in East Africa. Finally, possible applications of climate models in East Africa and their limitations will be discussed.

1.2 Overview of climate variability and change in East Africa

This study focuses on three countries in East Africa, namely Kenya, Uganda and Tanzania, which are located between 34^{o}E and 42^{o}E and between 11^{o}S and 4.8^{o}N (Figure 1.1). This region has a very heterogeneous topography which includes the highest peaks of Africa (Mount Kilimanjaro, Mount Kenya and Mount Meru), the greatest lakes (such as Lake Victoria and

Tanganyika, which is the longest lake in Africa) and furthermore the Great Rift Valley which passes across the three countries (Figure 1.1).

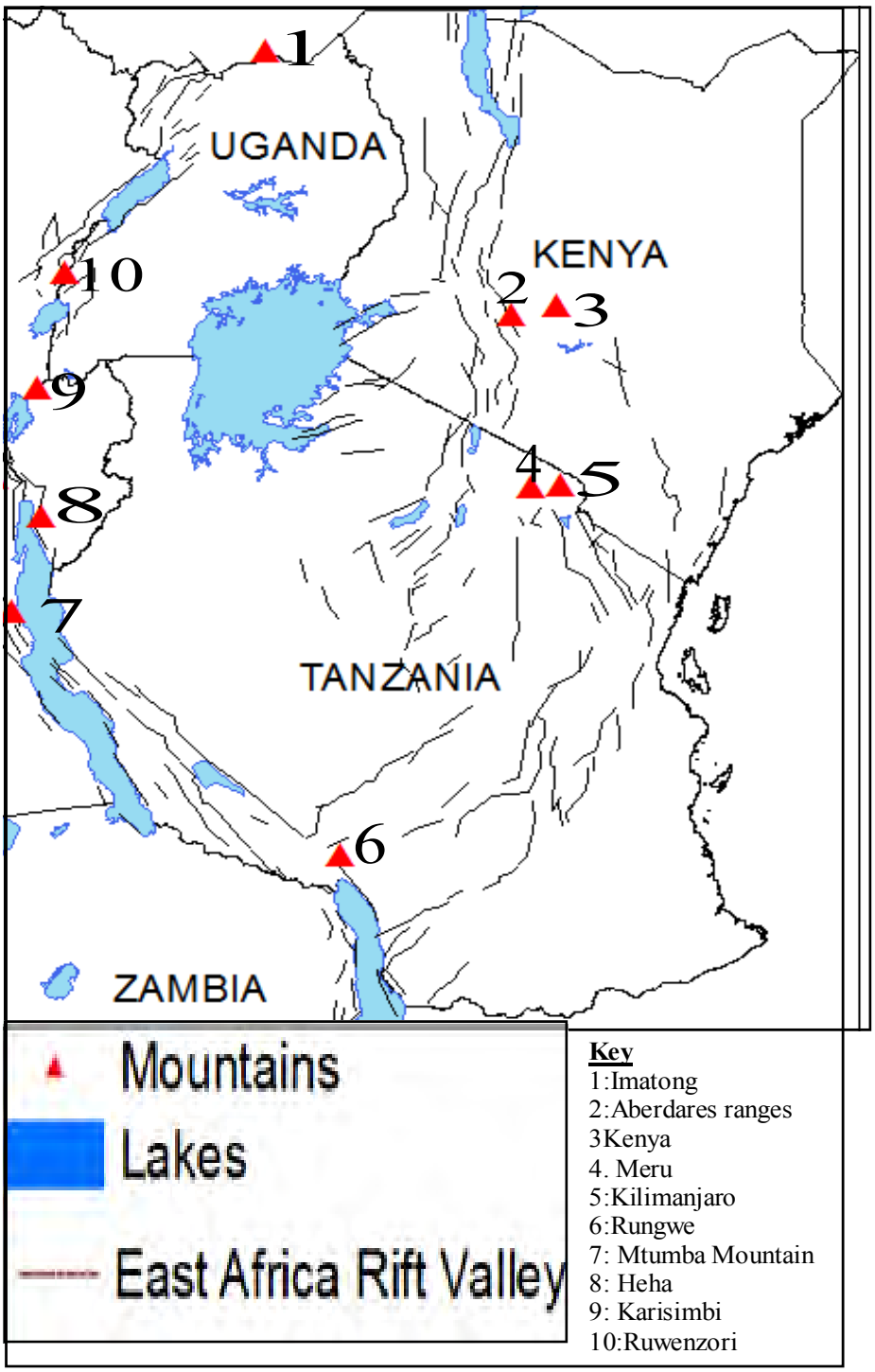

Figure 1.1: A map of East Africa showing a study domain with some physical geographical features covering Kenya, Uganda and Tanzania.

1.2.1 Climatology of East Africa

The climatology of East Africa has been studied in great detail, using both observations and climate model data (McClanahan 1988; Nicholson 1996; Mutai et al. 1998; Basalirwa et al. 1999; Indeje et al. 2000; Zorita & Tilya 2002; Camberlin & Philippon 2002; Camberlin & Okoola 2003; Omondi et al. 2013). These authors found that East African climatology is controlled by the Intertropical Convergence Zone (ITCZ), the subtropical highs and in addition the moist and warm air mass over the Congo Basin. This, the complex topography mentioned above and the Indian Ocean which modulates the large-scale atmospheric circulation patterns (Indeje et al. 2000; Slingo et al. 2005) all exert influence on climate in the region. These factors are discussed in detail in the following chapters.

Rainfall is a key climatic factor of concern in East Africa. It varies considerably in space and time. The south-north oscillation of the ITCZ in combination with atmospheric circulation features (Hadley cell) control the rainfall regime in East Africa (Indeje et al. 2000; Mpeta & Jury 2001; Zorita & Tilya 2002; Hastenrath 2001; Anyah & Qiu 2012). Principally, there are two rainy regimes: unimodal and bimodal rainfall regimes. The mode in the unimodal rainfall regime occurs from November to April over most parts of the southern portion of East Africa (central to southern Tanzania; McGregor & Nieuwolt 1998; Basalirwa et al. 1999). The mode in the bimodal rainfall regime has two wet and two dry seasons. It is the main regime over a large part of tropical East Africa and consists of '*vuli*' (the short rainfall season) which occurs from October to December and '*masika*' (the long rainfall season) which occurs from March to May (McGregor & Nieuwolt 1998; Odiyo et al. 1999; Indeje et al. 2000; Slingo et al. 2005; Conway et al. 2005;Mbululo 2012). The remaining months of the year, in particular from June to early September, are dry with relatively cooler temperatures.

However, rainfall distribution and magnitude in both regimes are not the same (McGregor & Nieuwolt 1998; Camberlin & Moron 2009). Atmospheric convergence over the region becomes stronger when the ITCZ is close to the equator. Rainfall maxima are observed during the long and short rainfall seasons around April and November respectively. However, larger amounts of rainfall are received during the long season, where the ITCZ tends to be broader and moves

slowly northward. Conversely, during October and November the ITCZ shifts more rapidly southward, particularly over the eastern part of East Africa and less rain is received (McGregor & Nieuwolt 1998).

Synoptic features such as high pressure cells, located in the south-east (Mascarene High) and south-west (St Helena High) of South Africa, together with the Arabian Ridge, play a great role in influencing the monsoon winds which prevail for a long time during the year (Schott & McCreary 2001; Manatsa et al. 2014). From December to March, East Africa experiences north-east monsoon winds which bring continental winds passing over the relatively cool Somali currents through the coast of East Africa where it transports some moisture and, as it passes further north to Lake Victoria, it brings some rain to the slopes of the mountains (Mt. Kilimanjaro and Kenya). The Congo air mass and orographic uplift over the slopes of mountains along the western rim of the Rift Valley (Virunga Mountains and Ruwenzori Range) cause rainfall during both monsoon seasons (McGregor & Nieuwolt 1998; Hession & Moore 2011). The dry season occurs during May to September (July and August) when the ITCZ is in the northern Hemisphere. At this period, the continental south-west monsoon winds (second monsoon systems), which originate from the high pressure cell over the eastern South Africa and Indian Ocean, dominate over the region. These monsoon winds (Camberlin & Moron 2009) draw away moisture from East Africa which is released as they pass over the eastern mountain ranges of Madagascar. Early onset of the Indian monsoon winds is connected to the shortage of rainfall in May over East Africa (Camberlin et al. 2010). Due to the geographical location and topography of East Africa, the rainfall and surface temperature are not uniform and vary greatly in space. Differential heating of the landmass is strongly influenced by topography, higher temperature over the low land and coast, with low temperature over the mountainous regions. Likewise, rainfall varies with topography; high amounts of rain fall over high ground compared to low land areas (Mutai & Ward 2000; Hession & Moore 2011). However, the inter-annual variability of East Africa's seasons is associated with the interaction of local topographical features with larger scale features (sea surface temperature, Indian Ocean and circulation patterns) (Mutai et al. 1998; Indeje et al. 2000).

Additionally, soil moisture feedback can also play part in influencing rainfall variability over the region. The soil moisture feedback can be caused by an increase in reduction of loud cover and

specific humidity above 700hPa and results in a net decrease/increase of column integrated precipitable water, despite the increase/decrease surface water flux, indicating reduction in moisture convergence. Soil moisture acts as the negative feedback to precipitation helping to buffer the system against any external forcing of ENSO (Cook et al. 2006). More factors such that, the ITCZ, subtropical highs will be discussed later. The focus of this thesis, however, is not on the drivers that affect climatology over East Africa, important as they are, but rather on the impact of increase of resolution in RCMs on projected climate variability and change. The following section gives an overview of the causes of climate variability and change in East Africa in a larger context.

Climate variability is associated with changes in mean and extreme climatic conditions over a given region and period. This chapter provides an overview of circulation patterns that control East Africa's climate. It introduces relevant circulation patterns that influence climate variability over East Africa. Additionally, it provides a general understanding of climate models, including global climate models and high resolution regional climate models.

1.3 Factors controlling the Tropical East African Climate

The mean climatological patterns over East Africa are controlled by regional and local factors including its complex topography. As elsewhere, more rainfall is observed over the highlands areas than the low land areas (Nicholson 2000). Hession & Moore (2011), using spatial regression, found that the topographic variables such as elevation and slope strongly influence rainfall in both short and long rainy seasons. Moreover, Slingo et al (2005) found that East Africa highlands systematically freshen the tropical Indian Ocean and act to focus the monsoon winds along the coast leading to greater upwelling and cooler sea surface temperatures.

However, rainfall variability in East Africa is linked to global circulation patterns (Nicholson & Selato 2000). On a more localised scale, Nicholson (1996) in her studies gave an overview of climate dynamics and causal mechanisms of climate variability in East Africa. She found that the inter-annual variability over East Africa is governed by three air streams: the Congo air mass,

north-easterly and south-easterly monsoon flows, and convergence zones such as the Congo air boundary zone and upper air convergence.

1.3.1 Intertropical Convergence Zone (ITCZ)

A wide belt formed in the centre of the tropical circulation, where the two trade winds from the northern and southern hemispheres meet along the equator is called the ITCZ (Nicholson, 1996; MacGregor & Nieuwolt, 1998). The rising limb of the air mass in the equatorial region occurs where there is maximum heating from the sun associated with a strong convergence (Figure 1.2). The position and timing of the movement of the ITCZ determines the onset and duration of rainfall in East Africa (Nicholson 1996; Basalirwa et al. 1999; Camberlin & Moron 2009; Kijazi & Reason 2012). The ITCZ is known to be the key component of the global circulation system located between 5^{o} N and 5^{o} S of the equator based on the pattern of the land and ocean (Nicholson 2000; Riddle & Cook 2008). The ITCZ varies throughout the year while it remains near the equator. It normally migrates towards the warming hemisphere at a seasonal and longer time scale. However, changes may occur depending on the variations of land and ocean temperature and especially during El Niño events (McGregor and Nieuwolt, 1998).

The differences in heat capacity of land surface and the neighbouring Indian Ocean contribute to the alignment of the meridional arm of the ITCZ over land in tropical East Africa. The meridional arm is a result of moist air masses from the Atlantic and Indian Ocean converging over land. This occurs normally between January and March, and it produces rainfall in the northern part of East Africa even if the main ITCZ is located further south.

The ITCZ passes over tropical East Africa twice a year. When it is active, many areas receive heavy rainfall (Camberlin & Okoola 2003). A delay of the onset of the rainfall season is therefore associated with the delay of onset of the ITCZ. On the other hand, the Indian monsoon early onset is also connected to early cessation of the long rainy season in East Africa (LinHo et al. 2008; Camberlin et al. 2010). Moreover, recent studies have highlighted that the south–northward oscillation of the ITCZ is characterised by rather abrupt jumps in rainfall amount

(Riddle & Cook 2008; Riddle & Wilks 2013). In the region between 5 and 10^{o} S and between the equator and 7^{o} N, two jumps in rainfall quantity exist over eastern Africa: in April and late May/early June (Riddle & Wilks 2013).

Furthermore, the normal movement of the ITCZ is altered by the topography. The mountains and the Great Rift Valley provide an environment conducive for complex interaction between regionally induced and large scale circulations (Indeje et al. 2000; Anyah & Semazzi 2006; Hession & Moore 2011). The aforementioned circulation patterns act independent of each other; however, their interactions combined with the ITCZ, local and synoptic features play a great role in the formation of East Africa's climate.

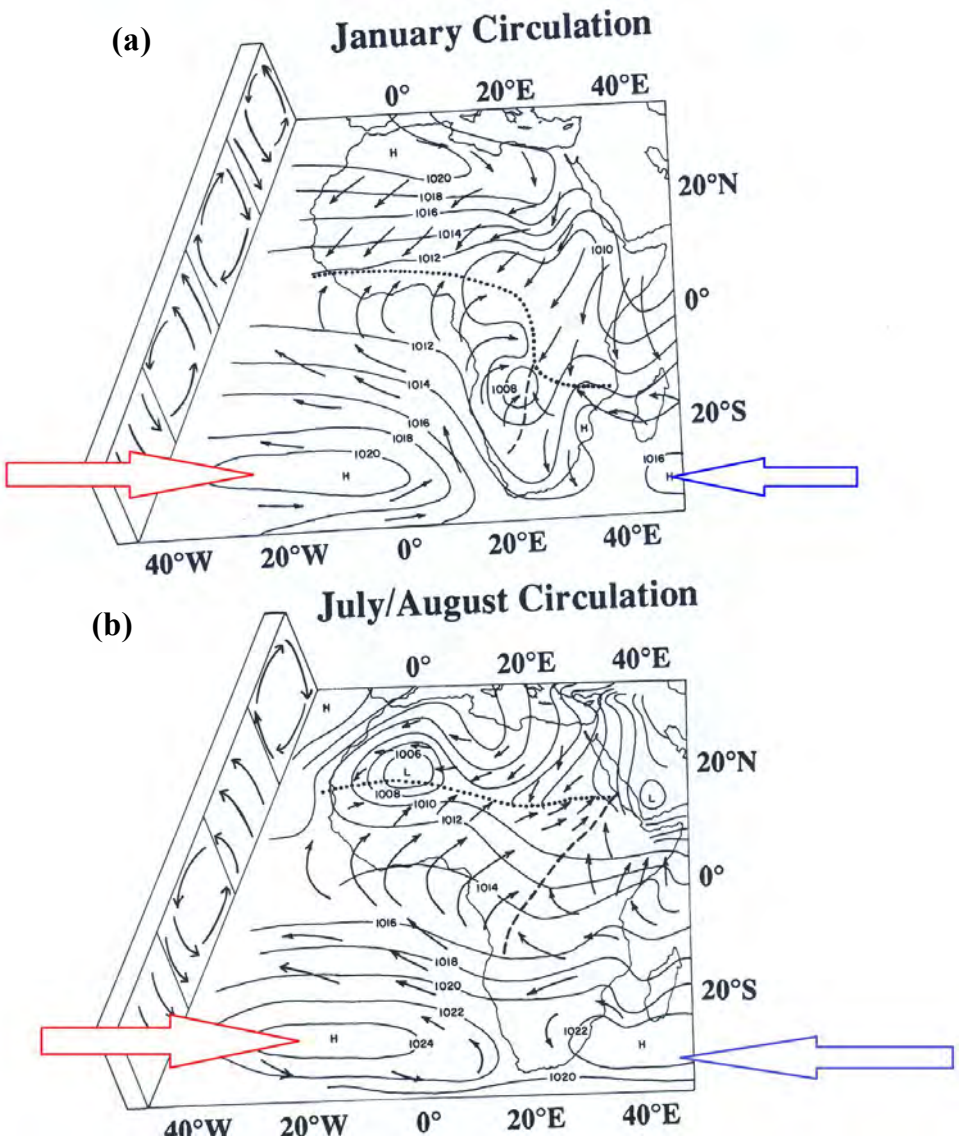

Figure 1.2 Schematic of the general patterns of winds (arrows), pressure (H for subtropical highs) and convergence over Africa. Dotted lines indicate the ITCZ, dashed lines other convergence zones (Source: Nicholson 1996). The blue arrows indicate the Mascarene High while the red arrows indicate the St Helena High.

Figure 1.2a shows January's circulation, in the period of high sun (austral summer) over the southern hemisphere, north-easterly and easterly flows are caused by the intensification of high pressure cells in the northern hemisphere which pushes the ITCZ southwards into the southern hemisphere. Likewise, Figure 1.2b shows July-August circulations, in the period of high sun over the northern hemisphere, when the ITCZ shifted to the northern hemisphere and subtropical

highs in the southern hemisphere intensify the southerly to south easterly flows which clears the weather over the southern hemisphere.

1.3.2 Subtropical highs

The subtropical highs are anticyclone centre cells, located at latitudes between 20^{o} to 40^{o} in both hemispheres (Figure 2.1). In the southern hemisphere they develop, among other places, over the Atlantic and hence are warm and moist. These high pressure centres are oriented in an east-west direction and dominate the surface pressure pattern over the large ocean basin throughout the year (Nicholson, 1996; McGregor & Nieuwolt 1998). The main dynamic factor is the Coriolis Effect (Ogata & Xie 2011). The upper level pole-wards movement of air in the Hadley cells is turned to the right in the northern hemisphere and to the left in the southern hemisphere, forming upper level westerly air flow in the subtropics where geostrophic balance is reached. Furthermore, upper-level pole-ward motion is thus prevented, and air converges at about 30° north and south of the equator. Intermittent upper level airflow also converges towards the same areas from the mid-latitudes. This convergence thus increases the atmospheric mass, creating a downward flow and thus high surface pressure. In turn, the high surface pressure generates the low level outflow required to balance the upper level convergence (Figure 1.2).

Meanwhile, during the peak period of sun in the southern hemisphere, the subtropical highs (Mascarene and St Helena) relax to give room for further southward movement of the ITCZ that enhances moisture and rainfall over the East African mainland (Manatsa et al. 2014). However, the peak period of the sun in the northern hemisphere is around June (Figure 2.1b); in the southern hemisphere the Subtropical Highs widen and intensify the south-easterly and easterly flows which push the ITCZ further to the northern hemisphere and weaken the Arabian and Azores Highs (Nicholson 1996; Mutai & Ward 2000; Hastenrath & Polzin 2003; Hastenrath et al. 2011; Mahongo et al. 2012; Manatsa et al. 2014).

The winds that blow to the equator from the northern hemisphere are called north-east trade winds, while those from the southern hemisphere are called south-east trade winds (Nicholson

1996). As these winds cross the equator they are called monsoon winds. Therefore, in East Africa two major monsoons dominate: the north-easterlies that originate from the Arabian high over north-eastern Africa and the Arabian Peninsula; and the south-easterlies that originate from the south-western region of the Indian Ocean in the Mascarene high (Figure 2.1). The north-easterly and south-westerly monsoons are thermally stable and are associated with the subsiding air, and therefore are relatively dry. However, previous studies have shown some influence of monsoon winds associated with anomalous rainfall in East Africa (Ashok et al 2001; Zorita & Tilya 2001; Tolbolt 2007). Tolbolt found that these winds have influenced drought conditions in East Africa about 5^{o}S to 10^{o}S of the equator.

Moreover, Zorita and Tilya (2001) found a relationship between rainfall anomalies in the month of May to be associated with the monsoon winds over northern Tanzania. They found that anomalous increases in SSTs over the Indian Ocean tend to weaken monsoon wind circulation in May which results in moisture advection from the Indian Ocean into the continent. At 200 hPa level, the opposite circulation is observed. During this same period more rainfall is observed at the coastal strip of East Africa, while in the interior rainfall decreases. In conclusion, they noted that there is a close relationship between the influences of ENSO and the Indian monsoon on rainfall in Tanzania during the month of May. During ENSO events, the monsoon winds were found to weaken over the Pacific Ocean, hence weakened pressure gradient between Indonesia and the South Pacific constitutes a prerequisite (Bjerknes 1969; Saji & Vinayachandran 1999; IPCC, 2001).

1.3.3 The Congo Air Boundary (CAB)

The Congo Air Boundary (Figure 1,2) separates easterly and westerly airflow (Nicholson 1996; Talbot et al. 2007; Kijazi & Reason 2009). It plays a fundamental role in controlling the hydro-climate in the African tropics (Tierney et al. 2011). It has been found that the CAB is a convergence that marks the confluence of Indian Ocean air with unstable air from the Congo basin which lies west of Lake Challa at all times of the year. Other studies have also shown an

influence of the Congo forest in combination with mechanisms of topographic and orographic uplift (Mapande & Reason 2005; Mchugh 2006; Hastenrath et al. 2010).

Via a westerly flow, the CAB brings a lot of moisture which enhances rainfall over the western area of Uganda and Tanzania (Camberlin & Philippon 2002; Reason et al. 2006; Samba & Nganga 2012). These authors also found that the moisture advection from the Atlantic Ocean through westerly flow is enhanced with the orientation of the CAB towards flow from the Atlantic to East Africa. In addition, the CAB was found to be associated with anomalous westerly from southern Congo and Zambia which leads to convergence of low–level moisture over western Tanzania. The air aloft, that is, the convergence zone aloft is the third convergence zone which separates the dry stable air from the Sahara and the moist southerly flow (Nicholson 1996; Talbot et al. 2007; Kizza et al. 2009).

Studies have shown the importance of these components of circulation as the controlling factor of East Africa's rainfall (Mapande & Reason 2005; Hastenrath 2007; Hastenrath et al. 2011). Kijazi & Reason (2012) noted that an anomalous wet condition during a long rainy season was enhanced by the advection of moisture from the Congo basin and Indian Ocean to the region. Moreover, the anomalous dry conditions during the long rainy season are linked to the deviation of moisture away from Tanzania. They found that this moisture is deviated by the cyclonic anomaly over the coast of Somali that turns the winds into a southerly flow.

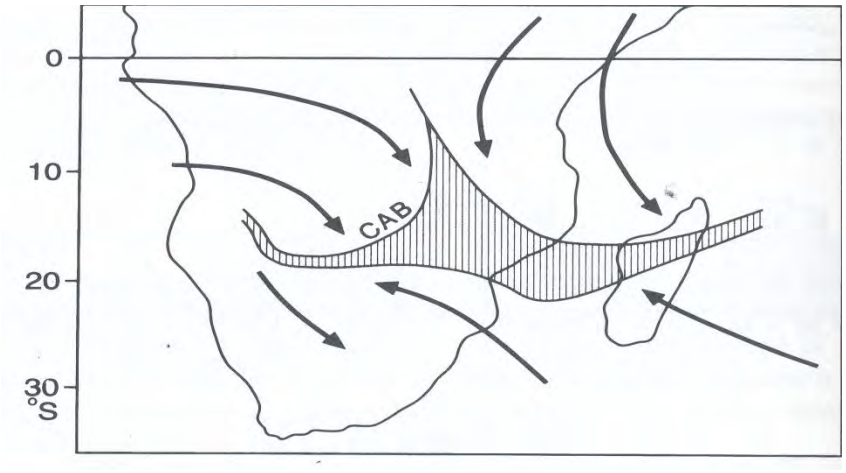

Figure 1.3 shows the approximate position of the ITCZ and Congo Air Boundary (CAB) (Source: McGregory & Niewolt, 1998).

1.3.4 Madden Julian Oscillation (MJO)

MJO is a shallow convective heating in the Indian Ocean and western central Pacific Ocean where it has pronounced impact. MJO is either characterised by upper tropospheric convergence/subsidence and lower tropospheric divergence/convergence which reduces/enhances convective activities which lead to reduction/increase of rain and thunderstorms. The tropical convection anomalies sink in the areas of the Congo and Amazon Basin. MJO modulates the moisture field, atmospheric stability, and convection over East Africa (Mpeta & Jury 2001). MJO produces a multi-week variability in winds, sea surface temperatures cloudiness and rainfall across the tropics. It also enhances the divergence in the upper troposphere and convergence in the lower troposphere. However, the MJO has strong year to year variability which is partly linked to ENSO years. The MJO has also found to play a part in intra-seasonal variability of the whole Africa over the warm pool sector (Kingdom 2004).

1.3.5 Walker Circulation and El Niño Southern Oscillation (ENSO)

Walker circulation is an east to west circulation along the equator, characterised by the ascent of air in the western Pacific in the region of Indonesia and descent in the eastern Pacific off the coast of South America. When this pattern shifts eastward it causes high pressure over the Indian Ocean which suppresses the monsoon winds, especially in spring when the monsoon begins to develop. Previous studies indicate that Walker circulation is controlled by sea surface temperature variation in the eastern and western Pacific (Bjerknes 1969; McGregor & Nieuwolt 1998). Bjerknes (1969) found that the maxima of the sea temperature in the eastern and central equatorial Pacific occur as a result of anomalous weakening of the trade winds of the Southern Hemisphere with inherent weakening of the equatorial upwelling. Over the Atlantic and Pacific oceans, the basic Walker circulation consists of easterly trade winds at the surface, with westerly aloft (in the upper atmosphere). In contrast, mean airflow over the Indian Ocean and Africa is westerly, with easterlies aloft (in the upper atmosphere). Dry/wet spells over East Africa are associated with strong/weak easterlies over the Indian Ocean (Mutai et al. 1998; Mpeta & Jury 2001; Mapande & Reason 2005).

Due to the increase in greenhouse gaseous emissions in the atmosphere, there is evidence of rapid increase of warming in the Indian Ocean which have altered East African rainfall (Mcmichael et al. 2005; Hansen et al. 2010; Hansen et al. 2011; Shongwe et al. 2011; Cook & Vizy 2013). These authors found that increased warming over the Indian Ocean has resulted in westward extension of warm pools which lead to the extension of Walker circulation. They suggested that an increase in SST favours a local enhancement of convection and precipitation over the tropical Indian Ocean with resultant latent heating altering regional wind and moisture flux patterns. Also, Funk et al. (2008) found that anthropogenic Walker-like circulation which has led to decreased rainfall during the months of March to June is expected to have a continued effect into the future. The result is that agricultural production and food security in the region will be negatively impacted.

They also found that increasing tropical Indian Ocean precipitation as a result of anthropogenic warming is associated with atmospheric ridging and anticyclonic moisture circulation over

eastern Africa. This disrupts the main onshore moisture flows, leading to a rainfall deficit. It was also found that Walker circulation favours rainfall in the short rainy season which occurs in the months between October and December (Saji & Yamagata 2003; Shongwe et al 2011). For example, Shongwe et al., (2011) found that in general**,** a change in the Eastern Hemisphere Walker circulation is consistent with an increase in precipitation over East Africa.

The quasi-periodicity disruption of the Walker Circulation manifests as ENSO events (introduced in the previous chapter). ENSO is the well-known multiyear mode which influences the climate of many regions of the world and also East Africa (Indeje et al. 2000; Nicholson 2000; Ashok et al. 2001; Manatsa et al. 2011). It is a result of anomalous warm/cold SST over the tropical Pacific Ocean, recurring approximately every 3 to 7 years. El Niño and La Niña events develop in association with swings in atmospheric pressure between the tropical Indo-Pacific and eastern Pacific Oceans (Saji & Yamagata 2003). Behera et al. (2005) found that anomalous SST gradients relevant for East Africa's rainfall were a perturbed Indian Ocean Walker cell. ENSO extends its reach beyond the tropical Pacific through atmospheric teleconnections that affect patterns of weather variability worldwide. Particularly, there have been investigations of different types of ENSO events according to the onset time and propagation characteristics.

1.4 Climate variability and change in East Africa

Climate change plays a major role in undermining socio-economic wellbeing in East Africa. Humans possess the ability to mitigate damage done through their activities, on a regional and global scale, by adhering to the mitigation measures as suggested by the reports from the Forth and Fifth Assessment reports of the IPCC (AR4, AR5) respectively. Other natural factors include: variations in solar output, shifts and wobbles of the earth's orbit (Milankovitch cycles), and volcanic activity. A wobbling of the earth's axis due to the gravitational pull of the sun and moon on the equatorial bulge has some influence on the earth's climatic changes (McGregor & Nieuwolt 1998; Wilson & Haubrich 2007; IPCC 2007). Volcanic eruptions as a natural factor have noticeably affected global temperatures and rainfall variability. For example, anomalies in

temperature (below normal) and rainfall (above normal) were observed after the Mount Pinatubo eruption in 1991 (McCormick et al. 1995; Easterling 1997; Hansen et al. 2010; Stott et al. 2010; Betts et al. 2011).

In addition to natural factors, human activities contribute to the increase in the emission of greenhouse gases into the atmosphere, which in turn have been cited as the major contributor to an increase in global temperatures (Wigley & Raper 2001; Stendel & Christensen 2002; Schreck & Semazzi 2004; Patz et al. 2007; McCarthy et al. 2010; Nicholls et al. 2011). Global emission of greenhouse gases has been shown to create positive trends in global surface temperatures. In the late 20th century the global average temperature increased by 1^{o}C which resulted in a rapid change of climate (Mitchell et al. 2006; IPCC 2007; Schwartz et al. 2010).

Moreover, human activities such as deforestation and desertification have severely impacted climate variability and impacted climate at local and national levels (IPCC AR4; Mango et al. 2011; Nogherotto et al. 2013). Deforestation is caused by human-induced or socio-economic factors, and natural factors such as fire events and drought. In East Africa, poverty, the desire for arable land and inequality has forced rural people to over-cultivate and expose land to erosion (Hepworth (2010a and 2010b); Mango et al. 2011)). Indeed, in most parts of East Africa deforestation is practiced for the purpose of income through wood harvesting for fuel, export, farming and urbanisation (Allen & Barnes 1985; Semazzi & Song 2001; IPCC 2007). Allen & Barnes (1985) found significant reduction in rainfall over deforested land and neighbouring regions. The impact of deforestation was also found to be comparable to that of greenhouse-warmed regional climates and the climates in tropical rainforest regions (Zhang & Mcguffie 2001).

Desertification is a process which can be caused by human activities or drought. This process is one whereby conditions predominantly associated with desert regions are brought about in an area where they previously did not exist (McGregor & Niewolt 1998, IPCC 2007). Land degradation, deforestation and overgrazing of land, for example, can lead to the destruction of the natural vegetation systems. This process is catalysed by natural factors such as drought, which compels people to graze herds over larger areas, thereby spreading the effects of

vegetation loss. Previous studies have shown that the frequency of droughts that appear in low latitudes including East Africa is attributed not only to global change but also to land-use change which occurs at a local to regional level (Lambin et al. 2003; Hein et al. 2009; Collier et al. 2008; Mango et al. 2011).

The mode and means of cultivation in many areas have changed owing to the changes in local climate driving and land changes such as deforestation and desertification. In recent years, in some areas in East Africa, for example the Kilimanjaro region in Tanzania, there has been a great change in land use. The main cash crop which was coffee has now declined due to economic challenges and population growth in this region (Maghimbi 2007). The coffee plantations have been cut down and even some forests have been cleared for the purpose of cultivating short period crops like vegetables.

It is apparent that in the absence of mitigation, more warming is projected by the end of the 21st century (e.g. IPCC 2013; Betts et al. 2011; New et al. 2011). The IPCC (AR5) corroborates previous studies and scenarios on climate change that find increasing greenhouse gases emission will cause the global average temperature to rise by 1.4 to 5.8^{o} C in the 21st century. The results of this warming are already noticeable and the impacts have already been experienced worldwide, specifically in East Africa (Patz et al. 2005). In East Africa, the average temperature is projected to increase by more than 2^{o} C by 2039 (Rowhani et al. 2011). The result of this warming will have significant impact on agricultural production. For example, in Tanzania food production of crops such as maize, sorghum and rice will decrease in the order of about 13%, 8.8% and 7.6% respectively (Rowhani et al. 2011). The precipitation projections are less certain, with some suggesting a likely increase of precipitation over East Africa (IPCC AR4, 2007; Shongwe et al. 2011; Marshall et al. 2012).

1.4.1 The role of the Indian Ocean in influencing climate variability and change

The increase in anthropogenic greenhouse gases and aerosol emissions contributes to anomalous warming of the Pacific and Indian Ocean which in turn influences the East African climate

variability. Previous studies have shown that the Indian Ocean plays a role in modulating East African climate (Marchant et al. 2006; Manatsa et al. 2011). For instance, it was found that widespread increase in temperature over the Indian Ocean–and especially near the coast– enhances the moisture flow towards the mainland which brings more rain during the short rainfall season. As the largest warm pool on the planet, the tropical Indian Ocean has a crucial role to play in influencing regional and global climate, ranging from intra-seasonal to interannual and longer time scales, most of which are coupled to the strong seasonal cycle (Schott et al. 2009).

The El Niño Southern Oscillation (ENSO), a result of anomalous warming over the Pacific and Indian Ocean, has been shown to have great impact on climate and weather worldwide and especially in East Africa (Latif et al. 1999; Behera et al. 2003; Indeje, Semazzi & Laban Ogallo 2000; Kijazi & Reason 2005; Marchant et al. 2006; Ummenhofer et al. 2009; Hastenrath 2009; Manatsa et al. 2011). These studies have found that above normal SST over the south-western Indian Ocean occur during the warm phase of ENSO (El Niño) while below normal SSTs occur during the cold ENSO phase (La Niña). They also found that warm ENSO, which brings warm moist air from the Indian Ocean over the East African land mass, was associated with above normal rainfall, while cold ENSO, which brings dry and cool air over the land mass, was related to below normal rainfall over East Africa. It is clear that ENSO affects rainfall intensity, distribution and season normality (e.g. early onset and late cessation of rainfall season with a warm ENSO). During the months of October to December, in years when ENSO begins, above normal rainfall with a peak in December was observed instead of November (Indeje et al. 2000). Furthermore, Kijazi & Reason (2009) found the short rainfall season shifted later during the positive phase of ENSO warm period in Tanzania.

The majority of previous studies have found a distinct correlation between the short rainfall season and the SSTs over the Indian Ocean (Mutai et al. 1998; Kabanda & Jury 1999; Basalirwa et al. 1999; Indeje et al. 2000; Behera et al. 2003; Black, Slingo & R. 2003; Black, Slingo & Sperber 2003; Schreck & Semazzi 2004; Hastenrath et al. 2010). Black et al., (2003) investigated the short rainfall season by looking at years with heavy rainfall events and constructed composites of SSTs, wind, rainfall, and humidity. They found that short rainfall

seasons were associated with large scale SST anomalies in the Indian Ocean which resemble those that develop during Indian Ocean Dipole (IOD) events. The Indian Ocean Dipole is a coupled atmosphere-ocean phenomenon the instability of which depends on the annual cycle of the basic state of wind. It is an episodic SST anomaly between the eastern and western tropical Indian Ocean (Saji & Yamagata 2003).

The positive phase of IOD above normal SST in the equatorial Pacific Ocean was found to be associated with ENSO during the peak of the short rain season (Spencer et al. 2005; Schott et al. 2009). However, not all IOD was found to be associated with ENSO (Slingo et al. 2005). Although IOD events happen rarely when compared to ENSO, they contribute to rainfall variability in East Africa (Ashok et al. 2001; Saji & Yamagata 2003; Schott et al. 2009). During the positive phase of IOD, above normal rainfall is observed while the negative IOD phase is associated with below normal rainfall (Marchant et al. 2006; Manatsa et al. 2011; Ummenhofer et al. 2009).

1.4.2 Overview of the direct impacts of climate variability and change

Global warming contributes to an increase in extreme climatic events such as extremely heavy rainfall and drought conditions (Mitchell et al. 2006; IPCC 2007, 2013 and 2014). The IPCC reports and many other studies have shown that future climate change may lead to an alteration in the frequency and intensity or even severity of extreme climate, such as heavy rainfall and drought events (Shongwe et al. 2011; IPCC 2011; Anyah & Qiu 2012; Goodess 2013). The impact of climate variability and change in East Africa is expected to continue to threaten the life and economy of poor communities which are most exposed and have less capacity to adapt (IPCC (SREX) 2012)). Given that agriculture is sensitive to climate, it will likely be highly impacted. The longer and more frequently these events persist, the more damage and loss to the community could be experienced.

Climate change has already contributed to changes in local/regional average temperature, frequency of tropical cyclones, seasonal and annual rainfall seasons (Nicholson, 2000; Ashok et

al. 2001; Yamagata et al. 2004; Semenov et al. 2007; Anyah & Semazzi 2007; Semenov et al. 2007, IPCC (AR4) 2007; Christy et al. 2009). Global warming has already contributed to variability of seasonal and annual rainfall which has led to a decrease in the growing period and yield (Washington et al. 2006; Rowhani et al. 2011; Hepworth 2010b; Moore et al. 2011; Ververs 2012). There is evidence of the disappearance of some staple foods due to drought conditions, and the shortening of the growing period (Thornton 2006; Funk et al. 2008; Thornton et al. 2011; Betts et al. 2011; Horlings & Marsden 2011; New et al. 2011). It is also projected that future climate change may see the decline in crop productivity and livestock (IPCC 2007). This has already been experienced as there is some evidence of drought in East Africa which has resulted in a food crisis and water shortage leading to lower hydropower output (Hastenrath et al. 2007; Kijazi & Reason 2009; Shongwe et al. 2011; Williams & Funk 2011).

Since the climate change projection shows increases in temperature, that means agricultural production for East Africa in the future is uncertain. Food and water are required to sustain life; the challenge for the East African community is the security of these resources. If these two things are uncertain, that means there will be more challenges to a normal human life. The continuous updating of climate change information could provide better options for adaptation strategies. Therefore, improved climate model projections are crucial for assessing and projecting the future climate over East Africa.

In addition, increasing climate variability and change is expected to add more stress on human health. An increase in malaria cases and deaths and even spread to the highlands of East Africa (Kenya, Tanzania) due to an increase in average temperature (Lindsay & Martens 1998; Hay et al. 2002; Patz et al. 2005; Chaves et al. 2012; Himeidan & Kweka 2012; Alonso et al. 2011) have been reported. Poor and insufficient information on climate variability and change in East Africa could lead to more economic and social stress. Therefore, more attention is needed on climate projections at a regional and local level which will assist in the impact assessment to enable the government authorities and policy makers in creating new strategic planning for mitigation and adaptation purposes.

1.5 Climate model application in East Africa and challenges

GCMs have been extensively used worldwide to provide realisations of climate change scenarios. GCMs are capable of simulating observed climate change at a global scale and can also be used for future climate change projections. They are also used to provide data to be used in RCM downscaling exercises. Most studies on climate change projections in Africa, including East Africa, are based on GCMs (Engelbrecht et al. 2009; Shongwe et al. 2011). However, due to their coarse resolution, GCMs cannot sufficiently resolve elements of topography such as heterogeneous land surfaces, vegetation cover, mountainous regions, and land-sea contrast, all of which influence climate at a regional level (IPCC AR4; Giorgi et al. 2009; Rummukainen 2010; Kim et al. 2013; Flato et al. 2013). In addition, GCMs are inadequate for capturing extreme climatic events occurring due to regional and local scale forcings. The information of local topography and associated extreme climatic events are very important for impact assessment (Giorgi et al. 2009; Hernández-Díaz et al. 2012; Kim et al. 2013).

The needs of addressing climate information at a regional and local level have driven scientists to develop RCMs (Mearns et al. 2001; Christensen et al. 2007; Rummukainen 2010), which are useful tools for generating high resolution climate change scenarios for use in climate impact and adaptation studies (Mearns et al. 1999). The RCMs developed are able to reproduce regional climate with more details than GCMs, and RCMs are now used in a wide range of climate applications, from palaeoclimate to anthropogenic climate change studies (Hostetler et al., 1994, 2000; IPCC 2007). There are various ways of downscaling, such as process based techniques with a focus on nested models and empirical techniques (Hewitson & Crane, 1996). The driving data of RCMs can be derived both from GCMs or analyses of observations and can include greenhouse gas emissions and aerosol forcing.

In contrast to GCMs, RCMs have been found to provide more realistic simulations of regional and local climate (Patricola & Cook 2010; Mcguffie & Henderson-Sellers 2001; Flato et al. 2013). High resolution RCMs are better capable of simulating the distribution and intensity of precipitation over heterogeneous topography (Hijmans et al., 2005; Cameron, Parra). Hijmans et

al. (2005) found that very high resolution models can be used to simulate precipitation in the highgrounds such as higher mountainous environments. Furthermore, the availability of high resolution RCMs data provides the possibility of evaluating model skill in relation to lower resolution models. Additionally, previous studies have found large biases in GCM simulations of regional climate (Pan et al. 2001; Gao et al. 2006; Lucas-Picher et al. 2012). As an example for Africa, Hudson & Jones (2002) studied the regional climate for present day and future climate by using Hadley Centre HadAM3H GCM and found that rainfall is overestimated over South Africa. Moreover, it was found that due to the influence of topography, the confidence and consistency in the projections of precipitation extremes by using GCMs were low at the regional level. In the case of East Africa, Shongwe et al. (2011) found evidence of a fairly strong and consistent signal of increased heavy precipitation in the future projection but generally the signals were weaker at a regional level. Tebaldi et al. (2006) also shows some consistency and significance in the GCMs projections, with fewer consensuses, especially in relation to regional patterns. GCMs, while good in simulating large scale climate, are not the favourite choice in the simulations of regional climate necessary for impact assessment (Flato et al. 2013).

Growing evidence of a changing climate and its direct impact on the community have encouraged many government authorities and various decision makers to seek more reliable information about climate variability and change at local and regional scales (Giorgi et al. 2001; Christensen et al. 2007; Hawkins & Sutton 2009; Sylla et al. 2013). Therefore, downscaling techniques have been developed to provide climate information at the smaller scales needed for many climate impact studies. Studies and reports established that there is high confidence that downscaling adds value both in regions with highly variable topography and for various small-scale phenomena (Christensen et al. 1998; Rummukainen 2010; Kendon et al. 2012; Flato et al. 2013).

Lower resolution models, however, can only skillfully represent the general climatological behaviour without the additional spatial details forced by the topography (Mearns et al. 1999; Dankers et al. 2007; Rummukainen 2010; Flato et al. 2013) Coppola et al. 2010). However, knowing that high resolution RCMs are better in simulating regional climate will not be enough.

A model needs to undergo various tests to assess its credibility in the simulation of relevant features in a specific region (Flato et al. 2013).

1.6 Summary

To date, limited information has been published on climate change projections in East Africa. While efforts have been made to study East Africa's climate, very little information on climate change projection is available and accessible. Those studies published are primarily based on coarse resolution GCMs (Shongwe et al. 2011; Anyah & Qiu 2012) and there are few RCM (Cook & Vizy 2013) simulations of climate change. While RCMs have shown some skill at a regional level when compared to GCMs, they still possess inherent bias in their forcing and have problems in their validation (Christensen et al. 1998; Hernández-Díaz et al. 2012; Nikulin et al. 2012). This thesis will therefore focus on the importance of increasing resolution of regional climate models in assessing climate variability and change in East Africa.

In order to have confidence in a given model for climate change projections, that model must be tested for its credibility in simulating the climatic behaviour of that region. Model credibility is partly based on the model's ability to represent the climatological patterns, such as the present or past mesoscale features that contribute to climate variability. Moreover, there must be some accurate information to validate the model such as observation datasets. However, in East Africa, there is limited data which constraints model evaluation. The observation stations are sparsely distributed of which most of them have inconsistency in reporting and questionable quality of the available data (Mutai & Ward 2000).

1.7 Research objectives

Building on the above understanding, the main aim of this thesis is to investigate the potential of increasing resolution in regional climate models in the simulation of climate variability and change over East Africa. In particular, this study will look at the HIRHAM5 (Christensen et al.2006) simulations at 50 km and 10km resolutions when driven by ECHAM5 (Roeckner. et al.

2003; Roeckner et al. 2006) and HIRHAM5 at 50 km resolution when driven by reanalysis, (ERA-Interim) data (Dee & Uppala 2008). These outputs of the models will be validated using observation datasets from Climate Research Unit (Mitchell et al. 2004) and African Climatology Version 2 for Famine Early Warning System (Novella & Thiaw 2013), and ERA–Interim reanalysis data,. Furthermore, observed data from selected stations in Tanzania Meteorological Agency (TMA) will be used. The core of this thesis is supported by the following specific objectives:

1. How well does HIRHAM5 simulate East Africa climatology and extreme climatic events?
2. Does increasing resolution of the HIRHAM model improve the simulation of East Africa climate variability?
3. How does increasing resolution of HIRHAM5 impact the projected climate change in East Africa?

Chapter 2

Models, data and methods

This chapter offers a detailed description of the climate model used in this thesis supported with the maps of the model and study domain. It also describes the field work conducted over the Great Ruaha River sub basin (GRR) in Tanzania and the gridded observation data sets used in the model validation. Additionally, the methodology used in this study is presented at the end of the chapter.

2.1 Climate models

Climate models are mathematical representation tools of the climate system based on physical, biological and chemical principles (Figure 2.3). Climate models use quantitative methods with complex mathematical equations and derivation to simulate the interactions of the atmosphere, oceans, land surfaces and ice (Harvey et al. 1997; Griffies & Adcroft 2008). Climate models can be regarded as the conceptual constructs that can be used to make projections about the outcomes of measurement (Randall & Wielicki 1997). The climate models used in this study are HIRHAM5 and ECHAM5 of which the summary attribute table is presented in table 1.

Table 1: Summary of the models used in this study

Name	Source	Data set used
ECHAM5/MPI-OM1)	Max Planck Institute for Meteorology (MPI-M) coupled atmosphere–ocean general circulation model (AOGCM)	Rainfall, 2 meter temperature, total cloud cover and winds at 700hPa level from 1950 - 2100
HIRHAM5 at 50km resolution forced by ECHAM5	Danish Meteorological Institute	Rainfall, 2 meter, maximum and minimum temperature, winds at 700hPa and 850 hPa, total cloud clover and moisture from 1950 to 2100
HIRHAM5 at 10km resolution forced with HIRHAM5 at 50km resolution	Danish Meteorological Institute	Rainfall, 2 meter, maximum and minimum temperature, winds at 700hPa and 850 hPa, total cloud clover and moisture in three time slices: 1980-1999, 2046-2065 and 2080-2099
HIRHAM5 at 50km forced with ERA Interim	Danish Meteorological Institute	Rainfall, surface temperature, winds, total cloud clover, mean sea level pressure from 1989 to 2008

2.1.1 The global model: ECHAM5-MPI/OM1

ECHAM5-MPI/OM1 is the fifth version of the coupled atmosphere-ocean circulation model (GCMs) generated by the Max Planck Institute for Meteorology, combining the ECHAM5 atmospheric general circulation model and MPI-OM1 ocean/ice model (Roeckner et al. 2003; Roeckner et al. 2006). This version of ECHAM5 was used in the state of art model in the IPCC (AR4 and AR5). The ocean model MPI-OM (Marsland et al. 2003) is a free surface primitive

equation model formulated on C grid and orthorgonal curvilinear coordinates. The model uses the spectral transform method for vorticity, divergence, temperature and the logarithm of surface pressure at T63 spectral truncation with 19 levels, up to 10hPa pressure. This truncation corresponds to about 2° x 2° (Roeckner et al. 2006).

The model has been used in the simulations and projections of climate change in various places including Europe, Asia and some areas in Africa (IPCC 2007; May 2008; Paeth et al. 2009; Matei et al. 2012; Springer et al. 2013). For Africa, ECHAM5 was used to force the Hamburg RCM REMO at 50km resolution (Paeth et al. 2009). The authors found a prominent spatial coherence between the ECHAM5/MPI-OM1 ensemble-mean pattern of precipitation changes over Africa and the multimodel ensemble-mean pattern in the IPCC AR4. They also found that REMO forced with ECHAM5 shows the spatial pattern and the amplitude of the precipitation changes governed by land degradation, whereas greenhouse forcing and land cover changes are equally important for the near-surface warming. In East Africa ECHAM5 was used in the assessment on the Indian Ocean Dipole Mode (IOD) and in the projection of future rainfall (Conway et al. 2007). It was found that the ECHAM5 and HadGEM1 models produced high correlation of rainfall in all seasons compared to other GCMs used. The ECHAM5 data used in this study are monthly rainfall 2 meter temperature and winds at 700hPa (Table 1). These datasets were obtained from the Danish Meteorological Institute through the CLIVET Project under the sponsorship of the Danida Fellowship Centre.

2.1.2 The regional model: HIRHAM5

HIRHAM is a regional atmospheric climate model based on a subset of the High Resolution Limited Area Model (HIRLAM) (Undén et al, 2002), combining the dynamics of the former model with the physical parameterisation schemes of ECHAM (Roeckner et al, 2003).

HIRHAM5 is the fifth version of the HIRHAM regional climate model (RCM), combining the most recent versions of HIRLAM, version 7 and ECHAM5 (Christensen et al.2006). It has been

developed in collaboration between the Danish Climate Centre at DMI and the Potsdam Research Unit of the Alfred Wegener Institute Foundation for Polar and Marine Research.
The model was implemented to extract the large scale circulation from the driving data, and impose this on the fields produced by the HIRHAM5 (Christensen. et al. 2007). The model has been used for a wide range of applications, including numerous experiments outside Europe, on climate variability and change studies. It was recently included in the international regional downscaling experiment CORDEX (Giorgi et al. 2009; Hernández-Díaz et al. 2012; Nikulin et al. 2012; Jacob et al. 2012; Endris et al. 2013; Meque & Abiodun 2014).

This thesis used downscaled model data in different resolutions which were obtained from DMI. These data include global climate model ECHAM5 used as boundary conditions for a simulation by DMI with the regional climate model HIRHAM5 running at 50km resolution. The output from this 50km simulation was further downscaled by the DMI with a second HIRHAM5 simulation running at 10km resolution. HIRHAM5 at 50km (0.44^{o} grid) resolution is generally run on a rotated lat-lon grid in order to have the (rotated) equator not too far from the centre of the model domain so that all grid boxes roughly have the same size. HIRHAM5 at 50 km resolution is available from 1950 to 2100 while HIRHAM5 datasets at 10km resolution are available in three time slices: 1980–1999; 2046–2065 and 2080–2099.

The hindscast of HIRHAM5 under ERAI Interim forcing, which is one of the CORDEX data in Africa (Giorgi et al. 2009), are also used. The HIRHAM5 at 50 km resolution was forced with ERAI reanalysis data as a hindcast from 1989 to 2008 at 50 km resolution following the CORDEX format. This will help to address the uncertainty in HIRHAM5 simulations of climate change projections over East Africa. It was suggested to also use the hindcast of HIRHAM5 at 10km; however, these data were not available at the time of undertaking the PhD (due to the computational constraints).

2.1.3 The model domain

In this study, the HIRHAM5 datasets used have two domains: all of Africa (Figure 2.1a), identical to the CORDEX Africa domain (Giorgi et al., 2009), and a tropical East Africa (Figure 2.1b) domain. That is, the larger domain is at a resolution of 50 km while the smaller domain is at a resolution of 10km. The region of interest is placed such that it is far enough from the relaxation zone (Lo et al. 2008). Note that, in the analysis for a smaller domain the extreme northern portion of East Africa is ignored due to the potential artifacts near the boundaries. Furthermore, the location of the boundaries are chosen so that the complex topographical features of East Africa such as the highest peaks of Africa (Mount Kilimanjaro) and Indian Ocean circulation (bordered to the east) fit within the domain.

The higher resolution (Figure 2.1b) model domain shows the topography as resolved in the simulations, which includes continental East Africa and the highlands of East Africa and Indian Oceans, extending from 15.956^{o} W to 52.056^{o} E and 28.035^{o} S to 4.035^{o} N.

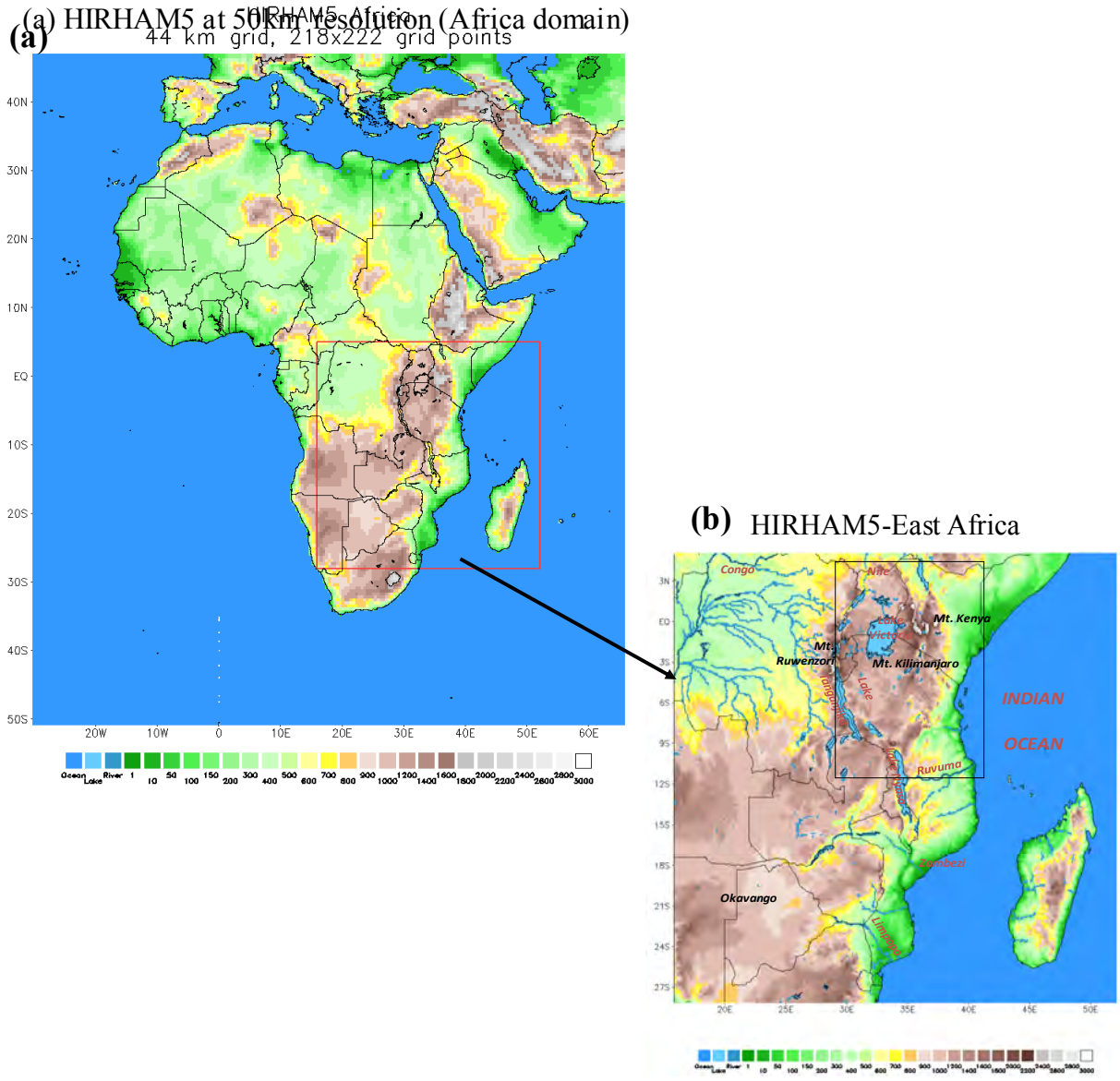

Figure 2.1: (a) The simulation domain for low resolution HIRHAM5 at 50 km resolution (CORDEX Africa) with a nested high resolution HIRHAM5 at 10km resolution (red box) showing the topography and (b) model domain for the nested HIRHAM5 at 10km resolution. The black box is the study domain covering Kenya, Uganda and Tanzania.

2.2 The field work, reanalysis and gridded observation data

This section presents a brief of field work conducted over GRR, reanalysis data from the ERA–Interim and observation datasets from the observed gridded, blended satellite data such as CRU, FEWS datasets and Multivariate ENSO Index (MEI). It also presents station data from the Tanzania Meteorological Agency.

2.2.1 Observation dataset from field work in GRR

The field work was conducted over the GRR to collect all available observed daily and monthly climatology from observation stations (Table 1). Since Tanzania Meteorological Agency works to observe, collect, archive and disseminate meteorological and related information for the United Republic of Tanzania that was the first port of call. It is found that in their archive they have over 146 observation stations in GRR which are registered. These stations are supposed to send their data to TMA for archiving. However, the data that were available at TMA had many missing years and months, and the stations had stopped sending their data to TMA. Therefore, it was decided to visit the stations for the purpose of filling the gaps and getting new data. The results show that out of the 48 stations that were visited (Appendix 1), only 2 stations had quality and consistent data. Some stations had problems of equipment; some inadequate observers (manpower); some data were missing due to poor storage (Appendix 1). It was also found that most of these stations were research centers, and after the intended project ended they operated for a short period and then stopped. Most of these stations are voluntary stations (Primary and Secondary Schools, Missions) who were expecting some incentives from the government; when the incentives stopped the stations became non-operational.

Therefore, the observations of two stations, namely Iringa and Dodoma were obtained from TMA to represent the unimodal rainfall regime and Kilimanjaro International Airport Meteorological station (KIA) for the bimodal rainfall regime in Tanzania. These two stations were taken as a point station to be used as the signals in the averaged area for model validation.

The following map and table indicate the location of the field work stations that were chosen to represent the unimodal (UN) and the added stations from the bimodal (BM) area regime in Tanzania. Note that Kilimanjaro is coloured red, Dodoma green and Iringa grey (Figure 2.2b)

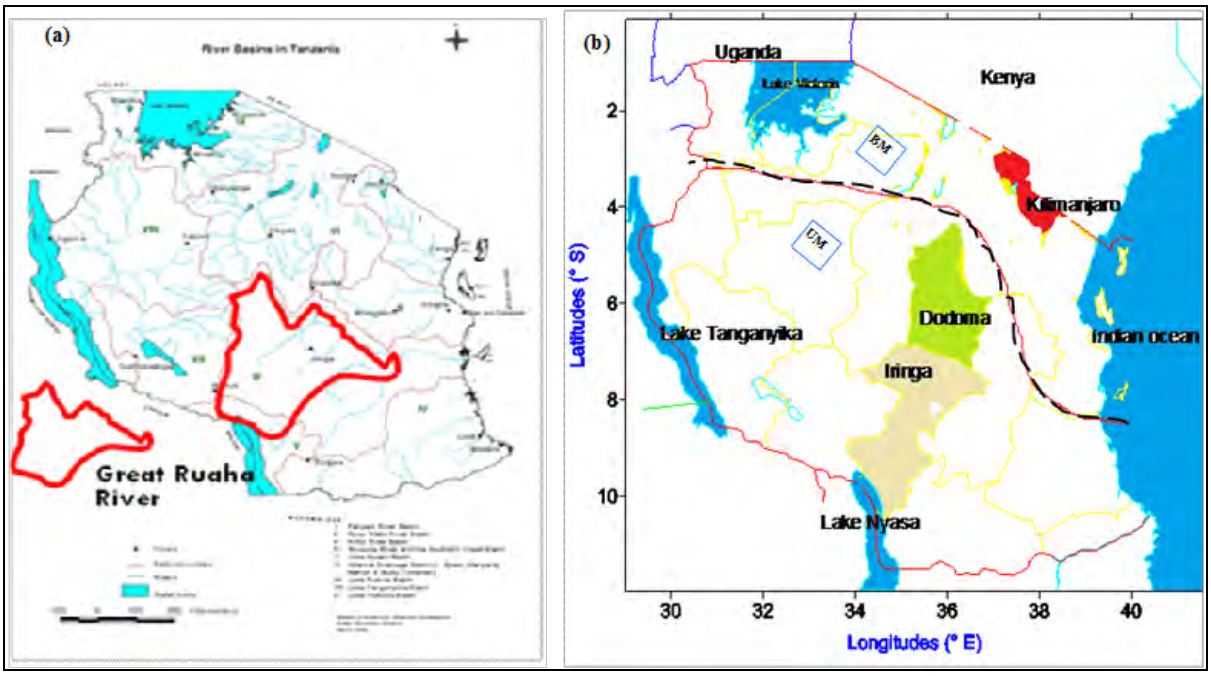

Figure 2.2: (a) Location of the Great Ruaha River sub-basin (GRR) in the map of Tanzania: Source Rufiji river basin Office and (b) Homogeneous rainfall zones in Tanzania (modified form TMA). The dotted line divides the country into Unimmodal (UN) and bimodal (BM) rainfall regime.

Table 2.1 Meteorological stations with locations in Tanzania.

WMO Code	Station name	Latitude	Longitude	Elevation (m)
63887	Iringa	7° 38' S	35° 46' E	1428
63862	Dodoma .	6° 10' S	35° 46' E	1120
63791	KIA	3° 25' S	37° 04' E	896

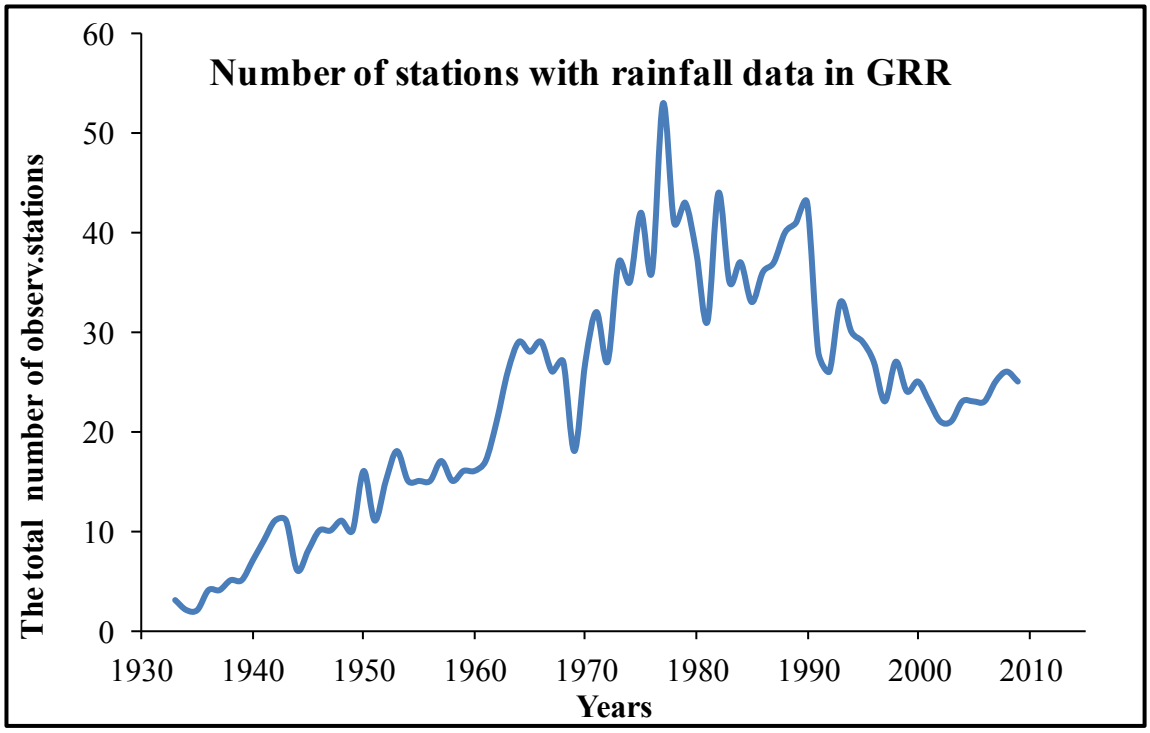

Figure 2.3: The number of climatological stations in the Great Ruaha River sub basin (GRR) sub basin with rainfall records: from 1933 to 2009.

Figure 2.3 indicates the number of stations with rainfall records after field research. The focus here is to show how many stations are active and have at least data. The total number of climatological stations in GRR sub basin is 148 but only 48 stations were found to operate and with data. Long term data records of rainfall and temperature were targeted but, as mentioned above, only 2 stations (Iringa and Dodoma) were found to have sufficiently long records (more than 20 years) of both rainfall and temperature. Therefore, the number of stations with records of rainfall was plotted because the stations with long term temperature records were sparse (below 5). The results show that there is no specific trend of rainfall stations over the region. For the reasons given earlier in this section, the rainfall stations in operation vary from year to year. This is a big challenge for any researcher when it comes to the issue of observation data. It is clear now that climate has changed and is projected to continue to change (IPCC 2007, 2013). The impact of climate change is also well known, especially for developing countries. For better adaptation and planning for mitigation measures, there is a need of continuous monitoring of climate at a local to regional level. This is only possible with quality and consistent observation

data. Most studies have found that a quality climate model is dependent on good observation data. The main challenge in climate projection for the impact assessment is observation data for climate model validation (Allan & Soden 2008; Rummukainen 2010; Nikulin et al. 2012, Kim et al. 2013).

Since the field work over the GRR did not give quality and spatial distribution data intended for validating high resolution RCMs, it was decided to use the estimated gridded observation datasets. The following section will present the details of reanalysis and gridded observation datasets.

2.2.2 Observation datasets from CRU and FEWS

The observation datasets from Climate Research Unit (CRU) and (FEWS datasets) African Rainfall Climatology, version 2 (ARC2) are presented in this section, followed by a brief description of observation station data used from the Tanzania Meteorological Agency.
The CRU datasets from the University of East Anglia (Mitchell et al. 2004) (UEA) is used in this thesis is monthly rainfall and surface temperature from 1980 to 2006, interpolated to a grid resolution of 0.5 x 0.5 degree latitude/longitude. CRU datasets have been used worldwide, including Africa, for various studies and climate experiments such as model validation and in climate assessment (Christensen et al. 1998; Omotosho & Abiodun 2007; Jung & Kunstmann 2007; Paeth et al. 2009). For example, recently most of the CORDEX Africa studies use CRU datasets as observations in the evaluation of regional cliamate models (Endris et al. 2013; Gbobaniyi et al. 2013; Omondi et al. 2013)

The FEWS project is the project developed by the United States Agency for International Development (USAID) Famine Early Warning System (FEWS) to assist in drought monitoring efforts for the African continent (Herman et al. 1997). This project developed a technique for estimation of rainfall over Africa with the augment that rainfall data available is sparsely distributed over the region. In this thesis, the dataset used is called African Rainfall Climatology, version 2 (ARC2). The datasets span from 1983 to 2013 at a spatial resolution of

0.1^{o} (Novella & Thiaw 2013). The ARC2 (FEWS) has been used in various experiments in Africa such as assessing the impact of rainfall on agriculture and water resource management (Funk & Brown 2006; Riddle & Cook 2008; Ahmed et al. 2009).

2.2.3 The reanalysis data (ERA Interim)

ERA Interim is the latest global atmospheric reanalysis produced by the European Centre for Medium Range Weather Forecasts (ECMWF) (Dee et al. 2011). Reanalysis is an activity which makes use of the modern Numerical Weather Prediction (NWP) system available today to reproduce past atmosphere, sea and land surface conditions using past observations (Dee et al. 2011). ERA-Interim uses the sets of observations obtained from its predecessor ERA-40, supplemented by data from later years from ECMWF's operational archive (Dee et al. 2011). The ERA-Interim dataset that is present for this study starts from 1989 to 2009. However, for standard procedure the first year of the simulation will be discarded to avoid spin-up of the model. The spin-up of the model is the time which the model takes to achieve its climate equilibrium (Denis et al.2002).

2.3 The Multivariate ENSO Index (MEI) data

It is known that El Niño Southern Oscillation (ENSO) is characterised by the complex interaction of the atmosphere-ocean coupled mode. The anomalous sea surface temperature (SSTs) was associated with rainfall anomalies over East Arica. ENSO is a dominant mode of inter-annual variability in East Africa (Latif et al. 1999; Indeje et al. 2000). Many indices have been used in studying ENSO events, most of which incorporate only a single variable. The well-known Southern Oscillation Index (SOI), NINO3.4 (5^{o} S–0; 44^{o} E-80^{o} E), and NINO3, NINO4, Central Equatorial Index NINO3.4 (5^{o} S–5^{o} N; 170^{o} W–110^{o} W), CEI (Central Equatorial Indian index) (15^{o} S-0; 44^{o} E–80E) use only one variable. However, recent studies have suggested to use the multivariate ENSO index MEI in studying the ENSO signal (Wolter & Timlin 2011). MEI is a bi-monthly index characterised by six observed variables: sea level pressure, zonal and meridional components of the surface wind, sea surface temperature (SSTs), surface air

temperature and cloudiness of the South Pacific Ocean using data from the International Comprehensive Ocean Atmospheric Data Set (ICOADS). For example, Wolter & Timlin (2011) found that MEI provides a more complete and flexible description of the ENSO phenomenon than single variable ENSO indices such as the SOI or Niño 3.4 SSTs.

Therefore, in the evaluation of HIRHAM5 in simulating ENSO (El Niño and La Niña) signals over East Africa, the Multivariate ENSO Index is used. The MEI data used in this study was downloaded from http://www.esrl.noaa.gov/psd/enso/mei/table.html.

2.4 Methods

This study will use the high resolution HIRHAM5 model to assess the climate variability and change over East Africa. In order to have confidence in using this model, this study will evaluate the model with reference to available observed data from the region. In the evaluation process of the present climate, the data from 1990 to 1999 will be used. This period was chosen for consistency's sake; that is, to also cover HIRHAM5 at 10km which is in time slices (first slice starting from 1980 to 1999). Moreover, HIRHAM-ERAI which has data starts from 1990 to 2007 will be used.

The climate models (HIRHAM5 and ECHAM5) will be evaluated in several steps. The evaluations will involve model representation of mean climatology of rainfall; temperature, winds, annual cycles of both rainfall and temperature, bias estimation relative to observation datasets (station data, gridded FEWS and CRU) and the spatial correlation of climate models relative to observed rainfall and temperature. Furthermore, in chapter 4 the annual variability of seasonal rainfall and temperature and ENSO signals as simulated by the models versus observation datasets are also presented. Furthermore, the Multivariate ENSO Index is also used to investigate HIRHAM5 representation of El Niño Southern Oscillation signals in simulations of rainfall and surface temperature. Moreover, in chapter 5, HIRHAM5 is used in the projection of mean and extreme climatic changes for rainfall and surface temperature over East Africa domain. Note that in all experiments HIRHAM5 simulation in both resolutions (50 km and

10km) is investigated in the representation of the bimodal regime, MAM and OND and JJA rainy seasons. However, in most of this thesis results only MAM season will be presented and where necessary the other seasons are presented in Appendix 2.

Finally, the possible projection of East Africa climate variability and change will be presented using ECHAM5 and HIRHAM5 at 50 and 10km resolutions. This will be done as outlined below. Does increasing resolution add value in the assessment of climate variability and change in East Africa? The following chapters will seek to answer this question.

Chapter 3

Evaluation of high resolution regional climate model HIRHAM5 in simulating East Africa climate

The aim of this chapter is to investigate the capability of the very high resolution RCM HIRHAM5 in simulating East African climate. Studies have shown that a model's skill can be defined by its realistic representation of the selected statistics of historical climate over a specified region (Mearns et al. 1999; Sylla et al. 2010). Such historical statistical features include model simulations of the annual mean climatology and annual cycle of rainfall and surface temperature, and ENSO signals (Jin et al. 2008). However, the model quality depends on the driving fields (Wilby et al. 2004; Kim et al. 2013), ERA-Interim (ERAI) and ECHAM5 (in this case).

3.1. Simulation of seasonal rainfall climatology over East Africa

This section presents the mean climatology of rainfall as exposed by the observation datasets and simulations of HIRHAM5 and ECHAM5 for MAM (OND in the Appendix 2) rainy season. The performance of HIRHAM5 simulations for the current climate (1980–1999) is examined in comparison to the observation datasets from CRU, FEWS and the boundary forcing from ERAI and ECHAM5. The 19 year period (1980–1999) is selected in order to accommodate observations, reanalysis (starts 1989 as CORDEX data) and the model especially HIRHAM5-10km (the present data covers 1980 to 1999) datasets. This will include the evaluation of HIRHAM5 in simulating mean and seasonal climatology, annual cycles and extreme climatic events. Additionally, correlation analysis relative to CRU and FEWS for both rainfall and

temperature are discussed. Furthermore, HIRHAM5 simulations of seasonal winds are presented with respect to CRU and ERAI followed with a summary of this chapter.

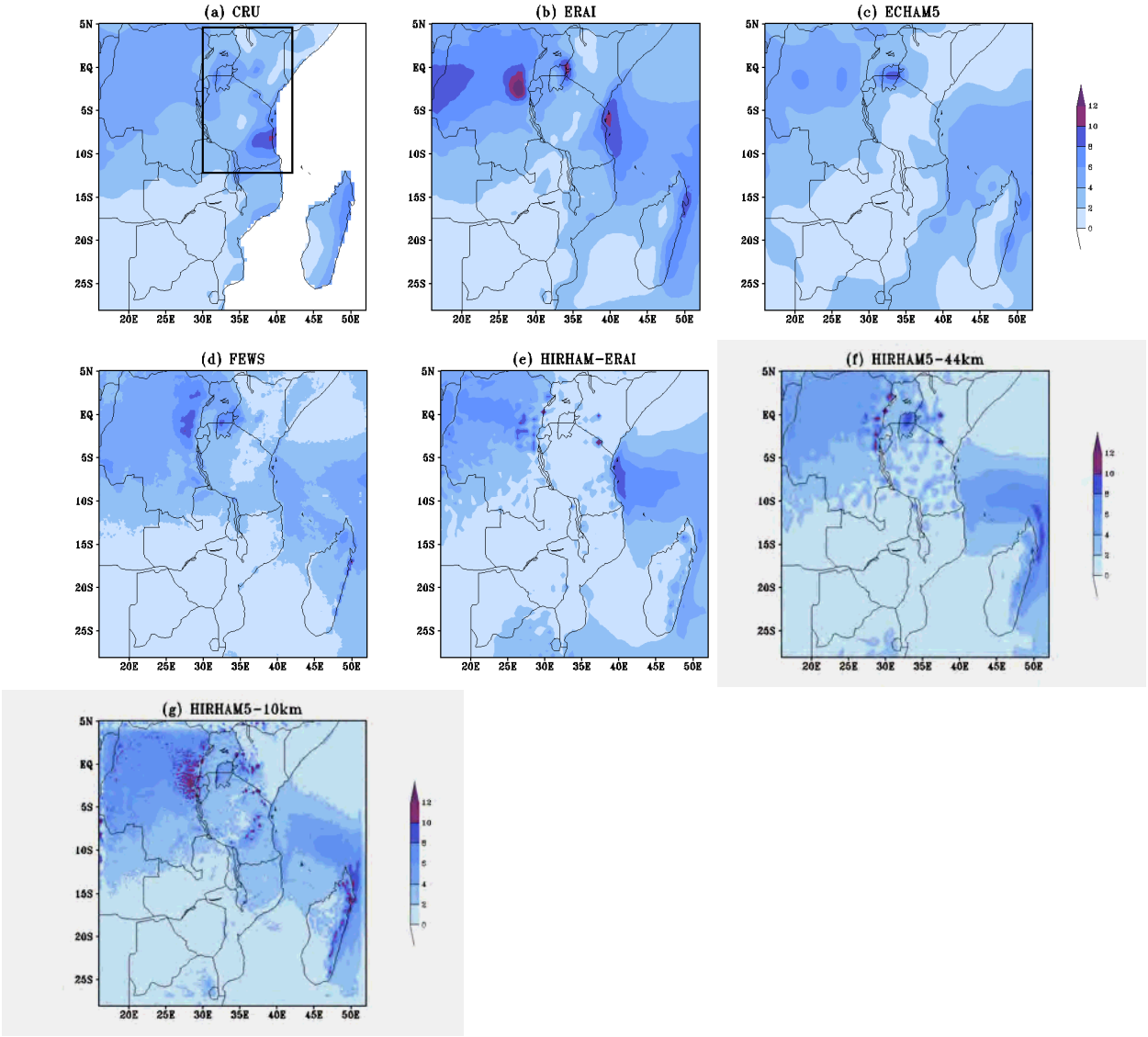

Figure 3.1: Mean rainfall (mm/day) climatology during MAM season by (a) CRU, (b) ERAI, (c) ECHAM5 (GCM), (d) FEWS, (e) HIRHAM5 driven by ERAI (HIRHAM-ERAI), (f) HIRHAM5 driven by ECHAM5 at 50km resolution (HIRHAM5-50-km) and (g) HIRHAM5 driven by ECHAM5 at 10km resolution (HIRHAM5-10km)

The results in Figure 3.1 show that all fields present some similarities in the distribution of the patterns, however with some differences in magnitude. The results show similarities in model simulations and observations, however with some differences. The observation datasets and the models reproduce more rainfall over the western portion of the domain, which include the coastal belts of Tanzania and Kenya, and over the Congo basin forest. However, the observation field (3.1(a and d) show some differences in magnitudes. CRU show higher amount of rainfall over the coast of Tanzania than FEWS (Sylla et al. 2013). In Figure (2.1d) FEWS shows less amount of rainfall over Kenya and north–eastern highlands of Tanzania. The best estimates, ERAI, also show some differences from the observations although the patterns look similar. ERAI shows more rainfall over southwestern Uganda and over the coastal regions of Tanzania (Zanzibar and Pemba) basin in comparison to CRU (6mm) and FEWS (9mm) than all observed fields. The differences in the two observation datasets could be related to the data source: FEWS is a blended satellite derived data, which might have missed some features over the ground, although it has a high resolution and spatial distribution compared to CRU dataset. CRU is gauge-based data which is known to have missing data over the high ground and remote area (Nikulin et al. 2012).

Furthermore, the low resolutions fields (ECHAM5) due its resolution do not distinguish the rainfall amount in the high grounds from lower elevations, it smoothens the mountainous areas that are subject to upslope. Therefore, ECHAM5 model simulations show some differences relative to the observations and with HIRHAM5 (especially over the high ground). On the hand HIRHAM5 simulations at different forcings and resolutions also show some similarities and differences. HIRHAM5-ERAI simulates less rainfall over larger portion of Tanzania and Kenya in comparison to HIRHAM5 at 50km and at 10km resolution. HIRHAM5-50km and HIRHAM-ERAI, although having the same resolution, show some differences especially in magnitude and over high ground (Figure 4.1e and f). Most of the previous studies have shown that the major bias in the RCMs is the driving GCMs (Kim et al. 2013; Flato et al. 2013). However, it is well thought-out that HIRHAM-ERA was supposed to at least look like its boundary forcing but the patterns show large departure from the boundary condition. It is suspected that the systematic error in the model formulation as this could play part as well. The analysis of the bias estimation

in the coming sections could probably give illustrations on HIRHAM-ERAI reproduces the observed rainfall relative to its boundary forcing. It is noted that climate model error can propagate through the entire assessment procedure to become a fundamental source of uncertainty (Kim et al. 2013). Although the two fields, HIRHAM5 at 10 and 50km seem to underestimate rainfall patterns, HIRHAM-ERA simulate rather less precipitation over the mainland of the three countries (Kenya, Uganda and Tanzania). The higher resolution, HIRHAM5-10km simulates more rainfall (~12mm/day) over the Congo basin, high ground and central Indian Ocean, maxima in CRU field is ~7mm/day. This result shows that increasing resolution of the model does not change the patterns but rather changes the magnitude. The same result is depicted for OND (Appendix2). The detailed discussion of the model comparison will be given in the following sections.

3.2 General estimation of bias in simulated rainfall climatology relative to the observations

The observation datasets are compared to each other, and the model simulations are compared to the observation datasets. The former intention is to get an overview of observation datasets representations of East Africa climatology, and the latter is model reproduction of the observed East Africa climatology. The discussion will also follow on the model bias estimation according to their boundary forcing and horizontal resolution. This chapter presents the fields for MAM rainy season, other fields OND rainy season where necessary are presented in the Appendix 2. The mean model bias and differences between the observation datasets in the present day climatology of rainfall is estimated by taking the difference between the models results and the observation dataset following the equation the equation adopted from Pan et al. (2001):

$$\Delta P_{RCM} = \frac{\sum_{i=1}^{N} W_i (P_i^m - P_i^0)}{\sum_{i=1}^{N} W_i} \quad \text{.....(1)}$$

Where Po and P^m are time means of observed and model simulated precipitation respectively. N is the total number of grids in the region while W is a latitudinal dependent weight (Cos φ_i), whereas φ_i is latitude of the grid point. However, for East Africa, the denominator is equal to 1 since the weight factor W is 1 for East Africa (Cos φ_i) =~1). Therefore the formula will finally be as follows:

$$\Delta P = \sum P^m - P^0 \quad \text{.....(2)}$$

Whereas ΔP is the differences between model (P^m) simulations and observation datasets (P^o).

3.2.1 Bias estimation in simulated rainfall climatology relative to CRU

In this subsection is undertaken to specify to what degree the models overestimate or underestimate the rainfall climatology in bimodal rainfall regime when compared to the CRU datasets. This will enable us to quantify the skill of the models with respect to the observation and resolutions. This is done by taking the difference between the models results and the observation dataset (Formula1).

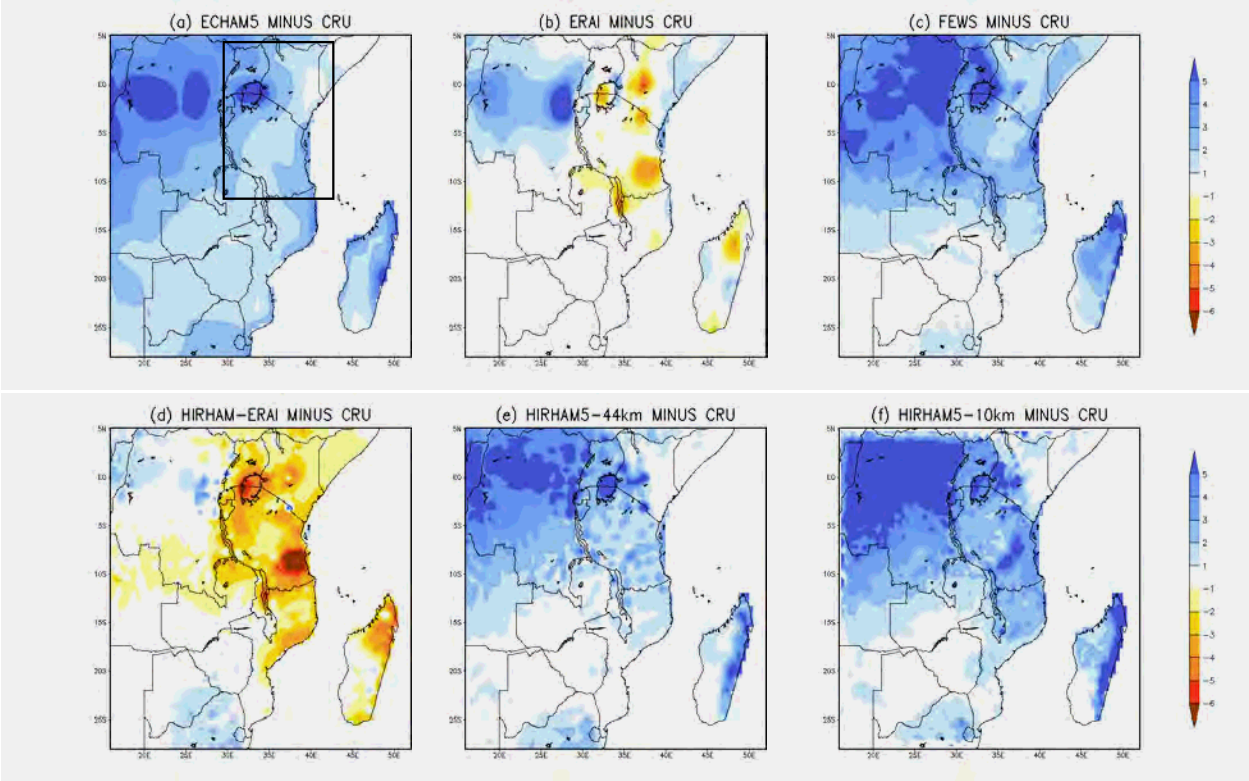

Figure 3.2: Comparison of the observed and simulated mean rainfall climatology (mm/day) over the East African domain during MAM season from 1990–1999. (a) ECHAM5 minus CRU; (b) ERAI minus CRU; (c) FEWS minus CRU; (d) HIRHAM5-ERAI minus CRU; (e) HIRHAM5-50km minus CRU; and (f) HIRHAM5-10km minus CRU. The black box in the figure (c) is the study domain

Figure 3.2 presents the comparison of the HIRHAM5 fields in two different resolutions and its boundary forcing, ERAI and ECHAM5 relative CRU. All models including the best estimate, ERAI simulate wet bias over the western portion of domain (Congo basin). ERAI in comparison to CRU datasets also presents dry bias over the highlands of East Africa (Mount Kilimanjaro, south-western highlands of Tanzania and in Kenya). The hindcast, HIRHAM-ERAI however, differ from other models, it simulates dry bias (> -5 mm/day) over the large areas covering Tanzania, Kenya and Uganda with the patterns similar to the boundary forcing. (Figure 3.2d). In this case the increased bias in the hindcast seems to be propagated to the boundary forcing.

Additionally, HIRHAM5-10km, HIRHAM5-50km (Figures 3.2 a, d and f) and their boundary forcing, ECHAM5 (Figure 3.2a) simulates wet bias over the entire East African region. The wet bias seems to be propagated from the boundary forcing.

Furthermore, the higher resolution HIRHAM5-10km simulates larger wet bias (above 5 mm/day) over the Congo basin forest and high ground of the East Africa compared to the lower resolution HIRHAM5-50km. These results were also depicted in OND rainy and JJA season (Appendix). This means the downscaled regional climate model biases are propagated from their boundary forcing (Filippo. & Gary. 1989; Nikulin et al,. 2011; Flato et al,. 2013). This result agrees with most of the previous studies that, higher resolution provides more details of topography than low resolution (Giorgi et al.2001, Nikulin et al. 2011; Flato et al., 2013). Additionally, a higher resolution simulates high amount of rainfall over the high grounds of the southwestern highlands of Tanzania which could be linked to high convection scheme of the model. It is also observed that the patterns in the higher resolution RCM look more similar to the patterns of the FEWS minus CRU (Figure 3.2(c and f). It is noted that model bias decreases with high resolution observation datasets (Cook & Vizy 2012; Nikulin et al. 2012). In this section the comparison of the model with low resolution observation datasets is presented, the following section (section 3.2.3) presents models bias relative to high resolution observation dataset, FEWS.

3.2.2 Correlation pattern of rainfall climatology simulations relative to CRU datasets

This subsection discusses correlation pattern of HIRHAM5, ECHAM5 and ERAI relative to CRU datasets for MAM rainy season (OND is shown in the Appendix2). This experiment is conducted to assess how well the model reproduces in each grid resolution.

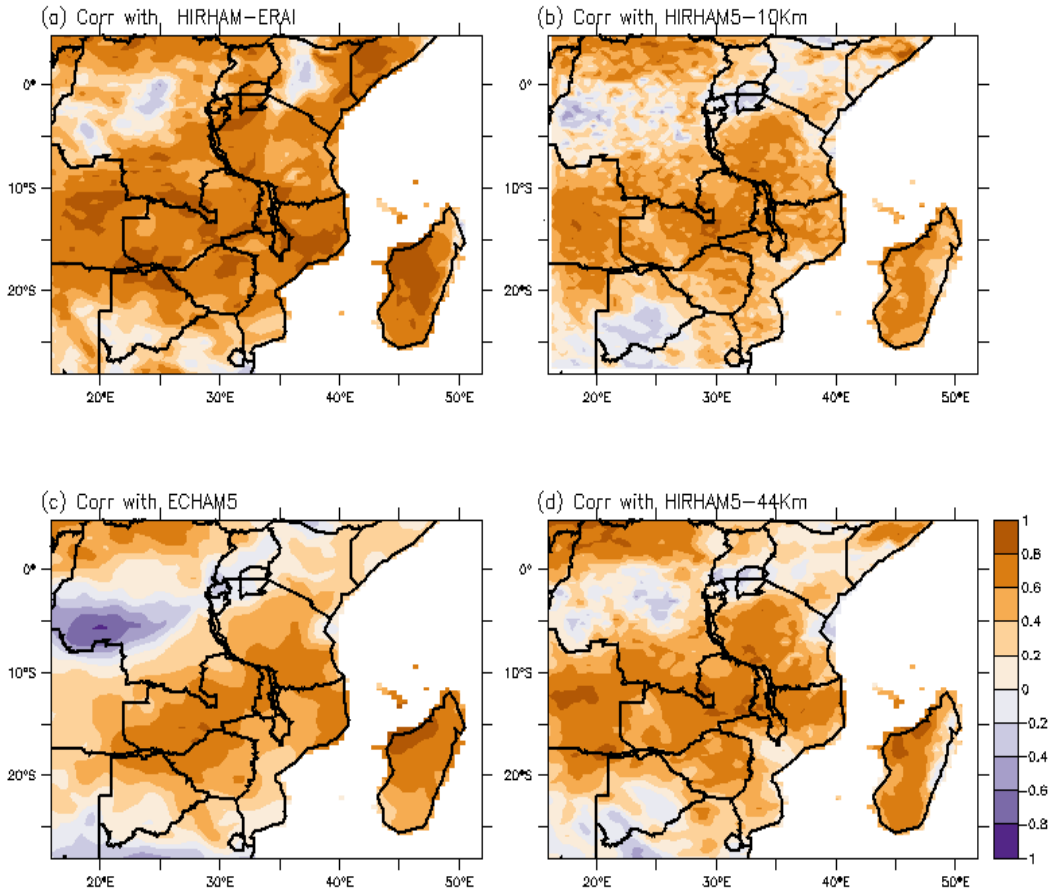

Figure 3.3: Rainfall climatology correlation (r) of MAM rainy season as simulated by (a) HIRHAM5-ERAI, (b) HIRHAM5-10km, (c) ECHAM5 (d) HIRHAM5-50km with reference to CRU datasets.

Figure 3.3 shows the results of the correlation pattern of the models relative to the CRU. The ECHAM5 show some good correlation with CRU. The highest correlation is simulated around 20° S to 10° S for all models. Although the patterns are similar with the same boundary forcing, the higher resolution, HIRHAM5-10km shows reasonable skill in comparison to HIRHAM5-50km over the large area of Tanzania, and especially north-eastern Kenya (Figure 3.4 e and f). The reason could be that increasing resolution improved model physics (capturing small scale features). However, the weak negative correlation (between -0.4 and 0.1) is more confined over the central to western Congo basin area, northern Tanzania and Kenya (and especially southern Kenya, and Lake Victoria). This is related to the topographical features over these areas. The

areas with weak correlation are remote areas which CRU data sets have missing data (Nikulin et al. 2012). For example over the northern Tanzania, north–west Kenya and Congo area the topographical features show poor correlation with ECHAM5 and HIRHAM5. On the other hand ECHAM5 is a coarse resolution which is limited by its resolution to resolve details features especially over the high grounds. As stated above, CRU has no data over remote areas. Therefore this is why the models show some poor correlation to some of these regions such as northern Tanzania, southern Uganda and south and northwest Kenya (along the Great Rift valley, Lake Eldoret) and in the remote areas over Congo basin forest. Despite the weakness, overall results show that HIRHAM5 and its hindcast demonstrates good skill with strong correlation ($r>0.8$) in simulating rainfall patterns compared to ECHAM5. The result is also depicted in OND season (not shown).

3.2.3 Bias estimation in simulated rainfall patterns relative to FEWS

The bias estimation of rainfall climatology of HIRHAM5 and its boundary forcing ECHAM5, ERA Interim relative to FEWS will be presented in this subsection. This experiment is conducted for the purpose of more understanding how well HIRHAM5 simulations relative to more spatial observation and high resolution datasets reproduce East Africa rainfall climatology. It was noted in the previous section (3.1) that CRU data set have missing data over the remote areas.

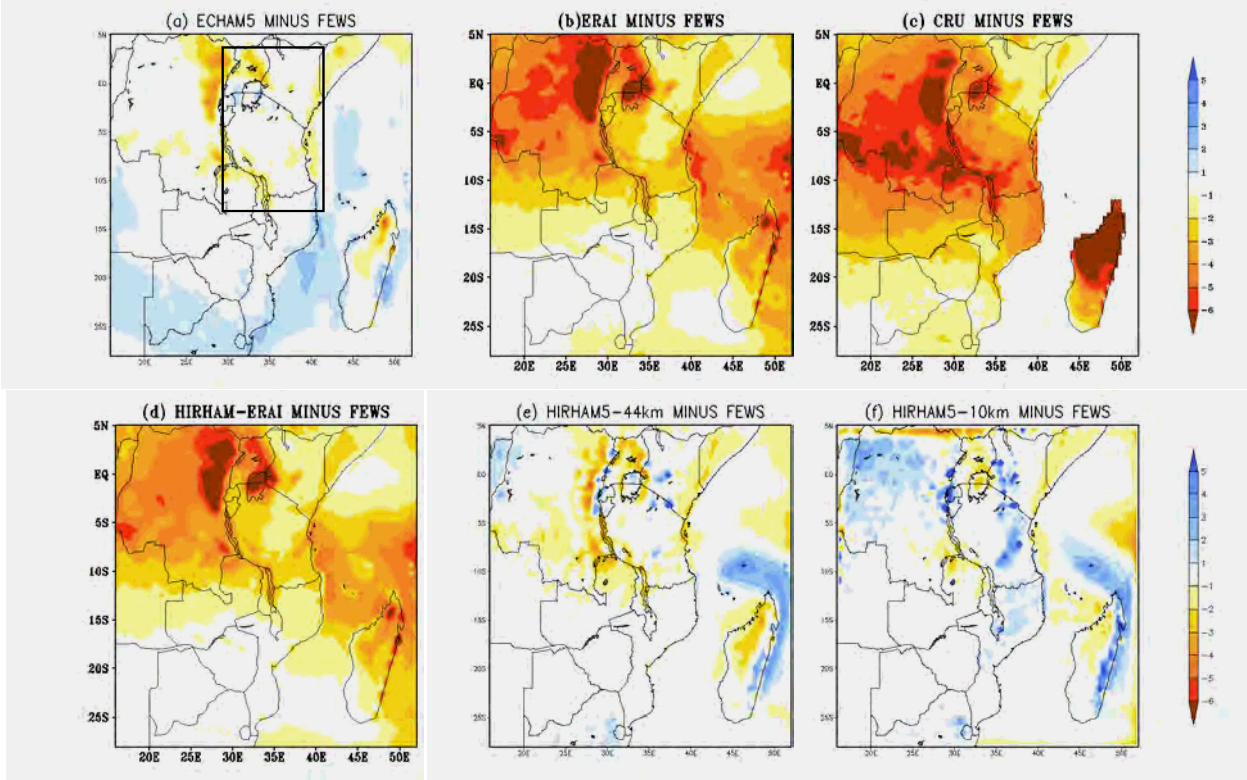

Figure 3.4: Comparison of the observed and simulated mean rainfall climatology (mm/day) over the East African domain during MAM season from 1990–1999. (a) ECHAM5 minus FEWS; (b) ERAI minus FEWS; (c) CRU minus FEWS; (d) HIRHAM5-ERAI minus FEWS; (e) HIRHAM5-50km minus FEWS; and (f) HIRHAM5-10km minus FEWS. The black box in the figure (c) is a study domain

Figure 3.4 presents the results of the comparison of observed high resolution dataset (FEWS) and simulated mean rainfall (mm/day) climatology over East Africa domain during MAM rainy season. The results show that the observed field like in the previous section (3.1.1), CRU and ERAI reproduces more rainfall over large areas of the domain. This results show substantial difference from previous analysis on bias estimation relative to CRU. For example, HIRHAM-ERAI simulates dry bias over the entire domain. The ECHAM5 and HIRHAM5 in both resolutions also show substantial differences in comparison to the previous bias estimations. The bias in HIRHAM5 are inherited from the boundary forcing as this can be seen in the patterns looking much similar for the hindcast with their boundary forcings (Flato et al. 2013). However,

the bias has substantially been reduced in FEWS than when comparison was undertaken with CRU (Section 3.1.1). In HRHAM5 at 10 km simulations the bias has been reduced from Figure 3.2f (+5mm/day) to Figure 3.4f (1-2 mm/day).

Furthermore, the evaluation of the resolution impacts shows that, higher resolution simulates increased wet bias over the high ground in comparison to low resolution (HIRHAM5-50km). This results agree with most of the previous studies that, high resolution overestimates rainfall over the high ground while low resolution underestimate rainfall over high ground (Polanski et al. 2010).

3.2.4 Simulated rainfall correlation pattern relative to FEWS

In this subsection the coefficient correlations between the HIRHAM5 models and ECHAM5 versus observation from FEWS dataset is presented for MAM season. As in the previous sections the analysis is based on MAM rainy season.

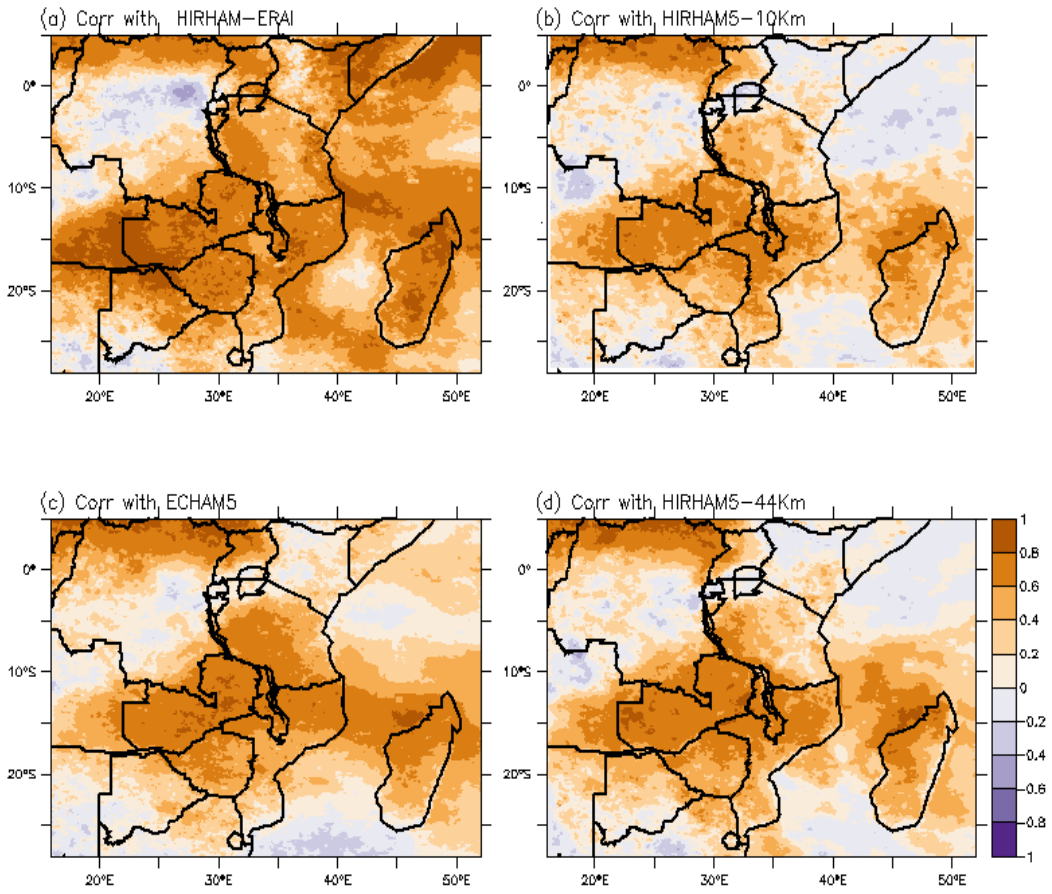

Figure 3.5: The correlation pattern of rainfall climatology as simulated by (a) HIRHAM5-ERAI, (b) HIRHAM5-10km, (c) ECHAM5 (d) HIRHAM5-50km relative to FEWS in MAM season

Figure 3.5 presents rainfall correlation coefficient of the models relative to FEWS during MAM season. The results of the model simulations show significant positive correlation over almost the entire study domain. Over the large parts of Tanzania (western portion) and Uganda (northern) the correlation is good ($r>0.7$). However, over the high ground and especially the regions where the Great Rift Valley passes the correlation is low (0.2). This could be related to the fact that the orographic features over these regions not well captured by the model or the observation's discrepancies in data estimation over the ground information. Note that FEWS is a blended satellite data as this could be the reason that the spatial data over this are either over estimated or not well represented. The recent study show that FEWS datasets show high frequency and low intensity over South and of East Africa (Sylla et al. 2013). In some regions

where the models in general did not capture well the correlation pattern is poor. In northern Kenya both ECHAM5 and HIRHAM5 simulate only weak positive correlations (r=~0.2) Furthermore, both GCM and RCMs simulate weak negative correlations (r=~-0.2) over Congo basin, northwest Indian Ocean, south of Mozambique Channel and southernmost of the domain. These are the areas of heterogeneous topography, such as the Great Rift Valley, highlands and the Lakes (Lake Victoria, Eldorate and Edward).

3.2.5 Annual rainfall cycles of East Africa

This section presents the annual cycles of rainfall total per month over the averaged area of the study domain. The study domain covers Kenya, Uganda and Tanzania (Figure 1.1). It then follows with the annual cycles of the selected region in Tanzania over the unimodal and bimodal rainfall regime (Figure 2.2b in Chapter 2). Additionally the analysis of temporal bias and correlations for each time series relative to the observed fields (CRU and FEWS) are presented followed with the discussion.

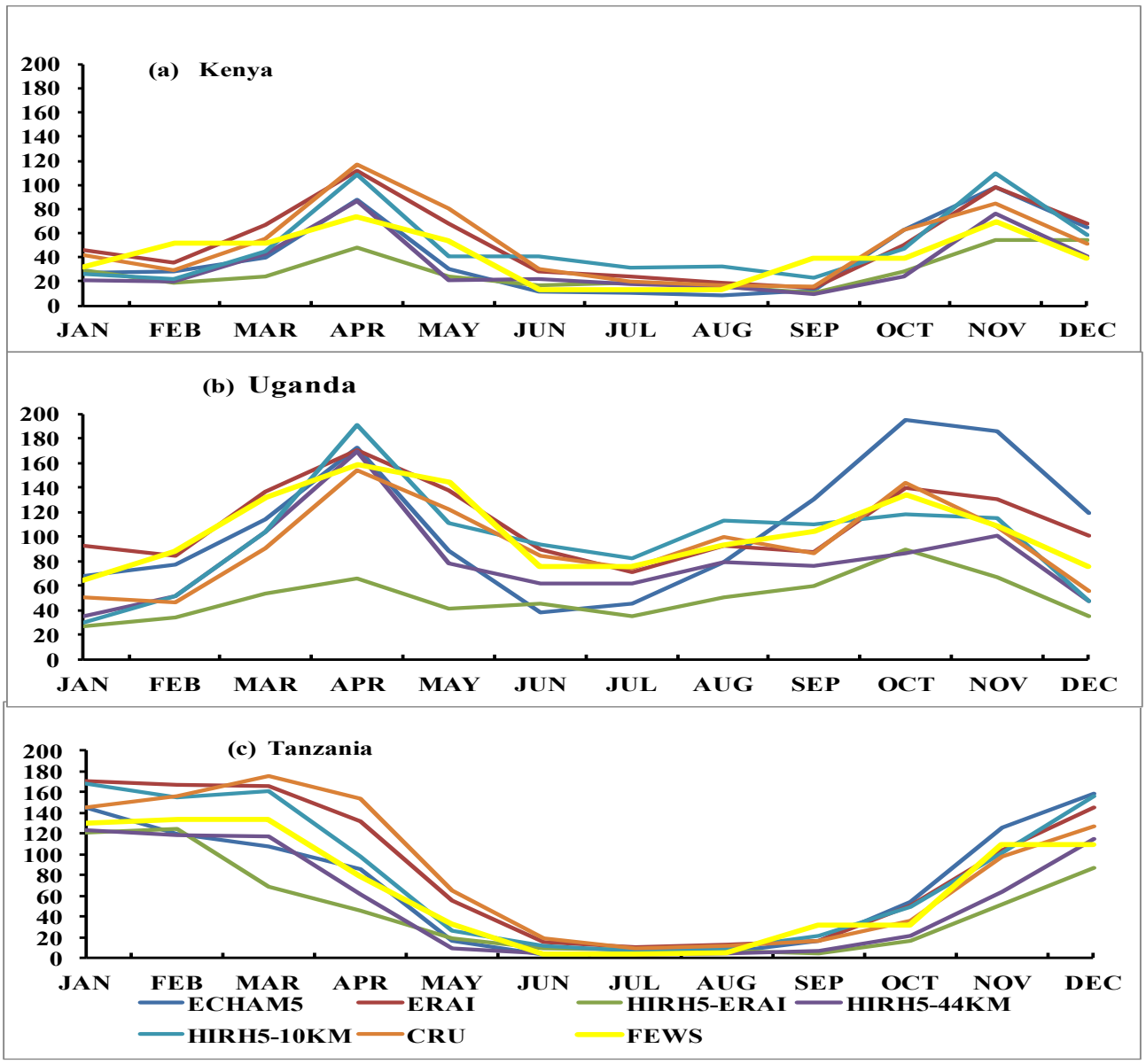

Figure 3.6: Annual cycles of rainfall (mm/month) for the selected averaged regions of the study domain of East Africa covering: (a) Kenya (3.6° S – 4.8° N, 34°E –41.7° E), (b) Uganda (1.8° S – 4.035° N, 29.5°W – 35° E) and (c) Tanzania (29° W – 41° E, 11° S – 1° S)

Figure 3.6 shows the results of the annual rainfall cycles as simulated by the dynamical downscaled HIRHAM5 with its two boundary forcings, ECHAM5 and ERAI, and observed gridded data (CRU). It is known that East Africa has two rainfall peaks during the seasons between MAM and OND which are associated with the movement of the ITCZ (Mutai & Ward 2000; Indeje et al. 2000). The results show that all the models were able to capture the main

patterns the two peaks with some differences especially in magnitude. For example, the peak of MAM rainfall season which occurred around April is well represented (Figure 3.6 (b and c)) over Uganda and Kenya. The peak of OND rainy season is significantly overestimated (<10mm/month) by ECHAM5. Furthermore, HIRHAM-ERAI simulation significantly underestimates rainfall peaks in all regions. More details of these biases will be presented in the coming analysis on the bias and correlation.

Further attempts were made to analyse the annual cycle for a smaller regions. The criteria for this selection were to have at least one observation station with quality (consistent, reliable and long term) data. In this experiment we used additional data from the field work conducted over GRR with the gridded observations data from FEWS and CRU to be able to get high spatial data for comparing with the models. The same data that was used in Figure 3.6 in addition to the merged gridded observation datasets, FEWS to represent the annual cycles of Tanzania for selected two regions of bimodal and unimodal rainfall regimes.

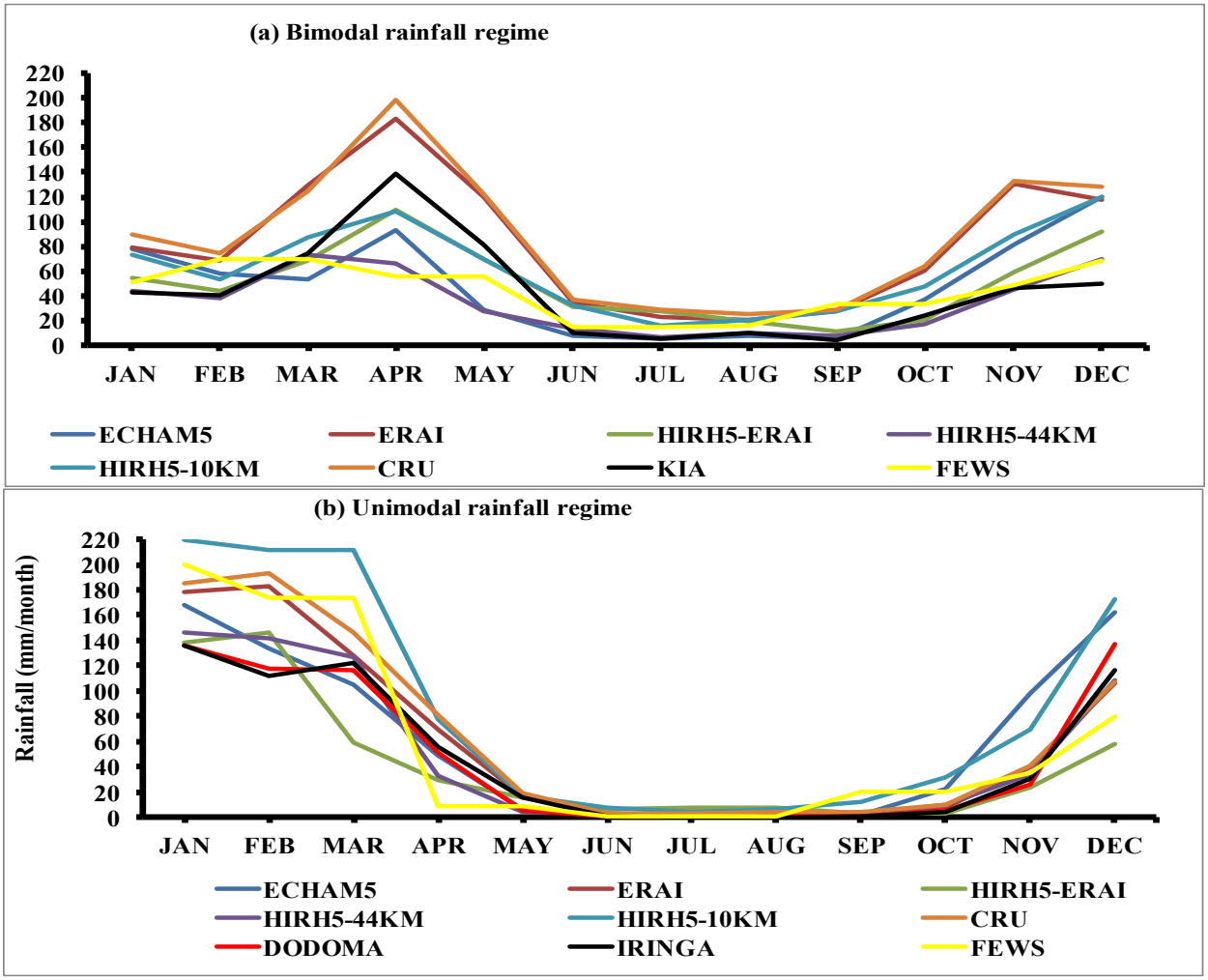

Figure 3.7: Annual cycles of rainfall (mm/month) for the selected averaged regions of Tanzania covering (a) southwestern highland in the unimodal (11° S – 7° N, 31.6°E –33.7° E) and (b) northeastern highland in the bimodal (5° S – 1.5° S, 35°E –38.5° rainfall regime in Tanzania

The results in Figure 3.7 show that, the models have good skill in reproducing the annual cycles of both rainfall regimes in Tanzania. The two peaks of rainfall during MAM and OND season are generally well captured by the models. For example, the models simulate well the long season peak (MAM) which is normally confined in April (Indeje et al. 2000). For unimodal rainfall regime, a peak occurs between November and December, of which the models are also able to capture the pattern. Despite capturing the patterns, both GCM and RCMs differ in magnitude as in the previous (Figure 3.6). For example, HIRHAM5-10km overestimates peaks in the unimodal rainfall regime (Figure 3:7b) and at the same time underestimates the peak in the

bimodal rainfall regime relative to CRU (Figure 3:7a). The observation results are also not the same; FEWS shows less rainfall than all observations especially in the bimodal rainfall regime cycles (Figure 3:7b). The same reason will apply as in the previous section that FEWS has less rainfall intensity over East Africa but with high frequency and spatial distribution. The following analysis present the summary bias and correlations of the simulated time series of rainfall cycles relative to the observed fields over the East Africa domain (Figure 3.8).

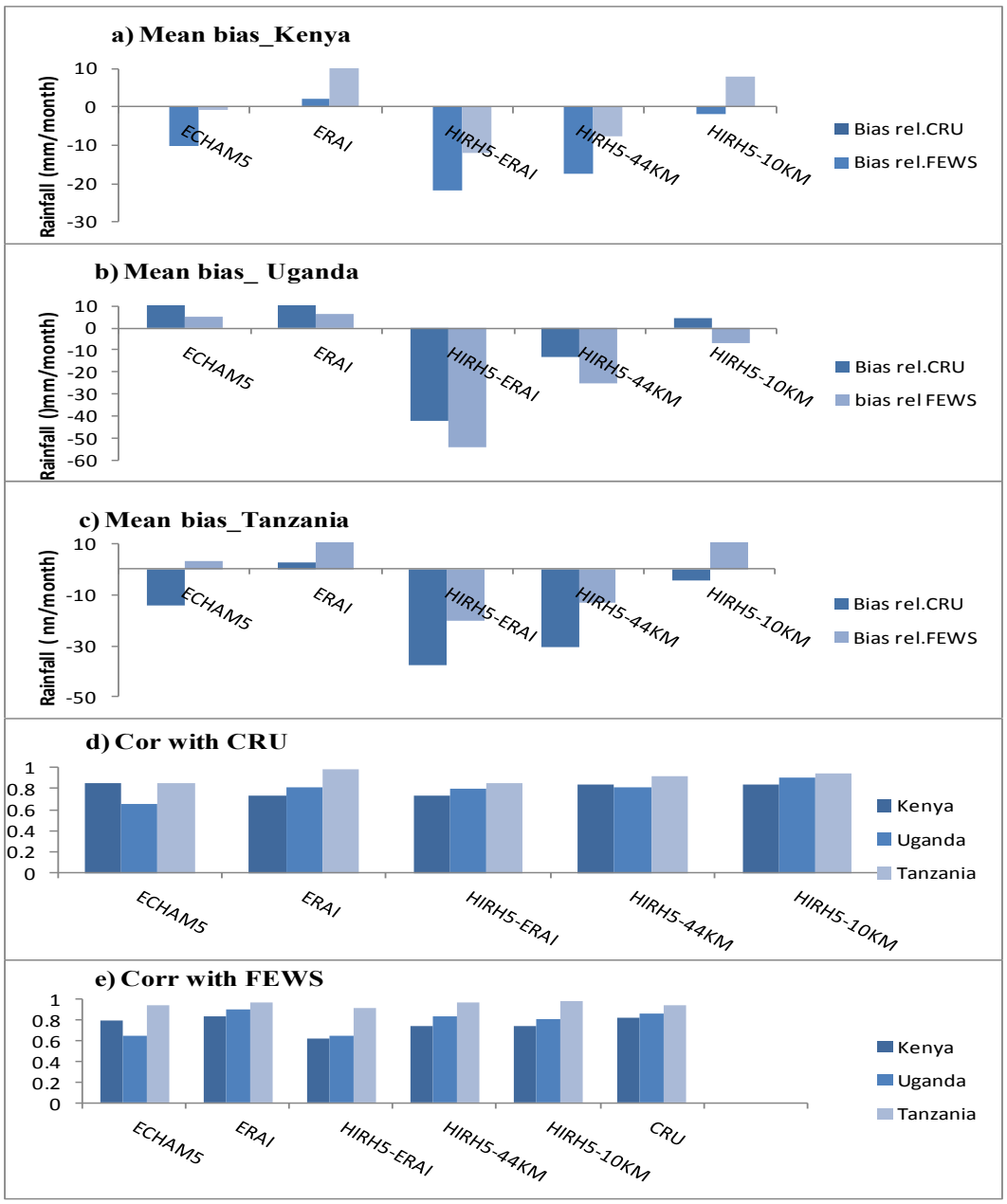

Figure 3.8: Model bias summary of the annual cycles for rainfall over the regions for (a) Kenya, (b) Uganda and (c) Tanzania as per time series in Figure (3:6), and (d, e) the correlation of rainfall cycles in each time series as simulated by the models relative to the observations (CRU and FEWS respectively).

Figure 3.8 (a, b and c) presents the summary bias of the model simulations estimated from each time series in Figure 3.6 relative to the observation datasets followed with the correlations of

each time series relative to the observations. The overall results of the mean bias show that the hindcast (HIRHAM-ERAI) and HIRHAM5-50km simulations show dry bias over all regions. The maxima dry bias is simulated by the hindcast relative to CRU (~ -57mm/month) over Uganda. The HIRHAM5-10km simulations show very smaller wet bias in comparison to the low resolutions HIRHAM5-50km. It simulates small wet bias over Kenya and Tanzania (~5mm/month).

Figure 3.8 (d, e) presents the correlation patterns of the annual cycles of rainfall. The overall results show good correlation of the model simulations with the observations datasets (CRU and FEWS). Both RCMs and their boundary forcing simulate very high positive correlation ($r \geq 0.96$) relative to CRU and FEWS. This gives confidence to proceed with the models in further analysis of the East African climate variability and change. Although, both simulations of HIRHAM5 at 50 and 10km show good skill, higher resolutions, HIRHAM5-10km show better skill in all experiments, it simulates small bias and the correlation is higher in comparison to the lower resolution.

3.2.6 Evaluation of HIRHAM5 model in simulating extreme precipitation over East Africa domain

This section examines how well increasing resolution of HIRHAM5 improves the model skill in capturing extreme rainfall events over East Africa. Two extreme values: the maximum number of consecutive dry days (CDD) and 90^{th} percentile of rainfall are presented. The extreme values are selected because of their significant impact to human life and the natural environment. A dry period is when rainfall is less than 1 mm a day. The 90th percentile of rainfall is the extreme heavy rainfall when the daily rainfall amount exceeds the 90^{th} percentiles in the calendar 5-day window for a given period (Frich et al. 2002; Zhang et al. 2011). Therefore, daily rainfall data for a 10 year period covering 1990–1999 during MAM and OND season is used. Both data sets are re-gridded to a common grid of 0.5^{o}. It is then followed by the comparison of HIRHAM-ERA simulations with FEWS and ERA-Interim followed with the calculation of their differences.

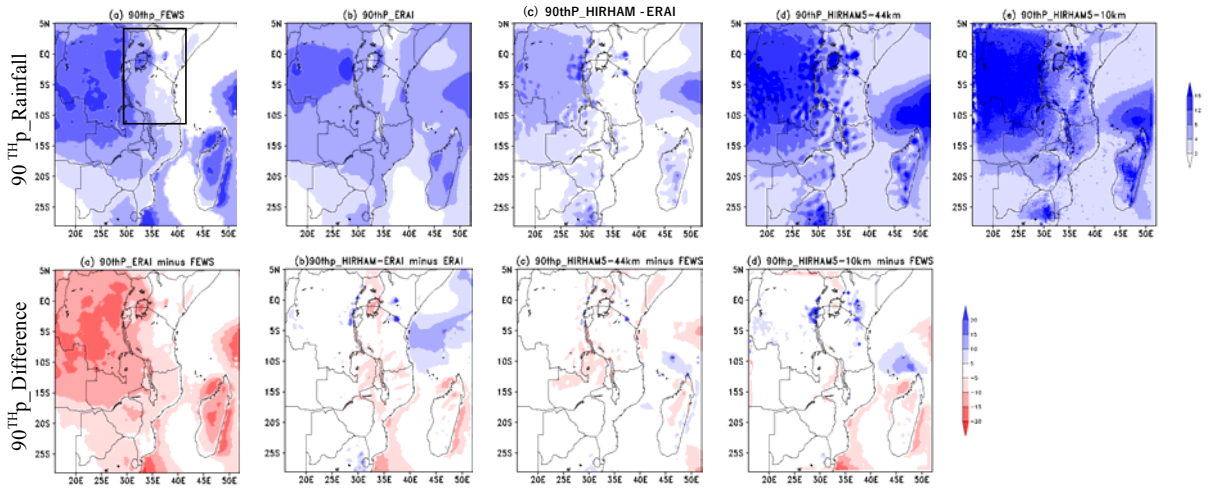

Figure 3.9: The 90th percentile of daily rainfall (mm/day) as presented by the observations from (a) FEWS, and the simulations from (b) ERA-Interim, c) HIRHAH-ERAI d) HIRHAM5-50km, e) HIRHAM5-10km (first row) and their differences from the observations in the second row for MAM (second row).

Figure 3.9 shows the 90th percentile of rainfall expressed in mm/day for HIRHAM-ERAI, FEWS and ERA Interim. The results show that the HIRHAM-ERAI simulation and ERAI presents less amount of the 90th percentile over entire region compared to the observations. In this case the error in ERAI (boundary forcing) is propagated to HIRHAM5. This can be seen easily in the Figure 3.9 (d) where the HIRHAM5-50km simulate high percentiles of rainfall (≥15 mm/day) with the same resolution as the hindcast (5≤mm/day) over Congo and the high ground. The same results are depicted in the OND rainy season (Appendix2). Both HIRHAM5-50 and HIRHAM5-10km simulates similar patterns, however with slight higher percentile in high resolutions especially over the high ground. The higher resolution also show better spatial distribution of the detailed features of the region compared to low resolution.

3.3 Seasonal temperature climatology over East Africa

This section focuses on how well HIRHAM5 reproduces the observed climatology of seasonal surface temperature over East Africa. Monthly data for CRU and ERA Interim (ERAI) fields are

used in this evaluation. A downscaled HIRHAM5 under two resolutions, 50km and 10km (forced with ECHAM5) is compared with a downscaled HIRHAM5 under boundary forcing of ERAI in simulating surface temperature climatology distribution over East Africa (as in the previous but for surface temperature). The seasonal mean climatology for all fields is presented followed by the extreme surface temperature.

3.3.1 Observed and simulated mean surface temperature climatology over East Africa

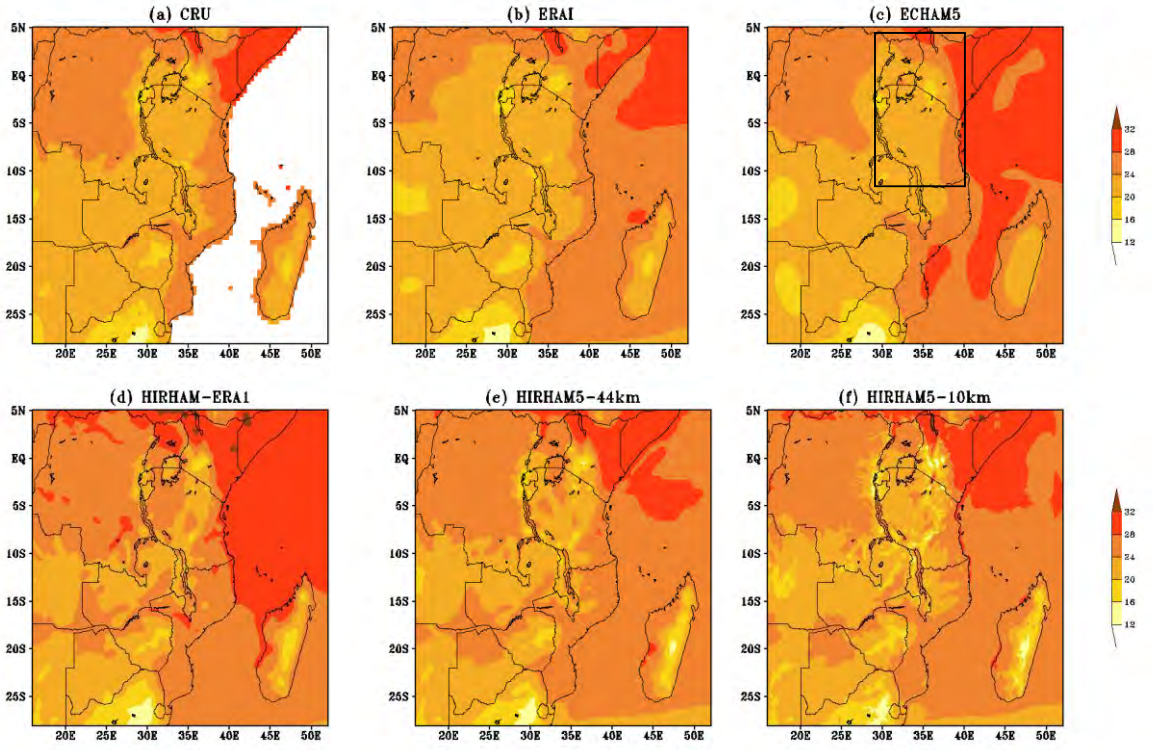

Figure 3.10: The mean surface temperature climatology (^{o}C) simulations in MAM season for (a) (a) CRU, (b) ERAI, (c) ECHAM5, (d) HIRHAM-ERAI, (e) HIRHAM5-50km and (f) HIRHAM5-10km over East Africa Domain.

Figure 3.10 presents the mean surface temperature for CRU and ERAI and the simulations of ECHAM5 and HIRHAM5 during MAM season. The CRU and ERAI fields show low temperature over the southern Kenya, Uganda and large parts of the western to southern portion

of the domain. The highest values are simulated over wetter areas, such as over the Ocean and Congo basin areas. CRU as in rainfall (previous sections) has no data over the Ocean, while the remaining patterns are similar to ERAI. Both ECHAM5 and HIRHAM5 also captured well most of the patterns in CRU and ERAI, however with slight differences. HIRHAM-ERAI is much warmer (above 30^{o} C) over the Ocean and above 27^{o} C over northern Kenya and Uganda and over the coast of Tanzania and Congo basin. Moreover, a high resolution and especially HIRHAM5 at 10km simulate low temperature (below 16^{o} C) over the high grounds of Tanzania and Kenya. This result is similar to most of the previous studies that high resolution RCMs has a cold bias over the high ground. This uncertainty could be related to the fact the observation dataset (CRU) does not have data over this area (Nikulin et al. 2011; Sylla et al. 2013).

3.3.2 Bias estimation in simulated surface temperature climatology relative to the observations

In this subsection the model bias are presented over the entire domain of East Africa instead of the study domain in order to allow more freedom for HIRHAM5 models to reproduce their own circulations within the domain. The HIRHAM5 at 50km and 10km under ECHAM5 boundary conditions and HIRHAM5 forced with ERA Interim at 50km resolution and ECHAM5 is compared with CRU data fields for both MAM rainy seasons (OND in the Appendix2).

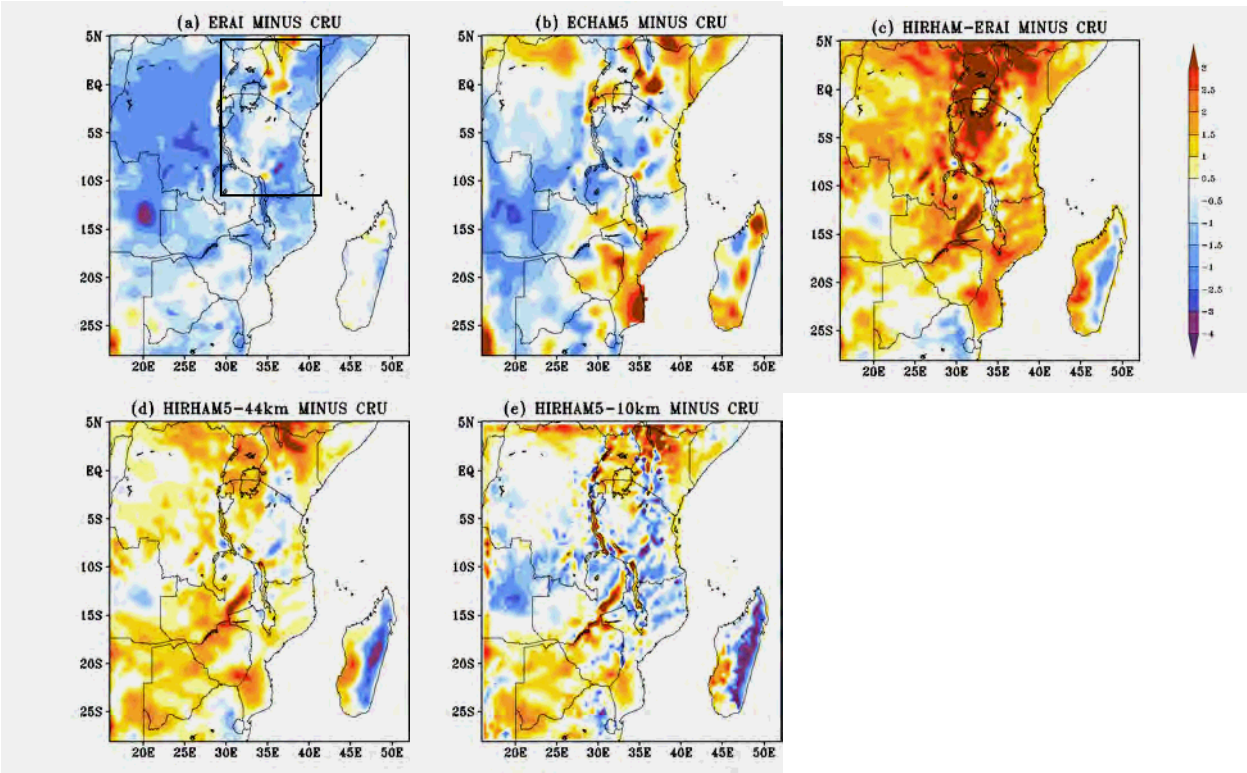

Figure 3.11: Comparison of the simulated mean surface temperature (^{o} C) climatology with the observations (CRU) in MAM rainy season from 1990-1999: (a) ERAI minus CRU; (b) ECHAM5 minus CRU; (c) HIRHAM5-ERAI minus CRU; (d) HIRHAM5-50km minus CRU; (e) HIRHAM5-10km minus CRU.

Figure 3.11 compares surface temperature bias as simulated by HIRHAM5 and the boundary forcings, ECHAM5 and ERAI relative to the observation datasets from CRU. The results show that the downscaled HIRHAM5 in both resolutions and boundary forcing simulates warm and cold bias but differ in magnitude. The high resolution simulates cold bias increase over the high ground in comparison to low resolution. The ERAI presents cold bias over large part of the domain, while the hindcast simulates warmer bias spread over large part of the domain. For example, it was expected that the warm bias (up to 2.5^{o} C) in HIRHAM-ERAI simulation was propagated from the boundary forcing, however the ERAI (Figure 3.12a) presents cold bias over almost the entire domain. There could be several reasons as to why both resolutions show biases. One general reason could be insufficient observation data over the region.

The second reason could be the model error, when these fields are compared even with the same resolution still there are some big gaps. For example, HIRHAM-ERAI show different field from its boundary forcing (Figure 3.12 (a, d)). The ERAI hindcast is warmer than the ECHAM5 hindcast, which show the boundary condition factor. On the other hand, the lower resolution RCM simulates much warmer ($\leq 1.5^{o}$ C) in comparison to the high resolution (~ -1 to -2^{o} C) model. This results show that the warming depends on the resolution likewise in the previous (Section 3.1) wetness also depends on the resolution. This results agrees with the previous studies that the high resolution RCM is able to capture the spatial patterns and the observed mesoscale signals and also reproduces the signals associated with orography (Hudson & Jones 2002). The large warm bias over Uganda (around Lake Victoria) could be related to the topographical features such as the Great Rift Valley and the lake effects (Lake Victoria, Edward and Eldoret) where CRU has no data. Therefore these biases could be associated with lack of observations and probably with the model error itself.

As mentioned earlier, that, the model's discrepancies could be associated with various factors. However, the HIRHAM5 model simulates warm bias ~ $\pm 1.5^{o}$ C, this bias agrees with most studies on using RCMs including some of the CORDEX data (Jacob et al. 2012; IPCC AR5) Some studies have also shown that the common assumption of bias cancellation (invariance) in climate change projections can have significant limitations when temperatures in the warmest months exceed 4–6 °C above present day conditions (Christensen et al. 2008).

3.3.3 Correlation of simulated surface temperature relative to CRU

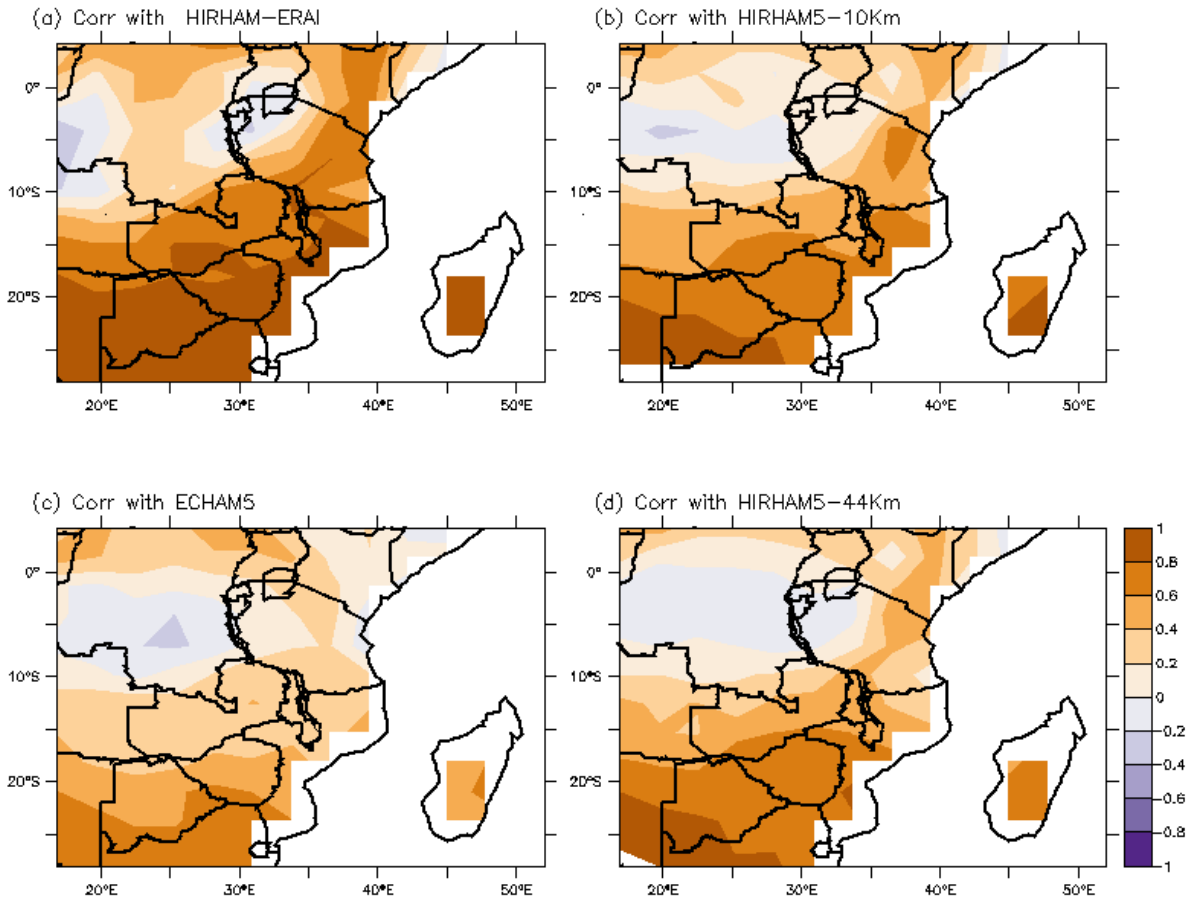

Figure 3:12 Correlation pattern analysis of mean surface temperature as simulated by models (HIRHAM5 and ECHAM5) versus CRU during wet season.

Figure 3.12 shows correlation pattern of mean surface temperature over East Africa domain as simulated by the downscaled HIRHAM5 at 50 and 10km resolution under ECHAM5 forcing and the hindcast (HIRHAM-ERA) in MAM season (OND is presented in the Appendix 2). The results depict previous (Figure 3.11). The model simulations show poor to moderate correlation (r= -0.2 t0 0.6) in simulating mean surface temperature relative to CRU dataset, especially over the western and northern portion of the domain: the Congo basin and the Lake Victoria and Great Rift Valley regions. All models (GCM and RCMs) simulate the weakest positive correlation (~r

±0.3) over these regions. This agrees with the previous analysis on the model bias that the models simulations have poor agreement with CRU due to major reasons that associated with the density of observation data over these regions. It is believed that the model is doing good job as with the case of rainfall it performed much better in comparison with temperature.

3.3.4 Annual cycles for surface temperature in East Africa

This subsection presents the evaluation of HIRHAM5 in the simulation of annual surface temperature cycles over the selected three regions of East Africa: Kenya (34^{o}–41.7^{o} E and 3.6^{o} S–4.8^{o} N), Uganda (29^{o} E–35^{o} E) and Tanzania (29.5^{o} E–41^{o} E and 11^{o} S–1^{o} S) respectively. The data spans 1990 to 1999 to cover the present day climate product that is available for this study.

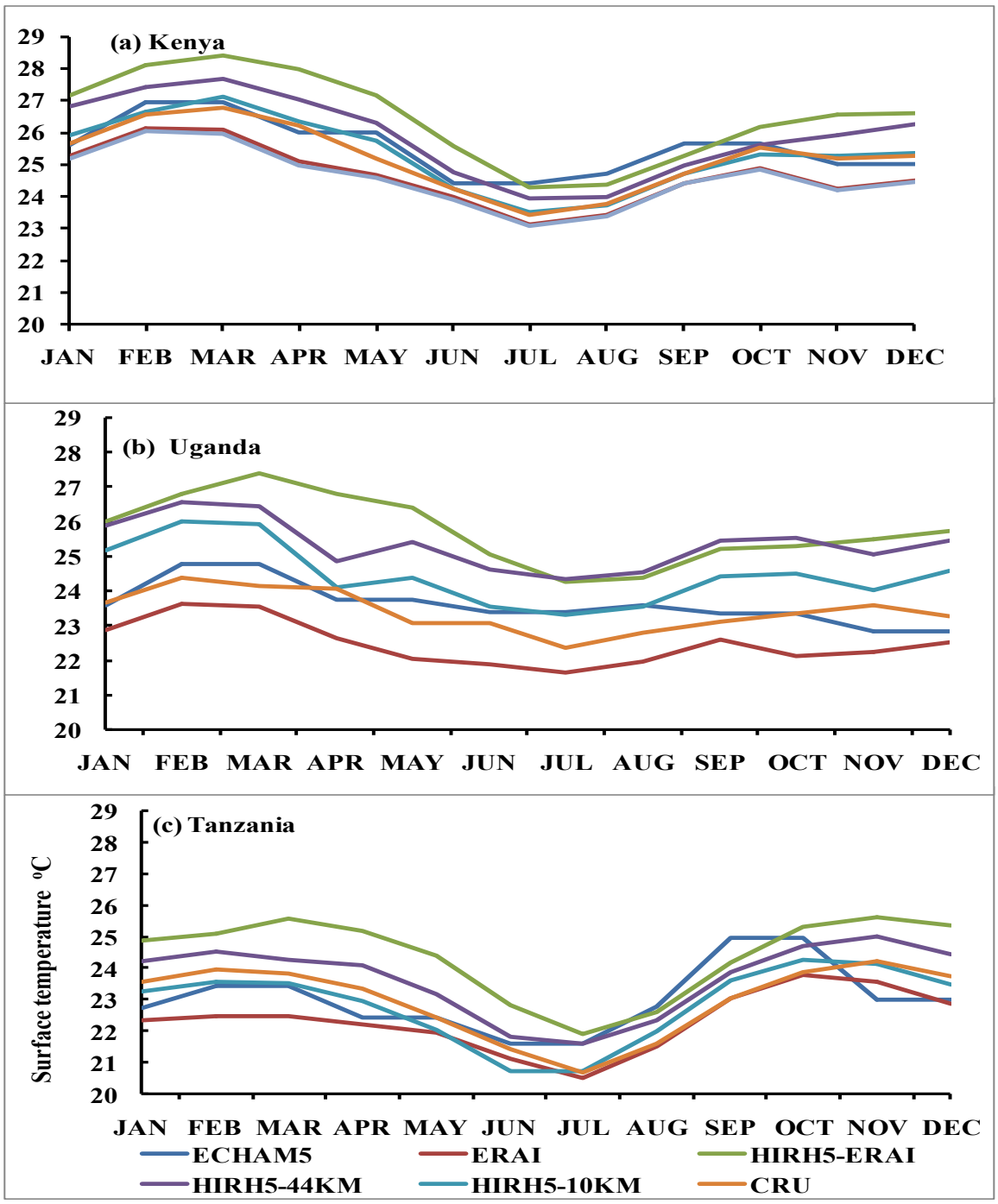

Figure 3:13: The annual cycles of the surface temperature (^{o} C) for observation datasets from CRU and reanalysis data from ERA-Interim and simulations from ECHAM5 and downscaled HIRHAM5 for (a) Kenya (3.6^{o} S – 4.8^{o} N, 34^{o}E –41.7^{o} E), (b) Uganda (1.8^{o} S – 4.035^{o} N, 29.5^{o}W – 35^{o} E) and (c) Tanzania (29^{o} W – 41^{o} E, -11^{o} S – 1^{o} S)

Figure 3.13 shows the annual cycles of surface temperature climatology as simulated by the models (HIRHAM5 and ECHAM5), ERAI and observation dataset from CRU. The results show that the models tolerably simulate the surface temperature cycles over East Africa over the selected regions (Kenya, Uganda and Tanzania). For example, the important phase cycle of MAM and OND double peak which normally occur between April and November respectively is well captured; furthermore, in June to August (JJA) when the surface temperature are minimum is also well captured. All models simulate minima around JJA as the observations and ERAI, however, with some discrepancy which is associated with location (topography) and the model backgrounds. Over all regions the minima temperature is around 19^{o} C while a maximum is ~29^{o} C.

However, the HIRHAM5-50km and especially the hindcast simulations overestimate the peaks of temperature in all regions. This was also shown in the previous analysis (Figure 3.13) that HIRHAM-ERAI overestimate surface temperature patterns and this is also true in the mean bias estimation. Overall the results of the HIRHAM5 simulations show an average skill.

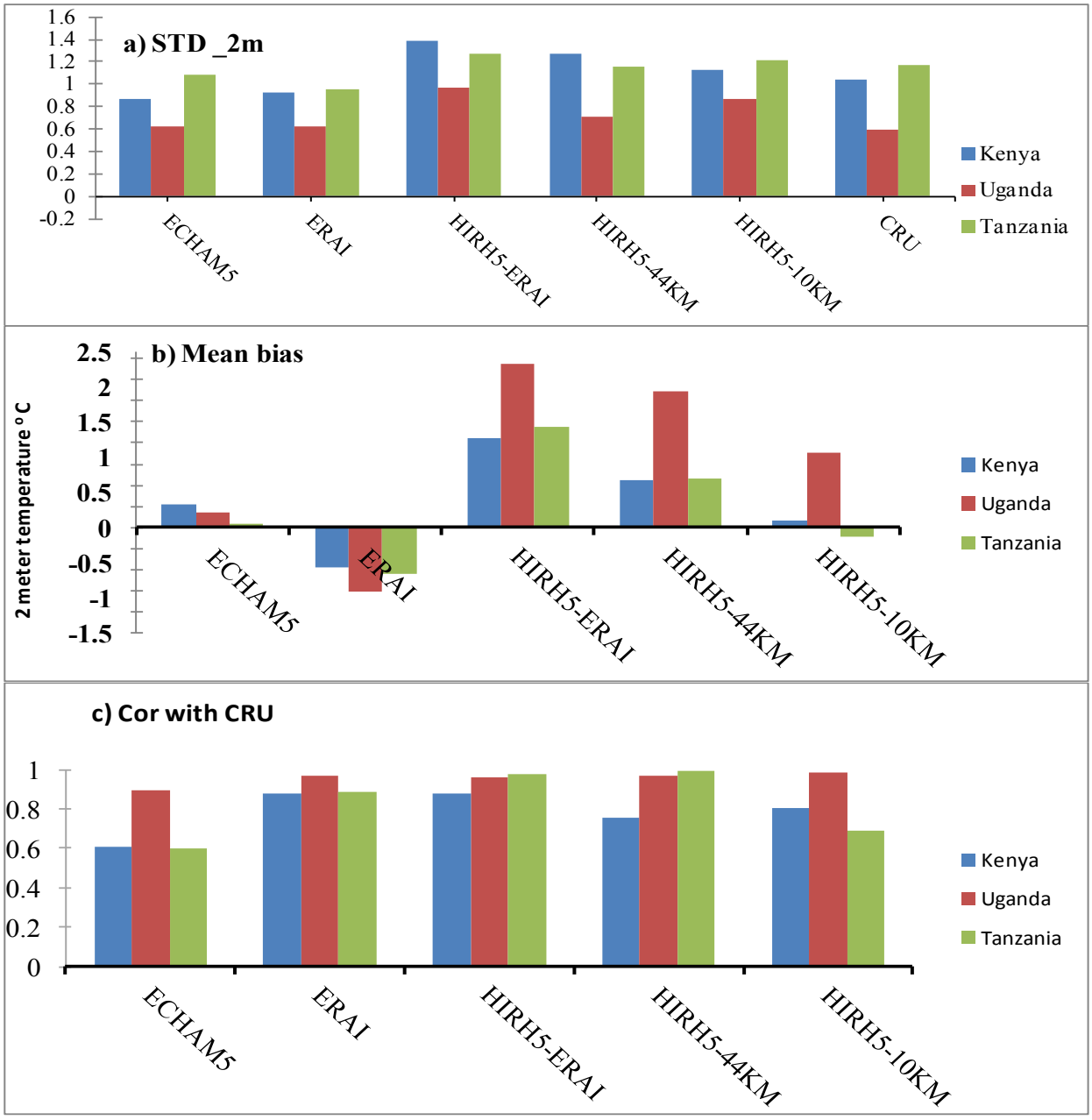

Figure 3.14: a) The standard deviation (STD) of 2 m temperature, (b) mean bias estimation of 2 meter temperature (^{o} C) and c) correlation of 2 m temperature as simulated by the models relative to CRU. The averaged area referred to Figure 3.14).

The overall results of the simulated standard deviation, mean bias and correlation relative to CRU dataset show that all model simulations are within the range of observation, however with small differences (Figure 3.14(a)). The maxima standard deviation is simulated by HIRHAM-ERAI (1.4^{o} C) while at the same time and the same region CRU show STD of 1.04^{o} C. On the

other hand the minima STD are simulated over Uganda by ECHAM5 (~0.6^{o} C) of which CRU has STD of 0.56^{o} C over the same region.

Furthermore, the results of mean bias (Figure 3.14b) show that the maxima warm bias are simulated in HIRHAM-ERAI (2.4^{o} C) over Uganda. Over all three HIRHAM5 products, the lowest bias is simulated in the highest resolution, HIRHAM5-10km. In Figure (3.14c), the model simulations of 2 meter temperature correlation with CRU show high correlation (above 0.96) over all regions and across the models. The highest correlation is simulated in HIRHAM5-10km (0.99). In summary the results show that HIRHAM5 simulations demonstrate reasonable skill in reproduction of the observed mean climatological and annual cycles of surface temperature over the East Africa domain.

3.3.5 HIRHAM5 evaluation in simulating extreme hot day and night

This subsection compares the extreme hot days and nights, expressed in the 90th percentiles of maximum and minimum temperature respectively. Warm nights and days are defined as the percentage of times in the year when minimum/maximum temperature is above the 90th percentile of the climatological distribution for that calendar day. When conducting this experiment daily maximum and minimum data for CRU were not available. Therefore, daily maximum and minimum surface temperature data from the simulation of the downscaled HIRHAM5 are compared with ERA Interim for MAM and OND season. For standard comparison the analysis is restricted to the hindcast and ERAI datasets.

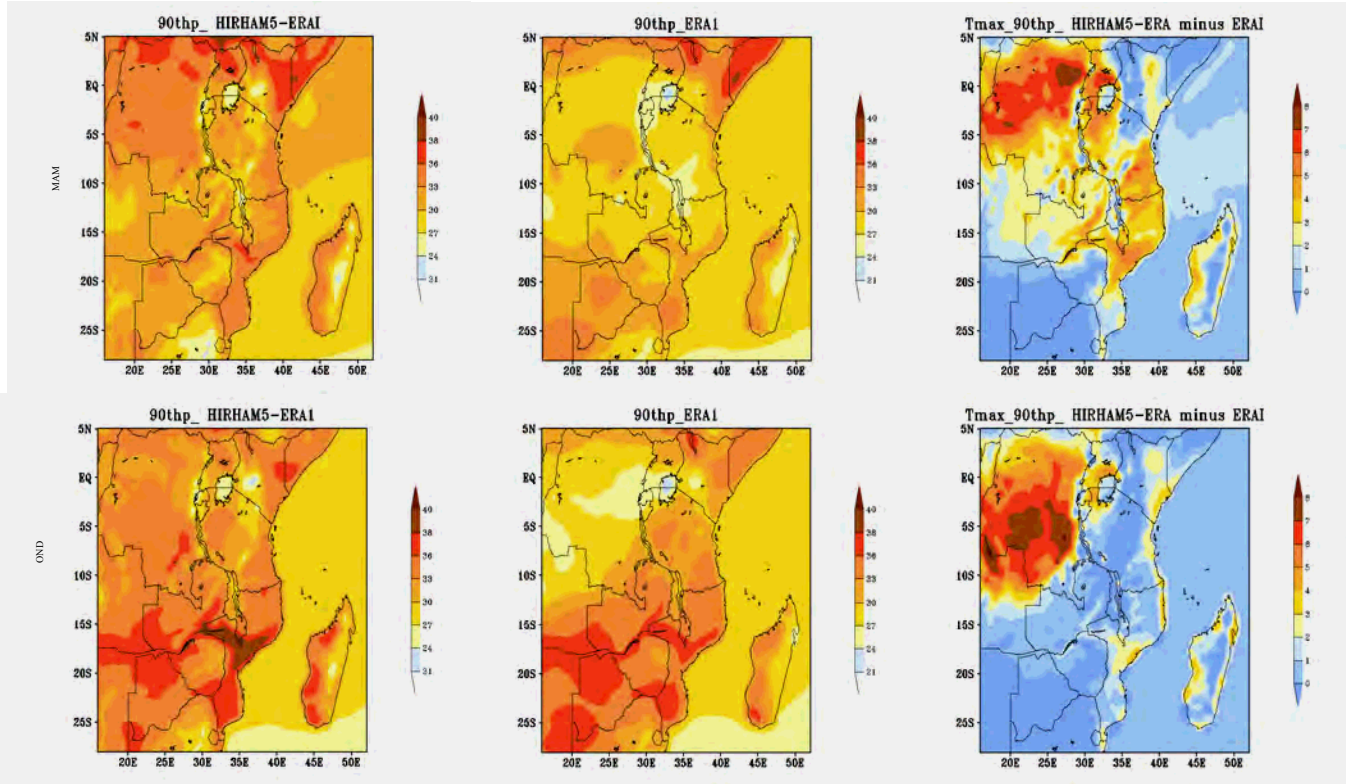

Figure 3:15: The 90th percentiles of maximum surface temperature (° C) as simulated by the downscaled HIRHAM5 under the boundary forcing of ERAI (first column) in comparison to ERAI (second column) and their differences (third column) for MAM (first row) and OND (second row).

Figure 3.15 shows the comparison of the extreme hot days expressed in the 90th percentile of surface maximum temperature as simulated by HIRHAM-ERAI with reference to ERAI. The data used spans 1990 to 2007. The results show that the model captures well some of the observed patterns (in ERAI) especially in the northern Kenya and Uganda, southern Tanzania and extreme southern portion of the domain (Zambia, Angola), however with some differences. Both fields of ERAI and HIRHAM-ERAI show less temperature in MAM than OND rainy seasons, showing some good agreement. It is noted that MAM is a long rainy season and when it is raining the temperatures are somehow cool. On the other hand the OND is a short rainy season with strong variability and even the ENSO events have great impact over this season this season (Indeje et al. 2000; Camberlin et al. 2001;Kijazi & Reason,2011; Wolff et al. 2011). The

maxima hot days (36^{o} C) are confined in the northern and southern portions of the domain in both ERAI and HIRHAM-ERAI (Figure 3.18, first and second column). The minima (~24^{o} C) is simulated in the southwestern highlands, northeastern highlands of Tanzania and the highlands of Kenya and Uganda, and further to the Congo basin area. The warm bias in HIRHAM-ERAI simulations (Figure 3.12c) also occur in the simulation of the extreme hot conditions. Despite it capturing well some of the patterns of extreme hot days, HIRHAM-ERAI overestimated the extreme hot days (above 7^{o} C) in the western Congo basin (Figure 3.18 (third column)) and more than 1–4^{o} C in MAM and 1–2^{o} C in OND season. It is also noted that HIRHAM-ERAI simulates large bias in MAM than in OND season. This could be related to the fact that, a MAM season is a long rainy season and so there is much moisture over the region and so the more the land is moist the warmer the atmosphere. Therefore, probably a model is configured to capture some of these features in this season and have high spatial data compares to the reference data. In other way ERAI is cooler in MAM than OND, therefore, that is why the differences is large from MAM compared to OND. Note that, in Chapter 2, the results of the field work have also shown the inadequate of observation stations and quality and reliable data. It is noted that in Africa and especially East Africa the observation data are sparsely distributed over the region. Even the available data is hard to get in digitised format (as most of the data are still in hard copy) and in good quality. Therefore, additional to the boundary forcing of the model/systematic error the warm bias which is highly confined over Congo basin is probably linked to lack of the observations as this region is a remote where there is dense forest and hence lack observation stations (Nogherotto et al. 2013). Additional reason could be related to the model error formulation, because if ERAI is a boundary forcing we expected the difference to be minor.

3.3.6 A potential for added value in HIRHAM5 Model simulations of rainfall and temperature climatology

A potential for added value is the measure of the extent to which the downscaled climate is closer to the observations than the model from which the boundary conditions were obtained (Flato et al. 2013). The added value of RCMs is expected to be in the representation of the detailed topography and extreme climatic condition associated with local features such as

topography and natural climate variability (Feser et al. 2011). The data used are downscaled HIRHAM5, which is to be evaluated relative to GCM (ECHAM5) and observation data set for CRU. HIRHAM5 model used is in three different datasets: HIRHAM5 at ~50km resolution under boundary forcing of ERAI and ECHAM5 at 50km resolution. Monthly rainfall and surface temperature data for 10 years, 1990 to 1999 were used. The idea of the potential for added value (PAV)is described in Di Luca et al. (2012). According to Di Luca et al. (2012; 2013), the added value (β), which is a measure of difference between GCM and RCM bias, is computed as follows:

$$\beta = (GCM' - OBS')^2 - (RCM' - OBS')^2 \quad \text{.....(2)}$$

Whereas, GCM' and RCM' corresponds to the mean bias estimated in ECHAM5, and HIRHAM5 relative to the observation (CRU) respectively.

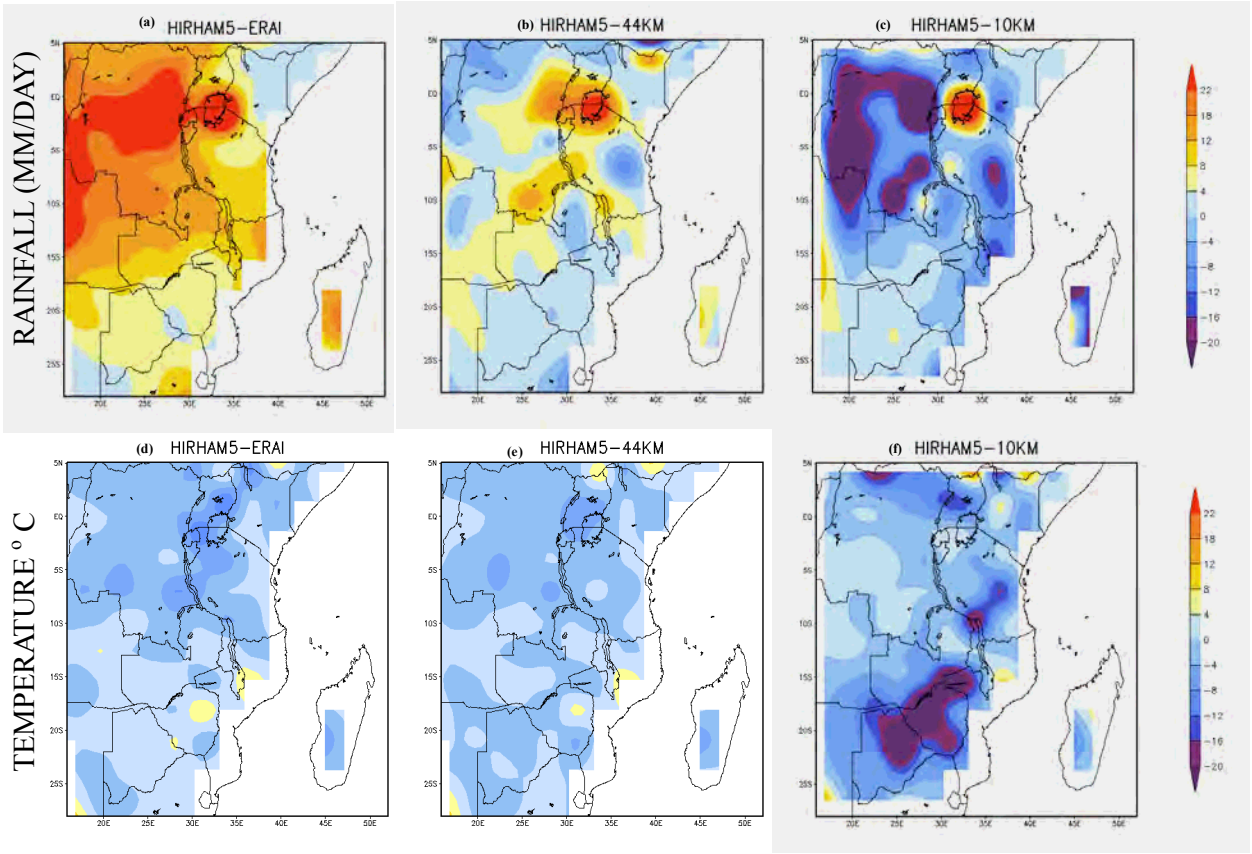

Figure 3:16: Mean climatology for rainfall in mm/day (first row) and temperature (°C) (second row) representing a potential for added value.

Figure 3.16 presents a potential for added value of rainfall and temperature climatology. The results show that HIRHAM forced with ERAI (HIRHAM-ERAI) shows some skill in simulating rainfall and temperature climatology followed with HIRHAM5-50km. The best skill occurs in rainfall climatology simulations. However, surface temperatures (Figure 3.16 in the second row) are poorly presented in both resolutions ($\beta < 0$), higher resolution (HIRHAM-10km) show poor skill in both rainfall and surface temperature simulations especially over high grounds. This was also pragmatic in the previous analysis that (Figure (3.1-3.8) and (3.10–3.14)) high resolutions (HIRHAM-10km) overestimates rainfall and underestimates temperature over high grounds. Nevertheless, high resolution RCMs simulate details of the topography, the added value here is less than 0 ($\beta < 0$), and more significant over the high grounds. This shows that HIRHAM-10km and HIRHAM-50km have shortcomings in simulating rainfall and temperature over East Africa. This could be related to some of the reasons already mentioned above. This result affirms the so called inadequate observation datasets over the region. This could be true because, both HIRHAM5 at 10 and 50km resolutions show negative values over the high ground. As already been said CRU has no data over the high ground and the spatial distribution of CRU over Africa land is poor (Nikulin et al. 2012). Therefore here the resolution factor is not well defined as the results show negative bias. However, there are some good results in HIRHAM-ERAI followed with HIRHAM5-50km. The large error in HIRHAM5-50km and HIRHAM5-10km is linked to the boundary forcing.

3.4 HIRHAM5 simulations of the surface winds at 700hPa

This section explores how well HIRHAM5 reproduces the current atmospheric circulations, based on winds at 700hPa (and 850hPa in the Appendix 2) and mean sea level pressure. Previous studies have shown that rainfall variability in East Africa is governed by the circulation patterns such as air streams and the ITCZ (Nicholson 1996). During wet seasons (OND and MAM), East Africa is dominated by weak easterly to south-easterly winds (Mapande & Reason 2005). These winds fetch moisture from the Indian Ocean and deposit it on the mainland of East Africa. On the other hand, during dry season (JJA) the ITCZ shifts north of the Equator in the

northern hemisphere, at this time of year most parts of East Africa experience dry and cool air blown by winds which are continental, and are originating from the southern hemisphere. The following figure will present wind patterns at 700 hPa which will help understand more of the circulation patterns.

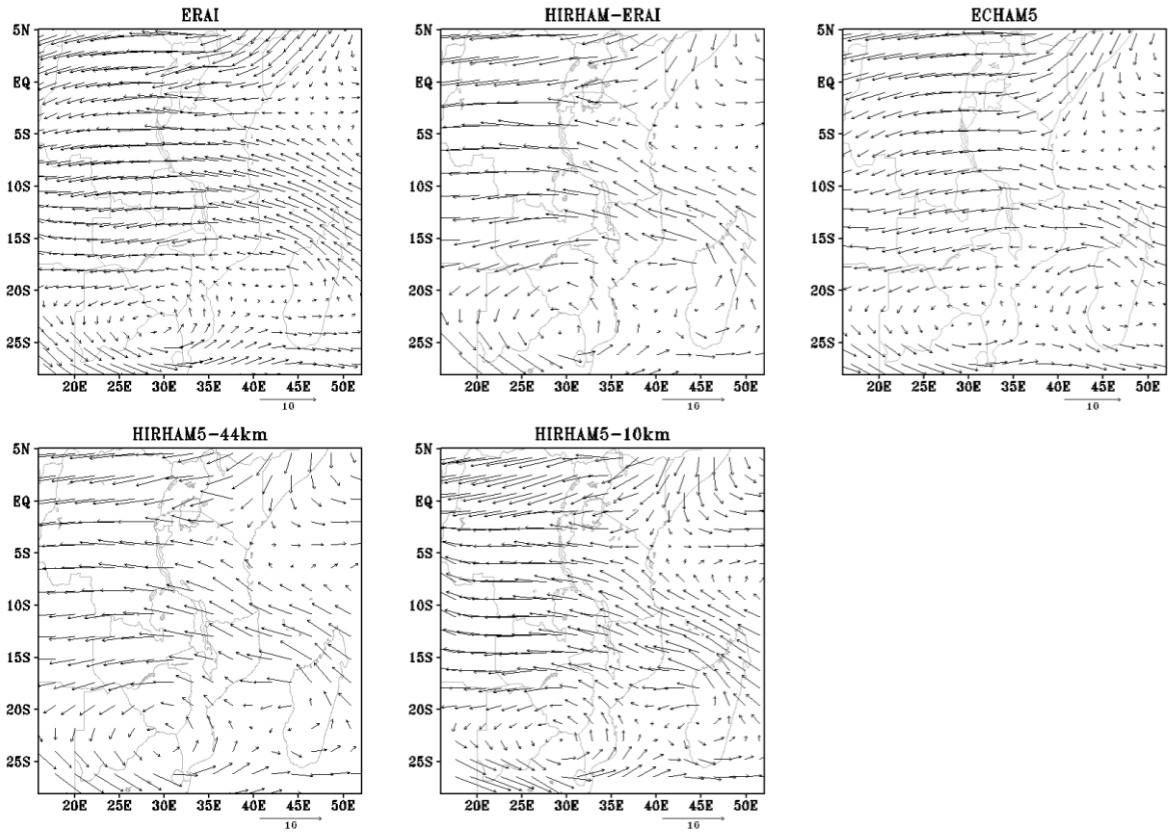

Figure 3.17: Climatology of winds flow at 700hPa in MAM season as presented by the ERAI (upper left panel), downscaled HIRHAM-ERAI (upper mid panel), ECHAM5 (upper right panel), HIRHAM5-50km (lower left panel) and HIRHAM5-10km (lower right panel). The arrows present wind vector (m/s)

Figure 3.17 shows the wind flow as presented by the downscaled HIRHAM5 at 50 and at 10km under ECHAM5 forcing and at 50km under ERAI forcing with the reanalysis from ERAI and the boundary forcing ECHAM5 data. The results show that the downscaled HIRHAM5 and its hindcast models under different resolutions capture well the wind patterns during the MAM season with some slight differences. The area of convergence in the western side of the domain (Congo basin area) and South Indian Ocean (SIO) are well captured by the models. The hindcast in the first panel (left column) in comparison to ERAI shows better skill, however the winds are stronger than ERAI. Moreover, the onshore winds (off–coast of Tanzania) which eject moisture from the Indian Ocean are also well captured. The HIRHAM5-50km and HIRHAM5-10km also

capture well the patterns (Figure 3.17, second row); however, with some differences. The winds are stronger over the western part of Kenya around the Great Rift Valley in HIRHAM–ERAI and HIRHAM-50km in comparison to HIRHAM5-10km and observation (ERAI). These patterns are also observed at 850hPa level winds (Appedix2). Generally, the patterns are similar but with increasing resolution the strength of the winds decreases. This explains the large dry/warm bias in rainfall simulations by HIRHAM-ERAI and HIRHAM5 simulations 50km over 10km in comparison to the observations and ERAI in the previous sections.

HIRHAM-ERAI simulation shows large dry bias (rainfall ~ -5–-6mm/day) over the entire regions (study domain). This could be linked with the winds simulations increase in strength(Figure 3.17, upper right panel) over entire domain which shows an indicator of rainfall deficit due to lack of moisture in the model (as the moisture is drawn away from region by the strong winds). The 10km resolution shows good agreement in comparison to ERAI as it captured even with the fine features, for example, the weak convergence areas in both areas (Congo and Indian Ocean) are well captured. The good news is that even the circulations over the high ground are as well captured (Figure 3.17, lower right panel). For example, the patterns around the Great Rift Valley northwest Kenya are well presented as in ERAI (also at 850hPa in Appendix 2). In the low resolution these pattern are not visible. The same results of MAM season are depicted in OND season below.

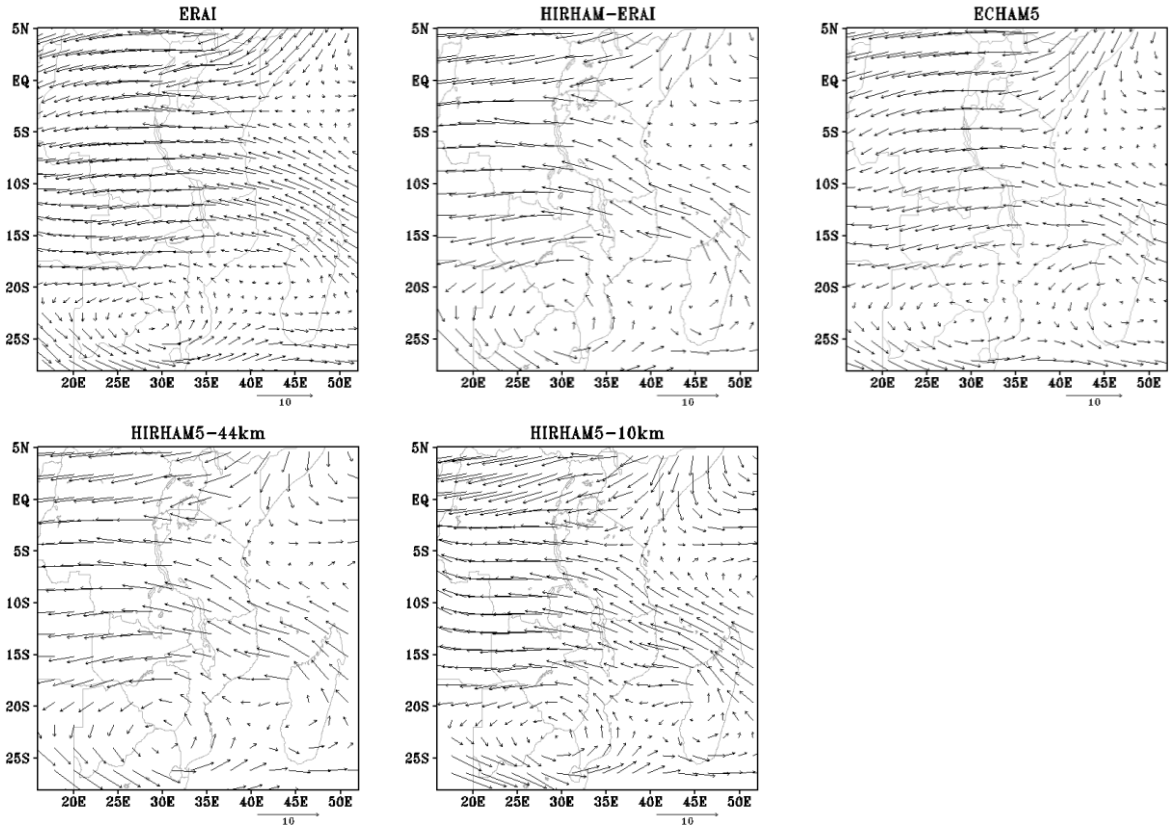

Figure 3.18: repeat the same as in the Figure 3.17 but for OND

Figure 3:18 compares HIRHAM5 simulations of wind patterns during OND season with ERA-Interim. The results show that the model is working well as it captured the wind patterns over most regions in the domain. In East Africa, this time of season is dominated by easterly winds and in the western side there is a convergence zone which normally originates from the meridional arm of the ITCZ. Therefore, larger parts of East Africa are dominated by the convergence flow: the winds are weaker, showing that there is a lot of moisture over the region (carried from the western side, Congo basin forest and Indian Ocean). Relevant areas of strong convergence can be seen especially over Congo basin, Indian Ocean (close to Tanzania and Kenya coast) and over the Mozambique Channel. Another interesting feature occurs over the Indian Ocean where winds are almost easterly (strong easterly waves) which allows penetration of moisture over Tanzania (Mapande & Reason 2005). HIRHAM5 in both resolutions and under boundaries of ERAI and ECHAM5 demonstrates good skill over all areas of the domain. On the

other side, a strong convergence zone can be seen over Congo forest basin (most of the area of the western domain) where the western regions of Tanzania and Uganda benefit from moisture influx from the Atlantic Ocean.

Overall results for both coarse and high resolution HIRHAM5 show better skill as they simulate the natural climatological feature of wind patterns at this specific season. HIRHHAM-ERAI show strong winds over the mainland of Tanzania and Kenya and which dictates the reason as why these areas have less rainfall than all other models. The coarse resolution overestimates wind strength compared to higher resolution (is depicted from previous Figure 3.17). This is observed in all seasons especially in the areas around northern Tanzania and southern Kenya and Uganda.

3.4.1 Model representation of mean sea level pressure

This subsection presents model representation of the circulation patterns of mean sea level pressure over the large domain of Africa. This thesis covers the domain of East Africa (Figure 2.1), however in this subsection a large domain of Africa is presented in order to see the general circulation pattern and the high pressure centers that contribute to the circulation patterns and climate variability over East Africa. As discussed in chapter 2, that there are two high pressure centers in the southern hemisphere (Mascarene and St. Helena Highs) which play a major role in East Africa rainfall variability. Therefore, it is important to present the model's ability in simulating this feature.

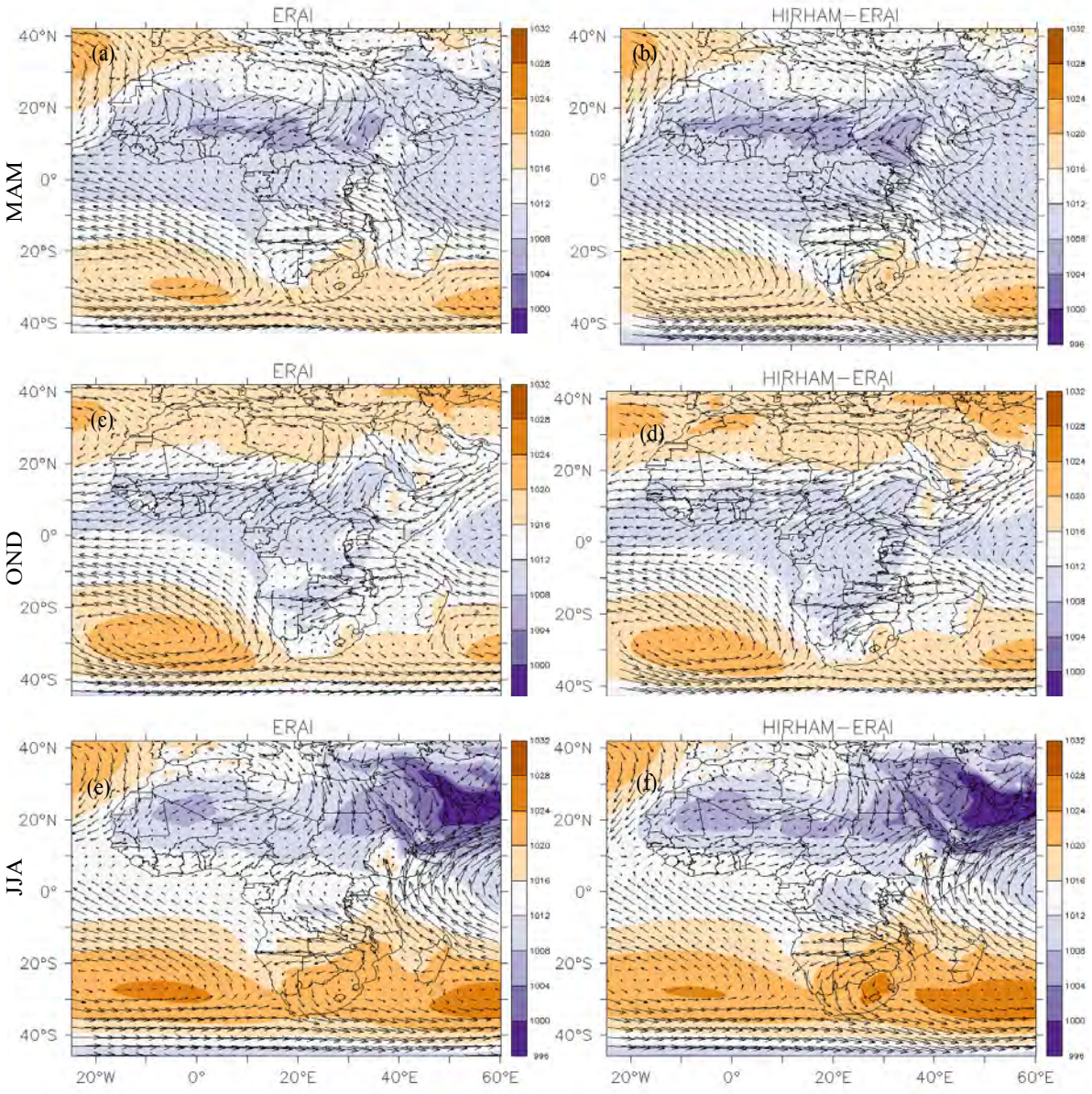

Figure 3.19: Comparison of HIRHAM-ERA (first column) with the reanalysis data from ERAI (second column) in the simulation of mean sea level pressure (shaded) with winds (m/s) at 850hPa level for MAM (first row), OND (second row) and JJA (third row). The arrows in each panel indicate winds strength (m/s); the lengths of the arrows indicate the wind strength at 850hPa level

Figure 3.19 presents the synoptic patterns taken over the large domain of Africa. The results show that HIRHAM-ERAI adequately simulates the synoptic features over the region for all seasons. The position of the pressure centers are well represented, although with some differences. The East Africa climate is influenced by two major anticyclones centres Arabian and Mascarene high pressure cells. Previous studies have shown the importance of these high pressure centers (Ogallo, 1989, 1994; Monatsa et al; 2013). The location of high pressure centers in the southern hemisphere, Mascarene and St. Helena high, are well represented. The low pressure belts located in around the equator between both hemispheres are well represented by the models however with some differences.

However, the HIRHAM-ERAI as presented in the previous section (Section 3.4) shows some discrepancies in wind strength. The HIRHAM-ERAI simulates stronger winds in both seasons in comparison to ERAI (Figure 3.19(left column)). Furthermore, the position of the subtropical highs in the southern Atlantic Ocean has shifted (weakened) southward which gives room for more southerly flow towards East Africa mainland. This could be connected to the increased continental southerly/south–easterly winds flow which carries less/no moisture to the East Africa mainland. In the contrary the ERAI show good south–easterly to easterly flow which advect maritime moisture to the mainland. It is therefore concluded that, the circulation patterns play a major reason for the increase/decrease of rainfall and temperature in the region.

Most of the previous studies have shown that that the anomalous easterly/westerly flow have great impact to rainfall variability in East Africa (Kiajzi & Reason 2012; Manatsa et al. 2014). For example, Kijazi & Reason (2012) found that during the rainy season the large part of Tanzania is covered by easterly moisture flux from the Indian Ocean and strong southeasterly moisture flux at the peak of rainfall season. On the other hand, recently Manatsa et al. (2014) found that when the Mascarene high is anomalously displaced to the west (east) of its normal position, the south east (SE) trade winds over the South Indian Ocean (SIO) anomalously strengthen (weaken). This enhances (reduces) the relatively cool and dry SE trade winds and induces cold (warm) sea surface temperature anomaly in the SIO. As a result, convection over the western equatorial SIO is suppressed (enhanced) and leads to rainfall deficits (excess) over East Africa.

3.5 Summary and discussion

This chapter presents the evaluation of HIRHAM5 simulations of rainfall, temperature and surface winds at 850hPa over East Africa. Additionally, the evaluation of HIRHAM5 in the simulation of the extremes of both rainfall and surface temperature were also presented. The observed and model datasets were used to study the seasonal climatology patterns and extreme climatic conditions over East Africa. The overall results show that HIRHAM5 demonstrates good skill in simulating both the climatology and extreme climatic conditions of East Africa. The model shows an acceptable performance in simulating the spatial and temporal distribution of the main precipitation and temperature features, with some variation in the resolution and the boundary forcings. HIRHAM-ERAI underestimated rainfall in all seasons; however, it simulated wet bias over the high grounds in some cases. The HIRHAM-ERAI also showed a discrepancy with its boundary forcing ERAI and HIRHAM5-50km at the same resolution. For example, the results of the bias estimation relative to high resolution observation dataset (FEWS) showed an increase in dry bias spread over the entire domain, which is different from ERAI and HIRHAM5 under ECHAM5 simulations. The later simulations showed a decrease in bias in high resolution observation datasets (FEWS, in this case).

It is also found that HIRHAM5 under ECHAM5 forcing, the same model but using a different resolution, showed similar patterns with slight differences in magnitude. The bias is significantly reduced in the high resolution HIRHAM5-10km. The correlation with the observations is also at its maximum in high resolution compared to the low resolution.

Despite its good performance, HIRHAM5's mismatch with observations in different resolutions and with the boundary forcing could be related to two main reasons. Firstly, it could be linked to the boundary forcing. It was found that HIRHAM5-50km and HIRHAM-ERAI simulations show large departures from one another although they are the same model and have the same resolution. In this case the differences could be the boundary forcing. It is noted in most of the recent studies that the great uncertainty of the RCM is connected to the boundary forcing (Rummukainen 2010; Kim et al. 2013). The second reason could be the effect of resolution and the convection scheme deficiency in the model, which hinders the low resolution in reproducing

details of local features. For example, in the simulations of wind patterns at 850hPa level (Appendix 2) over the Great Rift Valley (west of Kenya), the higher resolutions managed to capture the patterns while the lower resolutions failed (Figure 3.17). Studies have shown that higher resolution regional RCMs are capable of resolving details of the local/regional features associated with rainfall such as orographic rainfall over the steep topography and other local features compared to the coarse resolutions (Dankers et al. 2007; Kendon et al. 2012).

Chapter 4

Evaluation of HIRHAM5 simulations of the Annual variability of seasonal rainfall and temperature over East Africa

This chapter presents the results of the investigation of HIRHAM5 model's ability in reproducing the natural variability of seasonal rainfall and temperature. The reference dataset is the observation dataset from CRU as it has both rainfall and temperature (compared to FEWS which has only rainfall data) and it includes almost the full simulation period of HIRHAM-ERAI. Nevertheless, FEWS and ERAI datasets are also going to be used for more details and understanding in the further analysis. The second section of this chapter will present the composites of ENSO years relative to rainfall as simulated by HIRHAM-ERAI with reference to CRU and ERA Interim. Furthermore, a model representation of ENSO signals is investigated by means of a Multivariate ENSO Index (MEI) as a substitute of El Niño and La Niña years. The end of this chapter will provide further detail of the strength and weakness of HIRHAM5 in simulating East Africa's natural climate variability.

4.1 Annualvariability of seasonal rainfall and temperature over East Africa

In this section, the potential of HIRHAM5 in reproducing the annual variability of seasonal rainfall and temperature over the three climatic regions: Kenya, Uganda and Tanzania, are presented. The annual variability of seasonal rainfall and temperature is based on seasonal anomalies of rainfall and temperature over the selected regions in each year. This study case focuses on one rainy season in the bimodal regime, OND. The anomalies are calculated with respect to the rainfall climatology mean derived from the full period of 18 years (1990–2007). The area averages of both rainfall and temperature anomalies are normalised by the standard deviation derived from 1990–2007 time series. In order to quantify the model (HIRHAM-ERAI)

representation of the climate variability over East Africa, the correlation coefficient of the model for monthly rainfall and surface temperature are calculated with reference to CRU. Additionally, the correlation coefficients of its boundary forcing, ERA Interim, and FEWS with reference to CRU are also calculated for more understanding. Furthermore, the amplitude of the standardised anomalies (σ') for each datasets is assessed with reference to the standard deviation of the standardised anomaly of the CRU datasets. This can be summarised in the following equation:

$$\sigma' = \frac{\sigma_{HEF}}{\sigma_{Obs}} \quad \text{.....(3)}$$

whereas σ' is the amplitude of the standardised anomaly relative to the observation (CRU), σ_{HEF} and σ_{Obs} are the standard deviation of the anomalies from the model HIRHAM-ERAI, ERAI-Interim and FEWS relative to CRU respectively. If $\sigma'=1$, the model simulated the same variability as CRU and it shows that the model skill is good.

4.1.1 Annual variability of seasonal rainfall over East Africa

This subsection presents how well HIRHAM5 simulates the annual variability of seasonal rainfall over the selected three areas within East Africa: Kenya, Uganda and Tanzania. The annual variability of seasonal rainfall is shown in the following Figures (4.1,).

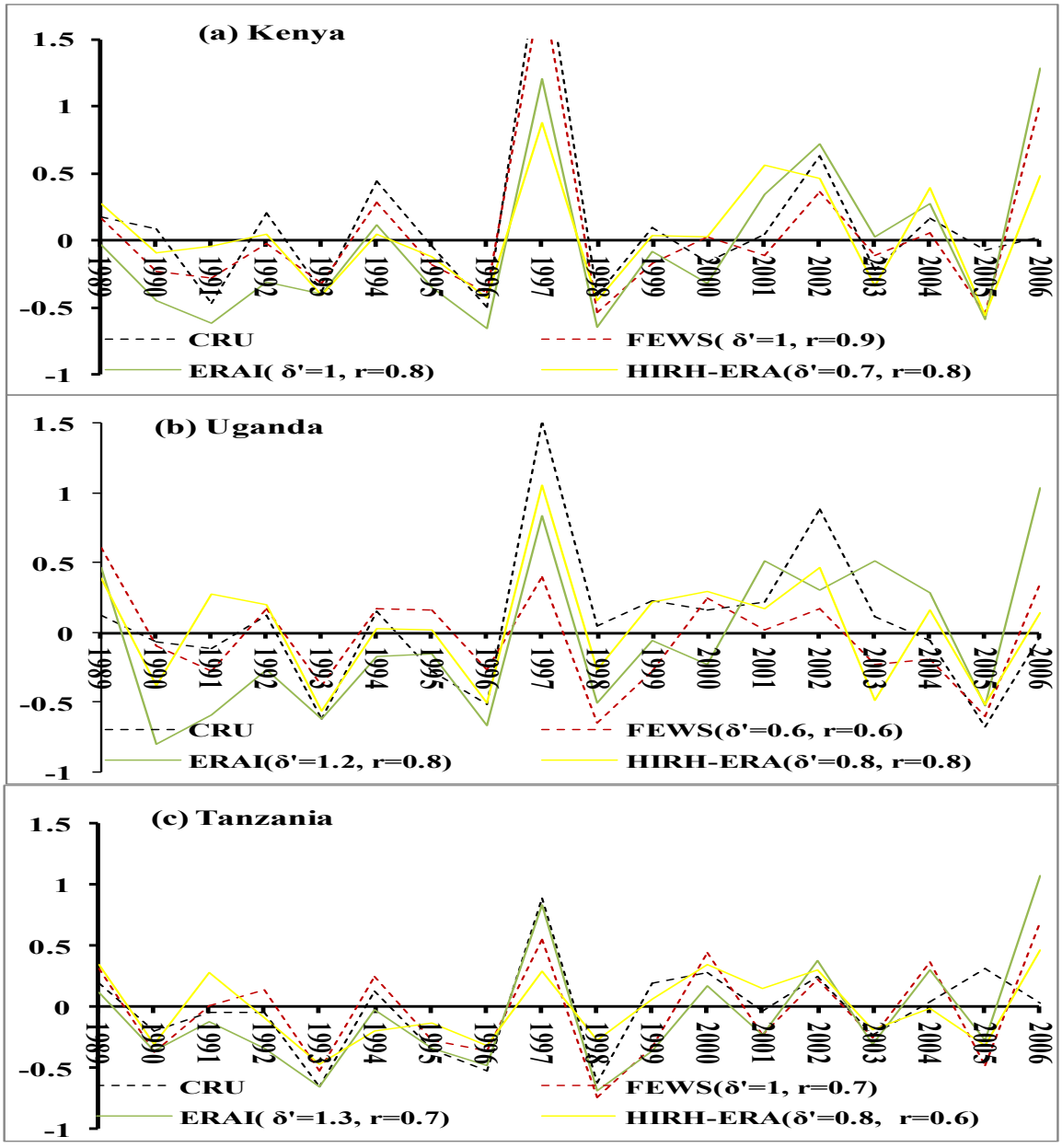

Figure 4.1: Annual variability of standardised anomalies of OND rainfall season over East Africa for (a) Kenya(-3.6° S – 4.8° N, 34°E –41.7° E), (b) Uganda (-1.8° S – 4.035° N, 29.5°W – 35° E) and (c) Tanzania (29° W – 41° E, -11° S – -1° S) from 1989 to 2006 as simulated by HIRHAM5-ERAI (HIRH-ERA), ERA Interim (ERAI), and observations from CRU and FEWS. The values in the brackets are correlation coefficients (r) with reference to CRU and normalised standard deviation (σ') for each datasets.

Figure 4.1, shows the results of the annual variability of the standardised anomalies of seasonal rainfall during the short rainy season (OND). It is has been studies that East Africa rainfall is highly variable during OND season (Schreck & Semazzi 2004, Anyah & Semazzi 2006; Wolff et al. 2011). OND season is characterised with stronger variability than MAM season. The results show that the model is able to capture most patterns of variability over the entire region. There is also good agreement of the model simulations with the observations over the entire region, in the years 1992, 1993, 1994, 1995, 1996, 1997, 1998, 2002 and 2005. HIRHAM-ERAI captures the maximum and minimum standardised anomalies as suggested by the observations over the three regions (Kenya, Uganda and Tanzania) showing strong variability of rainfall over the entire period. The strongest ENSO years, for example, 1997/98 (El Niño) and 1998/1999 (La Niña) are well captured by the model. However, there are some differences within the region: high correlation coefficient with FEWS occurs over Kenya (r=0.9) while in ERAI occurs in Kenya and Tanzania (r=0.7).

The model has a rather high correlation (r>0.6) with the observation datasets for all of the three regions. The highest correlation coefficient is 0.8, occurring in Kenya and Uganda (Figure 4.1 (a, b)). In general the model did good job to reproduce the key years of known climatic variability over East Africa.

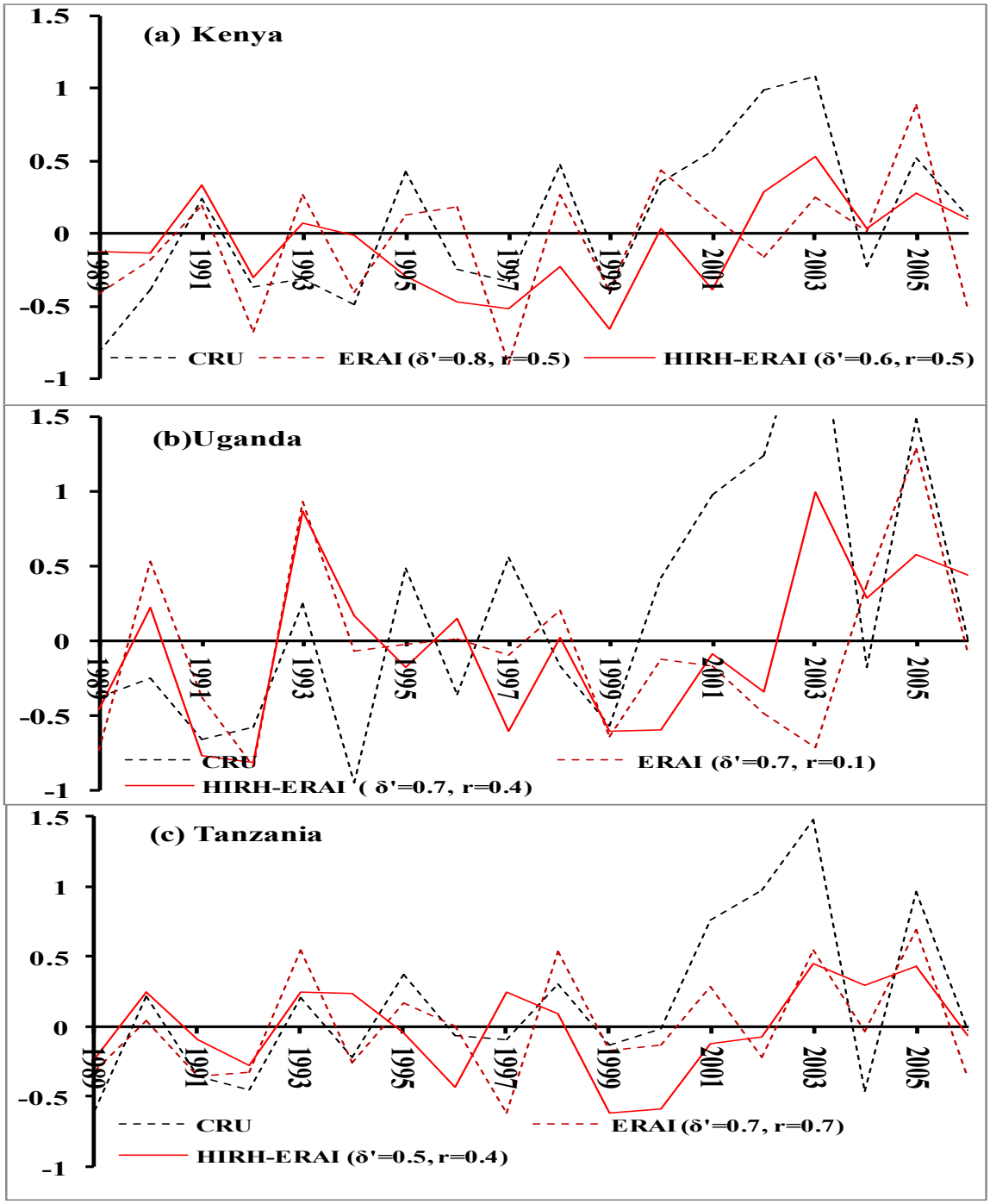

Figure 4.2: Annual variability of standardised anomalies of OND surface temperature season over East Africa covering averaged area of (a) Kenya(-3.6° S–4.8° N, 34°E–41.7° E), (b) Uganda (-1.8° S–4.035° N, 29.5°W–35° E) and (c) Tanzania (29° W–41° E, -11° S–1° S) from 1989 to 2006 as simulated by HIRHAM5 under boundary forcing of ERA Interim (HIRH-ERAI) and

observations from CRU and ERAI. The values in the brackets are correlation coefficients (r) and amplitudes of the standard deviation of the standardised anomalies (σ') with reference to CRU.

Figure 4:2 presents simulations of the standardised anomalies of surface temperature for HIRHAM-ERAI in comparison to the observation datasets from CRU, FEWS and reanalysis, ERAI during OND season. The results show some good skills of the model in capturing relevant patterns of the observed features. For example, the maximum and minimum standardised anomalies as suggested by the observation datasets are well captured, although not in all periods and locations. HIRHAM-ERAI simulations show good skill in capturing the La Niña events, 1991, where temperatures were below normal and El Niño years 1997/98 when surface temperature were above normal. Moreover, the maxima standardized anomaly (1.5) occurred in 2003 which indicate strongest variability in this year. This maxima was captured by the model, although the values of the model are below that figure. The minimum value of standardised anomalies, as presented by the observations, occurred in 1994 in Uganda in the same period as suggested by the observations. The model shows positive correlation with CRU over all regions where the strongest correlation coefficient (r=0.5) occurs in Kenya while moderate positive correlations (r=0.4) occur over and in Tanzania and Uganda. It is surprising that the model go well with ERAI throughout the, however, domain. This mismatch in extent between HIRHAM5 and the observations could be related to the model physical parameterisation and soil moisture.

It is already known that the rainfall variability in East Africa is influenced by the Indian Ocean which alters the local circulation patterns (for example the MJO) (Tierney et al. 2013). In this season a model demonstrated good skill in capturing the years of ENSO events although not in all regions. The strongest ENSO, 1997/98, is well captured over the Kenya region, while in Uganda and Tanzania in 1997 it is not well captured. The reason for this disparity could be related to the lateral boundary forcing. In the 1st chapter discussions the author discussed on the limitations of the RCMs, that, the high resolution RCMs (likewise HIRHAM5) are limited area models, and are constrained by their lateral boundary forcing. Moreover, a model quality depends on the quality of the driving lateral boundary forcing. There is also good agreement of the model simulations (Figure 4.2) with the observations over the entire region, in the years

1993, 1999, 2003 and 2005. The strongest La Nina year event, namely 1999/2000, is captured by all datasets as well as the model (Figure 4.2) while in Figure 4.1 is not well defined.

4.2 HIRHAM5 simulation of the observed impacts of sea surface temperature in ENSO years over East Africa

This section presents HIRHAM5 representations of the composite of the differences between December, January and February of ENSO years (El Niño and La Niña years) and rainfall climatology. This compositing approach allows meaningful comparisons between simulated and observed climatic signals. The anomalies are calculated from the departure of the control period (1990-2007) average of December, January and February (DJF). The observed fields are computed from CRU and reanalysis dataset, ERA Interim (ERAI), and the corresponding simulated field of HIRHAM5 under lateral boundary condition of ERAI (HIRHAM-ERAI). The following table 1 presents the ENSO years used in this experiment.

Table 2: The periods of El Niño and La Niña events over East Africa for this experiment:

El Niño	1991/92	1994/95	1997/98
La Niña	1998/99	1999/2000	

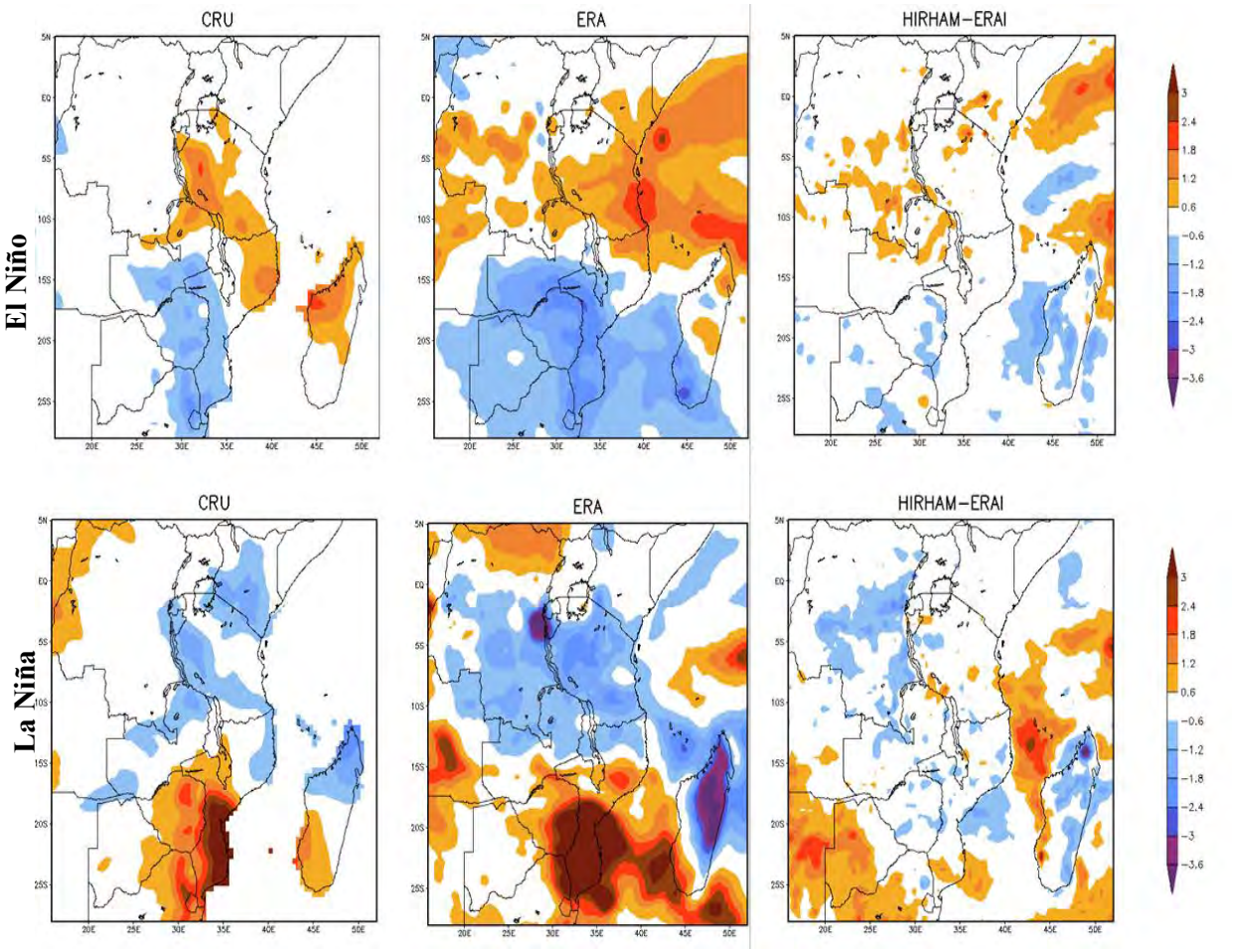

Figure 4.3: Comparison of simulated HIRHAM-ERAI ENSO years minus mean climatology composite OND rainfall with CRU and ERA Interim reanalysis (ERA).

Figure 4.3 shows the composites of El Niño and La Niña years relative to the mean rainfall climatology period (1989-2006). The observed fields, CRU, depict the wet anomalies during El Niño and dry anomalies during La Niña years. The reanalysis data captured very well both extreme wet anomalies in El Niño and drought in La Niña years over East Africa, showing the data is correct. It is therefore very important to assess HIRHAM5's ability in representing this crucial feature. HIRHAM-ERAI demonstrated good skill in capturing the ENSO signals in both events (El Niño and La Niña years) by simulating positive anomalies in El Niño and negative anomalies in La Niña years. This result agrees with the previous studies that East Africa has above normal rainfall during El Niño and below normal rainfall during La Niña years (Mutai et al. 1998; Indeje et al. 2000; Conway et al. 2005; Kijazi & Reason 2005; Hastenrath 2009; Wolff

et al. 2011). Therefore, this result provides a quantitative measure of possible application of the model in making projections for future changes in climatic variability and the statistics of extreme events under the influence of global warming.

4.3 HIRHAM5 simulation of Multivariate ENSO Index (MEI)

This subsection presents the correlation between November, December and January (NDJ) monthly rainfall and surface temperature with bi-monthly Multivariate ENSO Index. MEI, as already been noted in Chapter 2, is a bimonthly ENSO index based on six variables: pressure, zonal and meridional winds, sea surface temperatures, surface air temperature and total cloudiness fraction observed over the tropical Pacific region. The positive MEI values correspond to El Niño conditions, while negative values correspond to La Niña conditions (Wolter & Timlin 2011).

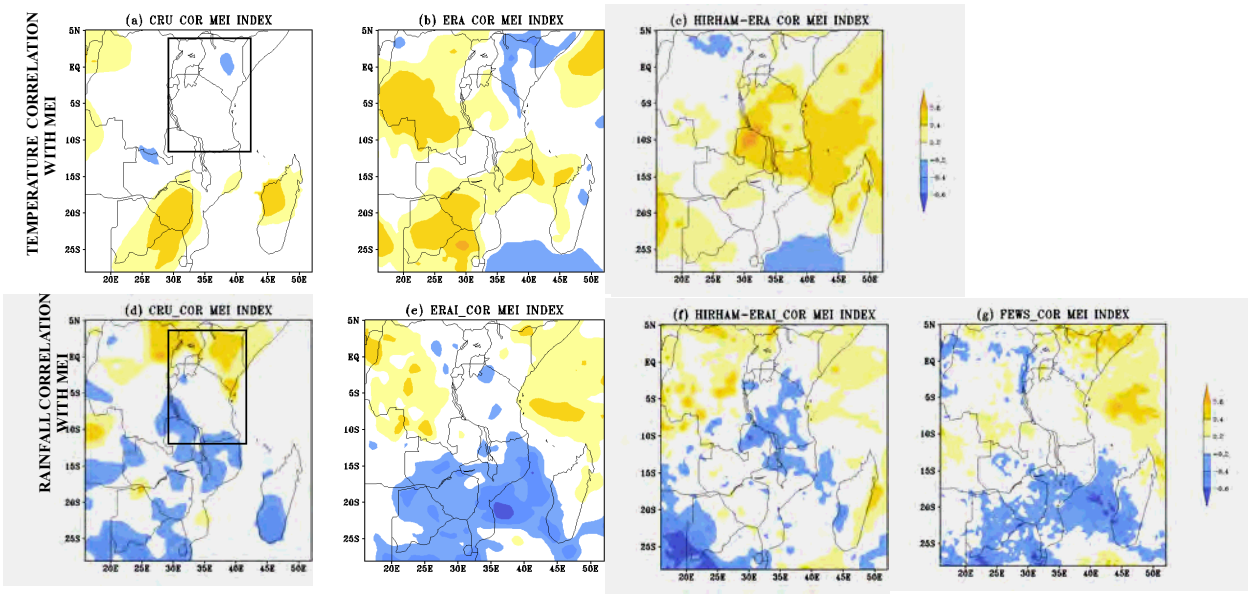

Figure 4.4: The correlation of MEI NDJ values with observed surface temperature climatology in (a) CRU, (b) reanalysis, ERA-Interim, and the simulated surface temperature in (c) HIRHAM-ERAI; and with the rainfall climatology (second row) in (d) CRU, (e) ERAI and the simulated rainfall in (f) HIRHAM-ERAI, and (g) FEWS for the mean annual sums of wet months of November, December and January (NDJ).

Figure 4.4 presents the results of the correlation between MEI values versus observed and simulated rainfall climatology during wet months (NDJ). The results show that, the observed fields, CRU and FEWS, and the reanalysis ERAI presented some similar patterns as well as different patterns to some regions. For example, CRU has no data over the remote areas and the ocean, that large portion remained blank (with no change). The positive correlation values occur more in the northern portion of the domain (12^{o} S–4^{o} N), while negative values occur south of 12^{o} S of the equator. This result seems to have uncertainty as FEWS and CRU show some dissimilar patterns. For example, on the rainfall correlation CRU presented moderate correlation ($r =\sim 0.6$) over Uganda and Kenya. On the contrary, FEWS presented weak positive correlation ($r \leq 0.2$), negative correlation over the western portion of Uganda (east f Congo and has data over the Indian Ocean with positive correlation ($r \geq 0.6$). The HIRHAM-ERAI simulation of surface temperature correlation in MEI show some good agreement with ERAI, however also show some discrepancies with the observation (Figure 4.4c). The results of the simulation of rainfall in

HIRHAM5-ERAI show some few agreements with the observations especially over Uganda and Congo basin area (Figure 4.4f). The patterns of MEI in rainfall simulations (Figure 4.4f) over Tanzania, show negative dipole (r= ~-0.4), weak positive correlation (r=0.2 and r=0.3) over Kenya and Uganda respectively.

Moreover, rainfall correlation with MEI values in ERAI shows some similar patterns as suggested by the two observation datasets, though differing in the extent from CRU and FEWS. These results reveal the quality of the observation datasets and reanalysis data used. Previous studies have shown that an increase in uncertainty in regional climate model evaluation is associated with the quality of the observation dataset used (Sylla et al. 2013) in this study case too.

Generally, the HIRHAM-ERAI performance show poor to moderate agreement with the observations in capturing the rainfall (and surface temperature) pattern in MEI proxy. This could be associated with the model limitations, due to its physical parametrisation. For example, here to blame is not a boundary forcing as ECHAM5 (not shown) and ERAI gives some good results which are likely close to HIRHAM-ERAI and HIRHAM5-50km (not shown). It is true that RCMs especially high resolutions are limited area models. The uncertainty of the RCMs due to lateral boundary condition forcing have been noted in previous studies (Nikulin et al. 2011; Kim et al. 2013) to have hindered the RCM to capture rainfall in association with moisture flux over the Indian Ocean due to the movement of the ITCZ. However, in this case, a model is limited to its error directed to physical parameterization

4.4 Summary and conclusion

This chapter presents HIRHAM5 simulations of the annual variability of seasonal rainfall and surface temperature covering three countries: Kenya, Uganda and Tanzania; the HIRHAM5 simulations of the ENSO signals using composite analysis for December, January and February of ENSO years (El Niño and La Niña years); and rainfall climatology. Furthermore, HIRHAM5 simulations of the Multivariate ENSO Index (MEI) is presented.

Overall, the results show the strengths of HIRHAM5 and some weaknesses in simulating observed climate variability over East Africa. The main strength of HIRHAM5 occurs in the simulation of the observed patterns of natural variability of both rainfall and temperature (Figures 4.1–4.2). HIRHAM-ERAI simulates almost the same amplitude of variability as CRU (σ'=~1) in both rainfall and temperature over the entire study domain. Moreover, the correlation coefficient is reasonable (r =~0.6) in all seasons and especially in OND (Figures 4.1). The ENSO signals are well captured; for example, in Figure 4.2 the model shows good agreement with the observations by simulating above normal rainfall during ENSO warm years (1997/98) and below normal rainfall during ENSO cold years (1998/99, 1999/2000). Moreover, HIRHAM-ERAI shows some good agreement in many areas of the domain with the observations in the simulations of the ENSO signals using composites of El Niño and La Niña years (Figure 4.3 third column).

Despite its strengths, HIRHAM5 simulations show some shortcomings. It fails to capture the peaks of rainfall and temperature in some regions (Figures 4.1, 4.2). HIRHAM5 shows weaker correlation in simulating inter-annual variability of surface temperature (especially in Uganda), compared to other regions. HIRHAM5 also shows weak to moderate correlation in simulating ENSO signals in both composite analysis and relative to MEI. Generally, HIRHAM-ERAI simulates moderate skill in simulating both ENSO signals in the rainfall composites and surface temperature in MEI proxy.

In the previous IPCC reports (AR4 and AR5), the regional climate models were reported to have significant errors which are related to the mismatches associated between the regional model's topography and local topography (Randall et al. 2007). East Africa has heterogeneous topography surrounded by the well-known high peaks of Africa (Mount Kilimanjaro, Kenya, Ruwenzori); the Indian Ocean (in the east), the great Lakes (Lake Victoria, Tanganyika) and the Congo forest basin. All these could create difficulties in the regional climate model's topography.

In this case, it is suggested that HIRHAM5 improves with increased resolution, although the bias may still remain. HIRHAM5, in comparison with its boundary forcing ECHAM5 and ERAI,

simulates realistic behaviour on a large scale and the model is able to reproduce the key features influencing East Africa's climate variability.

It is suggested that HIRHAM5 model could be used for probability projections of East African climate variability and change. However, in the future, this model needs more modification; as stated above, there some factors which could be linked to the model errors, including grid box and physical parameterisation of the model. Furthermore, there is need for more sets of high resolution regional climate models (apart from present CORDEX) to make an ensemble simulation over regions. It is noted that an ensemble of RCMs performs better than one RCM (Tebalti and Knutt 2007). Additionally, more reliable observation datasets at a high resolution with large coverage are needed for model evaluation.

Chapter 5

Projections of the future climate variability and change in East Africa

Unfortunately, most of the available climate studies in East Africa have been narrowed to the past and current climate, while most of the projections have focused on East Africa only from a global context. Moreover, the extreme climatic events which have already contributed to serious impact on human life and the environment in East Africa are less studied in the view of the future projection changes at a regional level (Shongwe et al. 2011). The regional climate change information is very important for impact assessment and early warning for preparedness and planning for development in mitigation and adaptation (IPCC, AR4, AR5). The knowledge on climate change projection at a local/national level also assists in rapid implementation of technology in the reduction of greenhouse gas emission.

The main aim of this chapter is to investigate whether increasing resolution of HIRHAM5 has impact on the projected rainfall and surface temperatures over East Africa. This study case examines the downscaled high resolution, HIRHAM5 in 50 km and 10km resolution, and the boundary forcing from ECHAM5 in the projected rainfall, surface temperature and moisture change for three time slices, following the A1B scenario, expressed as spatial distributions and time series relative to the control period. The projected change are assessed for the period 1980 to 2099 in three 20 year time slices: the control period, representative for present-day climate, is 1980–1999, "near future" climate (2046–2065) and "far future" climate (2080–2099). Furthermore, the extremes of both rainfall and surface temperature will be discussed. The time series are presented for three selected countries in East Africa: Kenya (3.6^{o}S – 4.8^{o}N, 34^{o}E – 41.7^{o}E), Uganda (1.8^{o}S – 4.035^{o}N, 29.5^{o}E – 35^{o}E), and Tanzania (11^{o}S –1^{o}S, 29^{o}E – 41^{o}E). Finally, the dynamics and thermodynamics of the impact of climate change are presented,

followed by the summary of this chapter. The results are presented for MAM season and (OND is shown in the Appendix2).

5.1 HIRHAM5 simulations of the projected seasonal annual rainfall change

This section examines the downscaled high resolution HIRHAM5 in 50 km and 10km resolution, and the boundary forcing ECHAM5 in the projected seasonal annual rainfall change for the three time slices. The time series are taken from the averaged area of the study domain as stated above. Furthermore, HIRHAM5 simulations of the projected change of extreme rainfall (defined as the 90^{th} percentile of daily precipitation) and the maximum number of consecutive dry days are presented.

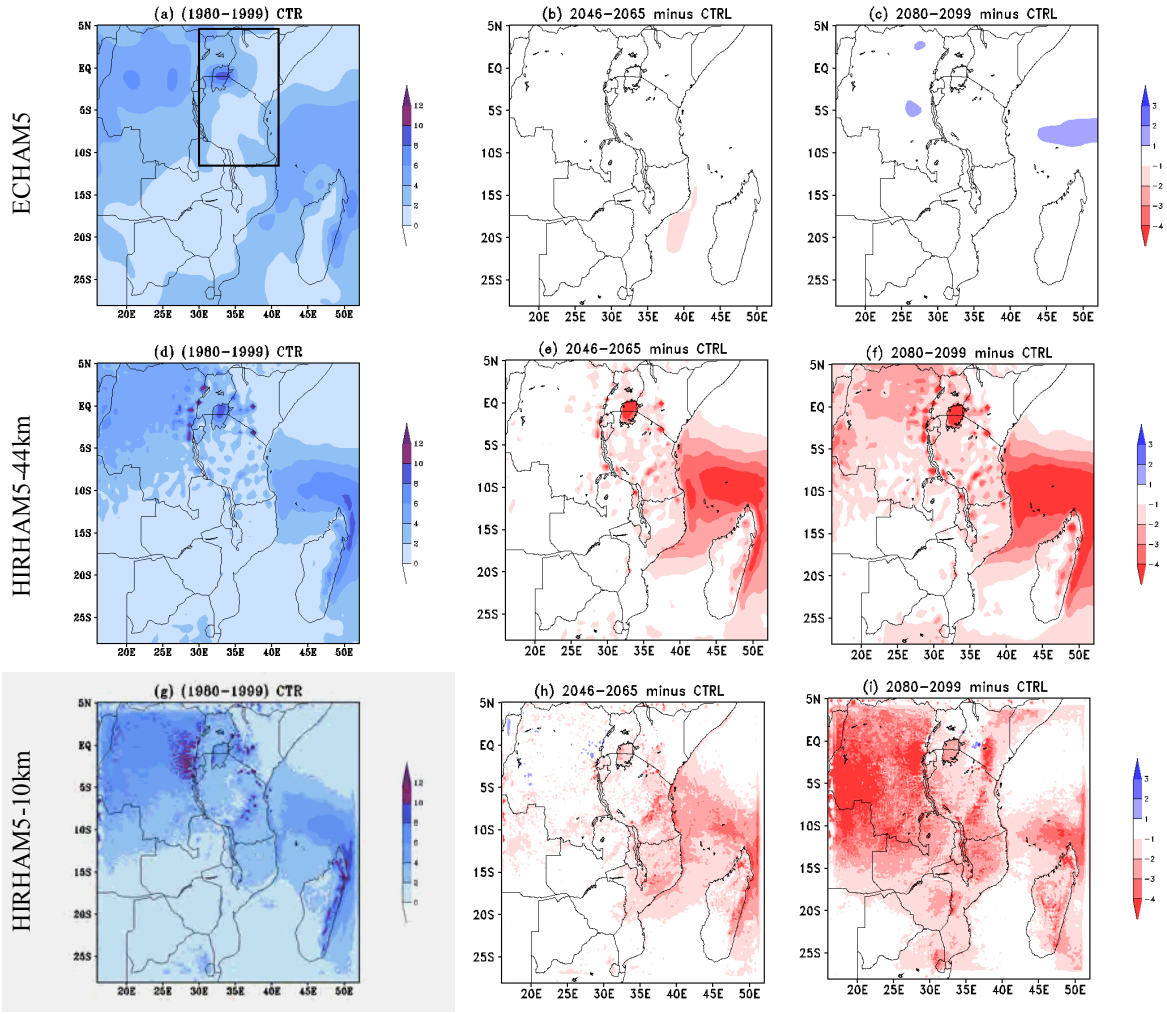

Figure 5.1: Mean MAM rainfall (mm/day) for the control period (1980-1999, left column) and changes with respect to the control period for near future (mid column) and far future (right column) for ECHAM5 (top row), HIRHAM5 at 50 km (middle row) and 10 km resolution (bottom row).

The results of the projected mean seasonal rainfall show some similar patterns in both RCMs and GCM, however the projections look different especially in the magnitude. HIRHAM5 at both resolutions projects a decrease in rainfall (~20%) over most regions in Tanzania, Kenya and Uganda in the near and far future. Moreover, the highest decrease in rainfall is projected in the far future (up to 50%) and especially over the western regions, Indian Ocean and highlands of

East Africa. Contrary to HIRHAM5 simulations, ECHAM5 projects small increase in rainfall in the far future projection (Figure 5.1 c).

The decrease in rainfall in the projected changes was also found by some of the resent studies over East Africa (Cook & Vizy 2013). They found that the reduction of rainfall in the future projection in Tanzania and Kenya is associated with the moisture flux (at 850hPa) anomaly over Congo basin forest. It is true that rainfall in East Africa is highly variable, and this variability is connected to the complex topography of East Africa, the adjacent Indian Ocean, and to ENSO (see Chapter 1). More discussion on the projected rainfall changes will also be discussed in the later section of which will focus on the changes of the thermodynamic impacts. It is noted that the Lake Victoria stands out differently (in all time slices); the reason for this difference is not clear.. However, there is no difference in the treatment of lakes in the 50km and 10km models.
This section also presents the amplitude of the projected change in rainfall, in order to understand as to whether the projected change is related to the local changes or climate variability as stated above. Therefore, Figures (5.2) presents time series of mean rainfall change and standard deviations (δ) of mean rainfall change. In order to quantify the variable nature of rainfall in East Africa, the standard deviation (δ) is calculated for each plot in each time slice and the amplitude (δ') is estimated. The magnitude of the projected mean change is estimated from the model projection calculated relative to the present day climate as follows:

$$\delta' = \frac{\delta_{future} - \delta_{present}}{\delta_{preset}} \quad \text{.....(3)}$$

where δ' is the amplitude of standard deviation in the projected mean changes relative to the control period ($\delta_{present}$), and (δ_{future} = (near future (nf) and far future (f)) in the Figure 5.2. If $\delta' > 1$, it means there is a climate change associated with the internal variability.

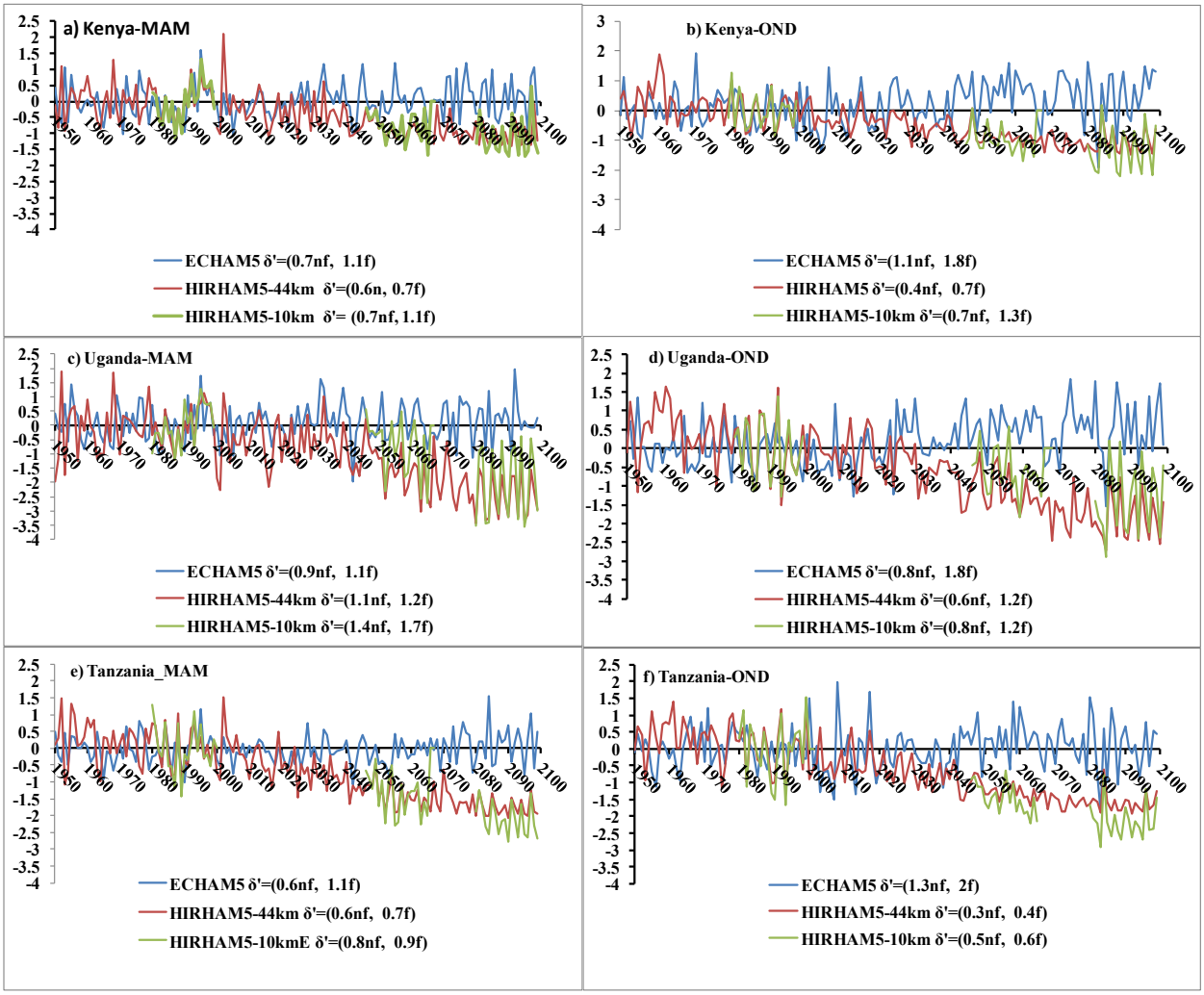

Figure 5.2: Climatology of rainfall change time series with reference to the control period (1980-1999) for Kenya, Uganda and Tanzania as simulated by HIRHAM5 at 50km (red) and 10km (green) resolution, as well as for ECHAM5 (blue line) for MAM(first column) and OND (second column). The standard amplitude of change is denoted by δ' (nf, near future and f, far future climate) in the brackets.

Figure 5.2 presents the time series of annual mean rainfall change. The results show some similarities and differences in both RCMs and GCM. In addition to the decrease in future rainfall (Figure 5.1), the amplitude of change is increasing towards the future. Both RCMs and the GCM simulate stronger variability with higher amplitude ($\delta' \geq 1$) in the far future than in

near future (Figure 5.2). Although all models project strong variability in the geographical distribution, they do differ in intensity distribution. In both future scenarios, HIRHAM5 at 10 km resolution simulates maximum standard deviation (δ' =1) and amplitude (δ'=1.4) over Uganda while at the same period over Kenya lower standard deviation (δ =0.7) and amplitude (δ'=0.8) are simulated. This result shows the high resolution project more increase in variability in the future in comparison to the lower resolution.

5.1.1: HIRHAM5 simulations of extreme heavy rainfall change

It is well known that extreme climatic events are the chief drivers of severe floods and droughts worldwide and especially in East Africa (Patz et al. 2005; Mitchell et al. 2006; Hastenrath et al. 2010; Kijazi & Reason 2009; Lyon & DeWitt 2012; IPCC, 2013). Mitchell et al. (2006) found that the large-scale warming is expected to be accompanied by increased frequency and/or intensity of extreme events such as heat waves, heavy rainfall, storms and coastal flood. It is clear that these events add more stress on life, socially, physically and economically in developing countries. Sasson (2012) noted that the cause of food insecurity is linked to the oscillation of climate due to ENSO impact (La Niña). In 1997/98, East Africa experienced very heavy rainfall associated with floods related to the strong El Niño event, which caused loss of life and property. Again, prolonged drought in 1998/1999, 1999/2000 which took place up to 2005 (to some regions in Tanzania and Kenya) were coupled with food insecurity, water shortage, hydropower outage and many other losses socially and economically. However, very few studies are available on the projection of extreme climatic changes over East Africa (WHO 2002, Patz et al. 2005; IPCC, 2007, 2013).

This subsection examines the performance of the downscaled HIRHAM5 at 50 and 10km resolutions in simulating the projected changes in annual indices of extreme precipitation and temperature events during MAM and OND seasons. The extremes are expressed in terms of the 20-year time slices (2046–2065 and 2080–2099) relative to the control period (1980–1999). The percentiles of rainfall and the number of consecutive wet and dry days are investigated.

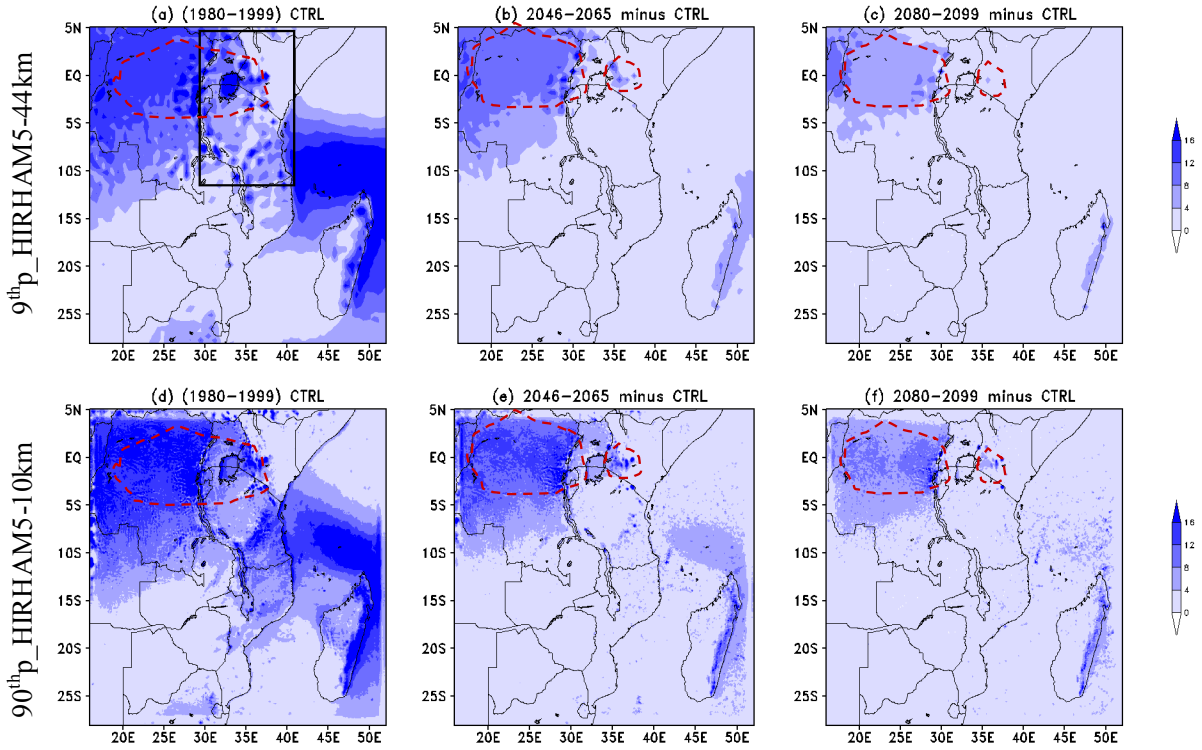

Figure 5.3: The 90th percentile of daily rainfall (mm/day) change in MAM season, as projected by HIRHAM5 at 50 km (first row) and at 10km resolution (second row) in near future (2046–2065, middle column) and far future (2080–2099, right column) relative to the control period (1980–1999), which is shown in the first column. The red dotted circle indicates areas of maxima extreme heavy rainfall.

Figure 5.3 shows the result of the projected mean changes of heavy rainfall expressed in the 90th percentile of daily rainfall during wet months of MAM. The control period shows how intensive the 10% heaviest rainfall are, heavy rainfall spread over most of the western regions, the Congo basin area, large parts of Tanzania (especially western portion) and more over the Indian Ocean (north and east of Madagascar). Both HIRHAM5 resolutions simulate similar patterns with slight differences, especially in the intensity. Slightly larger rainfall change occurs in HIRHAM5 at 10km over the coastal belts and the highlands compared to the 50 km resolution (Figure 5.3 e and f). This suggests the impact of resolution, that, increase of RCM resolution increases the chance of capturing more details over the surface (high grounds). In the near future

both RCMs simulations project increase in the heaviest rainfall (4mm/day) over the region marked with dots. The following section explores the frequency of rainy days over the area of significant change (Figure 5.3, first row).

5.1.2 HIRHAM5 simulations of the projected frequency and amount of daily rainfall

This subsection presents the projected frequency and amount of rainy days over a selected region in the model domain. Figure (5.1) showed that the higher resolution has smaller difference in the simulations of the projected patterns and temporal rainfall variability over East Africa domain. As discussed above, the annual mean change and the extremes of rainfall are projected to decrease in the future climate scenarios. This experiment focuses on the daily rainfall simulations from HIRHAM5-50km available at 1950 to 2010. The intention is to investigate amount and frequency of model rainfall relative to present-day and to find out why the model simulates less future rainfall. For this, an area was chosen where the models simulate significant change in the near and far future.

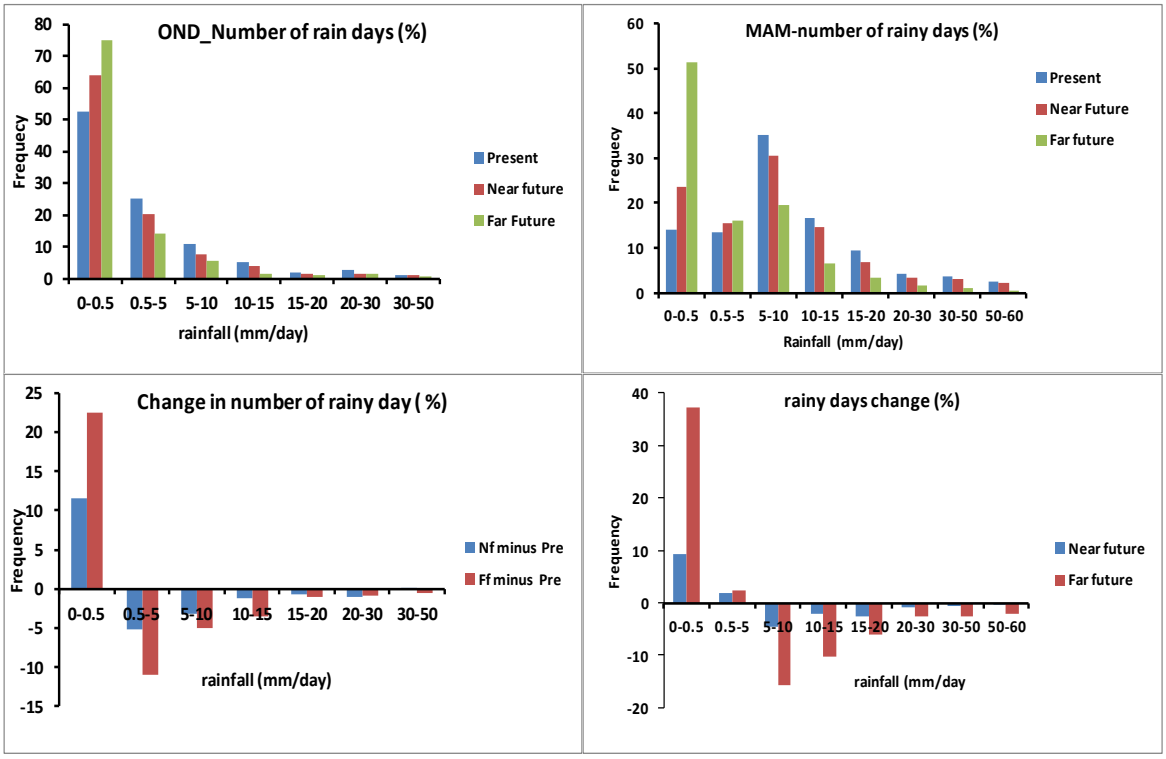

Figure: 5.4. HIRHAM5-50 km histograms of the number of rainy days (% of all days) over a selected grid point (Lon=28.6^{o} E; lat=3.3^{o} S) (first row) and projected change (%) in frequency rainfall amount (second row) for MAM (first column) and OND (second column).

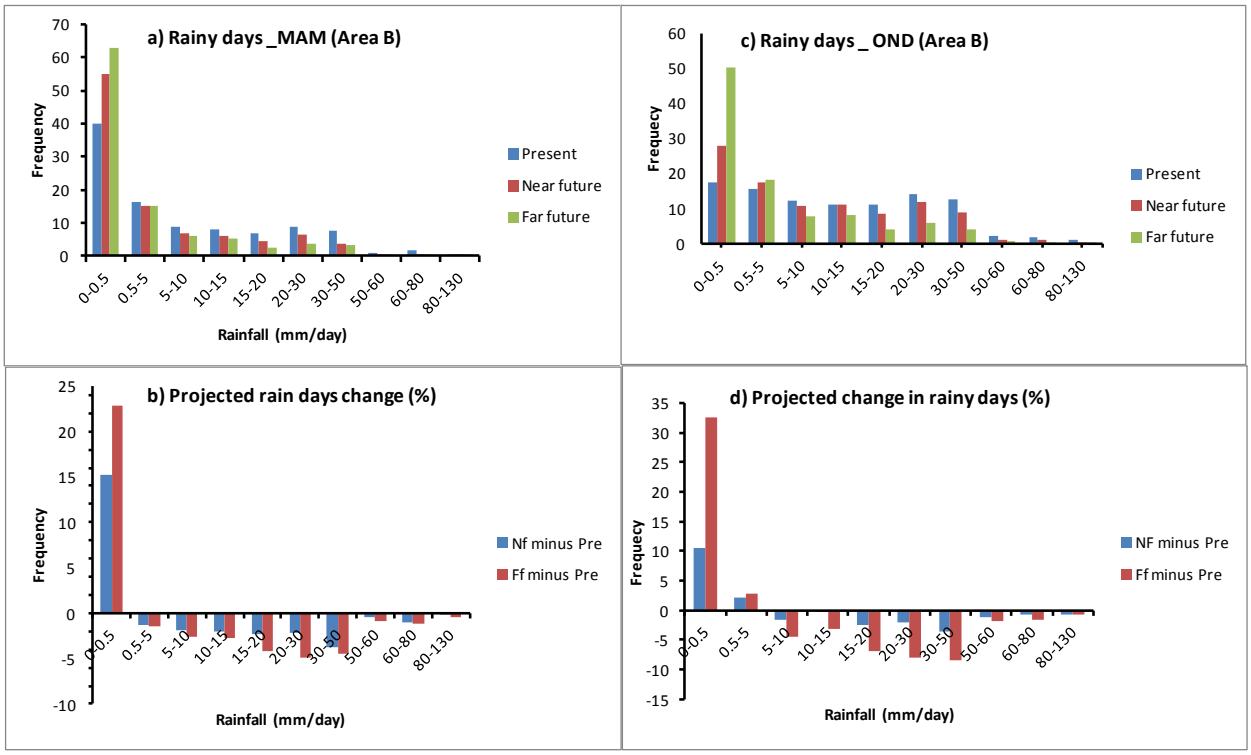

Figure 5.5: HIRHAM5-50km simulations of the number of rainy days over a selected grid point in the domain (Lon=22^{o} E; lat=0^{o}) in percentage (the first row) and projected change in rainy days (%) in the second row for MAM (first column) and OND (second column) rainy season.

The overall results show that the number of rainy days with less than 0.5 mm/day is increasing in the near and far future climate scenarios over the selected two grid points (Figures 5.4 and 5.5) . On the other hand the number of days with rainfall greater than 5mm/day is projected to decrease in the near and far future, in accordance with Figures (5.1–5.5). The reason of the decrease in rainfall could be linked to the changes in winds, total cloud cover, moisture and surface temperature. The following section will present the analysis of these parameters.

5.1.3 HIRHAM5 simulations of the maximum number of consecutive dry days

This subsection presents HIRHAM5 simulations of the extreme rainfall expressed in the maximum number of consecutive dry days using daily rainfall data in three time slices as in the previous analysis (section 5.1.1 and section 1.1.2). The HIRHAM5 simulations is the representative for a rather large region (100 and 2500 km^2, respectively for 10 and 50 km), a "dry day" cannot be defined as a day without precipitation. Instead, an amount of 1 mm/day is taken as a threshold. Then, CDD, or the number of consecutive dry days, is the maximum number of periods with more than 5 days occurring during the wet season when precipitation is less than 1 mm/day. CDD, in other words, is the maximum length of dry spells.

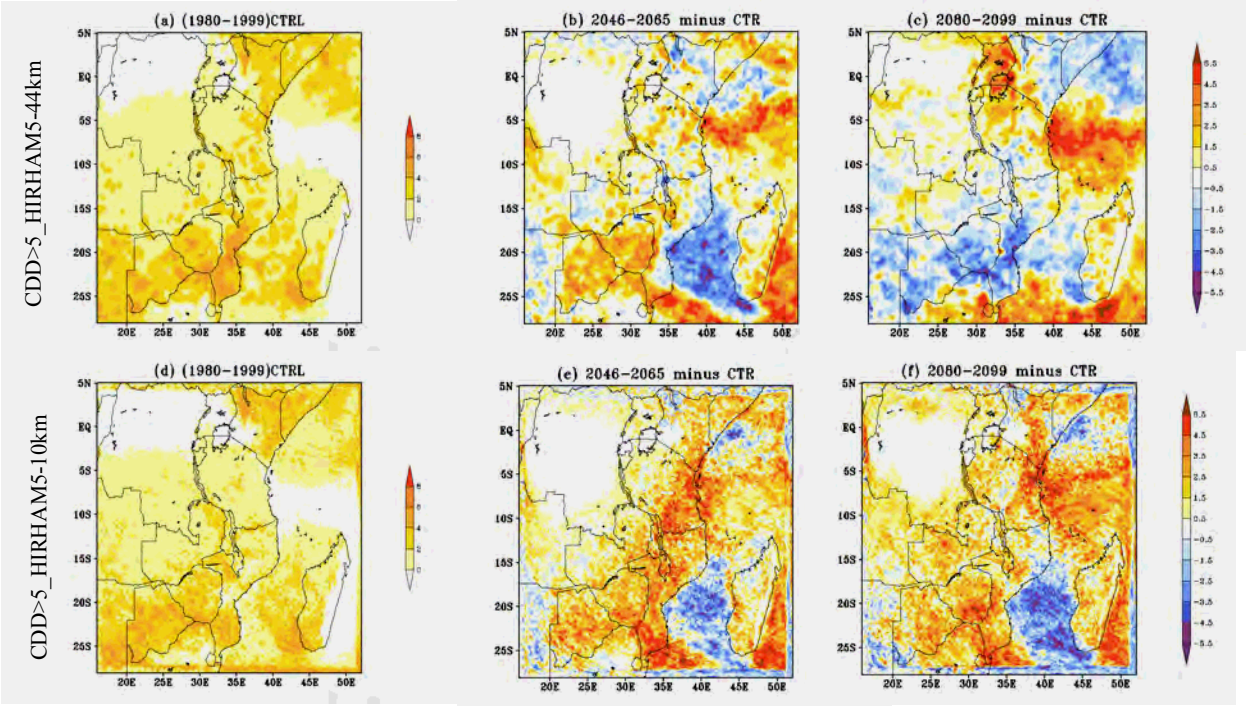

Figure 5.6: Daily change of maximum number of consecutive dry days relative to the control period (1980–1999, left column) as projected by HIRHAM5 at 50km and 10km resolution in the first and second row respectively.

Figure 5.6 presents HIRHAM5 simulations of the daily change in the maximum number of consecutive dry day index. In the control period (first column) the patterns look similar,

however with some slight differences (in magnitude). The area of maxima CDD has significant similarities in both resolutions in OND (not shown). The areas prone to drought over East Africa, central Tanzania and north-eastern Kenya are well captured by both resolutions in the control period. Likewise, both resolutions captured the wettest regions in the western portion of domain (Congo forest basin), high grounds and Indian Ocean.

The projected future change of CDD over much of the eastern portion of the domain shows variable patterns. The simulation of CDD in HIRHAM5-50km is lower in comparison to high resolution, which is consistent with the projected change of surface temperature Figures (in the following section). There is also substantial increase in CDD over the Indian Ocean, coast of Tanzania and northern Madagascar in the future in both HIRHAM5 resolutions. The increase in CDD agrees with the previous section where the number of rainy days with less than 0.5mm is increasing in the near and far future scenario. More increase in dry days is projected in the far future scenarios which reflects the projected changes in extreme rainfall expressed in the previous analysis of the 90^{th} percentile change

In summary, according to the RCMs simulations the central regions of Tanzania and northern Kenya will continue to be even drier in the future in comparison to present day climate. Likewise the wetter regions like Congo basin is projected to be wetter, however with decrease in magnitude and spatial distribution in the far future climate scenarios. High resolution shows more details spatial distribution (over high grounds) and slight increase in magnitude in comparison to lower resolution (Figure 5.2(1^{st} and 2^{nd} row) and 5.3 (second row). High resolution also projects more increase in CDD confined to the high grounds of Tanzania and Kenya in comparison to the lower resolution. More details of why these changes are projected in the future climate will be explored below.

5.2 HIRHAM5 simulations of the projected annual seasonal surface temperature change

As in the previous section for rainfall, this section presents the projection of the seasonal mean and extreme surface temperature changes over East Africa, as simulated by HIRHAM5 at 50 km

and 10km resolution, and mean surface temperature change only for ECHAM5. The projected changes are focused on the bimodal regime of East Africa (Figure 2.2b), the MAM and OND wet seasons. It will be examined whether increasing resolution of regional climate model has an impact on the projected surface temperature changes over East Africa.

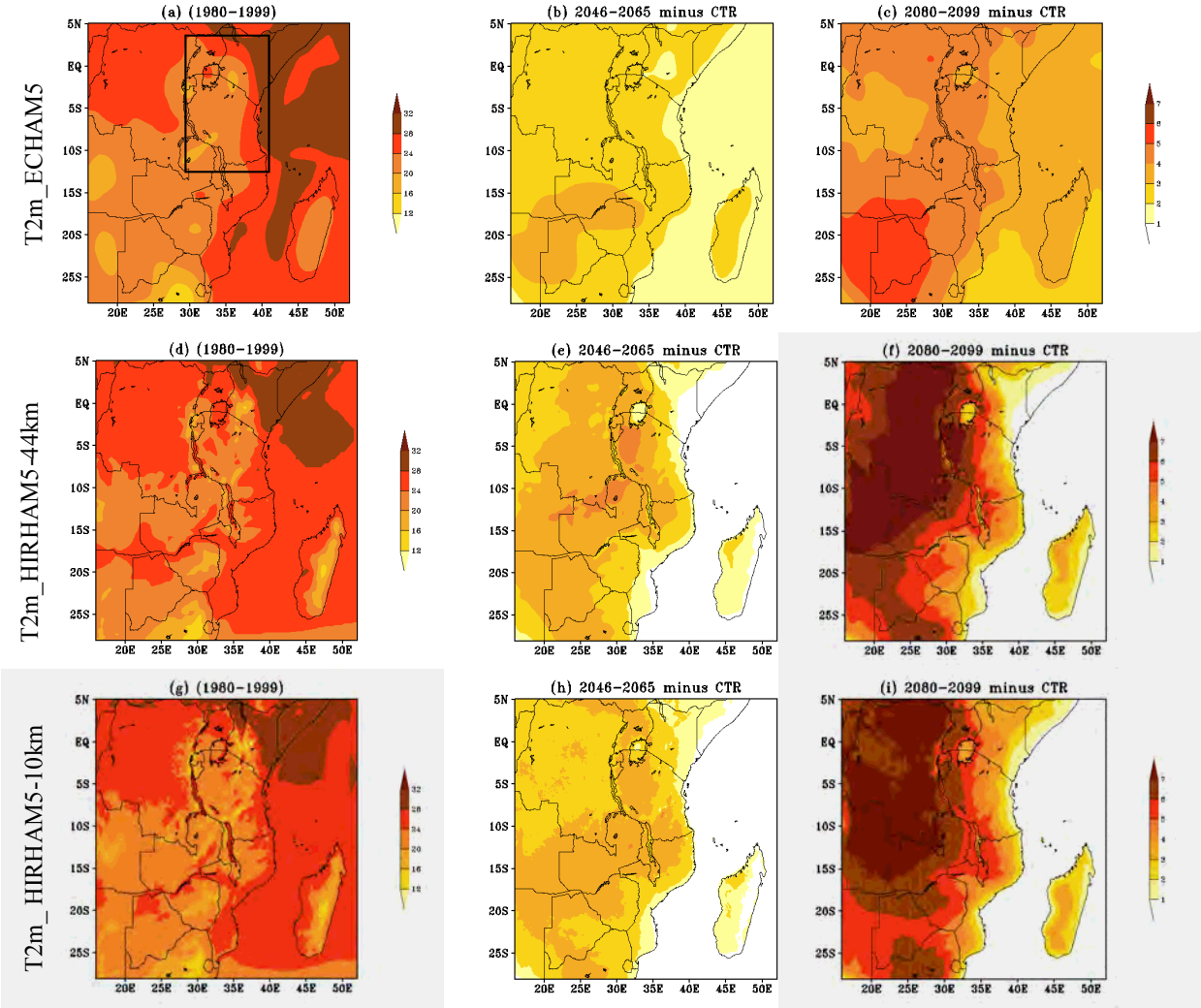

Figure 5.7: Mean surface temperature (^{o} C) change over East Africa domain as simulated by ECHAM5 (first row), HIRHAM5-50 (second row) and HIRHAM5-10km (third row) relative to the control period (1980–1999) in the first column, for the near future (2046–2065, second column) and far future (2080–2099) in the MAM season.

Figure 5.7 illustrates surface temperature change as simulated by ECHAM5 and HIRHAM5 for MAM season. In the control period, the patterns are similar in RCMs with slight difference in the high grounds of Kenya and Tanzania. In the projected changes, the warming is increasing over the land especially over the regions which are normally wet than over coastline (Figure 5.7

third column). This could be related to the impact of soil moisture reduction over the surface (Nikulin et al. 2011).

The GCM simulates lower temperature over the large portion of the domain (northern Tanzania, Kenya and north western regions). The projected changes of surface temperature in both seasons show significant difference between the GCM (Figure 5.7c) and RCMs (Figure 5.7(f and i). For example, over the western regions in Tanzania and Uganda, the RCMs simulations project higher temperature above 6^{o} C while GCM simulations show below 5^{o} C. The RCMs in both resolutions simulates large areas of warming in the far future (increasing over the study domain from 1 to ~5^{o} C) and the increased warming confined over the large portion of wetter region especially Congo and high ground East Africa in comparison to ECHAM5. HIRHAM5 simulations has clear signal of warming along the coastal belt and high ground in comparison to ECHAM5. HIRHAM5 simulates less warming over the high ground, coastal belt and over the neighboring Indian Ocean compared to other regions in the domain.

Over the ocean, ECHAM5 simulates warmer temperature than HIRHAM5; this is also linked to the boundary condition. It has been suggested that a small model domain could lead into an increased boundary condition impact (Paeth et al. 2009; Abiodun et al. 2012). Previous studies have also shown that surface temperature variations could be influenced by the inter-annual variability of sea surface temperatures. The anomalous warming/cooling of the sea surface temperature over the Indian Ocean (ENSO warm/cold) was found to have a great impact, especially in the OND season over East Africa (Rasmusson & Carpenter 1982). Despite the limitation of their boundary conditions, high resolution regional climate models have advantage over GCMs, in that they have good skill in representing regional/local climate features (Rummukainen 2010; Feser et al. 2011; Flato et al. 2013). The projected change of surface temperature as simulated in HIRHAM5 has maxima (~6^{o} C) confined largely over the western part of East Africa while in ECHAM5 the maxima around ~4^{o} C is confined in the extreme south-western portion of the East African domain (Zambia) in the far future climate scenario. The surface temperature is projected to increase from the coastal belts of East Africa towards the mainland of the regions. The projected mean surface temperature change simulations show an increase in minimum temperature (~2^{o} C) in the coastline to the maximum of ~6.5 ^{o} C in the

mainland areas of East Africa. This result is in agreement with most of the previous studies (in the IPCC reports) that in the future the warming will be higher over the land than over the Ocean, due the low heat inertia of land compared to the ocean. The ocean warms slower and loses heat slower than land.

An increase of resolution of the RCM shows small impact on the projected warming. In this case, higher resolution RCM is slight cooler in comparison to low resolution. However, the patterns and distribution of warming are quite similar in both fields.

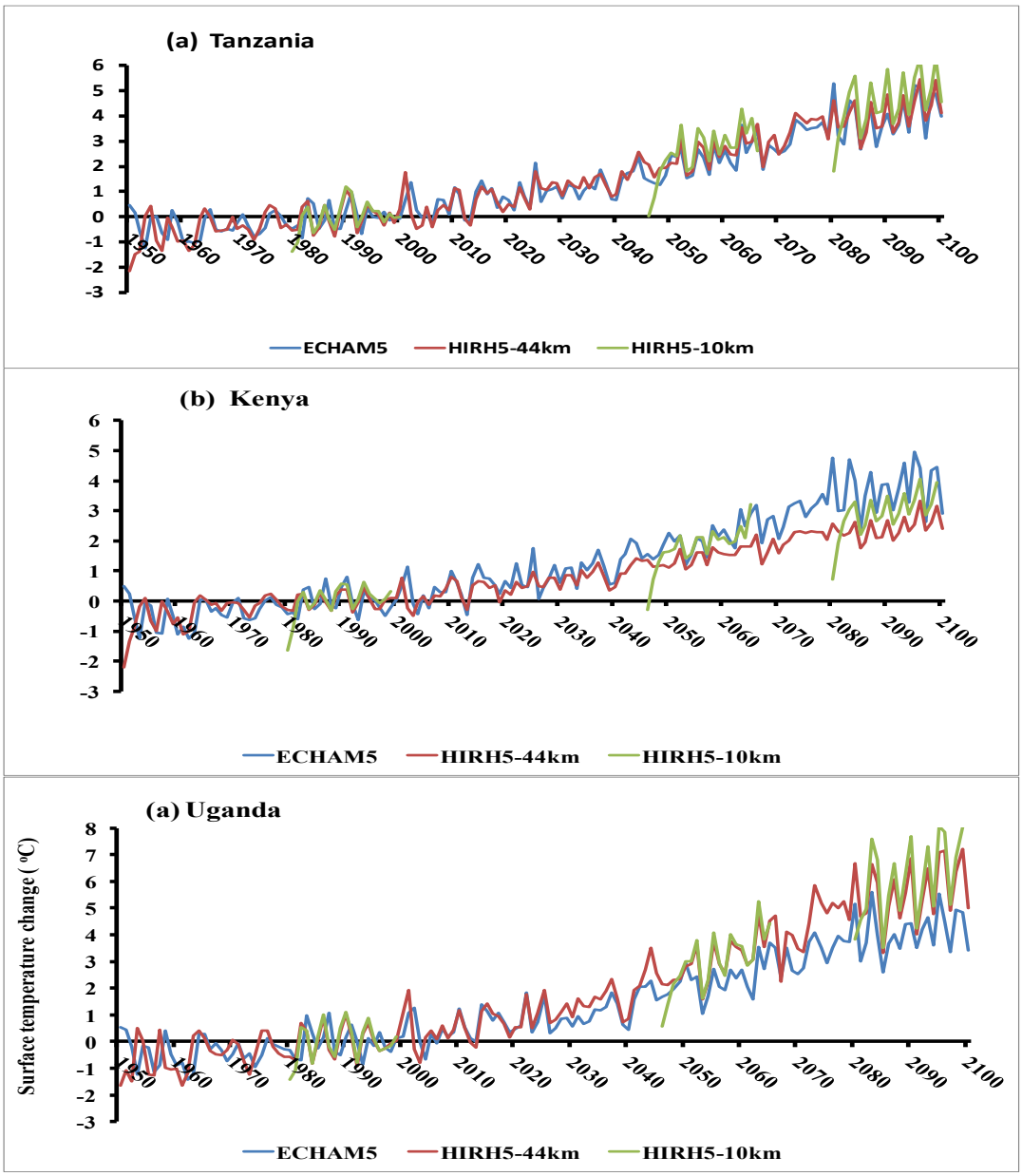

Figure 5.8: Mean surface temperature change time series (^{o} C) relative to control period (1980–1999) as simulated by HIRHAM5 downscaled in two resolutions, 50 km (HIRHAM5-50km) and 10km (HIRHAM5-10km), and their boundary forcing ECHAM5 for the selected three regions of East Africa: (a) Kenya, (b) Uganda and (c) Tanzania.

Figure 5.8 presents the results of the time series of surface temperature change relative to the control period (1980–1999) over the averaged area of the study domain (as in Figure 5.2). The

results show an increase in mean surface temperature change in the near future and far future climate scenario. As in the previous spatial patterns simulations in Figures (5.6 and 5.7), the minimum increment of temperature for the averaged entire regions ranges from 0.5–2^{o} C, while the maximum increment ranges from 5^{o} C to ~7^{o} C in the early and late 21st century respectively. This result agrees with most of the previous studies and the IPCC reports (AR4 and AR5) that the surface temperature has increased and is projected to increase in the 21st century due to an increase of greenhouse gases emission in the atmosphere, and the climate system's response to increased greenhouse gas forcing, which includes climate sensitivity and feedbacks.

This section presents simulations of surface temperature change over East Africa. All models simulate increase in surface temperature for the entire period. High resolution HIRHAM5 simulates higher increase in surface temperature over a larger area than ECHAM5. In all models the maxima temperature change (~7^{o} C) is concentrated over the western side of the domain, including western and southern regions of Tanzania, and the Congo basin area. This could be associated with the circulation pattern on both local and larger scale impacts, which will be discussed in section (Section 5.3).

5.2.1: HIRHAM5 simulations of the projected changes of extreme surface temperature

This section presents HIRHAM5 simulations of the projected changes of extreme surface temperature expressed in the 90th percentiles of daily maximum and minimum temperature in the MAM and OND seasons. One of the key messages in the recent IPCC (2012, AR5) reports, at the global context is that it is "**virtually certain** that increases in the frequency and magnitude of **warm daily temperature extremes** and decreases in **cold extremes** will occur ".

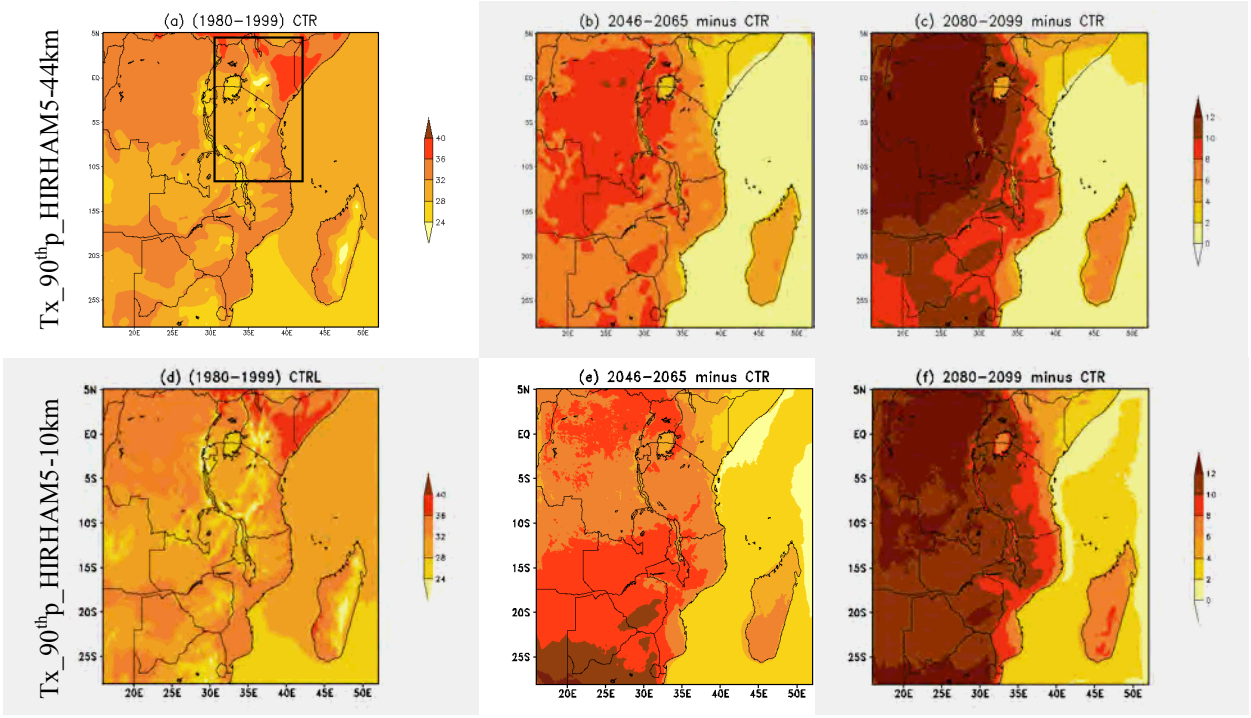

Figure 5.9: The 90th percentile of the maximum temperature (^{o} C) change in MAM season as simulated by HIRHAM5 at 50 km (first row) and 10km (second row) for control period (first column), near future (second column) and far future (third column).

Figure 5.9 shows the warmest days expressed in the 90th percentile of daily maximum temperature as simulated by HIRHAM5 over East Africa. The results show that the warmest days are increasing in both HIRHAM5 resolutions from present to far future climate scenarios. More increase in extreme maximum temperature is confined over the western side of the domain (the Congo basin area). The highest maximum temperature increase (~11^{o} C) is projected for the far future confined over the western portion of domain followed with the extreme over the western regions of Tanzania, Kenya, Indian ocean and over the northern portion of Madagascar (~8^{o} C). The lowest extreme maximum surface temperature is projected over the Indian Ocean and the coastal belts of the East Africa (the coastal region of Tanzania and Kenya) and the highlands. This result depicts previous studies and reports (IPCC 2007, 2013), that the surface temperature is increasing over the whole globe including the East Africa (Shongwe et al 2011;

Pachauri 2012, IPCC (AR5)). For example, one among the key messages in these reports, at the global context is that, "**Virtually certain** that increases in the frequency and magnitude of **warm daily temperature extremes** and decreases in **cold extremes** will occur".

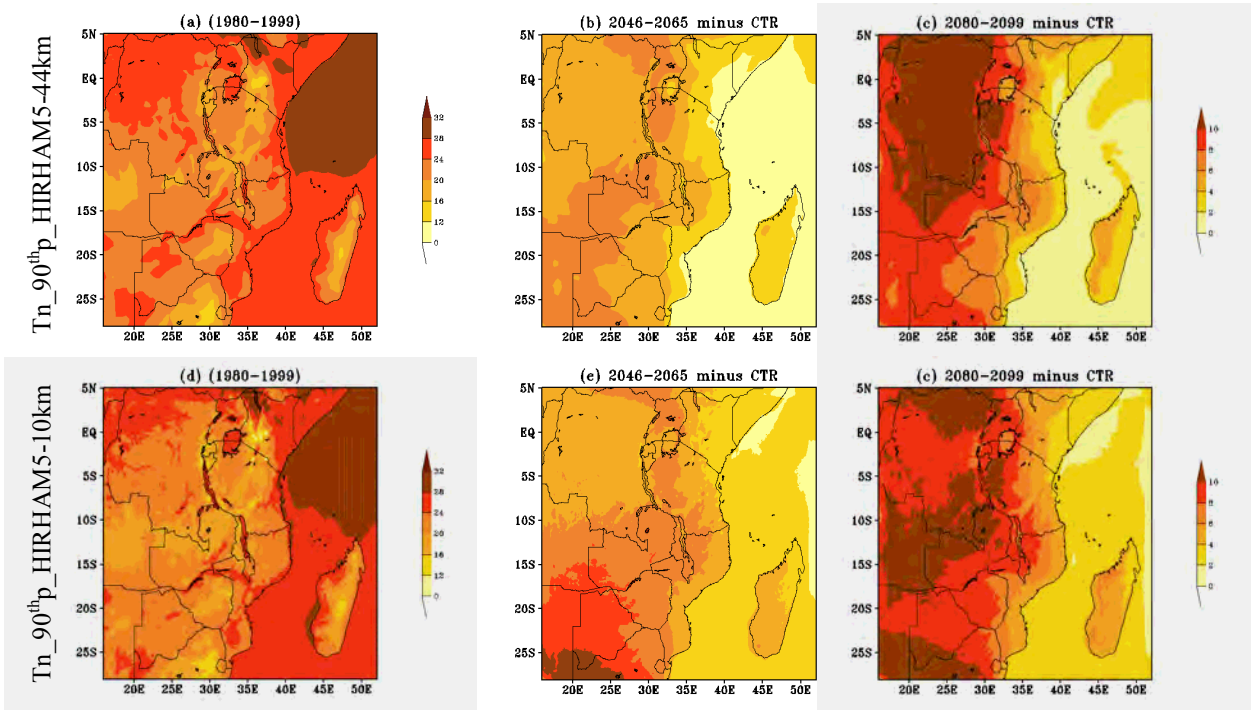

Figure 5.10: The 90th percentile of the minimum temperature (^{o} C) change in MAM season as simulated by HIRHAM5 at 50 km (first row) and 10km (second row) for control period (first column), near future (second column) and far future (third column).

Figure 5.10 presents the results of the projected changes of extreme minimum temperature following the procedure from the previous figure (Figure 5.3). The overall results show that the extreme minimum temperature (warmest night temperature) is increasing more in the near and far future climate scenarios. However, the two resolutions show some similarities, HIRHAM5-50 km simulates slight warmer increase in surface temperature projection in comparison to HIRHAM5-10km. The surface temperatures are increasing towards the mainland from the coastal (the Indian Ocean) belts of Tanzania and Kenya. The temperature along the coastal regions are projected to increase in the far future by around 4–5^{o} C which increases as one moves further into the mainland of East Africa. Increased warming is more confined to the west portion

of the domain which could be related to the influence of the warming over the South Pacific and South Indian Ocean (McHugh 2004). It has been shown that increased warming in Africa, and especially is linked not only to the global change but also to land use change (Moore et al. 2011; Omumbo et al. 2011). HIRHAM5 projects a maxima increase in extreme hot night temperature above ~7^{o} C which is confined over the southern and western portion of the domain (western regions of Tanzania to Congo basin area) in the near future. The coastal belts of East Africa and the high grounds are projected to have an increase in minimum temperature from 2 to 4^{o} C. In the far future, both resolutions project more increase in extreme minimum temperature, however, low resolution projects slight warmer in comparison to high resolution. As said before the temperatures are increasing from the coastline to the mainland of East Africa, showing the inertia property of the water surface and the land surfaces. Like 2m and maximum temperature the maxima extreme minimum temperature are confined over the western portion of the domain (western Tanzania, Congo basin area). The projected increase in extreme maximum (Figure 5.9) and minimum (5.10) temperatures could be associated with the changes in the thermodynamic patterns influenced by the increase in global warming.

5.3. The projected changes of the dynamic and thermodynamics variables

This section discusses the projected changes of the dynamic of the climate change over East Africa. The focus will be on the projected changes of surface winds, total cloud cover and specific humidity. The wind circulation patterns, discussed in Chapter 2, have impact on both rainfall and surface temperature. Previous studies (Nicholson 1996; Stefan Hastenrath & Polzin 2003; Mapande & Reason 2005; McHugh 2006; Mutai & Ward 2000; Hastenrath et al. 2011) have found that the surface circulation variability over Indian and south Pacific Ocean are associated with the climate variability over East Africa. McHugh (2004) found that circulation variability in the subtropical South Pacific Ocean has a significant but seasonally varying influence on East African rainfall on inter-annual timescales. Moreover, the impact of adiabatic uplift of moist Indian air masses over the highlands of East Africa as a prime source of rainfall generation, but suggests that negative SST anomalies over the Benguela current are associated with a strong anticyclonic circulation over the subtropical South Atlantic and inland penetration

of Atlantic air masses. Above normal sea surface temperature over Indian Ocean, which normally occur during ENSO events, are associated with weak easterly flow which enhance moisture inflow to the East African mainland and hence more rainfall receipt. In contrast, anomalous cold sea surface temperature over western Indian Ocean is characterised with strong easterly winds which draw away the moisture over the mainland of East Africa to the west, and hence the area remains dry.

In this section the projected changes of surface winds and other parameters will be investigated to see if there is a kind related to this extreme condition. Apart from winds, total cloud cover, moisture and evaporation will be investigated. Early studies have linked changes in total cloud cover with climate change through the large impact on the radiation over the planet (Manabe and Wetherald 1975; Zelinka et al. 2012). Moreover, moisture and evaporation are also found to have impact on rainfall and surface temperature. All these variables will be investigated on how they change with increasing resolution of HIRHAM5. The following figure presents projected changes in circulation patterns in the near and far future climate scenario relative to the control period.

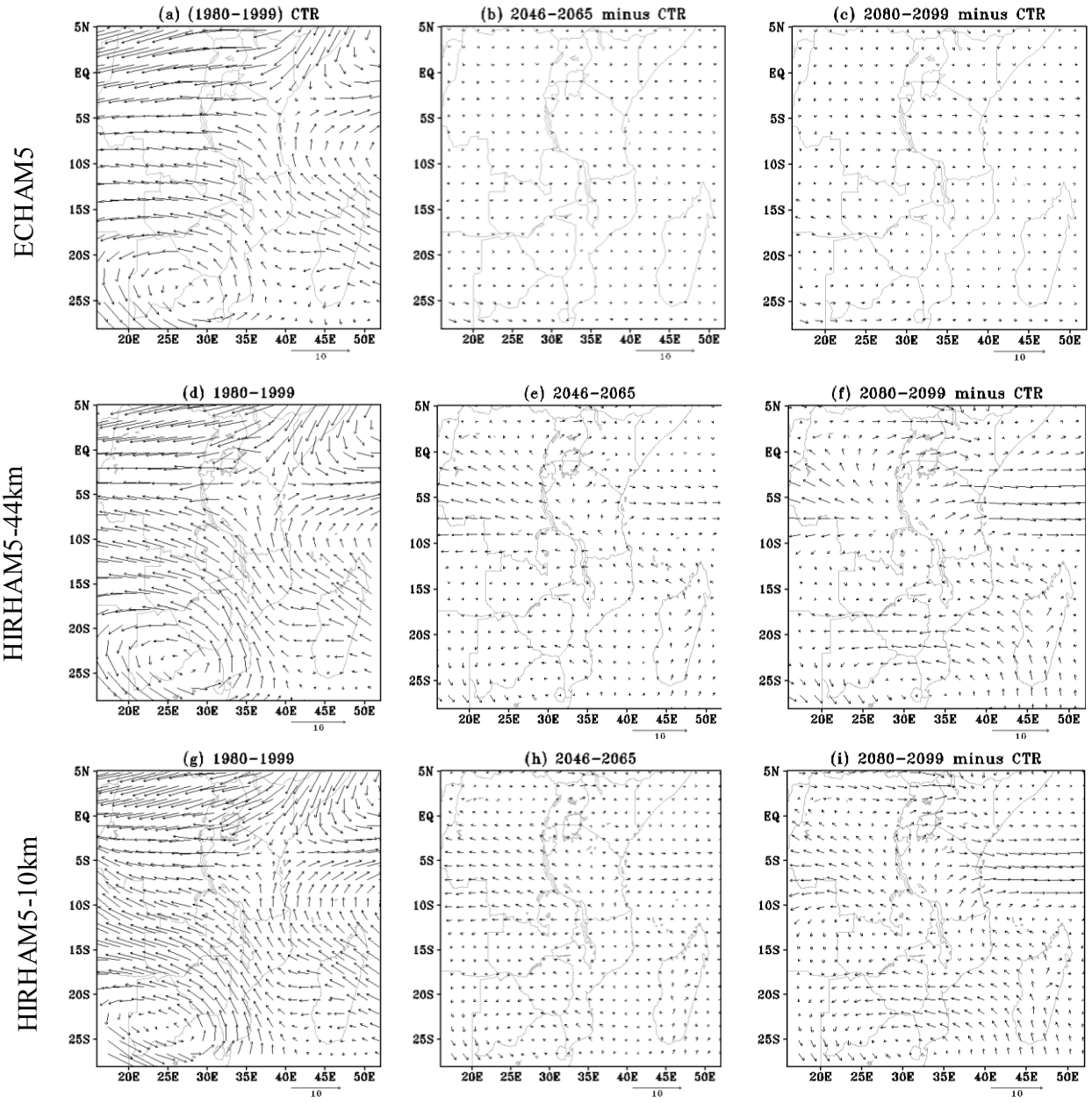

Figure 5.11: Rainy season (OND) wind vectors in 700 hPa (m/s) as simulated by ECHAM5 (first row), HIRHAM5 at 50 km (second row) and 10km (third row) in three time slices: control period (1980–1999) CTR in the first column and their differences: 2046–2065 minus CTR, and 2080–2099 minus CTR in the second and third column respectively in OND season.

Figure 5.11 presents the results of ECHAM5 and HIRHAM5 simulations of the projected changes of surface circulation anomalies relative to the control period. The results of the control

period (first column) for both ECHAM5 and RCMs simulate similar pattern distribution, which indicate some good agreement between RCMs and their boundary forcing, in terms of their physics and dynamics schemes. The results of the projected changes of the simulated winds in ECHAM5 show significant difference from the RCMs. In the near and far future the winds in ECHAM5 show very small change in comparison to RCMs. This is in agreement with the projected change in rainfall in ECHAM5, where the signals of changes were very small. On the contrary, HIRHAM5-50km and HIRHAM5-10km show significant changes in the near to far future. The winds are projected in both resolutions to increase in the near future and more increase is expected in the far future climate scenarios. In both RCMs, the westerly flow across the Western Indian Ocean, off-coast of Tanzania increases in strength, which is a sign of drawing away the moisture from the mainland of East Africa regions. Over the Congo basin forest, the main source of moisture in flow to the region the winds show decrease and diffluent pattern over the same area, the region which was expected to bring moisture to the region of interest (Uganda, Kenya and Tanzania).

Overall results show that in the future climate scenario surface wind anomalies are increasing in strength as they enter in the mainland of Kenya, Uganda and Tanzania. This is a sign that these winds draw away moisture from the mainland. Previous studies have shown that, weak westerly flow from Congo basin is a sign of rainfall over the East African mainland (Kijazi & Reason 2012; Cook & Vizy 2013). However, the projected change of winds show diffluent pattern which do not support moisture flux to the regions. Note that in the first section (Figures 5.1-5.3), mean rainfall is projected to decrease and more decrease is confined in the eastern portion of the domain (coastal belts of Kenya and Tanzania). The surface circulation pattern also project signals of these changes. In Figure 5.9 (second and third column) there is a divergent flow over the Congo Basin. The coastal belts of East Africa (entire eastern portion of Kenya and Tanzania) are projected to have strong diffluent pattern (over Kenya there is well defined core) and in all model simulations. This corroborates that the projected changes of rainfall and surface temperature are related to circulation patterns.

In contrast, over the western portion of the domain (especially over the northern Congo Basin) HIRHAM5 at both resolutions simulates a considerable decrease in extreme heavy rainfall and

increase drought condition (Figures (5.3 to 5.6)). The projected circulation patterns are also in agreement with this condition. In the Figure 5.3 (second and third column), over the western portion of the domain, the same region where it is projected to have an increase in extreme heavy rainfall, is projected to have strong convergence circulations. It is noted that the Congo Basin forest is one of the three key convective regions on the planet associated with global tropical rainfall (Washington et al. 2013). The model projects decrease in convective features in the near future and far future climate scenario. The sub-tropical highs, Mascarene and St Helena High which also play part in the rainfall variability over East Africa, is projected to shift to the mainland of southern South Africa where the winds change from south-easterly to easterly flow (specifically in MAM season) and therefore advect moisture from the Indian Ocean. Further north, the winds tend to turn into southerly flow, especially when it enters the mainland of southern portion of Tanzania. Further to the central regions the winds formulate an outflow and become strong westerly flow to the Indian Ocean. These results depict a previous scenario when the East Africa experienced extreme dry conditions (Lyon & DeWitt 2012). The anomalous 850hPa winds (Appendix 2) show westerly flow along the coastal East Africa and increases south of the equator which was associated with an abrupt decline of MAM rainy season in East Africa rainfall. This study presented the winds at 700hPa and the 850hPa level (Appendix3). All these results show remarkable shift of circulation patterns.

It is also important to note that the subtropical high pressure centers in the south Pacific (St Helena high) and southern Indian (Mascarene high) Ocean together with the Arabia high have great influence on East Africa climate variability. Early onset of the short rainy season (OND) was associated with the southward orientation of the Arabian high which weakened the Mascarene high to give room for the ITCZ southward movement (Sun et al. 1999). On the other hand, by relaxation of the Mascarene high, the St Helena high is enhanced which advect moisture from the Atlantic Ocean through Congo boundary air mass which enhances moisture flux to the East African mainland. The opposite is true for rainfall deficit. Moreover, the displacement of the position of these high pressure centers from the normal position also has impact on East Africa climate. Manatsa et al. (2014) have found that when Mascarene high is displaced to the west from its normal position, the south east trade winds over the South Indian Ocean (SIO) anomalously strengthen which enhances strong south easterly flow which is cool

and dry over the mainland and therefore results in a rainfall deficit over of East Africa. The projected surface winds changes in HIRHAM5 simulations show anomalous increase of westerly flow over the mainland of East Africa (Tanzania) and the south western Indian Ocean in the near and far future climate scenarios.

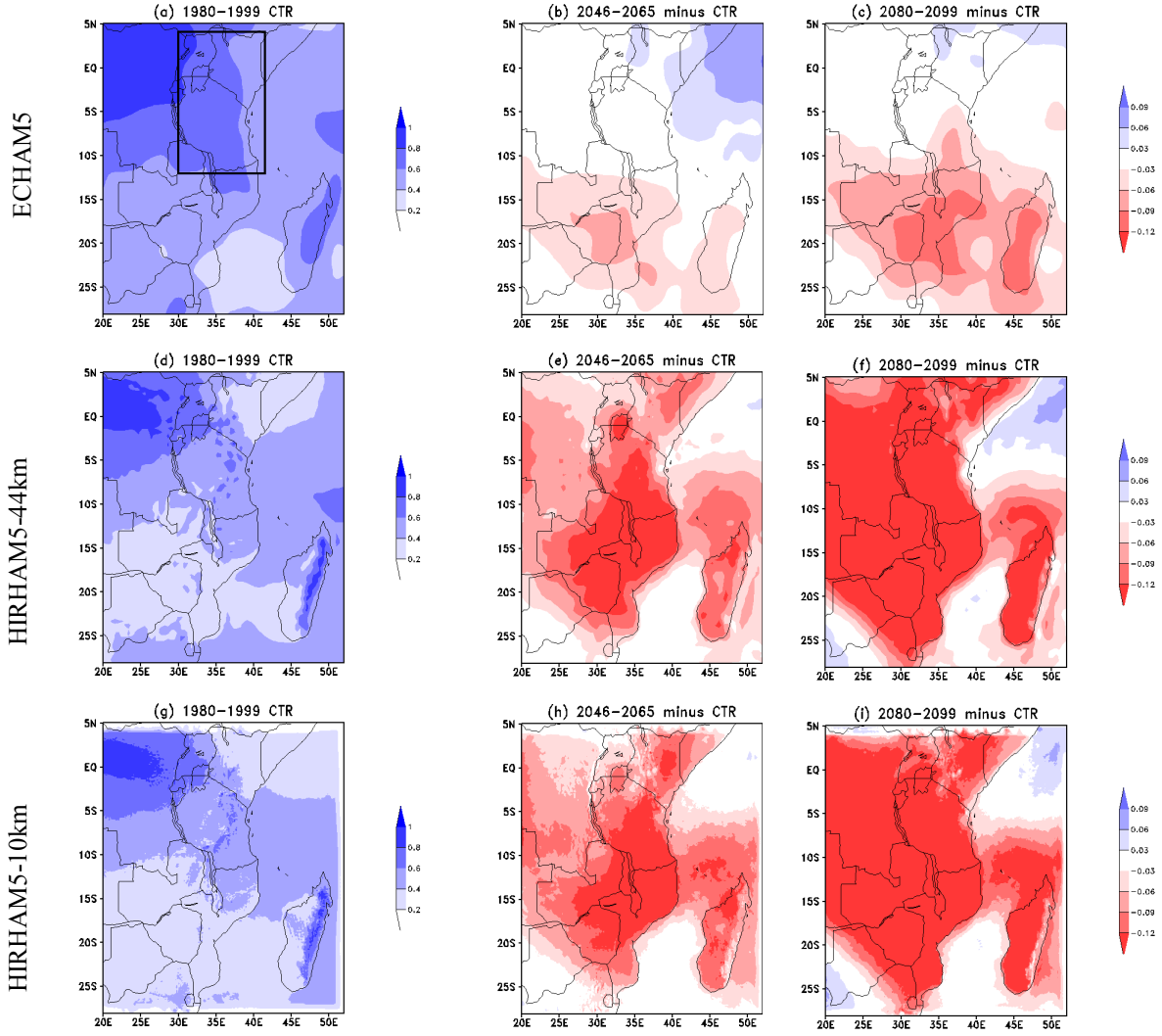

Figure 5.12: The projected mean change of the total cloud cover as simulated by ECHAM5 (first row), HIRHAM5 at 50 km (second row) and 10km (third row) in three time slices: control period (1980–1999) CTR in the first column and their differences: 2046–2065 minus CTR, and 2080–2099 minus CTR in the second and third column respectively in OND season.

Figure 5.12 presents the results of the projected change in total cloud cover calculated as the anomaly from the control period over East African domain. The results show similarities especially in the RCMs simulations. In the control period all model simulations show more cloud over the Congo basin area and the high grounds (more identified in the RCMs). The ECHAM5 simulation of the projected change of total cloud cover shows little change over large part of Tanzania, Kenya, and Uganda and Congo area. This could be related to resolution. ECHAM5 due to its coarse resolution can only to a limited extent capture the fine structure (surface moisture) over the region. It is noted that East Africa is associated with heterogeneous topography and this is why RCMs show more features compared to ECHAM5 with coarse resolution.

The overall results of the projected changes by RCMs simulations show decrease in total cloud cover in the near and far future climate scenario. The maxima decrease in total cloud cover (by 2 tenths) is projected over a large portion of north east Kenya, central to southern Tanzania towards Zambia and Mozambique in the near future, and almost the entire domain in the far future. The decrease in total cloud cover is linked to the increase in surface temperature (Figure 5.5 to 5.10) and surface winds (Figure 5.11).

The following equation presents the surface evaporation (E) change calculated from the latent heat flux (LHF) formula as follows:

$$E = \frac{Q_E}{\lambda} orE = \frac{Q_E}{2.5x10^6 Jkg^{-1}} \quad \text{.....(4)}$$

Whereas λ is the latent heat of evaporation a very large number. It is the number of Joules carried away from the surface per kilogram of water evaporating. Q_E is the latent heat flux in W/m^2.

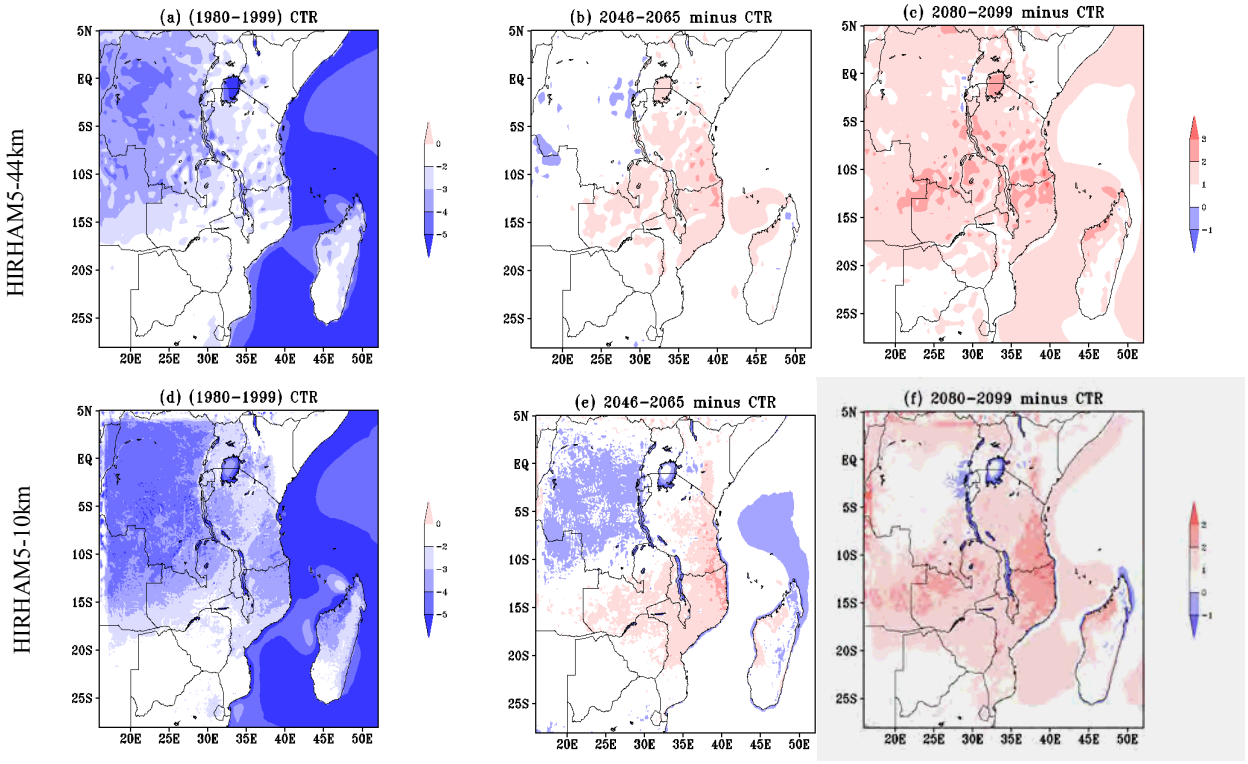

Figure 5.13: The projected mean change of evaporation (mm/day) as simulated by HIRHAM5 at 50 km (first row) and 10km (second row) in three time slices: control period (1980–1999) CTR in the first column and their differences: 2046–2065 minus CTR, and 2080–2099 minus CTR in the second and third column respectively in MAM season.

Figure 5.13 presents the projected mean change of evaporation as simulated by HIRHAM5 at 50 km and 10km resolution. It is clear that the evaporation sign is negative, indicating decrease in surface of moisture. The results show that in the control period the evaporation patterns in both resolutions have similar patterns, simulating more evaporation confined over the Indian Ocean and western portion of the domain (especially over Congo regions). The maxima (~5 mm/day) over the Indian Ocean and minima (trace or no evaporation) over eastern and northern Kenya and southernmost of the main domain is simulated in the control period. HIRHAM5 in both resolutions (50 and 10km), projects an increase in evaporation change in the near and far future climate scenario. The maxima decrease in evaporation (~3 mm/day) is confined over the western

portion of the domain in the far future in both resolutions (10 and 50 km). In contrast, in the near future the projection change is variable.

The overall results depict the physical relationship of patterns in the dynamic and thermodynamic changes. For example, the projection shows changes in surface temperature, winds and evaporation in the Figures (5.7–5.13). It is noticed that where there is decrease in evaporation, there is anomalous mean changes of zonal circulations, surface temperature and rainfall. This results agrees with the previous studies that soil moisture feedback have influence on rainfall over the region (Cook et al. 2006). They found that the increased soil moisture alters the surface energy balance, resulting in a shift from sensible to latent heating. This manifests in two ways relevant for precipitation processes. First, the shift from sensible to latent heating cools the surface, causing a higher surface pressure, a reduced boundary layer height, and an increased vertical gradient in equivalent potential temperature. These changes are indicative of an increase in atmospheric stability, inhibiting vertical movement of air parcels and decreasing the ability of precipitation to form. Second, the surface changes induce anomalous surface divergence and increased subsidence. This causes a reduction in cloud cover and specific humidity above 700 hPa and results in a net *decrease* of column integrated perceptible water, despite the increased surface water flux, indicating a reduction in moisture convergence. Based on this and a previous study, soil moisture may act as a negative feedback to precipitation in southern Africa, helping to buffer the system against any external forcing of precipitation (e.g ENSO).

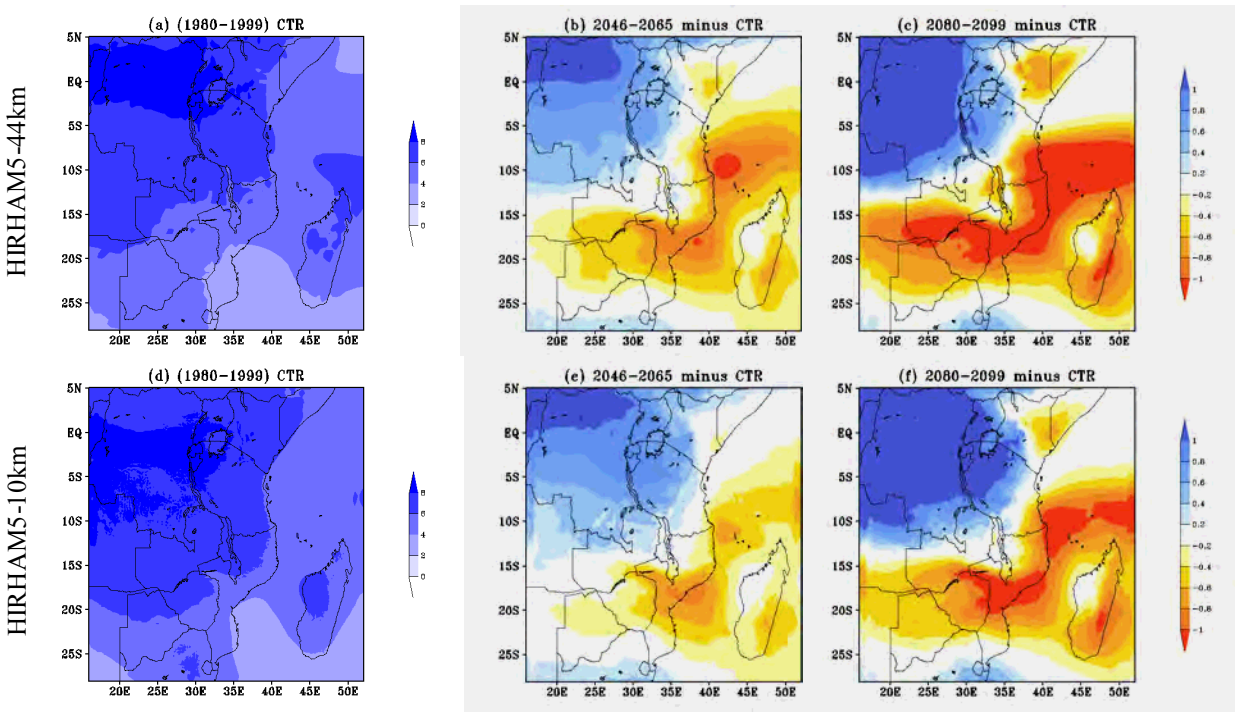

Figure 5.14: Projected mean change of 700 hPa specific humidity (g/kg) in the wet season (MAM season) as simulated by HIRHAM5 at 50 km (first row) and 10 km (second row) for present-day climate (1980–1999, left column) and the differences to present-day climate for 2046-2065 (mid column) and 2080-2099 (right column).

Figure 5.14 presents the surface moisture change projection as simulated by the downscaled HIRHAM5 at 50 km (first row) and 10km resolution (second row) in MAM season. The results show similar patterns in both coarse and high resolution of HIRHAM5. In the control period more moisture is confined in the northern part and over a large portion of the domain. The maxima in the control period (~8 g/kg) are confined over the western portion of the domain (Congo basin area) and the high grounds of Tanzania, Kenya and southern portion of Uganda. On the other hand the lowest moisture is confined over the extreme south of the domain, followed by north East of Kenya (Figure 5.13c). HIRHAM5 in both resolutions projects decrease in moisture over a large portion of the domain.

However, the large part of the remaining regions such as the coastal belt of Kenya and Tanzania, the southern Tanzania and north east Kenya are projected to have less moisture in the near and far future climate scenarios. More decrease in moisture is projected in the far future and slightly more decrease in the low resolution in comparison to the high resolution. In the near future over the north east Kenya and the coastal and southern regions of Tanzania are projected to have significant decrease (-1g/kg) in moisture in the near and far future as well as significant decreases in total cloud cover, whereas winds at 700 hPa and 850 hPa (not shown) are projected to increase in strength and become more westerly. For example in the Figure (5.11, second and third column in each simulation) there is a strong westerly flow passing over the mainland of Tanzania which sweeps away the moisture to the Indian Ocean. This result supports the projected decrease in rainfall and increase in drought condition in the future scenario over the region. Higher resolution reproduces the same, however with a slightly smaller magnitude. HIRHAM5-10km simulates maxima along the southern coast (slight shift and in smaller area (5.11f)) in comparison to low resolution (5.11c) where the maxima is projected over the large portion of northern to southern Coast of Tanzania.

Furthermore, the projected increase in moisture is confined over the warmest temperature (Figure 5.12), which is clear, since warm air can hold larger amounts of moisture than cold air. On the other hand, the projected decrease in specific humidity is also confined over the north-east Kenya decreasing area increases in the far future (Figure 5.12 (b, c)). The coarse resolution projects more decrease in moisture change (also slight increase mainly over Congo) in the future in comparison to the high resolution (Figure 5.22, third column). This result also is related to the previous results of rainfall, temperature and total cloud cover. The area of maxima total cloud cover is where the specific humidity is high and the opposite is true.

5.4 Summary

This chapter explored the projection of mean and extremes of rainfall and surface temperature changes over East Africa during MAM and OND (in the Appendix 2) season. Moreover, the dynamic and thermodynamic changes of the projected variables such as surface winds, total

cloud and moisture ere explored. The HIRHAM5 simulations results are not far from the state of the art models used on the assessment of the IPCC AR5 report. HIRHAM5 simulates changes in mean and extreme heavy rainfall and surface temperature in the future climate scenario over East Africa. It is also noted that climatic variables are transient, and these changes are related to each other (Figure (5.1 to 5.13). The total cloud cover is projected to decrease in the near and more significant decrease is projected in the far future. This could be related to the increase in temperature. In this study, total cloud cover decreases in the near and far future which reflects a decrease in albedo. From the previous studies, decrease in albedo is reflected to increase surface temperature. It is also noted that HIRHAM5 in both resolutions projects increase in surface temperatures both in mean and extreme terms. Furthermore, the specific humidity decreases over the regions with strong diffluent pattern, more noticeable the northern coast of Tanzania (Dar es Salaam, Pemba and Zanzibar). This area has significant change even in the total cloud and precipitation.

It is not easy to assess the credibility of the projected changes. Seen in terms of dynamical variables, the model demonstrates good skill. Moreover, the projected increase in mean and extreme surface temperature is consistent with most of the previous studies, though they are in a global context (IPCC, 2007, 2013). However, the results of precipitation vary with GCMs simulation; there are some similarities in the previous and with the present study. HIRHAM5 in both resolutions projects an increase in extreme heavy rainfall change over the entire domain, considerably confined over Congo basin forest. Meanwhile, HIRHAM5 projected decrease in drought over western domain mainly Congo basin forest and increase in drought over the remaining portion of East Africa (eastern portion of domain). These results are similar to those from GCM projection (IPCC, 2007, Shongwe et al.2011) and even more similar to the RCM projection (Cook & Vizy 2013). It is important to note that GCMs are limited in their capacity of resolving East African climate due to their resolution limitation (Flato et al. 2013).

HIRHAM5 in both resolutions also projects an increase in surface winds in all seasons. It is known that East African climate is influenced by surface circulation patterns. Strong /weak easterlies could enhance or decrease rainfall over East Africa. Moreover, enhanced (reduced) westerly moisture flux from the southern Congo basin occurring during the wet (dry) seasons is

associated with heavy rainfall over East Africa. This is also true during warm ENSO years (Mutai & Ward 2000; Indeje et al. 2000). During ENSO warm years, over the western Indian Ocean close to the Tanzania and Kenyan coast, winds are south-easterly to easterly and weaken as they enter the East African mainland resulting in above normal rainfall.

In this study, HIRHAM5 at both resolutions projects an increase in surface wind anomalies over the mainland of Tanzania and Kenya, with a decrease in surface moisture over the same region and an increase in surface temperature. Overall results show that rainfall and surface temperature changes are related to the changes in total cloud cover, surface moisture, evaporation and vertical uplift winds which are considerably decreasing in the future climate scenarios.

Increasing resolution also shows some impact on the projected changes in circulation patterns. The projections show positive anomalies of surface winds around 4 to 6 m/s in HIRHAM5-50km while in HIRHAM5-10km around 2 to 3 m/s in the near and far future respectively. As discussed above, wind speed has an impact on surface moisture, as strong winds lead to a decrease in surface moisture and hence rainfall. As such, it is not surprising to observe that HIRHAM5-50km simulates more decrease in rainfall than HIRHAM5-10km. In our case, surface temperatures and surface pressure are projected to increase (not shown). In the south-west portion of the domain there is anomalous increase in surface winds showing intensification of surface temperature in the near future. This is where the surface temperature is also very high, and there is more reduction of rainfall.

The overall results show some links in the changes of both rainfall and temperature. For example, the surface winds are noted to increase in the near and far future, total cloud cover is decreasing in the near and far future; surface evaporation is decreasing in most cases, although in the near future there are some traces of an increment over the western portion of Uganda. Indeed, there is clear relationship of this variable. It is observed that any change, whether positive or negative, affects the other. The vertical uplift of winds from 850 to 700hPa also shows a decrease in the near and far future; however, over Congo and most of the western portion where the winds are slightly weak, the vertical uplift shows a slight decrease.

Higher resolution (10km) simulates better representation of these features compared to low resolution (50 km). This result is in line with Cook & Vizy (2013) who projected reduction of rainfall in MAM season and increase in extreme precipitation in the future projection over East Africa. This study focused on the resolution dependency in the simulation and projection of East African climate. The overall results show that rainfall simulation in HIRHAM5 is resolution dependent. Moreover, more increase in rainfall is projected in higher resolution than in low resolution.

For surface temperature change projections, mean surface temperature changes and extreme surface temperature changes expressed in the 90th percentile for MAM, OND and JJA season were presented. The overall results show increase in surface temperature over the entire domain and in all season and models. The maxima mean temperature change as projected by HIRHAM5 in both resolution is ~6^{o}C which is confined between 17^{o} E–34^{o}E and 27^{o}S–4^{o} N of the equator in the far future climate scenario. The minima increase occurs over regions close to the Indian Ocean (East African coast, the area between 33^{o} E–44^{o} E). The main differences between coarse resolution (ECHAM5) and HIRHAM5 occur in the intensity and distribution. Moreover, ECHAM5 also projects increase in mean surface temperature change with maxima (~5.7^{o} C) confined over the extreme south-west of the domain in all seasons in the far future. The minima (3.5^{o} C) are confined over the coastal belts of East Africa (between 35^{o} E–40^{o} E) and the Indian Ocean (north and eastern portion of Madagascar). This was also noted earlier in the evaluation of HIRHAM5 in simulating present day climate.

Chapter 6

Synthesis

High resolution regional climate model offers advantages in simulating regional climate variability and change at a local/regional level. This thesis aimed at investigating the resolution dependency which is the key factor in the simulation and projection of climate variability and change over East Africa. The model's ability to represent mean and extreme rainfall and surface temperature climatology as well as possible dynamic and thermodynamic impacts of the projected changes was discussed. The following specific questions have been addressed to increase the understanding of the significance of increasing resolution in regional climate models:

1. How well does HIRHAM5 simulate East African climatology and extreme climatic events?
2. Does increasing resolution of HIRHAM5 model improve the simulation of East African climate variability?
3. How does increasing resolution of HIRHAM5 impact the projected climate change in East Africa?

In order to answer the first question, in chapter 3 HIRHAM5 model performance was evaluated in reproducing observed relevant climatic features in East Africa. The seasonal climatology of rainfall and surface temperature were explored relative to the observation datasets from CRU and FEWS. Moreover, the annual cycles of rainfall and temperature, and seasonal circulation patterns were also investigated.

In order to answer the second question, in chapter 4 HIRHAM5 simulations of the inter-annual variability of rainfall and surface temperature were compared with the observation datasets from

CRU and FEWS. Correlation coefficients for each dataset relative to CRU were done in simulating both spatial and temporal variability. Furthermore, composites of ENSO years when rainfall was above normal (El Niño) and below normal (La Niña) (Indeje et al. 2000) were explored relative to the observation. Additionally, the correlation analysis of both rainfall and surface temperature relative to the sea surface temperature anomalies using Multivariate ENSO Index (MEI) for the selected wet months of NDJ was explored. The data used in this question spans from 1990 to 2007.

In answering the third question on climate change projection over East Africa, in chapter 5 the projections of both mean and extreme rainfall and surface temperature changes relative to present day climate over East Africa using HIRHAM5 at 50km, HIRHAM5 at 10km and the boundary forcing, ECHAM5 were explored. Furthermore, using both resolutions of HIRHAM5 and ECHAM5, projected future climate variability and change in three time slices were presented. The results were compared to present day climate (1980–1999), for the near future (2046–2065) and far future climate (2080–2099) scenarios. Furthermore, the study investigated the dynamic and thermodynamics of the changes of climate variables in the same way (three time slices), where the climate change relative to the changes in the surface winds and vertical uplifts, total cloud cover, surface evaporation and specific humidity at 700hPa were assessed.

6.1 Discussion

Chapters 4–5 presented findings on the ability of HIRHAM5 in reproducing observed climatology and climate variability over East Africa. The two questions are answered together because they are related. It is clear that in the model evaluation rainfall is more challenging than temperature (Flato et al. 2013). The model simulation of the annual cycles of rainfall and surface temperature were also well represented. HIRHAM5 driven by ECHAM5 at 10km and 50 km resolution represented reasonably well the annual cycles without missing the months of maxima and minima. It is noted that during MAM rainy season the maxima occur around April while in OND the maxima occur around November. However, the higher resolution HIRHAM5 at 10km shows better skill in representing the local topography than HIRHAM5 at 50km (Mutai et al.

1998). In the simulation of rainfall climatology of present day climate in comparison to FEWS, HIRHAM5at 10km simulates better than HIRHAM5 at 50km resolution, in accordance with previous studies which show that higher resolution regional climate models perform better than the coarser ones (Dankers et al. 2007; Wilby & Fowler 2010; Lucas-Picher et al. 2012). Dankers et al. (2007), in the evaluation of high resolution regional climate models in the simulation of the small scale features (river flow), found that 12 km resolution represented the orographic precipitation patterns and extreme rainfall better than the 50km resolutions. Likewise, Lucas-Picher et al. (2012) found that increasing resolution decreases bias in rainfall and surface temperature.

Furthermore, HIRHAM5 model simulations show good skill in representing the circulation patterns in the geographical differences and seasons relative to the observed field. The areas of strong convergence and divergence are realistically represented by the model during the wet and dry season respectively (Hastenrath et al. 2011; Mbululo 2012). The high pressure centres in southern and northern Africa were well represented as suggested by observed fields and previous studies (Nicholson 1996), showing that the model skill is good. Furthermore, in the model evaluation with focus to the boundary forcing impact using PAV method (potential for added value) using the idea in Di Luca et al. (2012) is presented. HIRHAM-ERAI showed better skill than the rest of the models. However, HIRHAM5 at 50km and HIRHAM5-10km simulate large errors which is suggested to be linked to the model parameterisation, as noted when HIRHAM5 simulations were evaluated in Chapter 4 relative to their resolution and boundary forcing.

In the simulation of the inter-annual variability, using the composite of warm and cold ENSO years, HIRHAM-ERAI demonstrated good skill over most parts of the study domain by simulating positive anomalies during ENSO warm and negative anomalies during ENSO cold years. It is noted that in East Africa, above normal rainfall was associated with warm ENSO while below normal rainfall is linked with cold ENSO (Indeje et al. 2000; Wolff et al. 2011). In this case, the analysis of the inter-annual variability of East African climate using HIRHAM5-ERAI simulations of rainfall for 17 year data simulation (1990–2007) relative to the observed field, found that the model successfully reproduced the overall features of ENSO signals over the study domain. For example, HIRHAM5-ERAI simulated moderate positive correlation ($r \geq 0.6$)

over the entire domain in OND season. HIRHAM5 also showed some skill in the simulation of surface temperature correlation (especially HIRHAM5-10km) with MEI relative to the observed field.

Despite these strengths, HIRHAM5 showed some weakness in the simulation of the extent of rainfall and surface temperature. In the simulation of the extreme drought conditions expressed in the maximum number of periods with dry days when rainfall is less than 1 mm/day during the wet period, HIRHAM5 overestimated the drought condition or almost could not capture the pattern over the north-western portion of the domain (Congo basin). HIRHAM5 also underestimated drought conditions over the rest of the portion of East African domain. Moreover, HIRHAM5 at 50 km underestimated climatology of rainfall over low ground and overestimated over high ground and the Indian Ocean. Moreover, the model overestimated surface temperature in all seasons especially over the mainland and underestimated over the high ground and Indian Ocean. The coarser resolution HIRHAM5 (50 km) underestimated rainfall and overestimated surface temperature, while the finer resolution HIRHAM5-10km overestimated rainfall and temperature. Moreover, both resolutions of HIRHAM5 have wet and warm bias over high ground. The physical parameterisation of the model such as soil moisture and albedo can be sources of bias in the regional climate model. The model simulations of the heterogeneous land surfaces and topography, due to albedo contrast could increase bias of the model.

HIRHAM5 as a limited area model has inherited the physical parameterisation of the general circulation model used in the forcing, ECHAM5. Due to the limitation of its boundary, HIRHAM5 under ECHAM5 was limited in capturing some features in large circulation patterns. This is noted that in the simulation of ENSO relative to MEI values. HIRHAM5 at 50km and HIRHAM5 at 10km simulations of rainfall correlations with MEI differ from that of CRU and FEWS. However, better skill was manifested in the higher resolution HIRHAM5-10km when compared with CRU in surface temperature correlation with MEI. The large bias in HIRHAM5 rainfall correlation with MEI is suggested to be associated with the boundary condition. This was noted when HIRHAM-ERAI rainfall simulation was correlated with MEI. In this case,

HIRHAM-ERAI demonstrated good skill with ERAI (as the best estimate) and moderately with CRU and FEWS.

The answers for question 1 and 2 above have highlighted the understanding on the significant of increasing resolution in regional climate model, HIRHAM5. Furthermore, the evaluation of HIRHAM5 in both resolutions and under different boundary conditions (ERAI and ECHAM5) revealed the skill level of the model in reproducing East African climate variability and change.

Chapter 5 presented the findings regarding the performance of the downscaled HIRHAM5 model in the projected changes of mean and extreme rainfall and surface temperature over East Africa. Moreover, this chapter presented the dynamics and thermodynamics of the impact of changes in tonal and vertical winds, total cloud cover, specific humidity at 700 hPa level and evaporation. It is clear in this study and most of the previous studies that the projections indicate changes in both rainfall and surface temperature (IPCC AR4, AR5). In this thesis results, HIRHAM5 at 50km and HIRHAM5-10km project significant reduction of mean rainfall climatology in the future scenarios. For the extreme rainfall, the models projected an increase (not significant) in very heavy rainfall more confined to the western region over the Congo basin area; however this amount is decreasing significantly over the same portion in the far future climate scenarios (Figures 5.4 and 5.5). Other regions have shown less or no change in extreme heavy rainfall.

Moreover, the number of rainy days with more than 5 mm/day is projected to decrease in the near and far future. Furthermore, the number of rainy days with rainfall amounts less than 1mm is increasing in the near and far future. On the other hand, an increase in the maximum number of dry days occurring in the wet season (more than 5 days) is confined to the eastern portion of the domain which includes the mainland of the coastal belt of Tanzania and Kenya, and over the western Indian Ocean). These results agree with the recent study conducted over East Africa in using RCM simulations (Cook & Vizy 2013) who found that the East African long rainy season (MAM rainy season) is projected to decrease in the future climate scenarios.

Conversely, previous studies using GCMs differ in the simulation of the projected mean rainfall change from HIRHAM5 (Wit et al. 2005; Shongwe et al. 2011). In the projected mean and

extreme rainfall change using GCMs, Shongwe et al., (2011) found an increase in rainfall and reduction of drought over East Africa. In this thesis, it is also found the reduction of drought, though not for the entire region, mostly in the western portion of the domain. However, Cook and Vizy (2013), in using 6 members of regional climate models simulations at 90-km resolution projected future reduction of rainfall over larger parts of East Africa. They stressed that rainfall in boreal spring (MAM) over Tanzania and Kenya is reduced throughout the season in the future simulation. The results of the projection using HIRHAM5 simulations (in this study) also projected reduction of mean rainfall change over the entire domain (Tanzania, Kenya and Uganda) with, however, a considerable increase in extreme heavy rainfall over the Congo basin area. For projected changes of mean rainfall change, the model projected an increase only in small traces which are confined over a very limited area around extreme south-western Kenya and over small portions of the central western Congo.

This study also investigated the GCM which was used as the lateral boundary forcing of the downscaled HIRHAM5. It is surprising that ECHAM5 projected significantly different rainfall patterns in the near and far future in all seasons as both for near and far future climate, ECHAM5 projects an increase in rainfall in the near future during OND season. Moreover, in the projection of mean change of surface temperature, both GCM and RCMs project positive trends with differences in extent and distribution. In the future projection HIRHAM5 projected more of an increase in surface temperature changes over the entire domain consistent with previous studies and reports over East Africa (Collins et al. 2013). They projected more of an increase in surface temperature at a regional than a global mean scale. More warming is projected over the mainland than the coastal areas and over the oceans. The results of the projected changes of surface temperature show that surface temperature increases from the ocean towards the mainland. However, the projected changes of increase in surface temperature are not as dramatic over the ocean as the increase between the coastal belts and the mainland. Higher increase in temperature is located in the western portion of the domain, over the Congo basin and the extreme south-western portion of the domain, in the area of the anticyclonic flows (high pressure centre).

This study intends to add to the understanding that increasing resolution of RCMs provides more reliable results in comparison to coarse resolution. However, this was not evidenced overwhelmingly clearly due to a combination of model biases and the observations used in the model evaluation. This study has found that the major shortcomings of higher resolution HIRHAM5-10km are the overestimation of rainfall over the high ground and over the western Indian Ocean. The main reason here could be the boundary condition of the model. Moreover, the hindcast (HIRHAM-ERAI) poorly reproduced the observed rainfall and surface temperature under the ENSO influence over the East African mainland and Indian Ocean (Figure 4.3, third column). This could be linked to the error in model formulation. It is also noticed that the hindcast reproduces different from the boundary forcing. The discrepancy in HIRHAM-ERAI was also found in some of the previous CORDEX studies over the region (Meque & Abiodun 2014).

6.2 Caveat

The main limiting issue encountered in this body of work is in difficulties in evaluating the high resolution HIRHAM5 due to the constraints of observational data. The main task was to evaluate the impact of increasing resolution in simulating East Africa's climate. The main task to start with was to look for quality available observation data to evaluate the model.

The observation datasets from the meteorological stations along the Great Ruaha sub basin was used as the reference in the beginning of the RCM evaluation process. This area has great economic potential for Tanzania and East Africa in general due to the presence of the great dams which supply hydropower to Tanzania. Moreover, the area is less studied and is located in the transition region between bimodal and unimodal rainfall regime. Therefore, it is postulated to be a good representative of East Africa. However, this region has inadequate observation networks, poor and inconsistent observation data. It is finally decided to pick 3 stations from Tanzania Meteorological Agency (TMA) as the point stations for location of the bimodal and unimodal rainfall regime (TMA). In order to capture spatial and temporal patterns of East Africa, FEWS and CRU datasets were used. Nonetheless, these two datasets differ from their source and

resolutions. FEWS is a high resolution data (0.1^{o}) gridded satellite-derived precipitations estimate covering the entire African continent while the CRU is a low resolution (0.5^{o}) dataset which includes rain gauge station-based monthly precipitation, and surface temperature. Note that FEWS has only rainfall data while CRU has both monthly rainfall and surface temperature. For the wind data, the reanalysis data ERA-Interim was used as the best estimate. Using different observation datasets, it is found that every observed field reproduced significantly differently, especially in extent. For example, in the comparison of the spatial distribution of the observed rainfall data in CRU relative to FEWS, it is found that CRU show less rainfall in all seasons and over the entire domain. Also, in the comparison of the observed rainfall data in ERAI relative to CRU, the results show less rainfall in CRU throughout the domain and in all seasons (Figure 3.8). Therefore, different observation datasets in this thesis work reveal some difficulties in deciding the level of skill of the model. However, due to the fact that the model was able to show some skill within the constraints posed by the observational reference data, it is found that the evaluation of HIRHAM5 model does not disqualify it from further use for climate change studies.

The effort was made to then collect data from the meteorological stations (Tanzania Meteorological Agency) and from the cited region of reference. However, the data that was collected did not meet the requirements due to the inadequacy of the observation networks and poor quality of the data. This is the case for many stations in East Africa. Therefore, Therefore, the blended satellite with gauge data from FEWS along with CRU data sets which cover large areas and with better quality were used. Despite their spatial and temporal coverage, these datasets have different quality which sometimes made the evaluation process difficult, as they have different types of observed data (satellite and reanalysis). Moreover, CRU datasets have only monthly (no daily data) datasets and without wind data. In order to evaluate model performance in relation to winds, instead of CRU as observed data, ERAI as the best estimates was used. However, ERAI is also at coarse resolution like the CRU dataset (~50km) when compared to FEWS. Moreover, CRU has no data over the remote areas (over the Indian Ocean and high ground). Instead, FEWS which has higher resolution and daily rainfall data with large coverage were used . Despite good quality and coverage, FEWS has only rainfall data; therefore, other parameters had to come from the CRU and ERAI datasets. Consequently, different

datasets provided quite different representations of rainfall and surface temperature. Although HIRHAM5 showed good skill in simulating some patterns, for example annual cycles of rainfall and inter-annual variability of rainfall and surface temperature, the observation confused some of these results. This is evidenced, for example, with Sylla et al. (2013) who found uncertainty in observations as a key factor in preventing a rigorous and unambiguous evaluation of climate models over Africa.

Moreover, in the model evaluation the target was to use two pairs of HIRHAM5 datasets: the hindcasts of HIRHAM5 under boundary forcing of ERAI at 10km and 50 km resolution, and HIRHAM5 at 50 km and 10km resolution under GCMs (ECHAM5) forcings. However, HIRHAM5 at 10km resolution under boundary forcing of ERAI was missing. This also made the findings somewhat incomplete. HIRHAM5 in general simulated warm bias in mean surface temperature (-1.5 to +1.5^{o} C) and rainfall (-5 to +.5 mm/day) in all seasons and resolutions at present day climate. It is also found that in the inter-annual variability, HIRHAM-ERAI simulations showed poor rainfall correlation impacted by ENSO in MEI values with better surface temperature correlation with ENSO. Moreover, this was also shown in the potential for added value (PAV) analysis, where rainfall showed positive values (as well represented by the model) while surface temperature indicated negative values in all model resolutions (Figure 3.36a).

Previous studies have noted that the bias in regional climate models is associated with boundary forcing of the GCM and reanalysis data used to force the model. Furthermore, studies have shown that regional climate models have uncertainties due to the observation datasets used in the validation of the models and lateral boundary forcing (Sylla et al. 2013). However, some studies have indicated that precipitation bias in RCMs may be related to the model resolution (Jacob et al., 2007; Rasmussen et al., 2012). In this study it is noticed that increasing resolution of an RCM decreases bias. This is also observed in the case boundary forcing, HIRHAM5 simulations under different boundary forcing show different results especially in magnitude.

6.3. Conclusions and perspective

This PhD study has recognized some of the aspects and potential of increasing resolution in regional climate models. The study has contributed to the understanding of the importance of increasing the resolution in regional climate models in simulating East African climate variability and change. Moreover, this study contributes to a greater understanding of the possible changes of climate in the future, both in mean and extreme terms, and the underlying impact of the dynamic and thermodynamic processes. Low resolution regional climate models have been found to have larger bias in both rainfall and surface temperature in comparison to high resolution models. Moreover, larger bias was simulated in surface temperature compared to rainfall. For example, HIRHAM5 at 50 km simulates cold bias (-1.5^{o} C) and wet bias (+5mm/day) over the high ground. Therefore, while the higher resolution HIRHAM5 is generally reliable, caution must be exercised in forming conclusions from the results, especially over the high ground and remote areas where there was inadequate observation data.

This thesis work in the overall projection of rainfall and surface temperature over East Africa found that both variables are changing. In the future projections, rainfall is highly variable in all seasons. The amount of mean rainfall change is projected to decrease considerably in the far future over the western portion of the domain, southern regions and in the highlands of Tanzania and Kenya (northern Kenya). This is also true for the western Indian Ocean (northern Madagascar). Moreover, warming is resolution dependent, with more warming projected in the higher resolution HIRHAM5 than in the coarser ECHAM5. HIRHAM5 at 10km is slightly warmer than HIRHAM5 at 50 km. So it is that rainfall is also a resolution dependent. More rainfall is simulated in the higher resolution than coarser resolution.

Studies on climate variability and change using high resolution RCMs are very limited over the East African region. Nevertheless, high resolution RCMs are essential for impact assessments at a regional/local level. Moreover, East Africa is among those developing regions which are highly vulnerable to climate variability and change (IPCC, AR4; Thornton et al. 2009). Therefore, it is very important to continuously assess the impact of climate variability and change at the spatial and temporal resolution at which impacts occur. The most promising

method for assessing and projecting climate variability and change over East Africa is the use of high resolution regional climate models.

This study also investigated the dynamics and thermodynamic changes of climate variables such as total cloud cover, surface winds and vertical uplifts, surface moisture which demonstrated the above findings. For example, total cloud cover is projected to decrease more in the far future with an increase in surface winds. Moreover, surface temperature is projected to increase considerably in the far future climate scenarios. The surface winds are also projected to increase in the near future and more significantly in the far future climate scenarios. The vertical uplift, total cloud cover and surface moisture are also projected to decrease in the near future and more significantly in the far future. The projected changes in rainfall and surface temperature show physical relationships with other climatic variables (cloud, moisture, surface winds and evaporation).

6.4 Recommendations

There is no model which is perfect. All models are associated with uncertainties which limit them to some extent. High resolution regional climate models are better at resolving details of topography than their coarse counterparts. However, they are limited in resolving some features that are associated with large scale circulation which has an influence on local/regional climate. It is important to note that GCMs are the drivers of RCMs. Therefore, there is need for improving higher resolution regional climate models in order to resolve these important features that remained in GCMs which have an influence at a regional level. High resolution regional climate models remain the best models in resolving climate variability and change at a small scale necessary for impact assessment. More effort is needed to improve the available high resolution RCMs (for example, the CORDEX data) necessary for resolving a complex climate like that of East Africa. More effort is also needed to improve the observation datasets at the local to regional level. High resolution observation datasets are more reliable than coarse ones, as this was already been observed in the differences between CRU (~50km) and FEWS (10km) datasets. The CRU field showed less spatial rainfall distribution in the remote areas (Congo

forest basin, high grounds) in comparison to FEWS; as a result, when compared with the models, the models simulate large wet bias. Moreover, the CRU dataset used had neither wind data nor daily data for rainfall and surface temperature. Therefore, it was difficult to be consistent in this analysis. If the author had to rely solely on FEWS, which has higher resolution, FEWS has the disadvantage of having only rainfall data. Therefore, it is important to improve network stations and observation data over the land and neighbouring remote areas (ocean and mountainous areas).

The reliability of the climate models in reproducing observed relevant climatic feature is a key indicator of their potential use for future climate change projections. In this thesis, HIRHAM5 demonstrated good skill in capturing mean climatology, annual cycles and the annual variability of seasonal variability of rainfall and surface temperature over East Africa. Therefore, the author suggests that the model is skilled enough for assessing climate variability and change in East Africa, the information most needed for impact assessment. HIRHAM5 at 10km resolution shows better representation of East Africa climate than the coarse HIRHAM5 at 50 km resolution. However, the former needs improvement in terms of resolution and boundary conditions. It is suggested that the future work will be to focus on the understanding of the use of the high resolution multiple RCMs which will provide more understanding of the added value of increasing the resolution of the RCMs for assessing East Africa climate variability and change.

Therefore, the proposed anticipated future work will focus on the utilisation of the different high resolution regional climate models such as the ensemble simulations of CORDEX Africa outputs (if they are higher than 50km resolution, it will be an added advantage).

REFERENCES

Abiodun, B.J., Z.D. Adeyewa, P.G. Oguntunde, A.T Salami & V.O. Ajayi, 2012. Modeling the impacts of reforestation on future climate in West Africa. *Theor Appl Climatol Theor Appl Climatol,* 110), 77–96.

Ahmed, S.A., N.S. Diffenbaugh & T.W.Hertel, 2009. Climate volatility deepens poverty vulnerability in developing countries, *Environ. Res. Lett.*, 4, doi:10.1088/1748-9326/4/3/0334004.

Allan, R.P. & B.J. Soden, 2008. Atmospheric warming and the amplification of precipitation extremes. *Science*, 321, 1481–1484.

Allen, J.C. & D.F.Barnes, 1985. The causes of deforestation in developing countries. *Annals of the Association of American Geographers*, 75,163–184.

Alonso, D., M.J.Bouma & M. Pascual, 2011. Epidemic malaria and warmer temperatures in recent decades in an East African highland. *Proc. R. Soc. B.,* 278,1661–1669.

Anyah, R.O. & F.H.M. Semazzi, 2007. Variability of East African rainfall based on multiyear RegCM3 simulations. *Int J Climatol*, 27, 357–371.

Anyah, R.O. & W. Qiu, 2012. Characteristic 20th and 21st century precipitation and temperature patterns and changes over the Greater Horn of Africa. *Int J Climatol,* 32, 347–363.

Ashok, K., Z. Guan & T. Yamagata, 2001. Impact of the Indian Ocean dipole on the decadal relationship between Indian monsoon rainfall and ENSO, *Geophys. Res. Lett*., 28, 4499–4502.

Barker, P. & F. Gasse, 2003. New evidence for a reduced water balance in East Africa during the Last Glacial Maximum: implication for model-data comparison. *Q Sci Rev*, 22, 823–837.

Basalirwa, C.P.K., J.O. Odiyo, R.J Mingodo. & E.J. Mpeta,1999. The climatological regions of Tanzania based on the rainfall characteristics. *Int J Climatol,* 19,69–80.

Behera S., J. Luo, S. Masson, T. Yamagata, P. Delecluse, S. Gualdi & A. Navarra, 2003. Impact of the Indian ocean dipole on the East African short rains. A CGCM study. *CLIVAR-Exchanges,* 27, 1–4

Behera, S. K., J.J. Luo, S. Masson, P. Delecluse, S. Gualdi, A. Navarra, & T. Yamagata, 2005. Paramount impact of the Indian Ocean dipole on the East Africa short rains:ACGCM study. *J. Climate,* 18, 4514–4530.

Betts, R. A., M. Collins, D. L.Hemming, C. D. Jones, J. A. Lowe & M. G. Sanderson, 2011. When could global warming reach 4^{o} C? *Phil. Trans.A,* 369, 67–84.

Bjerknes, J., 1969. Atmospheric teleconnections from the Equatorial Pacific. *Mon. Wea. Rev.*, 97, 163–172.

Black, E., J. Slingo, & K.R. Sperber, 2003. An Observational Study of the Relationship between Excessively Strong Short Rains in Coastal East Africa and Indian Ocean SST. *Mon. Wea. Rev*, 131, 74–94.

Camberlin, P., B. Fontaine, S. Louvet, P. Oettli & P.Valimba, 2010. Climate adjustments over Africa accompanying the Indian Monsoon Onset. *J. Climate*, 23, 2047–2064.

Camberlin, P., S. Janicot & I. Poccard, 2001. Seasonality and atmospheric dynamics of the teleconnection between African rainfall and tropical sea-surface temperature: Atlantic vs. ENSO. *Int J Climatol,* 21, 973–1005.

Camberlin, P. & R.E. Okoola, 2003. The onset and cessation of the "long rains" in eastern Africa and their interannual variability. *Theor Appl Climatol,*75, 43–54.

Camberlin, P. & N. Philippon, 2002. The East African March-May rainy season: Associated atmospheric dynamics and predictability over the 1968–1997. *J. Climate,* 15, 1002–1019.

Camberlin, P., V. Moron, R. Okoola, N. Philappon & W.Giteau, 2009. Components of rainy seasons' variability in Equatorial East Africa: onset, cessation, rainfall frequency and intensity. *Theor. Appl. Climatol.,* 98, 237–249.

Chaves, L.F., A. Satake, M. Hashizume & N. Minakawa, 2012. Indian Ocean dipole and rainfall drive a Moran effect in East Africa malaria transmission. *J. Infect Dis.*, 205, 1885–1891.

Christensen, O.B., J.H.Christensen, B. Machenhauer & M. Botzet, 1998. Very High-Resolution Regional Climate Simulations over Scandinavia,Present Climate. *J. Climate*, 11, 3204–3229.

Christensen, O. B., M. Drews & J. H. Christensen, 2006. The HIRHAM regional climate model version 5. DMI Tech. Rep. 06-17, 22 pp.

Christensen, J. H., B. Hewitson, A. Busuioc, A. Chen, X.Gao, I. Held, R. Jones, R.K.Kiolli, W.-T. Kwon, R. Laprise, V. Magaña Rueda, L. Mearns, C. G. Menéndez, J. Räisänen, A. Rinke, A. Sarr &, P. Whetton, 2007. Regional climate projections. In: Climate Change 2007: Th e Physical Science Basis. Contribution of Working Group I to the Fourth Assessment Report of the Intergovernmental Panel on Climate Change. In: Solomon S, Qin D, Manning M, Chen Z, Marquis M, Averyt KB, Tignor M, Miller HL (ed) Climate Change 2007. Cambridge University Press, Cambridge, pp 847–940

Christensen, J.H., F. Boberg, O. B. Christensen & P. Lucas-Picher, 2008. On the need for bias correction of regional climate change projections of temperature and precipitation. *Geophys.l Res.Lett.*, 35, L20709, doi:10.1029/2008GL035694.

Christy, J.R., W.B. Norris, & R.T. McNider, 2009. Surface Temperature Variations in East Africa and Possible Causes. *J. Climate*, 22, 3342–3356.

Collier, P., G. Conway, & T. Venables, 2008. Climate change and Africa. *Oxf Rev Econ Policy*, 24, 337–353.

Collins, M., M., R. Knutti, J. M. Arblaster, J.-L. Dufresne, T. Fichefet, P. Friedlingstein, X. Gao, W. J. Gutowski, T. Johns, G. Krinner, M., Shongwe, C. Tebaldi, A. J. Weaver & M. Wehner, 2013. Long-term Climate Change: Projections, Commitments and Irreversibility*:* In:Climate Change, 2013. The Physical Science Basis. *Contribution of Working Group I to the Fifth Assessment Report of the Intergovernmental Panel on Climate Change* [Stocker, T.F., D. Qin, G.-K. Plattner, M. Tignor, S.K. Allen, J. Boschung, A. Nauels, Y. Xia, V. Bex and P.M. Midgley (eds.)]. Cambridge University Press, Cambridge, United Kingdom and New York, NY, USA.

Conway D., E.H. Allison, R. Felstead & M. Goulden, 2005. Rainfall variability in East Africa: implications for natural resources management and livelihoods. *Phil Trans R.Soc. A*., doi:10.1098/rsta.2004.1475.

Conway, D., C. E. Hanson, R. Doherty & A. Persechino, 2007. GCM simulations of the Indian Ocean dipole influence on East African rainfall: Present and future. *Geophys. Res. Lett*., doi: 10.1029/2006GL027597.

Cook, B.I., G.B. Bonan & S. Levis, 2006. Soil moisture feedbacks to precipitation in Southern Africa. *J. Climate*, 19, 4198–4206.

Cook, K.H. & E.K. Vizy, 2012. Impact of climate change on mid-twenty-first century growing seasons in Africa. *Clim Dyn*, 39, 2937–2955.

Cook, K.H. & E.K. Vizy, 2013. Projected changes in East African rainy seasons. *J. Climate*, 26, 5931–5948.

Cooper, P. J. M., J. Dimes, K. P. C. Rao, B. Shapiro,, B. Shiferaw & S. Twomlow, 2008. Coping better with current climatic variability in the rain-fed farming systems of sub-SaharanAfrica: An essential first step in adapting to future climate change? *Agric. Ecosys. Environ.*, 126, 24–35.

Dankers, R., O. B. Christensen, L. Feyen, M.Kalas, & A.P.J. DeRoo, 2007. Evaluation of very high-resolution climate model data for simulating flood hazards in the Upper Danube Basin. *J. Hydrol.*, 347, 319–331.

Dee, D.P. et al., 2011. The ERA-Interim reanalysis: configuration and performance of the data assimilation system. *Q. J. R. Meteorol. Soc.*, 137, 553–597.

Denis, B., R. Laprise & D. Cava, 2002. Downscaling ability of one-way nested regional climate models: The Big-Brother Experiment. *Clim Dyn*, 18, 627–646.

Di Luca, A., R. Elía, & R. Laprise, 2012. Potential for added value in temperature simulated by high-resolution nested RCMs in present climate and in the climate change signal. *Clim Dyn*, 40, 443–464.

Easterling, D.R., 1997. Maximum and Minimum Temperature Trends for the Globe. *Science*, 277, 364–367.

Endris H.S., P. Omondi, S. Jain, C. Lennard, B. Hewitson, L. Chang'a, J.L. Awange, A. Dosio, P. Ketiem, G. Nikulin, H.J. Panitz, M. Büchner, F. Stordal, L. Tazalika, 2013. Assessment of the performance of CORDEX regional climate models in simulating East African rainfall. *J Clim,* 26,8453–8475.

Engelbrecht, F.A., J.L. McGregor & C.J. Engelbrecht, 2009. Dynamics of the conformal-cubic atmospheric model projected climate-change signal over southern Africa. *Int J Climatol 29, 1013–1033*, 1013–1033.

Feser, F., B. Rockel, H. Von Storch, J.Winterfeldt & M. Zahn, 2011. Regional Climate Models Add Value to Global Model Data: A Review and Selected Examples. *Bull. Amer. Meteor. Soc.,* 92, 1181–1192.

Flato, G., J. Marotzke, B. Abiodun, P. Braconnot, S.C. Chou, W. Collins, P. Cox, F. Driouech, S. Emori, V. Eyring, C. Forest, P. Gleckler, E. Guilyardi, C. Jakob, V. Kattsov, C. Reason & M. Rummukainen, 2013: Evaluation of Climate Models. In: Climate Change 2013: The Physical Science Basis. Contribution of Working Group I to the Fifth Assess- ment Report of the Intergovernmental Panel on Climate Change [Stocker, T.F., D. Qin, G.-K. Plattner, M. Tignor, S.K. Allen, J. Boschung, A. Nauels, Y. Xia, V. Bex and P.M. Midgley (eds.)]. Cambridge University Press, Cambridge, United Kingdom and New York, NY, USA

Funk, C., M.D. Dettinger, J. C. Michaelsen, J. P. Verdin, M. E. Brown, M. Barlow & A. Hoell, 2008. Warming of the Indian Ocean threatens eastern and southern African food security but could be mitigated by agricultural development. *PNAS*, 105, 11081–11086.

Gao, X., Y. Xu, Z. Zhao, J.S. Pal & F.Giorgi, 2006. On the role of resolution and topography in the simulation of East Asia precipitation. *Theor Appl Climatol.*, 86, 173–185.

Gbobaniyi, E., A. Sarr, M.B. Sylla, I. Diallo, C. Lennard, A. Dosio, A. Dhiédiou, A. Kamga, NAB, Klutse, B. Hewitson, G.Nikulin, B. Lamptey., 2013. Climatology, annual cycle and interannual variability of precipitation and temperature in CORDEX simulations over West Africa. Int J Climatol, 34, 2241–2257.

Giorgi F., B. Hewitson, J. Christensen C. Fu, R. Jones, M. Hulme, L. Mearns, H. Von Storch, P. Whetton, 2001. Regional climate information – Evaluation and projections. In Climate Change 2001: The Scientific Basis, Houghton JT, Ding Y, Griggs DJ, Noguer M, van der Linden PJ, Xiaosu D (eds). Cambridge University Press: Cambridge; 583–638.

Giorgi, F., 2006. Climate change hot-spots. *Geophys. Res. Lett*., 33, L08707, doi:10.1029/2006GL025734.

Giorgi, F., C. Jones & G.R. Asrar, 2009. Addressing climate information needs at the regional level : the CORDEX framework. *WMO Bull*, 58, 175–183.

Giorgi, F., E. Coppola, F. Solmon, L. Mariotti, M. Sylla, X. Bi, N. Elguindi, G. Diro, V. Nair, G. Giuliani, U. Turuncoglu, S. Cozzini, I. Güttler, T. O'Brien, A. Tawfik, A. Shalaby, A. Zakey, A. Steiner, F. Stordal, L.Sloan & C. Brancovic, 2012. RegCM4: model description and preliminary tests over multiple CORDEX domains. *Clim Res*, 52, 7–29.

Goodess, C.M., 2013. How is the frequency, location and severity of extreme events likely to change up to 2060? *Environ. Sci. Policy,* 27, 4–14.

Hagemann, S., K. Arpe & E. Roeckner, 2006. Evaluation of the Hydrological Cycle in the ECHAM5 Model. *J. Climate*, 19, .3810–3827.

Hansen, J., M. Sato, P. Kharecha, and K. von Schuckmann, 2011: Earth's energy imbalance and implications. Atmos. *Chem. Phys.,* 11, doi:10.5194/acp-11-13421-2011.

Hansen, J., R. Ruedy, M. Sato & K. Lo, 2010. Global surface temperature change. *Rev. Geophys.,* 48, RG4004, doi:10.1029/2010RG000345.

Harvey, D., S. Leybourne & P. Newbold, 1997. Testing the equality of prediction mean squared errors. *Int J Forecasting*, 13, 281–291.

Hastenrath, S., 2001. Variations of East African climate during the past two centuries. *Climatic change*, 50, 209–217.

Hastenrath, S. & D. Polzin, 2003: Circulation mechanisms of climate anomalies in the equatorial Indian Ocean. *Meteor. Z.*, 12, 81–93.

Hastenrath, S., 2009. Past glaciation in the tropics. *Q Sci Rev*, 28, 790–798.

Hastenrath, S., D. Polzin & C. Mutai, 2007. Diagnosing the 2005 Drought in Equatorial East Africa. *J. Climate*, 20, 4628–4637.

Hastenrath, S., D. Polzin & C. Mutai, 2010. Diagnosing the Droughts and Floods in Equatorial East Africa during Boreal Autumn 2005–08. *J. Climate*, 23, pp.813–817.

Hawkins, E. & R. Sutton, 2009. The potential to narrow uncertainty in regional climate predictions. *Bull. Amer. Meteor. Soc.,* 90, 1095–1107.

Hastenrath, S., D. Polzin & C. Mutai, 2011. Circulation mechanisms of Kenya rainfall anomalies. *J. Climate*, 24, 404–412.

Hay, S.I., J. Cox, D.J. Rogers, S.E. Randolph, D.I. Stern, G.D. Shanks, M.F.Myers & R.W., 2002. Climate change and the resurgence of malaria in the East African highlands. *Nature*, 415, 905–909.

Hein, L., M.J Metzger & R. Leemans., 2009. The local impacts of climate change in the Ferlo, Western Sahel. *Clim Change*, 93, 465–483.

Hepworth, N D., 2010. Climate change vulnerability and adaptation preparedness in Tanzania. Heinrich Böll Foundation, Nairobi, Kenya.

Hepworth, N D., 2010. Climate change vulnerability and adaptation preparedness in Uganda. Heinrich Böll Foundation, Nairobi, Kenya.

Hernández-Díaz L., R. Laprise L. Sushama, A. Martynov, K. Winger & B. Dugas, 2012. Climate simulation over the CORDEX-Africa domain using the fifth generation Canadian Regional Climate Model (CRCM5). *Clim Dyn.* 40,1415–1433.

Hession, S.L. & N. Moore, 2011. A spatial regression analysis of the influence of topography on monthly rainfall in East Africa. *Int J Climatol,* 31, 1440–1456.

Hewitson, B. & R. Crane, 1996. Climate downscaling: techniques and application. *Climate Research*, 7, 85–95.

Hijmans, R.J., S.E. Cameron, J.L. Parra, P. Jones & Jarvis, 2005. Very high resolution interpolated climate surfaces for global land areas. *Int J Climatol,* 25, 1965–1978.

Himeidan, Y.E. & E.J. Kweka, 2012. Malaria in East African highlands during the past 30 years: Impact of environmental changes. *Frontiers in physiology*, doi: 10.3389/fphys.2012.00315.

Hudson, D. A. & R.G. Jones, 2002. Regional climate model simulations of present-day and future climates of southern Africa. *Hadley Centre Technical Note*, 39,41.

Indeje, M., F.H.M. Semazzi & L.J.Ogallo, 2000. ENSO signals in East African rainfall seasons. *Int J Climatol.*, 20, 19–46.

IPCC, 2001. Climate Change 2001: The Scientific Basis. Contribution of Working Group I to the Third Assessment Report of the Intergovernmental Panel on Climate Change. In: Houghton, J. T., Y. Ding, D. J. Griggs, M. Noguer, P. J. van der Linden, X. Dai, K. Maskell, and C. A. Johnson (eds). Cambridge University Press, Cambridge, United Kingdom and New York, NY, USA, 881pp.

IPCC, 2007. Climate change 2007: The physical science basis. In: Solomon S, Qin D, Manning M, Chen Z, Marquis M, Averyt KB, Tignor M, Miller HL (eds) Contribution of Working Group I to the fourth assessment report of the intergovernmental panel on climate change. Cambridge University Press, Cambridge, 996 pp

IPCC, 2011. Special Report on Managing the Risks of Extreme Events and Disasters to Advance Climate Change Adaptation (SREX). Summary for Policymakers. IPCC Secretariat, Geneva, Switzerland.

IPCC, 2012. IPCC WGI/WGII Special Report on Managing the Risks of Extreme Events and Disasters to Advance Climate Change Adaptation (SREX). [Field, C.B., V. Barros, T.F. Stocker, D. Qin, D.J. Dokken, K.L. Ebi, M.D. Mastrandrea, K.J. Mach, G.-K. Plattner, S.K. Allen, M. Tignor, and P.M. Midgley (Eds.)]. Cambridge University Press, The Edinburgh Building, Shaftesbury Road, Cambridge CB2 8RU England, 582 pp.

IPCC,2013. Climate Change 2013. The Physical Science Basis. Contribution of Working Group I to the Fifth Assessment Report of the Intergovernmental Panel on Climate Change [Stocker, T.F., D. Qin, G.-K. Plattner,M. Tignor, S.K. Allen, J. Boschung, A. Nauels, Y. Xia, V. Bex and P.M.Midgley (eds.)]. Cambridge University Press, Cambridge, United Kingdom and New York, NY, USA, 1535 pp.

Jacob, D., L. Bärring & O. Christensen, 2007. An inter-comparison of regional climate models for Europe: model performance in present-day climate. *Clim Change*, 81, 31–52.

Jacob, D., A. Elizalde A. Haensler, S. Hagemann, P. Kumar, R. Podzun, D. Rechid, A.R. Remedio, F. Saeed, K. Sieck, C. Teichmann & C. Wilhelm, 2012. Assessing the Transferability of the Regional Climate Model REMO to Different COordinated Regional Climate Downscaling EXperiment (CORDEX) Regions. *Atmosphere*, 3, 181–199.

Jin, E.K., J.L. Kinter, B. Wang, C-K. Park, I-S. Kang, B.P. Kirtman, J-S. Kug, A.Kumar, J-J.Luo, J. Schemm, J. Shukla & T.Yamagata, 2008. Current status of ENSO prediction skill in coupled ocean–atmosphere models. *Clim Dyn*, 31, 647–664.

Jones, P.D., K.R. Briffa, T.P. Barnett and S.F.B. Tett, 1998. High-resolution palaeoclimatic records for the last millennium : interpretation, integration and comparison with General Circulation Model control-run temperatures. *Halocene*, 8, 477–483.

Jung, G. & H. Kunstmann, 2007. High-resolution regional climate modeling for the Volta region of West Africa. *J. Geophys. Res,* 112, 1–17.

Kabanda, T. & M.Jury, 1999. Inter-annual variability of short rains over northern Tanzania. *Clim. Res.*, 13, 231–241.

Kemp, A.C., B. P.Horton, J. P.Donnelly, M. E.Mann, M. Vermeer & S. Rahmstorf, 2011. Climate related sea-level variations over the past two millennia. *PNAS*, 108, 11017–11022.

Kendon, E., N. Roberts, C. Senior & M. Roberts, 2012. Realism of rainfall in a very vigh resolution regional climate model. *J. Climate*, 25, 5791–5806.

Kijazi, A. L. & C. J. C.Reason, 2005. Relationships between intraseasonal rainfall variability of coastal Tanzania and ENSO. *Theor Appl Climatol,* 82, 153–176.

Kijazi, A. L & C. J. C. Reason, 2009. Analysis of the 1998 to 2005 drought over the northeastern highlands of Tanzania. *Clim. Res.*, 38, 209–223.

Kijazi, A.L. & C.J.C. Reason, 2009. Analysis of the 2006 floods over northern Tanzania. *Int J Climatol,* 29, 955–970.

Kijazi, A.L. & C.J.C. Reason, 2012. Intra-seasonal variability over the northeastern highlands of Tanzania. *Int J Climatol*, 32, 874–887.

Kim, J., D.E. Waliser, C.A. Mattmann, C.E. Goodale, A.F. Hart., P.A. Zimdars, D.J. Crichton, C. Jones, G. Nikulin, B. Hewitson, C. Jack, C. Lennard & A. Favre, 2013. Evaluation of the CORDEX-Africa multi-RCM hindcast: systematic model errors. *Clim Dyn*, 259, doi: 10.1007/s00382-013-1751-7.

Lambin, E.F., H.J. Geist & E. Lepers, 2003. Dynamics of Land-Use and Land-Cover Change in Tropical Regions. *Annu. Rev. Environ. Resour.*, 28, 205–241.

Latif, M., D. Dommenget, M. Dima & A. Grotzner, 1999. The Role of Indian Ocean Sea Surface Temperature in Forcing East African Rainfall Anomalies during December–January 1997/98. *J. Climate*, 12, 3497–3504.

Lindsay, S.W. & W.J. Martens, 1998. Malaria in the African highlands: past, present and future. *Bull. World Health Organ*, 76, 33–45.

LinHo, L.H., X. Huang, & N.-C. Lau, 2008. Winter-to-Spring Transition in East Asia: A Planetary-Scale Perspective of the South China Spring Rain Onset. *J. Climate*, 21, 3081–3096.

Lo. J. C. F.,Z.L. Yang and R. A. Pielke. Sr., 2008: Assessment of three dynamical climate downscalling methods using the Weather Research and Forecasting (WRF) model. J. Geophys.Res, 113, D09112, doi:10.1029/2007JD009216.

Lucas-Picher, P., M. Wulff-Nielsen, J. Christensen, G. Adalgeirsdottir, R. Mottram and S. Simonsen, 2012. Very high resolution regional climate model simulations over Greenland: Identifying added value. *J. Geophys. Res.*, 117, doi:10.1029/2011JD016267.

Lyon, B. & D. G. DeWitt, 2012: A recent and abrupt decline in the east African long rains. *Geophys. Res. Lett.*, 39, L02702, doi:10.1029/2011GL050337.

Maghimbi, S., 2007. Recent changes in crop patterns in Kilimanjaro region of Tanzania : The decline of coffee and rise of maize and rice. *African Study Monography,* pp.73–83.

Mahongo, S.B., J. Francis & S.E. Osima, 2012. Wind Patterns of Coastal Tanzania : Their Variability and Trends. *Western Indian Ocean*, 10, 107–120.

Manatsa, D., C.H. Matarira & G.Mukwada, 2011. Relative impacts of ENSO and Indian Ocean dipole/zonal mode on east SADC rainfall. *Int J Climatol*, 31, 558–577.

Manatsa, D., Y. Morioka, S.K. Behera, C.H. Matarira & T. Yamagata, 2014. Impact of Mascarene High variability on the East African "short rains". *Clim Dyn*, 42, 1259–1274.

Mango, L.M., A. Melesse, M. E.McClain, D. Gann & S. G. Setegn, 2011. Land use and climate change impacts on the hydrology of the upper Mara River Basin, Kenya: results of a modeling study to support better resource management. *Hydrol. Earth Syst. Sci.*, 15, 2245–2258.

Mann, M.E. Z. Zhang, M. K. Hughes, R. S. Bradley, S. K.Miller, S. Rutherford & F. Ni, 2008. Proxy-based reconstructions of hemispheric and global surface temperature variations over the past two millennia. *PNAS,* 105, 13252–13257.

Mapande, A. T. & C.J.C. Reason, 2005. Links between rainfall variability on intraseasonal and interannual scales over western Tanzania and regional circulation and SST patterns. *Meteorol. Atmos. Phys.* 89, 215–234.

Mapande, A.T. & C.J.C. Reason, 2005. Interannual rainfall variability over Western Tanzania. *Int J Climatol,* 25, 1355–1368.

Marchant R, C. Mumbi, S. Behera & T. Yamagata, 2006. The Indian Ocean dipole–the unsung driver of climate variability in East Africa. *Afr. J. Ecol,* 45, 4–16.

Marshall, M., C. Funk & J. Michaelsen, 2012. Examining evapotranspiration trends in Africa. *Clim Dyn*, 38, 1849–1865.

Marsland, S.J., H. Haak, J. H. Jungclaus, M. Latif & F. Roeske, 2003. The Max-Planck-Institute global ocean/sea ice model with orthogonal curvilinear coordinates. *Ocean Modelling*, 5, 91–127.

Matei, D., H. Pohlmann, J. H. Jungclaus, W. A. Müller, H. Haak & J. Marotzke, 2012. Two tales of initializing decadal climate prediction xperiments with the ECHAM5/MPI-OM Model. *J. Climate*, 25, 8502–8523.

May, W., 2008. Climatic changes associated with a global "2° C-stabilization" scenario simulated by the ECHAM5/MPI-OM coupled climate model. *Clim Dyn*, 31, 283–313.

Mbululo, Y., 2012. Climate Characteristics over Southern Highlands Tanzania. *Atmos & Clim. Sci.,* 02, 454–463.

McCarthy, M.P., M.J. Best & R.A. Betts, 2010. Climate change in cities due to global warming and urban effects. *Geophys. Res. Lett*., 37, doi: 10.1029/2010GL042845.

McCormick, M.P., L.W.Thomason & C.R. Trepte, 1995. Atmospheric effects of the Mt Pinatubo eruption. *Nature*, 373, 399–404.

McGregor, J.L., 1997. Meteorology, and Atmospheric Physics Regional Climate Modelling. *Meteorol. Atmos. Phys.* 117, 105–117.

McGuffie, K. & A. Henderson-Sellers, 2001. Forty years of numerical climate modelling. *Int J Climatol,* 21, 1067–1109.

McHugh, M.J., 2006. Impact of South Pacific circulation variability on east African rainfall. *Int J Climatol,* 26, 505–521.

McHugh, M.J., 2004. Near-Surface Zonal Flow and East African Precipitation Receipt during Austral Summer. J. *Clim*, 17, 4070–4080.

McMichael, A.J., R.E. Woodruff & S.Hales, 2006. Climate change and human health: Present and future risks. *Lancet*, 367, 859–869.

Mearns, L.O., I. Bogardi, F Giorgi, I. Matyasovszky & M.Palecki, 1999. Comparison of climate change scenarios generated from regional climate model experiments and statistical downscaling. *J. Geophys. Res.*, 104, 6603-6621.

Mearns L.O., M. Hulme, T.R. Carter, R. Leemans, M. Lal & P. Whetton, 2001. Climate scenario development (Chapter 13). In: Climate Change 2001: The Scientific Basis, Contribution ofWorking Group I to the Third Assessment Report of the IPCC, Houghton JT, Ding Y, Griggs DJ, Noguer M, van der Linden PJ, Dai X, Maskell K, Johnson CA (eds). *Cambridge University Press*, 583–638.

Mearns L.O., F. P. Giorgi, D. Whetton, M. Pabon, M. Hulme & M. Lal, 2003. Guidelines for use of climate scenarios developed from Regional Climate Model experiments, IPCC Task Group on Scenarios for Climate Impact Assessment (TGCIA). Web link: http://www.ipcc-data.org/guidelines/dgm no1 v1 10-2003.pdf.

Meque, A. & B.J. Abiodun, 2014. Simulating the link between ENSO and summer drought in Southern Africa using regional climate models. *Clim Dyn*, 1881–1900.

Mitchell, T. D., T.R. Carter, P.D. Jones, M. Hulme, & M. New, 2004. A comprehensive set of high-resolution grids of monthly climate for Europe and the globe: the observed record (1901-2000) and 16 scenarios (2001-2100).

Mitchell, J.F.B., J. Lowe, R.A.Wood & M. Vellinga, 2006. Extreme events due to human-induced climate change, *Philos. Trans. R. Soc.A,* 364, 2117–2133.

Moberg A, D.M. Sonechkin, K. Holmgren, N.M. Datsenko & W. Karlen, 2005. Highly variable Northern Hemisphere temperatures reconstructed from low- and high- resolution proxy data. *Nature,* 433, 613–617.

Mongi, H., A.E. Majule & J.G. Lyimo, 2010. Vulnerability and adaptation of rain fed agriculture to climate change and variability in semi-arid Tanzania. *AJEST*, 4, 371–381.

Moore, N., G. Alargaswamy, B. Pijanowski, P. Thornton, B. Lofgren, J. Olson, J. Andresen, P. Yanda & J. Qi, 2011. East African food security as influenced by future climate change and land use change at local to regional scales. *Clim. Change*, 110, 823–844.

Mpeta, E. & M. Jury, 2001. Intra-seasonal convective structure and evolution over tropical East Africa. *Clim. Res.*, 17, 83–92.

Murray, V. & K.L. Ebi, 2012. IPCC Special Report on Managing the Risks of Extreme Events and Disasters to Advance Climate Change Adaptation (SREX). *J Epidemiol Community Health*, 66, 759–760.

Mutai, C.C., M. N. Ward & A. W.Colman, 1998. Towards the prediction of the East Africa short rains based on sea-surface temperature–atmosphere coupling. *Int J Climatol,* 18, 975–997.

Mutai, C.C. & M.N.Ward, 2000. East African Rainfall and the Tropical Circulation/Convection on Intraseasonal to Interannual Timescales. *J. Climate*, 13, 3915–3939.

Mölg, T., G. Kaser & N.J. Cullen, 2010. Glacier loss on Kilimanjaro is an exceptional case. *PNAS*, 107, 68–70.

New, M., B. Hewitson, D. B. Stephenson, A.Tsiga, A. Kruger, A. Manhique, B. Gomez, C. A. S. Coelho, D. N. Masisi, E. Kululanga, E. Mbambalala, F. Adesina, H. Saleh, J. Kanyanga, J. Adosi, L. Bulane, L. Fortunata, M. L. Mdoka & R. Lajoie 2006. Evidence of trends in daily climate extremes over southern and west Africa. *J. Geophys. Res.,* 111. D14102, doi:10.1029/2005JD006289.

New M., D. Liverman, H. Schroeder & K. Anderson, 2011. Four degrees and beyond: the potential for a global temperature increase of four degrees and its implications. *Philos Transact A Math Phys Eng Sci.,* 369, 6–19.

Nicholls, R.J., N. Marinova, J. Lowe, A. Brown, S. Vellinga, D. De Gusmão, J. Hinkel, & R.S.J.Tol, 2011. Sea-level rise and its possible impacts given a "beyond 4°C world" in the twenty-first century. *Phil. Trans. R. Soc. A,*369, 161–81.

Nicholson S.E., 1996. Areview of climate dynamics and climate variabil- ity in eastern Africa. In The Limnology, Climatology and Paleoclima- tology of the East African Lakes, Johnson TC, Odada E (eds). Gordon and Breach: Amsterdam, 25–56.

Nicholson, S.E. & J.C. Selato, 2000. The influence of La Nina on African rainfall. *Int J Climatol*, 20, 1761–1776.

Nicholson, S., 2000. The nature of rainfall variability over Africa on time scales of decades to millenia. *Global and Planet. Change*, 26, 137–158.

Nicholson, S., 2001. Climatic and environmental change in Africa during the last two centuries. *Clim Res.*, 17, 123–144.

Nikulin, G., E. Kjellström, U. Hansson, G. Strandberg & A. Ullerstig, 2011. Evaluation and future projections of temperature, precipitation and wind extremes over Europe in an ensemble of regional climate simulations. *Tellus A*, 63, 41–55.

Nikulin G., C. Jones, P. Samuelsson, F. Giorgi, M.B. Sylla, G. Asrar, M. Büchner,R. Cerezo-Mota, O.B. Christensen, M. Déqué, J. Fernandez, A. Hänsler, E. van Meijgaard & L. Sushama, 2012. Precipitation Climatology in an Ensemble of CORDEX-Africa Regional Climate Simulations. *J. Climate*, *in press.*

Nogherotto R., E. Coppola, Giorgi F. & L. Mariotti, 2013. Impact of Congo Basin deforestation on the African monsoon. *Atmos Sci Lett.*, 14, 45–51.

Novella, N.S., & W.M. Thiaw, 2013. African Rainfall Climatology Version 2 for Famine Early Warning Systems. *J. Appl. Meteor. Climatol., 49,* 52, 588–606.

Ogata, T., S.-P & Xie, 2011. Semiannual Cycle in Zonal Wind over the Equatorial Indian Ocean. *J. Climate*, 24, 6471–6485.

Omumbo,J. A., B. Lyon, S. M. Waweru, S. J.Connor, & M. C.Thomson, 2011. Raised temperatures over the Kericho tea estates: revisiting the climate in the East African highlands malaria debate. *Malar. J.*, 10, 12.

Pachauri, R.K., 2012. The way forward in climate change mitigation. *WIREs Energy Environ.*, Available at: http://dx.doi.org/10.1002/wene.36.

Paeth H, K. Born, R. Girmes, R. Podzun & D. Jacob, 2009. Regional Climate Change in Tropical and Northern Africa due to Greenhouse Forcing and Land Use Changes. *J. Climate*, 22, 114–132.

Pan, Z., J.H. Christensen, R.W. Arritt, W.J. Gutowski, E.S. Takle, and F. Otieno, 2001. Evaluation of uncertainties in regional climate change simulations. *J. Geophys. Res.*, 106, 17735-17751.

Patricola, C.M. & K.H. Cook, 2010. Northern African climate at the end of the twenty-first century: an integrated application of regional and global climate models. *Clim Dyn*, 35, 193–212.

Patz, J.A., D. Campbell-Lendrum, T. Holloway & J.A. Foley, 2005. Impact of regional climate change on human health. *Nature,* 438, 310–317.

Patz, J.A., H.K. Gibbs, J.A. Foley, J.V. Rogers & K.R. Smith, 2007. Climate Change and Global Health: Quantifying a Growing Ethical Crisis. *EcoHealth*, 4, 397–405.

Polanski, S.,A. Rinke & K. Dethloff, 2010. Validation of the HIRHAM-Simulated Indian Summer Monsoon Circulation. *Advances in Meteorology*, 1–14.

Randall DA., R.A. Wood, S. Bony, T. Fichefet, J. Fyefe, V. Katsov, A. Pitman, J.Shukla, J. Srinivasan, R.J. Stouffer, A. Sumi, K.E.Taylor, 2007. Climate models and their evaluation. In: Solomon S et al (eds) Climate Change 2007: The physical science basis. Contribution of Working Group I to the Fourth Assessment Report of the Intergovernmental Panel on Climate Change. Cambridge University Press, Cambridge and New York, pp. 589–662.

Randall, D.A. & B.A. Wielicki, 1997. Measurements, models and hypotheses in the atmospheric sciences. *Bull. Am. Met. Soc*., 78, 399- 406.

Rasmusson, E.M. & T.H. Carpenter, 1982. Variation in tropical seas surface temperature and surface winds associated with the Southern Oscillation/El Nino. *Mon. Wea. Rev*., 110, 354-384.

Riddle, E. E., & K. H. Cook, 2008. Abrupt rainfall transitions over the Greater Horn of Africa: Observations and regional model simulations. *J. Geophys. Res.*, 113, D15109, doi:10.1029/ 2007JD009202.

Riddle, E.E. & D.S. Wilks, 2013. Statistical indices of the northward rainfall progression over eastern Africa. *Int J Climatol,* 33, 356–375.

Roeckner, E., G. Bäuml, L. Bonaventura, R. Brokopf, M. Esch, M. Giorgetta, S. Hagemann, I. Kirchner, L. Kornblueh, E. Manzini, A. Rhodin, U. Schlese, U. Schulzweida & A. Tompkins, 2003. Part 1: The atmospheric general circulation model ECHAM5, Part I: Model description. *Max Planck Institute for Meteorology report 349*, 140 pp.

Roeckner, E., R. Brokopf, M. Esch, M. Giorgetta, S. Hagemann, L. Kornblueh, E. Manzini, U. Schlese & U. Schulzweida, 2006. Sensitivity of Simulated Climate to Horizontal and Vertical Resolution in the ECHAM5 Atmosphere Model, *J. Climate*, 19, 3771–3791.

Rowhani, P., D.B. Lobell, M. Linderman & N. Ramankutty, 2011. Climate variability and crop production in Tanzania. *Agric & Forest Meteorol.*, 151, 449–460.

Rummukainen, M., 2010. State-of-the-art with regional climate models, *WIREs Clim Change*, 82–96.

Ruosteenoja, K., T.R. Carter, K. Jylhä & H. Tuomenvirta, 2003. Future climate in world regions: an intercomparison of model-based projections for the new IPCC emissions scenarios. The Finnish Environment 644, *Finnish Environment Institute*, 83 pp.

Saji, N. H., B. N. Goswami, P. N. Vinayachandran & T. Yamagata,1999. A dipole mode in the tropical Indian Ocean, *Nature,* 401, 360-363.

Saji, N. & T. Yamagata, 2003. Possible impacts of Indian Ocean Dipole mode events on global climate. *Clim Res*, 25, 151–169.

Sasson, A., 2012. Food security for Africa: an urgent global challenge. *Agriculture & Food Security*, doi:10.1186/2048-7010-1-2.

Schott, F. A., S.-P. Xie, & J. P. McCreary, 2009. Indian Ocean circulation and climate variability, *Rev. Geophys.,* 47, RG1002, doi:10.1029/2007RG000245.

Schreck, C.J. & F.H.M. Semazzi, 2004. Variability of the recent climate of eastern Africa. *Int J Climatol,* 24, 681–701.

Schwartz, S. E., R. J. Charlson, R. A. Kahn, J. A. Ogren & H. Rodhe, 2010: Why hasn't Earth warmed as much as expected? *J. Climate*, 23, 2453–2464

Semazzi, F. & Y. Song, 2001. A GCM study of climate change induced by deforestation in Africa. *Clim Res*, 17, 169–182.

Shongwe, M. E., G. J. van Oldenborgh, B. van den Hurk & M. van Aalst, 2011. Projected changes in mean and extreme precipitation in Africa under global warming. Part II: East Africa. *J. Climate*, 24, 3718–3733.

Slingo J., H. Spender, B. Hoskins, P. Berrisford, E. Black, 2005. The meteorology of the Western Indian Ocean, and the influence of the East African Highlands. *Phil. Trans. R. Soc. A* 363: 25–42.

Spencer, H., Sutton, R.T. Slingo, J.M., Roberts, M. & Black, E, 2005. Indian Ocean climate and dipole variability in Hadley Centre coupled GCMs. *J. Climate*, 18, 2286–2307.

Springer, C., C. Matulla C, W. Schöner, R. Steinacker & S. Wagner, 2013. Downscaled GCM projections of winter and summer mass balance for Central European glaciers (2000-2100) from ensemble simulations with ECHAM5-MPIOM. *Int J Climatol,* 33, 1270–1279.

Stendel, M. & J.H. Christensen, 2002. Impact of global warming on permafrost conditions in a coupled GCM. *Geophys. Res. Lett*., 29, doi: 10.1029/2001GL014345.

Sun, L., F. H. M., F. Semazzi, F. Giorgi & L.A. Ogallo, 1999. Application of the NCAR Regional Climate model to Eastern Africa. Part 1: Simulation of the short rains of 1988. *J. Geophys. Res.,* 104, 6529–6548.

Sylla M.B, E. Coppola, L. Mariotti, F. Giorgi, P.M. Ruti, A. Dell'Aquila & X. Bi, 2010. Multiyear simulation of the African climate using a regional climate model (RegCM3) driven by the high resolution ERA-Interim reanalysis. *Clim Dyn.* 35: 231–247.

Sylla, M.B., F. Giorgi, E. Coppola & L. Mariotti, 2013. Uncertainties in daily rainfall over Africa: Assessment of gridded observation products and evaluation of a regional climate model simulation. *Int J Climatol,* 33, 1805–1817.

Tebaldi C, K. Hayhoe, J.M. Arblaster & G.E. Meehl, 2006. Going to the extremes: an intercomparison of model-simulated historical and future changes in extreme events. *Clim Change,* 79:185–211

Tebaldi, C., and R. Knutti, 2007. The use of the multi-model ensemble in probabilistic climate projections. *Philos. Trans. Roy. Soc.*, 365A, 2053–2075.

Thompson, L.G., 2005. Tropical ice core records: evidence for asynchronous glaciation on Milankovitch timescales. *J Quat Sci.*, 20, 723–733.

Thompson, L.G. et al., 2010. Response to Mölg et al: Glacier loss on Kilimanjaro is consistent with widespread ice loss in low latitudes. *PNAS*, 107, 69–70.

Thompson L, H.H. Brecher, E. Mosley-Thompson, D.R. Hardy & B.G. Mark, 2009. Glacier loss on Kilimanjaro continues unabated. *Proc Natl Acad Sci USA*, 106, 19770–19775.

Thornton, P.K., P.G. Jones, G. Alagarswamy, J. Andresen, 2009. Spatial variation of crop yield response to climate change in East Africa. Global Environmental Change, 19, 54–65.

Thornton, P. K., P.G. Jones, T. Owiyo, R.L. Kruska, M. Herrero, P. Kristjanson, A. Notenbaert, N. Bekele & A. Omolo, 2006. Mapping climate vulnerability and poverty in Africa. Report to the Department for International Development, *ILRI,* Available at: http://www.dfid.gov.uk/research/mapping-climate.pdf.

Tierney, J., J. Smerdon, K. Anchukaitis & R. Seager, 2013. Multidecadal variability in East African hydroclimate controlled by the Indian Ocean. *Nature*, 493, 389–392.

Talbot, M.R., M.L. Filippi, N.B Jensen, J.-J. Tiercelin, 2007. An abrupt change in the African monsoon at the end of the Younger Dryas. *Geochemistry, Geophysics, Geosystems*, 8, Q03005.doi:10.1029/2006GC001465.

Tumbo,S.D, F.C. Kahimba, B.P Mbilinyi,., F.B.Rwehumbiza, H.F. Mahoo,W.B. Mbungu & E. Enfors, 2012. Impact of Projected Climate Change on Agricultural Production in Semi Arid Areas of Tanzania: A Case of Same District. *African Crop Science Journal*, 20, 453-463.

Ummenhofer, C. C., A. Sen Gupta, M. E. England & C. J.C. Reason, 2009. Contribution of Indian Ocean sea surface temperatures to enhanced East African rainfall. *J. Climate*, 22, 993–1013.

Ververs, M., 2012. The East African food crisis: did regional early warning systems function? *Nutrition*, 142, 131–133.

Washington, R., M. Harrison, D. Conway, E. Black, A. Challinor, D. Grimes, R. Jones, A.Morse, G. Kay & M. Todd, 2006. African climate change: Taking the shorter route. *B. Am.Meteorol. Soc*., 87, 1355-1366.

Washington R., R. James, H. Pearce, W.M. Pokam, & W. Moufouma-Okia, 2013. Congo Basin rainfall climatology. Can we believe the climate models? *Phil. Trans. R. Soc,* B 368, doi: 10.1098/rstb.2012.0296.

Wigley, T.M., & S.C. Raper, 2001. Interpretation of high projections for global-mean warming. *Science,* 293, 451–454.

Wilby R.L., S.P. Charles, E. Zorita, B. Timbal, P.Whetton & L.O. Mearns, 2004. Guidelines for use of climate scenarios developed from statistical downscaling methods. Data Distribution Centre of the Intergovernmental Panel on Climate Change. *University of East Anglia*, U.K., 27 pp. Available at: ipcc-ddc.cru.uea.ac.uk/guidelines.

Williams, A. P. & C. Funk, 2011. A westward extension of the warm pool leads to a westward extension of the Walker circulation, drying eastern Africa. *Clim Dyn*, 37, 2417–2435.

Wilson, C.R. & R. A. Haubrich, 2007. Meteorological Excitation of the Earth's Wobble. *Geophys. J. R. Astr. Soc.*, 46, 707–743.

Wolff, C., G. H. Haug, A. Timmermann, J.S. Sinninghe Damste´, A. Brauer, D. M. Sigman, M. A. Cane & D. Verschuren, 2011. Reduced interannual rainfall variability in East Africa during the last ice age. *Science*, 333, 743–747.

Wolter, K. & M.S. Timlin, 2011. El Niño/Southern Oscillation behaviour since 1871 as diagnosed in an extended multivariate ENSO index (MEI.ext). *Int J Climatol.,* 31, 1074–1087.

Yamagata, T., S. K. Behera, J. J. Luo, S. Masson, M. R. Jury & S. A. Rao, 2004. Coupled ocean-atmosphere variability in the tropical Indian Ocean. In: Wang C, Xie SP, Carton A (eds) Earth's Climate*:* the ocean–atmosphere interaction. *Geophys. Monogr*., 147, Amer. Geophys. Union, pp.189-212.

Zelinka, M.D., S.A. Klein & D.L. Hartmann, 2012. Computing and Partitioning Cloud Feedbacks Using Cloud Property Histograms. Part II: Attribution to Changes in Cloud Amount, Altitude, and Optical Depth. *J. Climate*, 25, 3736–3754.

Zhang, H. & K. Mcguffie, 2001. The compounding effects of tropical deforestation and greenhouse warming on climate. *Climatic Change*, 49, 309–338.

Zhang, X., L. V. Alexander, G. C. Hegerl, P. Jones, A. Klein Tank, T.C. Peterson, B. Trewin, & F. W. Zwiers, 2011. Indices for monitoring changes in extremes based on daily temperature and precipitation data. *Wiley Interdisci. Rev. Clim. Change*, 2, 851–870.

Zorita, E. & F. Tilya, 2002. Rainfall variability in Northern Tanzania in the March-May season (long rains) and its links to large-scale climate forcing. *Clim Res*, 20, 31–40.

Appendix 1

Meteorological stations along the Great Ruaha sub River basin

The GRR is located in the south-western highlands of Tanzania in the area of unimodal type of rainfall regime (Figure 1a). Figure 3.1b shows a map of Tanzania with the division of the two regimes: bimodal area regime located in the northern part while unimodal area regime located in southern part of the country. The following plates (1 and 2) indicate the results of the field work conducted in the south-western part of Tanzania along the GRR which was conducted by in the period 2011 and 2012.

Table 1.Name of the stations visited during the field work conducted 2011-2013 in GRR

No.	WMO - CODE	STATION NAME	START	END	LATITUDE	LONGTUDE	ELEVATIO
1	9535008	BAHI WD & ID	1962	2009	-5.57	35.18	
2	9535017	PARANGA MISSION	1973-1976,1979,1980-1993,1995	2009-2010	-5.90	35.52	1400
3	9538018	BAHI MISSION	1962-1995,1999,2000,2002	2008-2009	-5.57	35.20	853
4	9635010	KINUNGURU	1959	2010	-6.90	35.47	
5	9635011	ILANGALI	1959-1999,2002-2005,2007-2009	2009	-6.80	35.08	762
6	9635013	MLOWA DAM	1962-1985,1990-1995	1997	-6.55	35.75	914
7	9635014	MATAMBULU DAM	1962	1995	-6.30	35.77	1067
8	9635026	BIHAWANA SEMINARY	1986-1996,2001-2010	2010	-6.23	35.65	
9	9734000	MKOPURE	1960	1988	-7.93	34.57	
10	9734001	MSEMBE FERRY	1967	2009	-7.75	34.90	2600
11	9735002	ILOLE MISSION	1941-1956,1959-1987	1987	-7.68	35.83	1524
12	9735003	TOSAMANGANGA	1941-1974,1993	1993	-7.85	35.60	1524
13	9735004	KIMANDE DISP	1972-1975,1967,1972-1976,1980,1981,	2008	-7.37	35.52	883
14	9735007	IHIMBU FARM	1972-2001,2006-2008	2008	-7.90	35.82	1737
15	9735013	IRINGA MET	1960	2010	-7.63	35.77	1428
16	9735014	IRINGA MAJI	1960	2010	-7.78	35.70	
17	9735015	IRINGA EXPER	1961-1970,1972-1976,1978-1992,1995,	2010	-7.77	35.68	1548
18	9736003	ILULA PR	1943	1999	-7.67	36.00	1372
19	9736017	MTERA	1981	2010	-7.10	36.00	710
20	9737029	KILOMBERO Sugar Company	1962	2010	-7.67	37.00	304
21	9833003	ALLSA FARM	1935	1957	-8.92	33.92	1828
22	9833025	UYOLE AGROMET	1970	2010	-8.88	33.65	1798
23	9834000	MADIBIRA MAJI	1923-1939,1953-1992,1995,1998-2000	2000	-8.23	34.82	1158
24	9834002	CHIMALA RIVER	1935-1957,1963	1963	-8.83	34.03	1219
25	9834003	RUJEWA MISSION	1942	1981	-8.68	34.33	1067
26	9834004	ILEMBULA MISSION	1946	1965	-8.88	34.60	1463
27	9834005	LUHANYANA FARM	1950-1991,1994-1997,2003-2010	2010	-8.90	34.83	1673
28	9834006	IGAWA MAJI	1976-1958,1960-1991,1994-1997,2003-	2010	-8.77	34.38	1067
29	9834008	MBALALI IRRG	1957	2007	-8.67	34.25	1047
30	9834010	KIMANI	1956-1958,1961-2009	2009	-8.83	34.17	1189
31	9834013	MATAMBA	1971-1976,1979,1983-1986,1989-1990,	2000	-8.93	34.02	
32	9834016	UHENGA PR	1974-1976,1977-1980,1982-1987,1990-	2009	-8.75	34.70	1295
33	9835015	IFUENGA FARM	1946	1949	-8.05	35.72	1767
34	9835016	LUGANGA	1948	1951	-8.28	35.35	1829
35	9835017	ULETE MISSION	1951-1984,2003,2005-2009	2009	-8.12	35.40	1676
36	9835027	MTITU ESTATE	1952	1958	-8.02	35.85	1860
37	9835033	MAFINGA BOMANI	1963-1969,1971-2010	2010	-8.25	35.33	1829
38	9835036	URUNDI HILL	1963-1975,1978-1984,1986-1993,1997-	2010	-8.47	35.27	1737
39	9835039	MAFINGA JKT	1967-1972,1974,1976-1995,2000-2001,	2010	-8.32	35.30	2072
40	9835040	SAO HII	1971-1987,1995-2001	2001	-8.33	35.30	2072
41	9835044	USOKANI PR	1982-1988,1991-1994,1997-1998,2000	2000	-8.22	35.57	
42	9835050	BOMA LA NG'OMBE PR	1974-1975,1977-1980,1993-1994,1996,	1998	-8.22	35.88	
43	9835053	DABAGA SEED FARM	1978	2010	-8.08	35.80	1829
44	9933022	MWAKALELI SCHOOL	1959	1962	-9.00	33.83	1828
45	9934034	WANGAMA	1972-1981,1986,1988-1989,1994	1994	-9.05	34.82	1889
46	9934039	KILOLELO FARM	1975-1991,1993-1996,2004-2010	2010	-9.18	34.78	2021
47	9833001	MBEYA MET	1970	2010	-8.56	33.28	1758
48	9635001	DODOMA	1970	1970	-6.10	35.46	1120

Plate 1: (a) abandoned station became grazing land, (b) broken rain gauge and measuring cylinder, (c) a rock on top of rain gauge waiting for the rainfall to be removed, (d) poorly installed rain gauge (e) station under obstacles (big trees left and right), (f, g, h) discussion with stakeholders and leaders of the voluntary stations.

Plate 1a and 1c show abandoned observation stations. The station in Plate 1a is located at Bahi Ward in the Dodoma region and used to be a complete observation station with all equipment. It used to operate very well and some of the data are available in TMA archive. The equipment is now rusty and some is broken. Plate 1 (c), and 1(d) show volunteer stations located at primary schools. The observers here acknowledged what was going on. They said when there is no rain, they normally keep the funnel and the bottle inside to avoid breakage and been displaced. To protect the gauge from dust and other obstacles, they put a rock on top of a gauge (Plate 1c). If it rains in the presence of a rock, the observer just records what is available as if the gauge was placed in its standard normal condition. If this scenario is taken into consideration, the amount of rainfall that falls on the rock splashes out and some rainfall may or may not enter the gauge. These kinds of stations were ignored in this study. Plate 1b was just a bottle and funnel which were broken and caused the station to stop operation for more than 3 years. The following Plate is one of the climatological archives visited during the field work survey for the purpose of data collection to fill the gaps of the data.

(a) Data collection from the observation station **(b) Data archives—Dodoma**

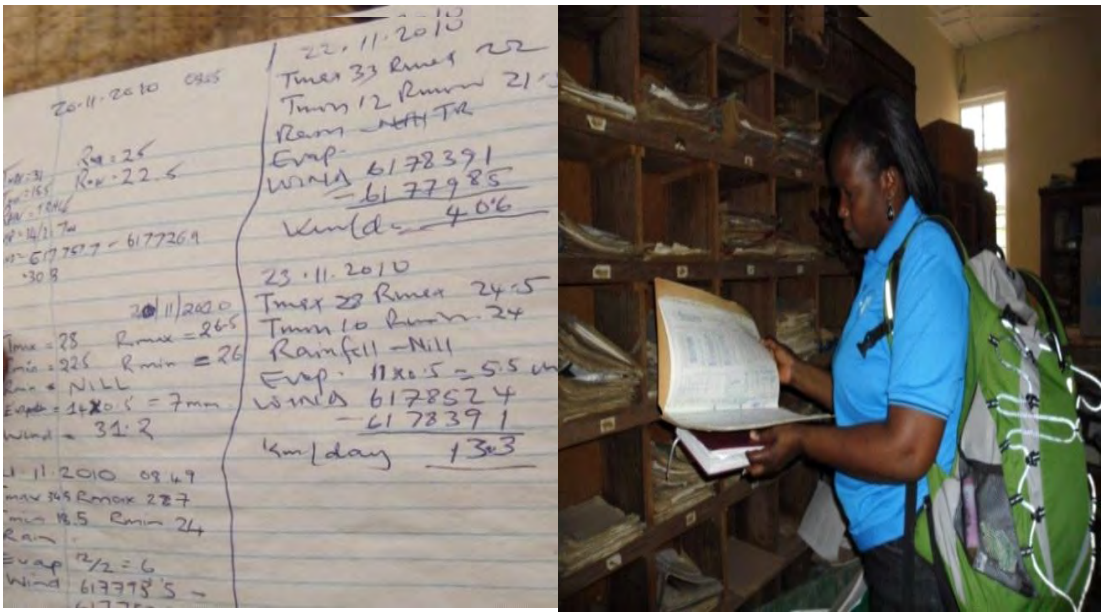

Plate 2 (a): Data records (b) Data archives

Plate 2 (a, and b) show an example of data storage and recording format found during the field survey over GRR area in Dodoma region. In this centre there were very few data stored in digital format while most of the data were stored as hard copies (Plate 2 b). Some of these data were torn out, some were lost; generally speaking this centre had very few data which were consistent, but that only for a short period.

Most of the data found in the voluntary stations are stored in hard copies and some papers were already old and torn and changed their colour. Plate 2 (b) shows one of the data storages in Dodoma–Water Office. The aim of visiting this archive was to collect data to fill gaps of the missing data which was first collected from TMA archive. This Center is supposed to have all the data records over this region and especially over the GRR on the side of Dodoma. The results of searching data to replace the gaps were not successful as most of the data were found in hard copies with a lot of gaps; discoloured paper (difficult to read) and some pages were missing.

Appendix 2

HIRHAM5 simulations of East Africa climate variability and change

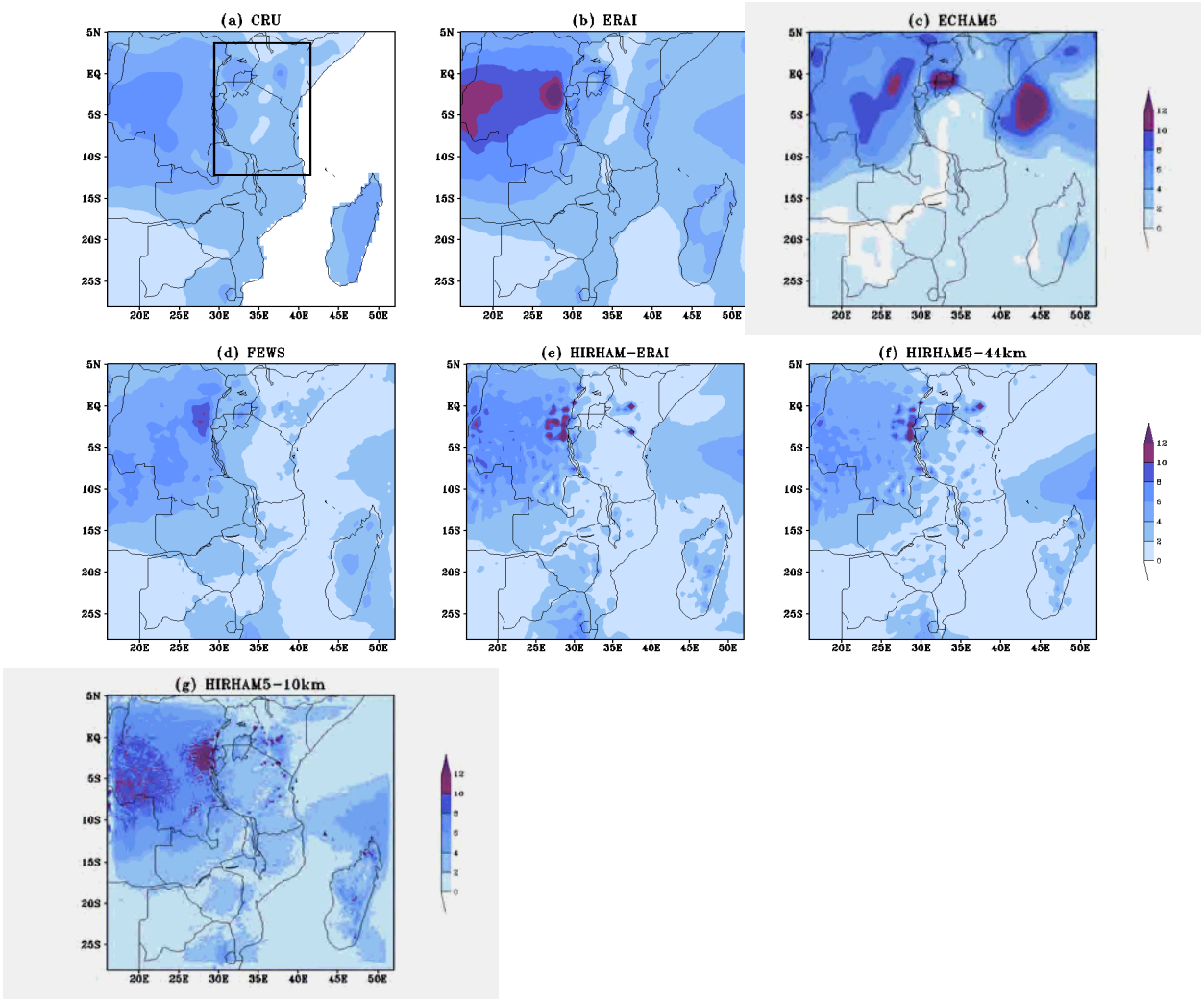

A2.1: Mean rainfall (mm/day) climatology during OND season by (a) CRU, (b) ERAI, (c) ECHAM5 (GCM), (d) FEWS, (e) HIRHAM5 driven by ERAI (HIRHAM-ERAI), (f) HIRHAM5 driven by ECHAM5 at 50 km resolution (HIRHAM5-50km) and (g) HIRHAM5 driven by ECHAM5 at 10km resolution (HIRHAM5-10km)

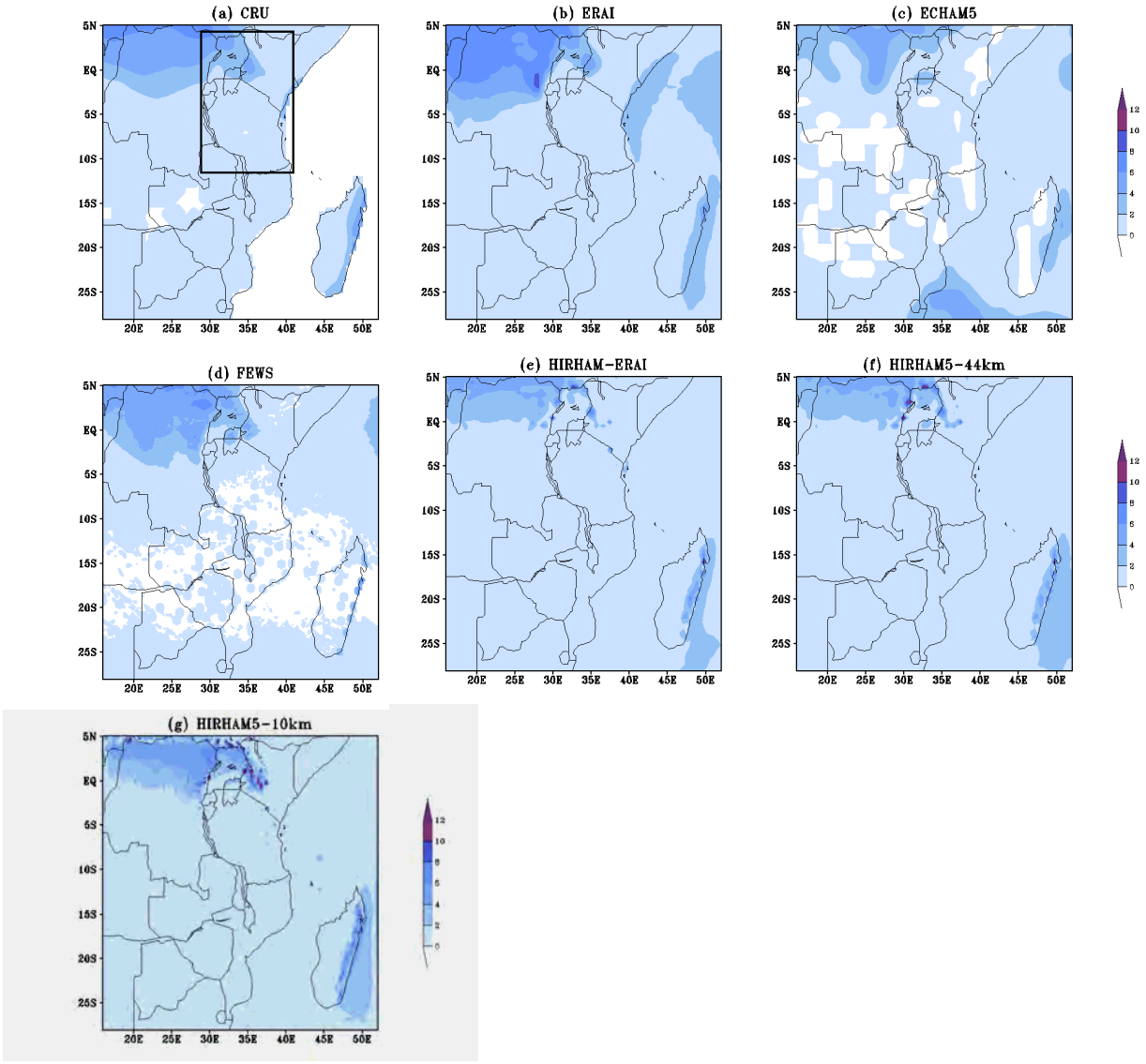

A2.2: Repeat the same as in A2.1 but for JJA season

2.1 General estimation of bias in simulated rainfall climatology relative to CRU

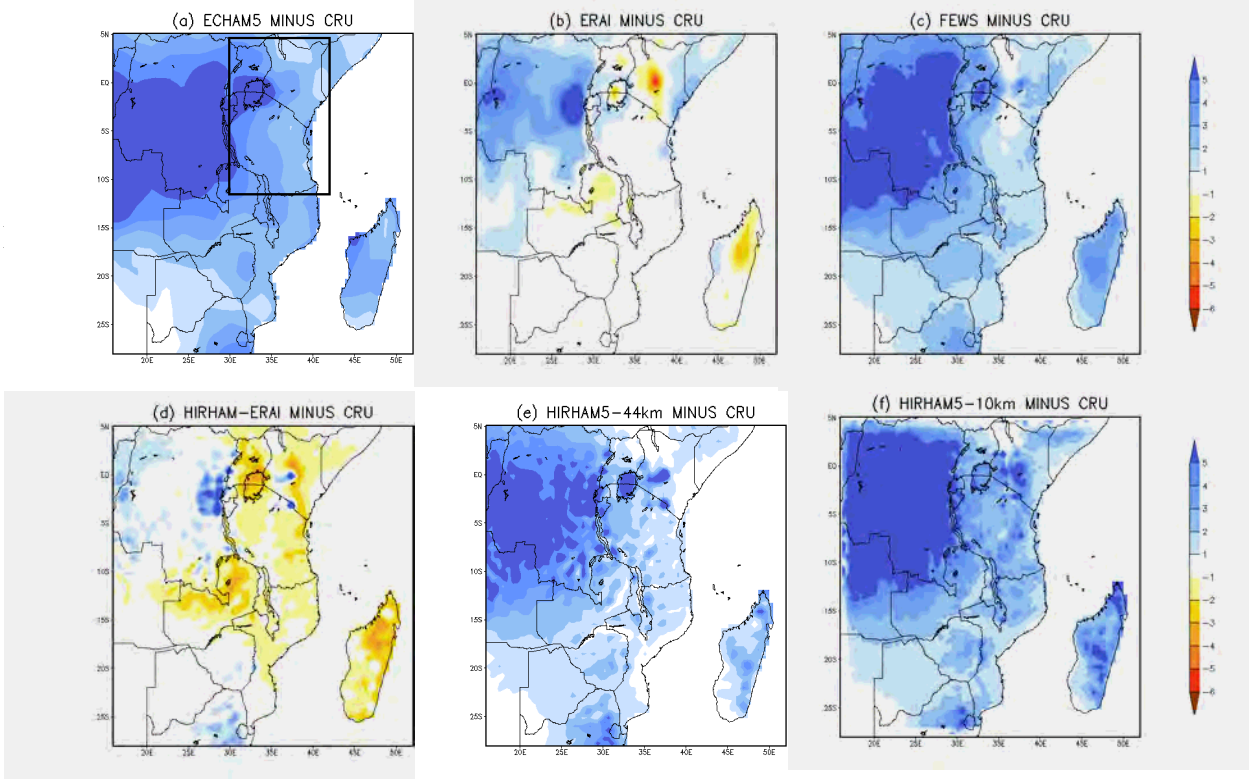

A2.3: Comparison of the observed and simulated mean rainfall climatology (mm/day) over the East African domain during OND season from 1990–1999. (a) ECHAM5 minus CRU; (b) ERAI minus CRU; (c) FEWS minus CRU; (d) HIRHAM5-ERAI minus CRU; (e) HIRHAM5-50km minus CRU; and (f) HIRHAM5-10km minus CRU. The black box in the figure (c) is a study domain

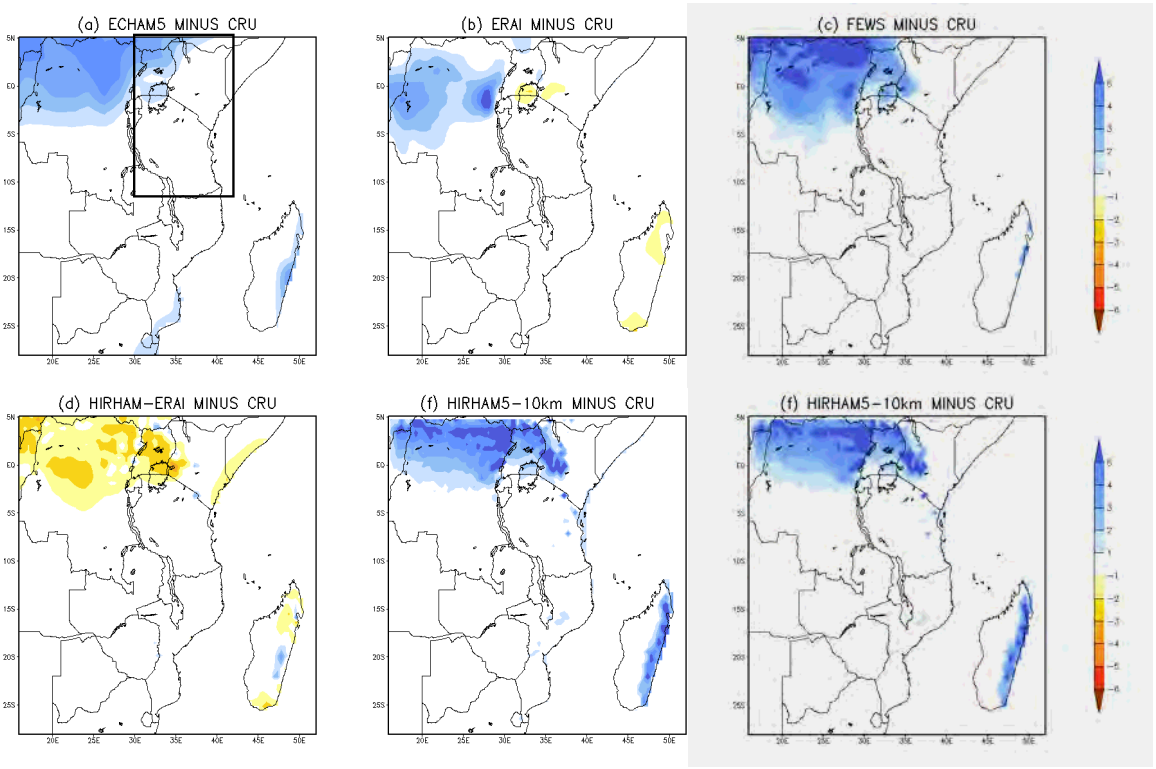

A2.4: Repeat the same as in A2.3 but for JJA season

2.2 General estimation of bias in simulated rainfall climatology relative to FEWS

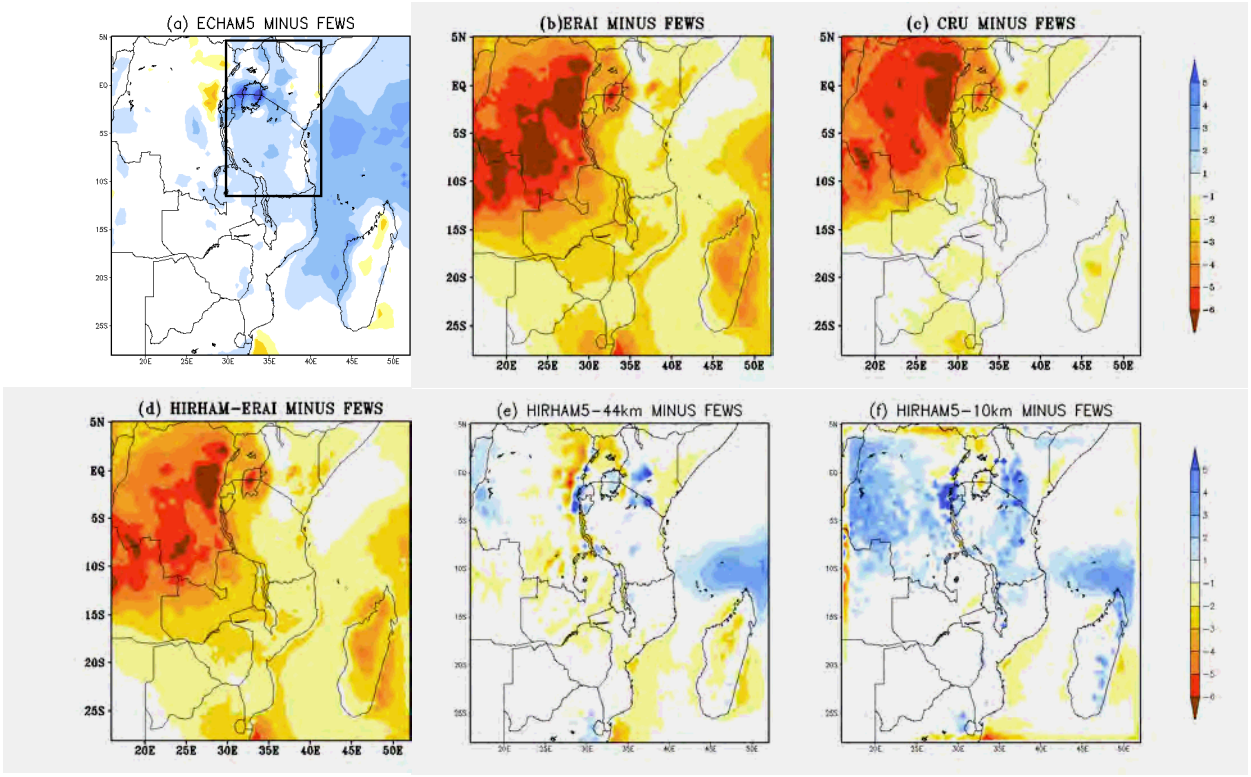

A2.5: Comparison of the observed and simulated mean rainfall climatology (mm/day) over the East African domain during OND season from 1990–1999. (a) ECHAM5 minus FEWS (b) ERAI minus FEWS; (c) CRU minus FEWS; (d) HIRHAM5-ERAI minus FEWS; (e) HIRHAM5-50km minus FEWS; and (f) HIRHAM5-10km minus FEWS. The black box in the figure (c) is a study domain

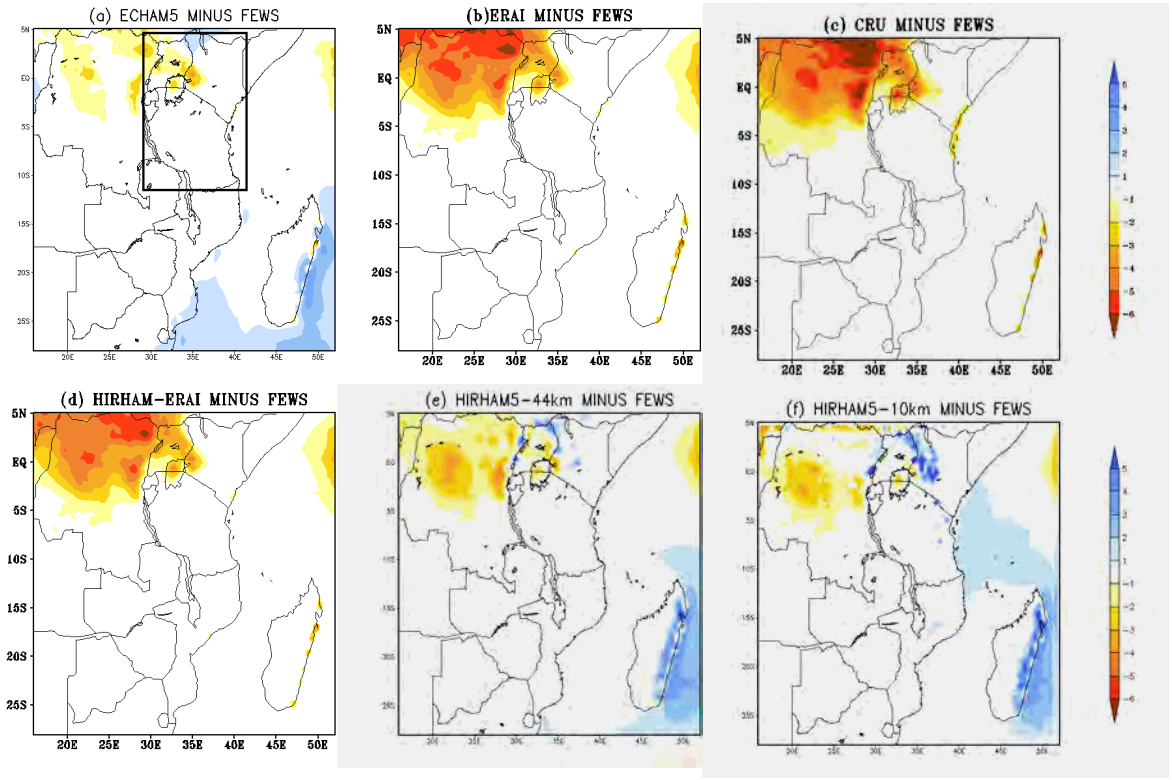

A2.6: Repeat the same as in A2.5 but for JJA season

2.3 Correlation pattern of simulated rainfall and observations

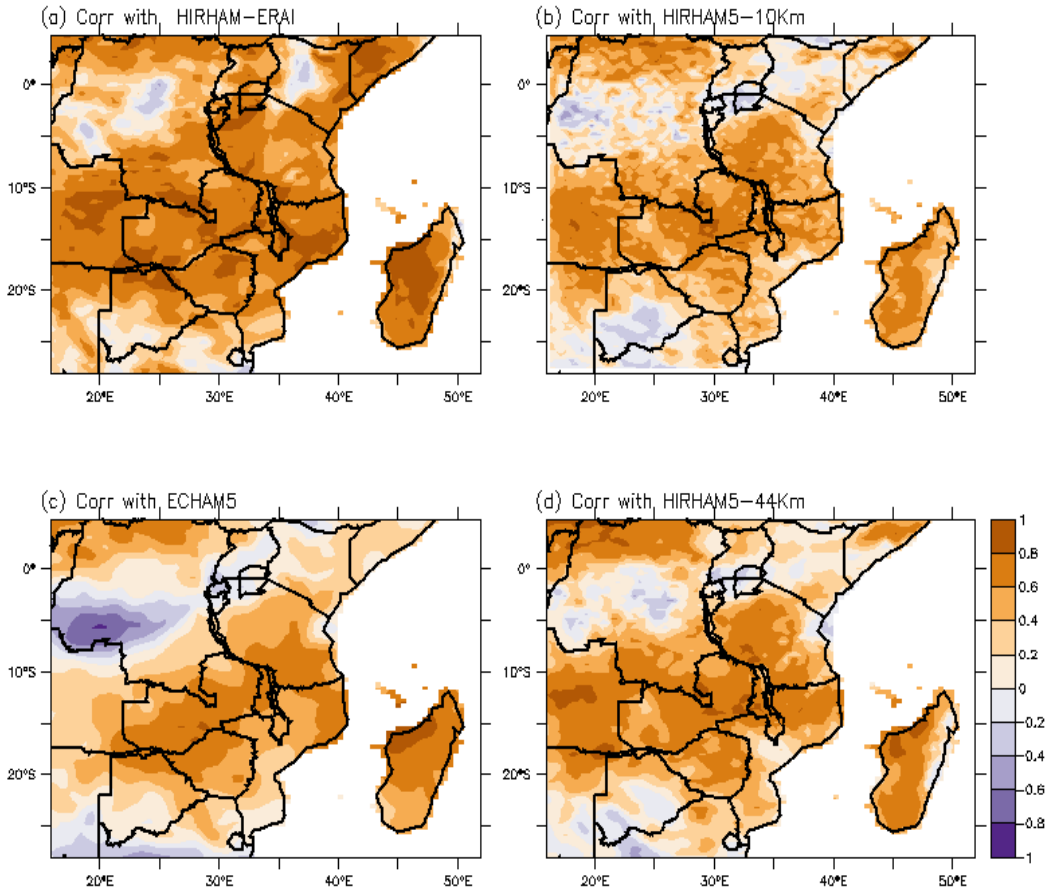

A2.7: Rainfall climatology correlation (r) for OND season as simulated by (a) HIRHAM5-ERAI, (b) HIRHAM5-10km, (c) ECHAM5 (d) HIRHAM5-50km with reference to CRU datasets.

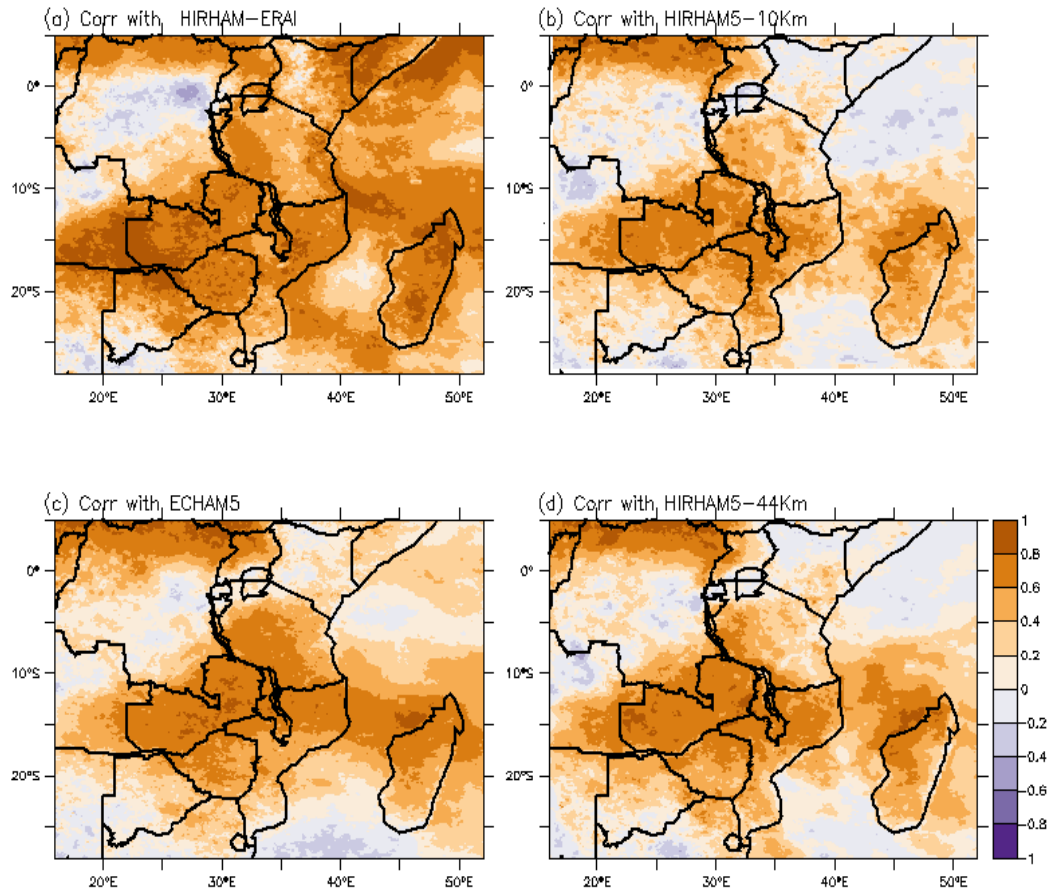

A2.8: Rainfall climatology correlation (r) for OND season as simulated by (a) HIRHAM5-ERAI, (b) HIRHAM5-10km, (c) ECHAM5 (d) HIRHAM5-50km with reference to FEWS datasets.

2.4 The evaluation of HIRHAM5 simulations in reproducing the 90th percentile rainfall over East Africa

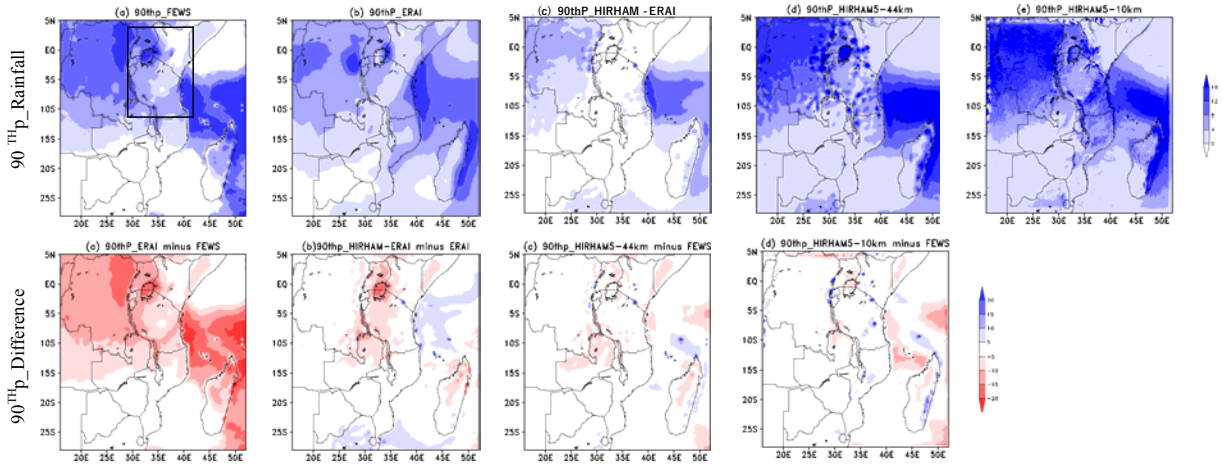

A2.9: The 90th percentile of daily rainfall (mm/day) as presented by the observations from (a) FEWS, and the simulations from (b) ERA-Interim, c) HIRHAH-ERAI d) HIRHAM5-50km, e) HIRHAM5-10km (first row) and their differences from the observations in the second row for OND (second row).

2. 5 Simulations and observations representation of mean Rainfall Climatology

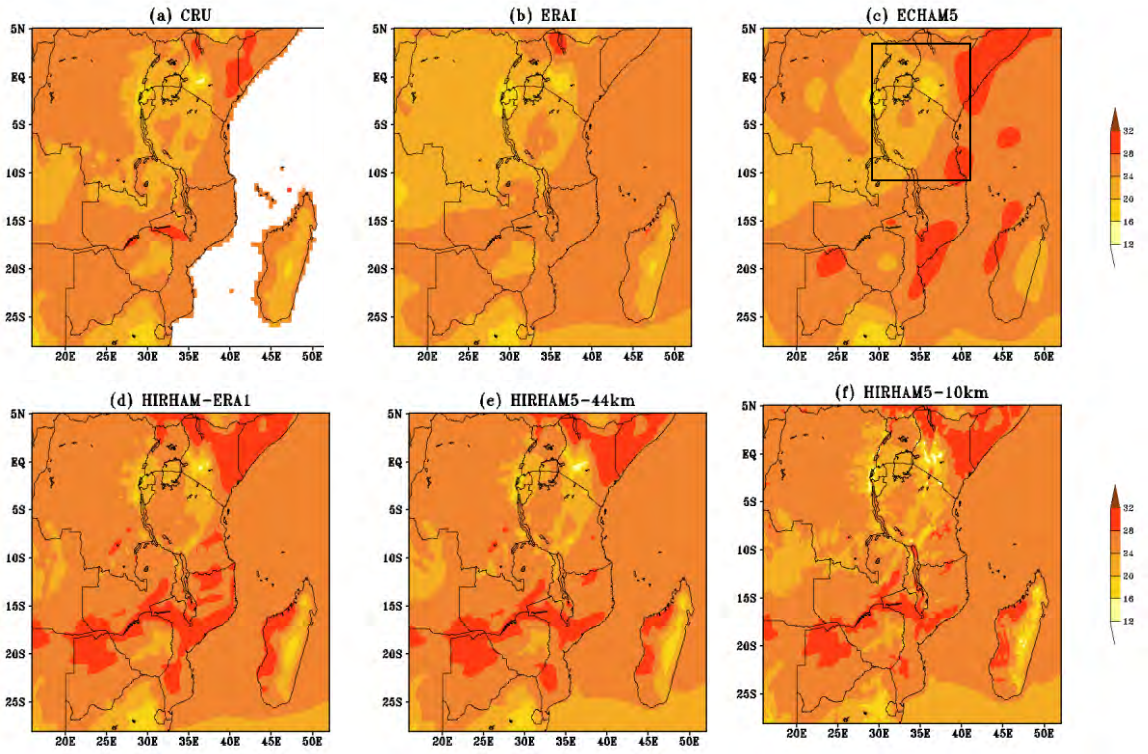

A2.10: The mean surface temperature climatology (^{o}C) simulations in OND season for (a) CRU, (b) ERAI, (c) ECHAM5, (d) HIRHAM5-ERAI (e) HIRHAM5-50km and (f) HIRHAM5-10km over East Africa Domain.

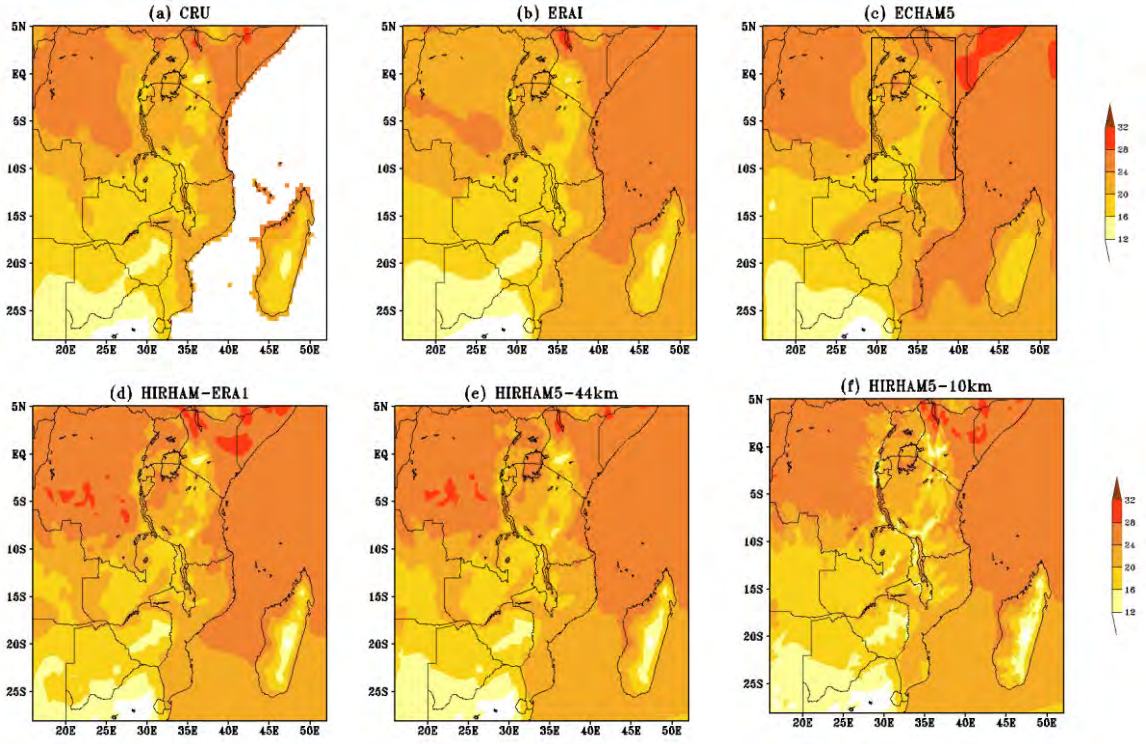

A2.11: Repeat the same as in A2.10 but for JJA season

2.6. Mean bias estimation of the simulated surface temperature Climatology relative to observations

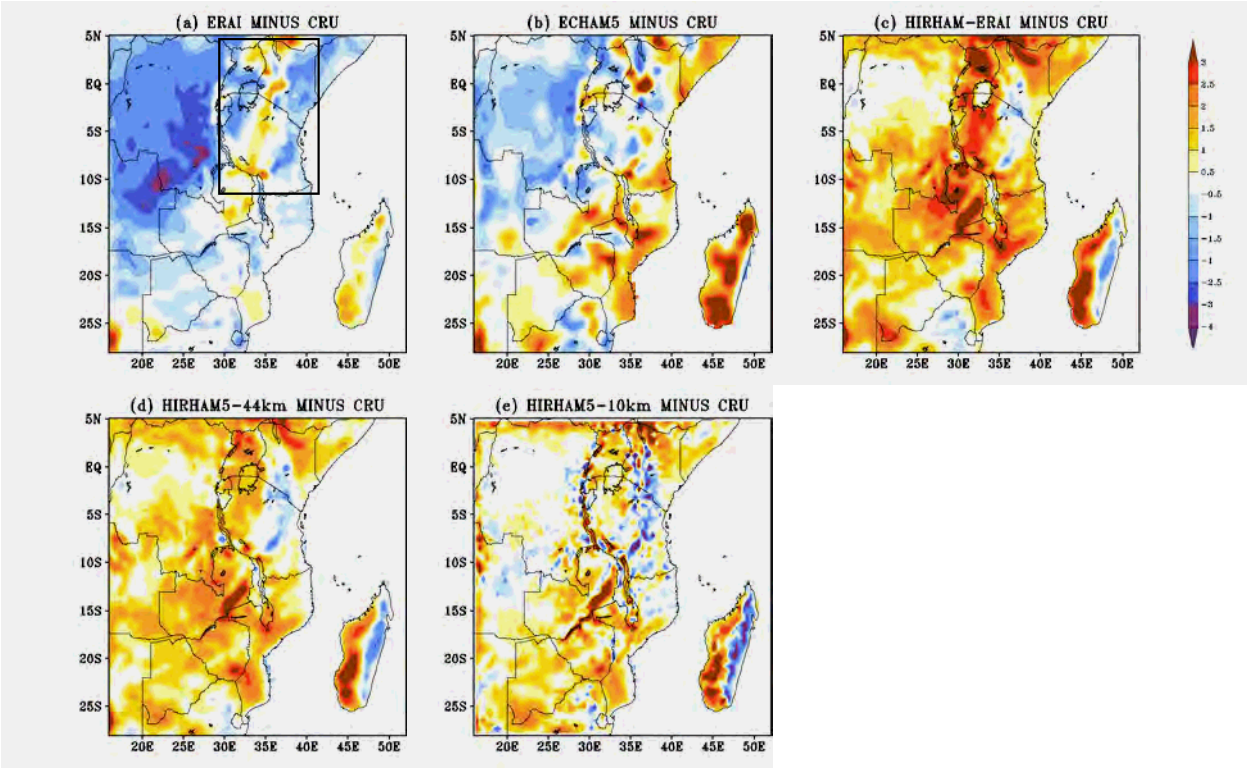

A2:12 Comparison of the simulated mean surface temperature (^{o} C) climatology with the observations (CRU) in OND rainy season from 1990-1999: (a) ERAI minus CRU; (b) ECHAM5 minus CRU; (c) HIRHAM5-ERAI minus CRU; (d) HIRHAM5-50km minus CRU; (e) HIRHAM5-10km minus CRU.

2.4 Correlation pattern of the simulated surface temperature relative to the observation

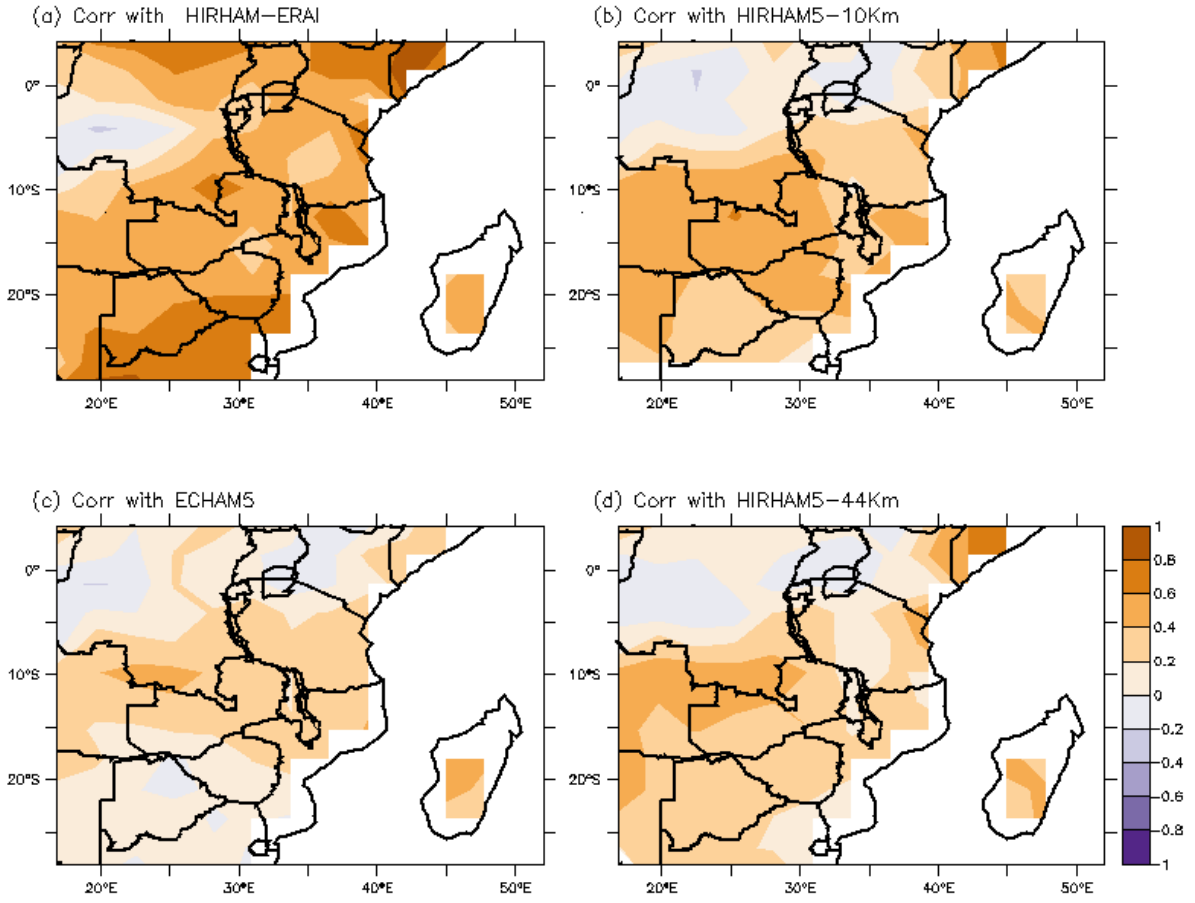

A2.13: Correlation analysis of mean surface temperature as simulated by models (HIRHAM5 and ECHAM5) versus CRU during OND season.

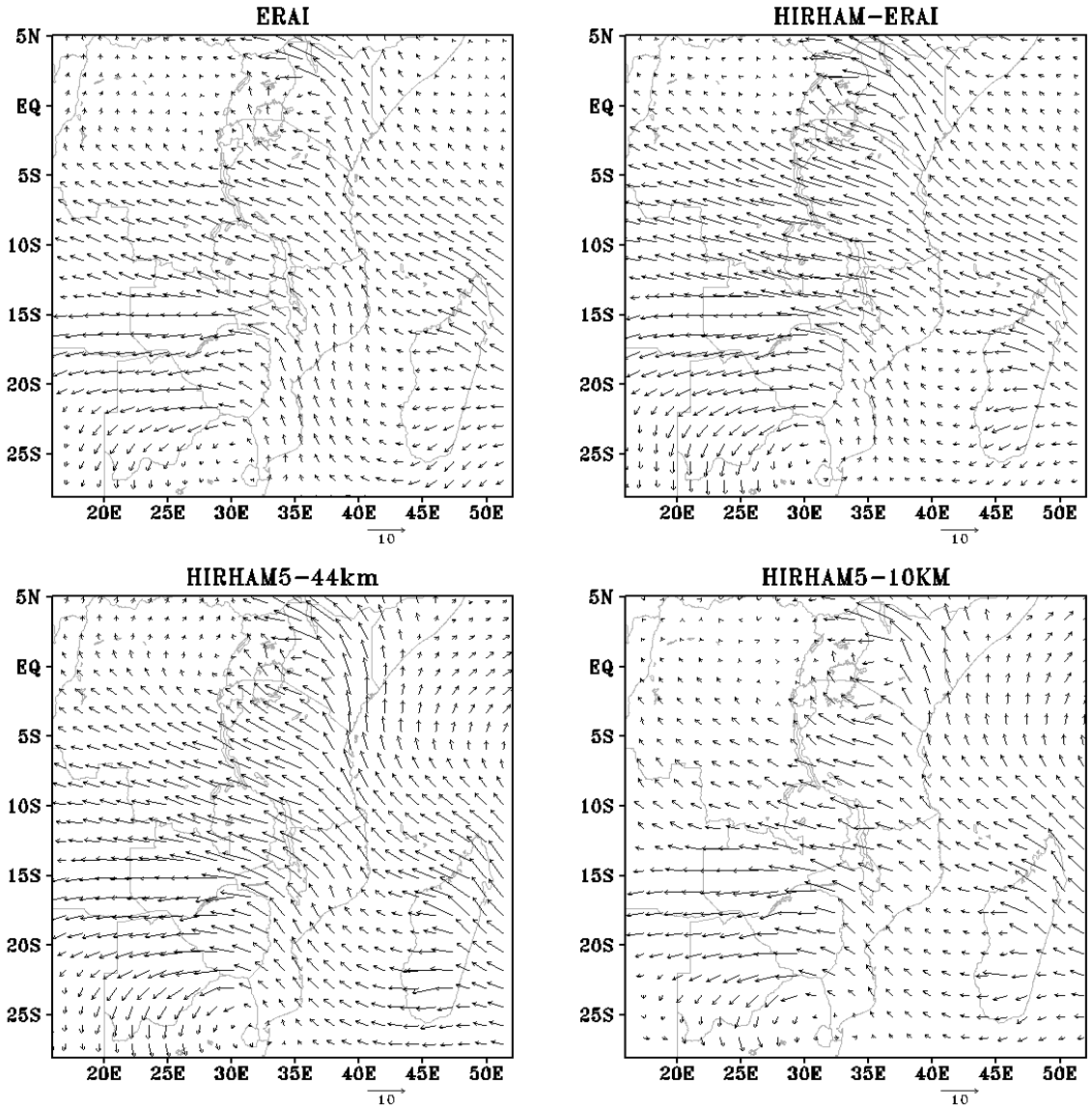

A2.14: Climatology of winds flow at 850hPa in MAM season as presented by the downscaled ERAI (upper left panel), HIRHAM-ERAI (upper right panel), HIRHAM5-50km (lower left panel) and HIRHAM5-10km (lower right panel). The arrows present wind vector (m/s)

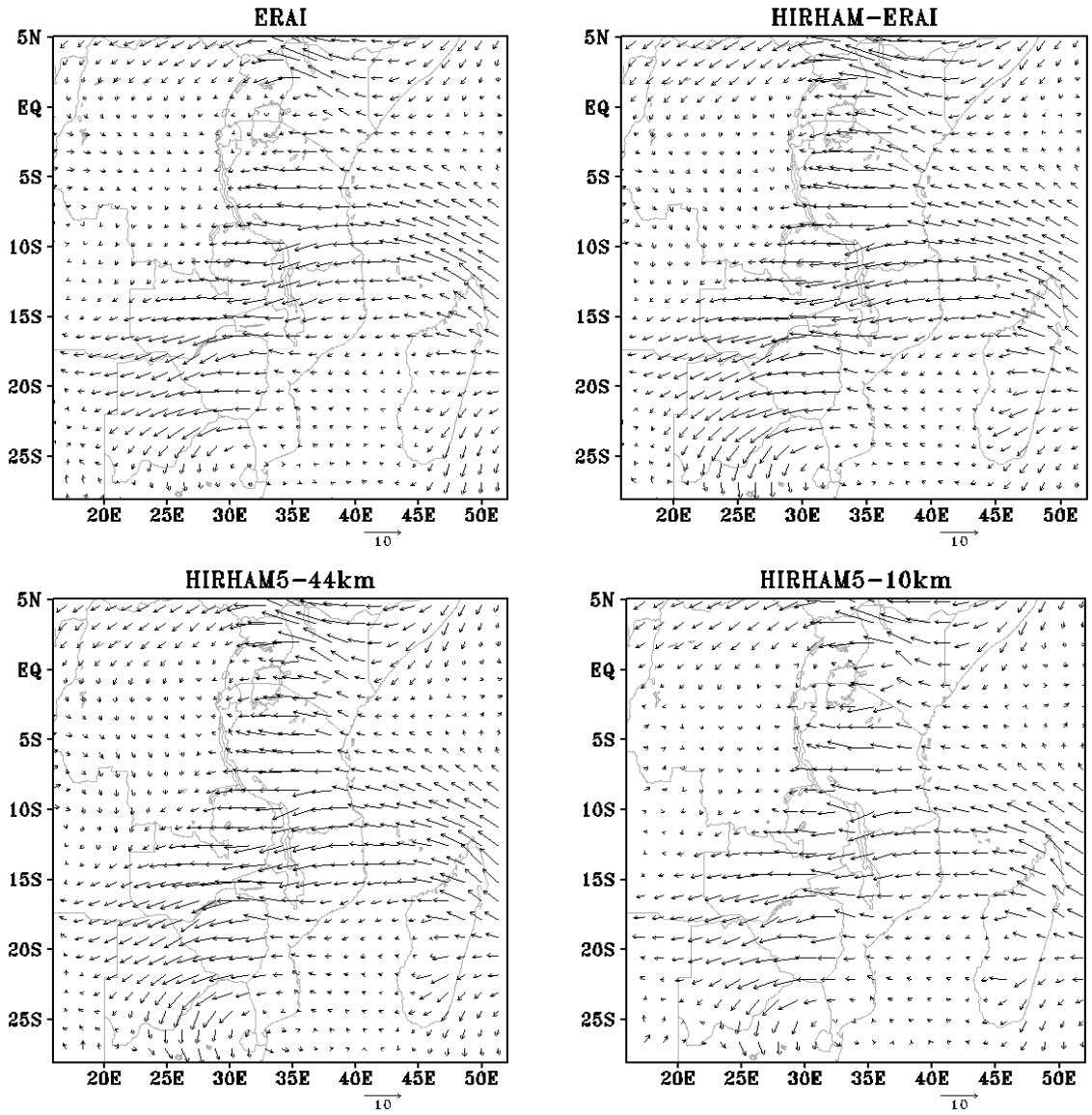

A2.15: Repeat the same as in A2:14 but for OND

Appendix 3

HIRHAM5 simulations of the projected climate change and variability over East Africa

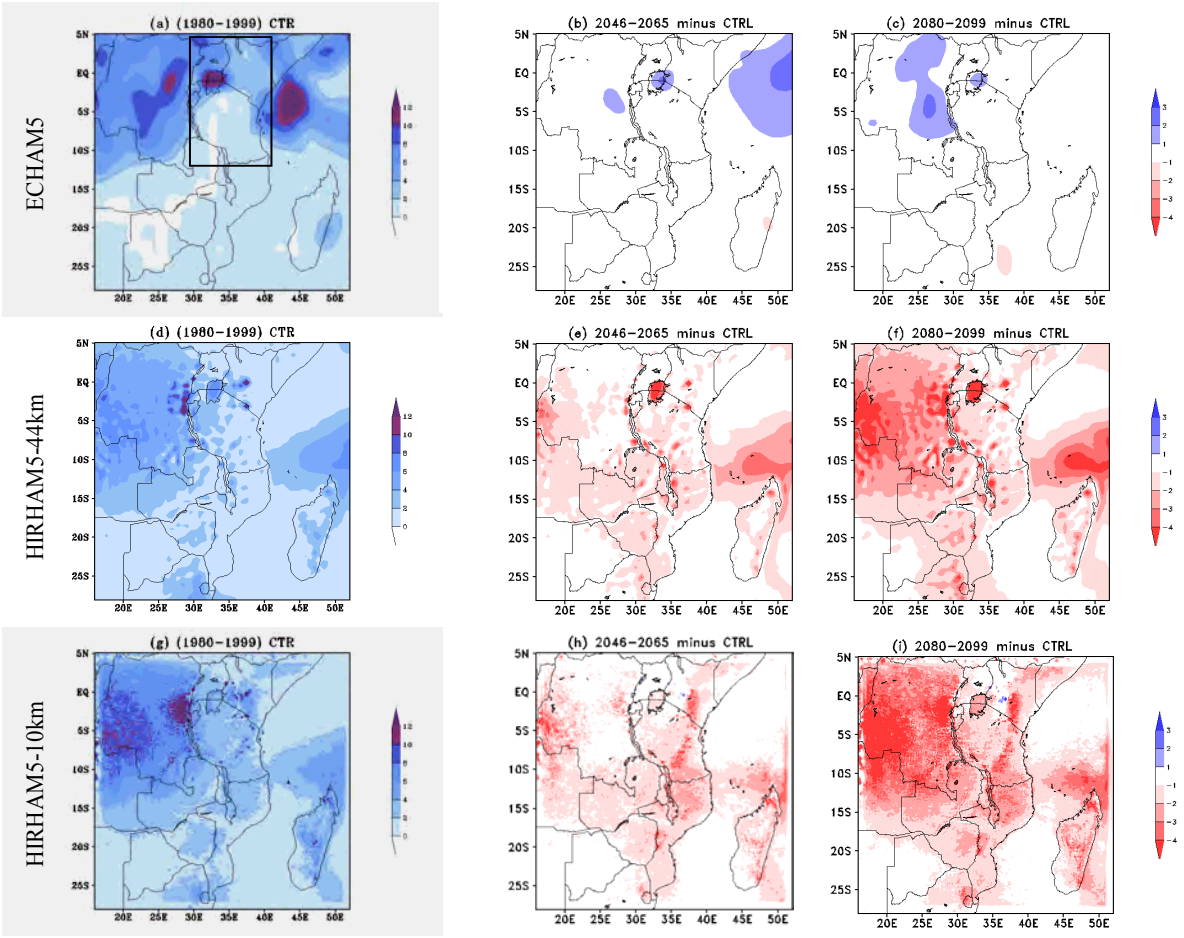

A3.1: Mean OND rainfall (mm/day) for the control period (1980-1999, left column) and changes with respect to the control period for near future (mid column) and far future (right column) for ECHAM5 (top row), HIRHAM5-50 km (middle row) and 10 km resolution (bottom row).

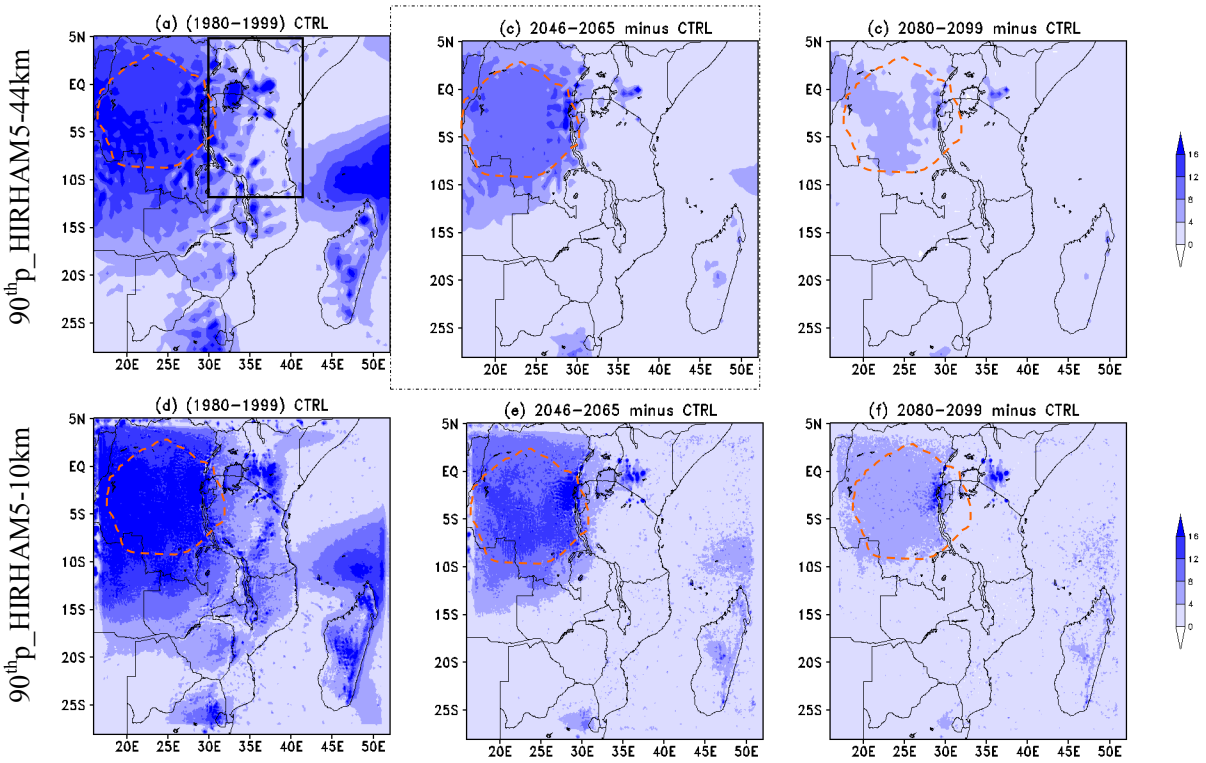

A3.2: The 90th percentile of daily rainfall (mm/day) change in OND season, as projected by HIRHAM5-50 km (first row) and at 10km resolution (second row) in near future (2046–2065, middle column) and far future (2080–2099, right column) relative to the control period (1980–1999), which is shown in the first column. The red dotted circle indicates areas of maxima extreme heavy rainfall.

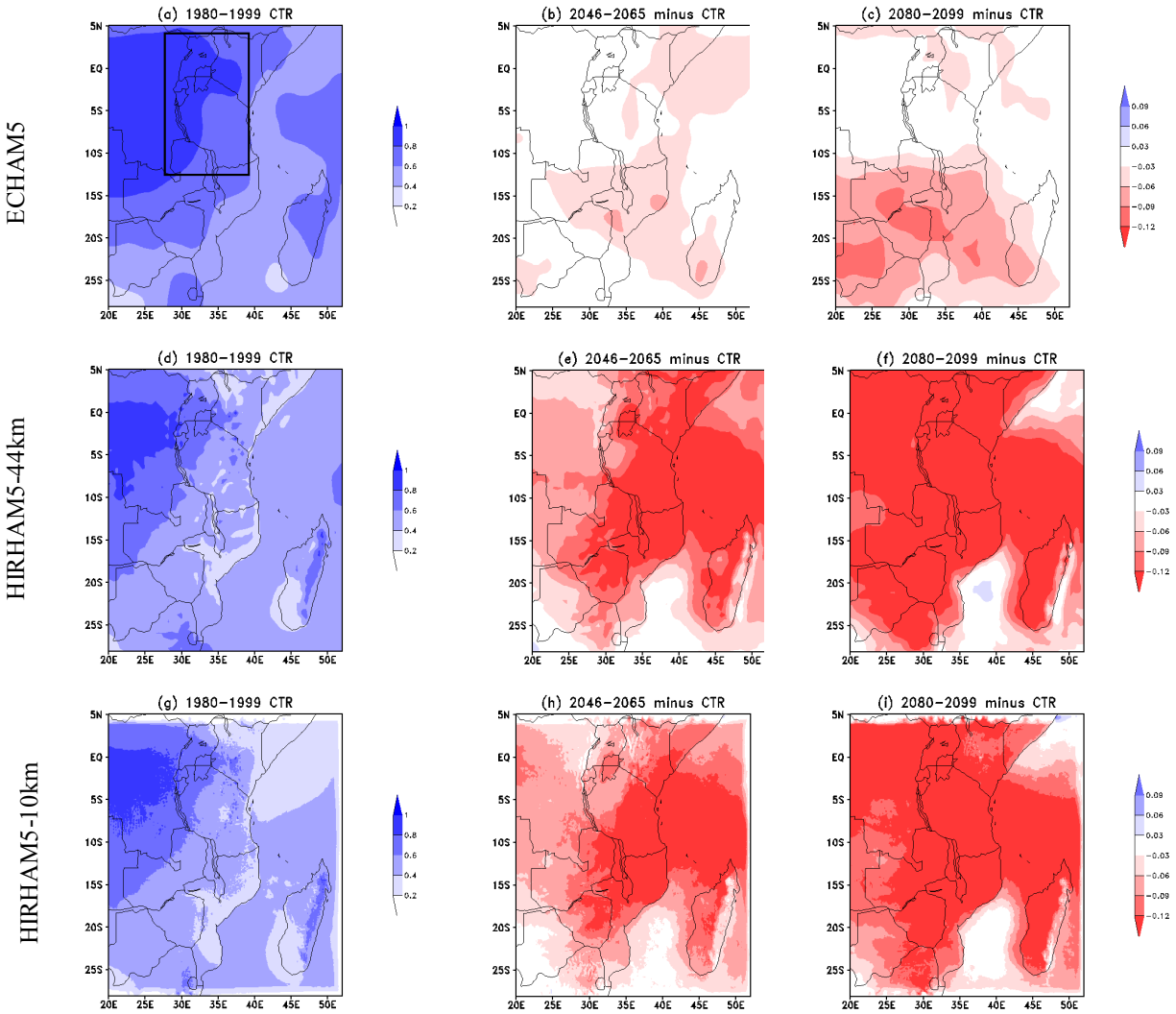

A3.3: The projected mean change of the total cloud cover as simulated by ECHAM5 (first row), HIRHAM5 at 50 km (second row) and 10km (third row) in three time slices: control period (1980–1999) CTR in the first column and their differences: 2046–2065 minus CTR, and 2080–2099 minus CTR in the second and third column respectively in OND season.

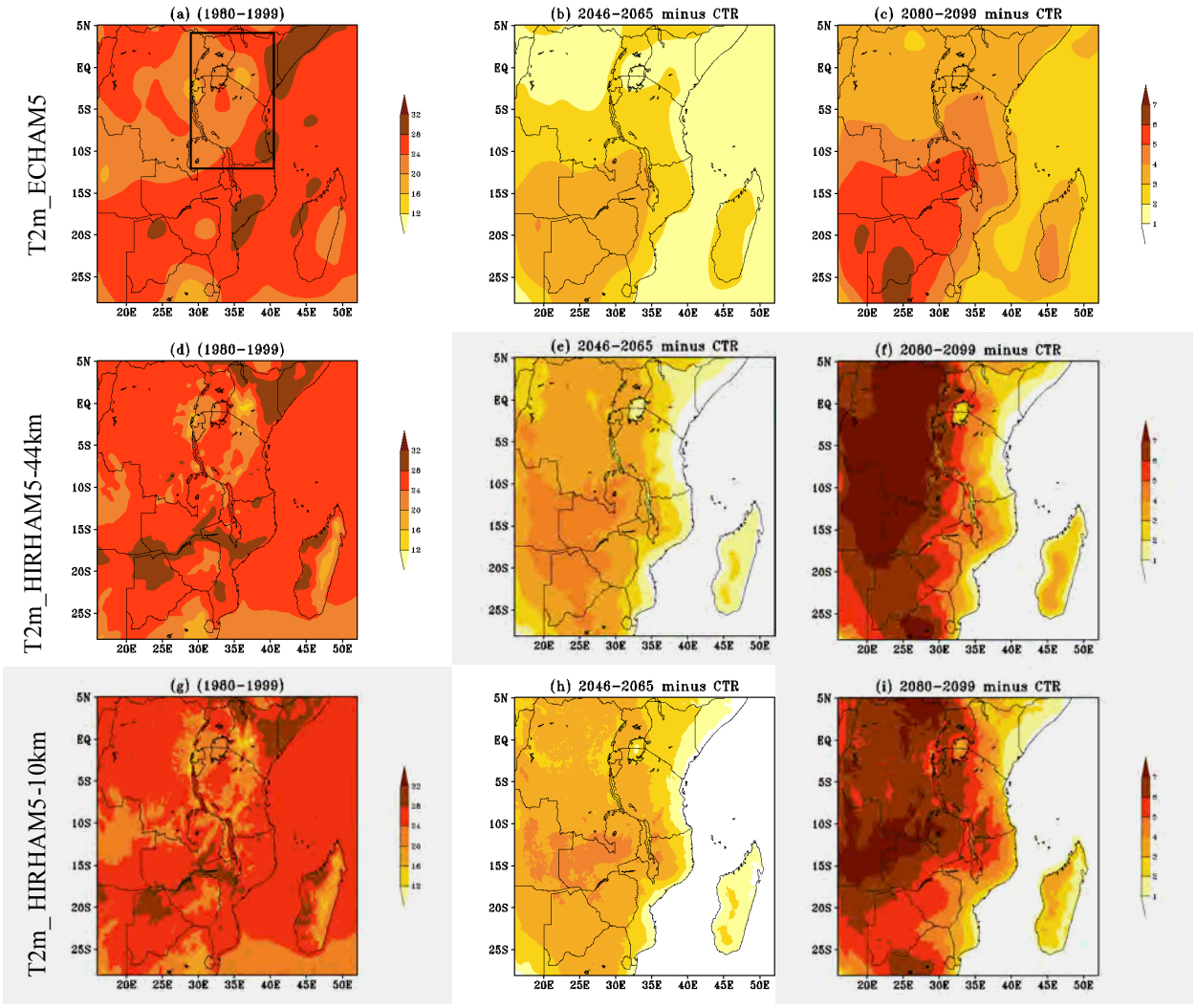

A3.4: Mean surface temperature (^{o}C) change over East Africa domain as simulated by ECHAM5 (first row), HIRHAM5-50 (second row) and HIRHAM5-10km (third row) relative to the control period (1980–1999) in the first column, for the near future (2046–2065, second column) and far future (2080–2099) in the OND season.

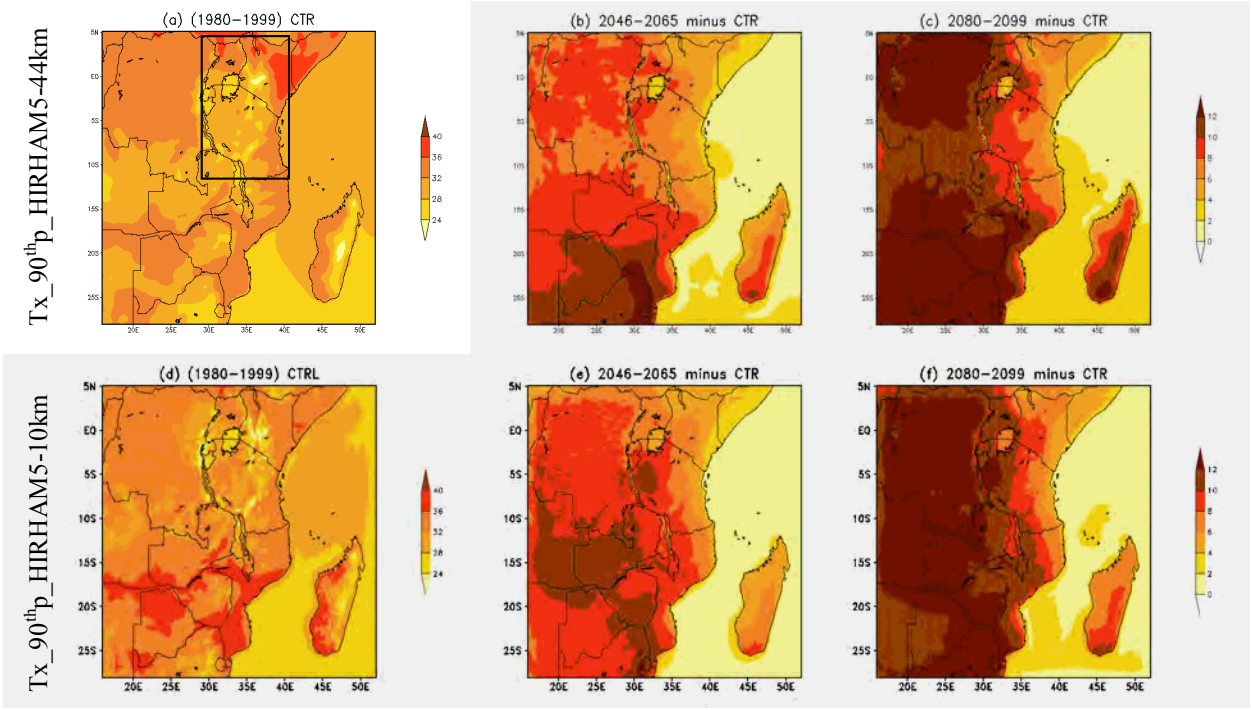

A3.5: The 90th percentile of the maximum temperature (^{o}C) change in OND season as simulated by HIRHAM5 at 50 km (first row) and 10km (second row) for control period (first column), near future (second column) and far future (third column).

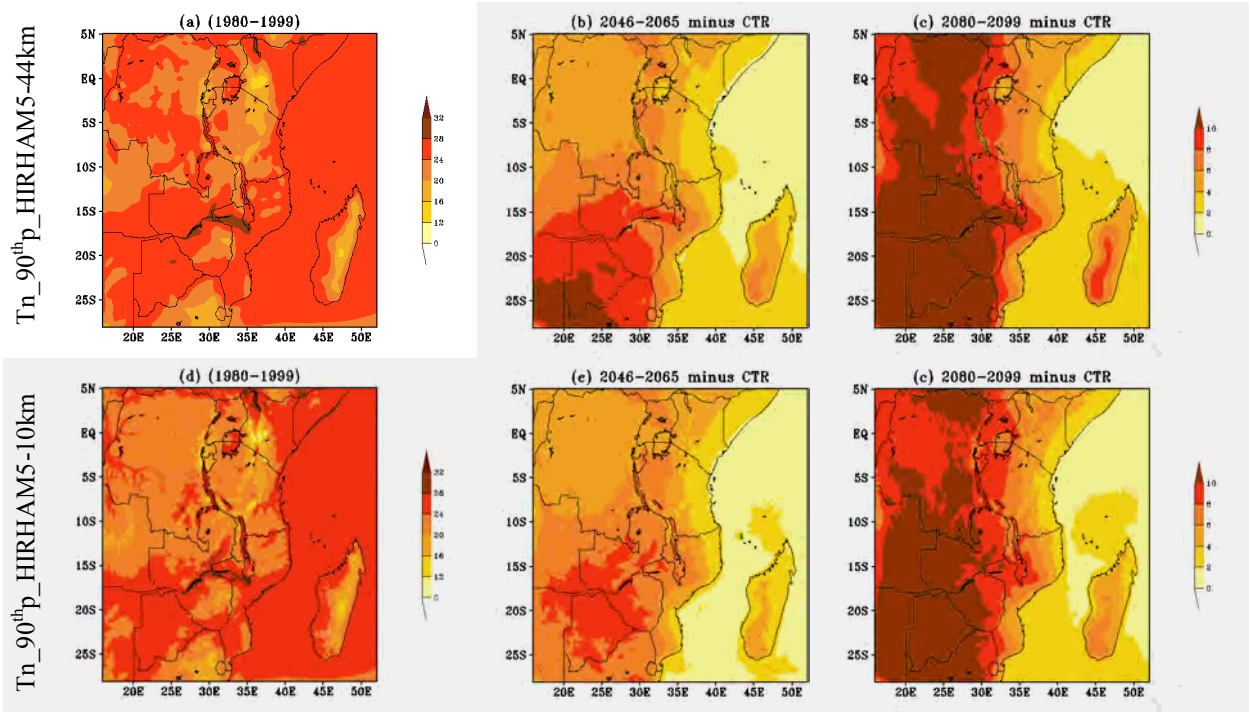

A3.6: The 90th percentile of minimum temperature (^{o} C) change in OND season as simulated by HIRHAM5 at 50 km (first row) and 10km (second row) for control period (first column), near future (second column) and far future (third column).

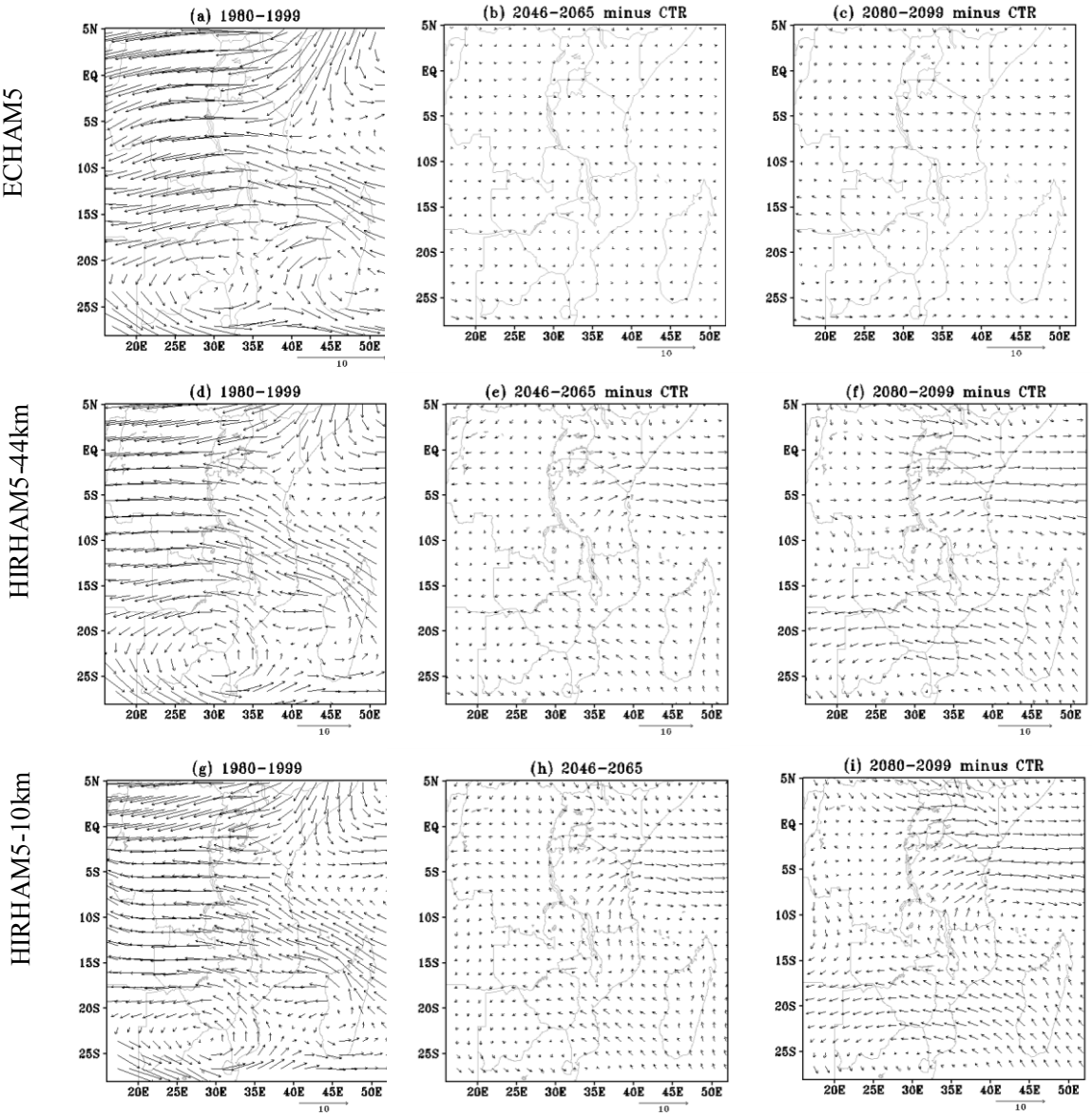

A3.7: Rainy season (OND) wind vectors in 700 hPa (m/s) as simulated by ECHAM5 (first row), HIRHAM5 at 50 km (second row) and 10km (third row) in three time slices: control period (1980–1999) CTR in the first column and their differences: 2046–2065 minus CTR, and 2080–2099 minus CTR in the second and third column respectively in OND season.

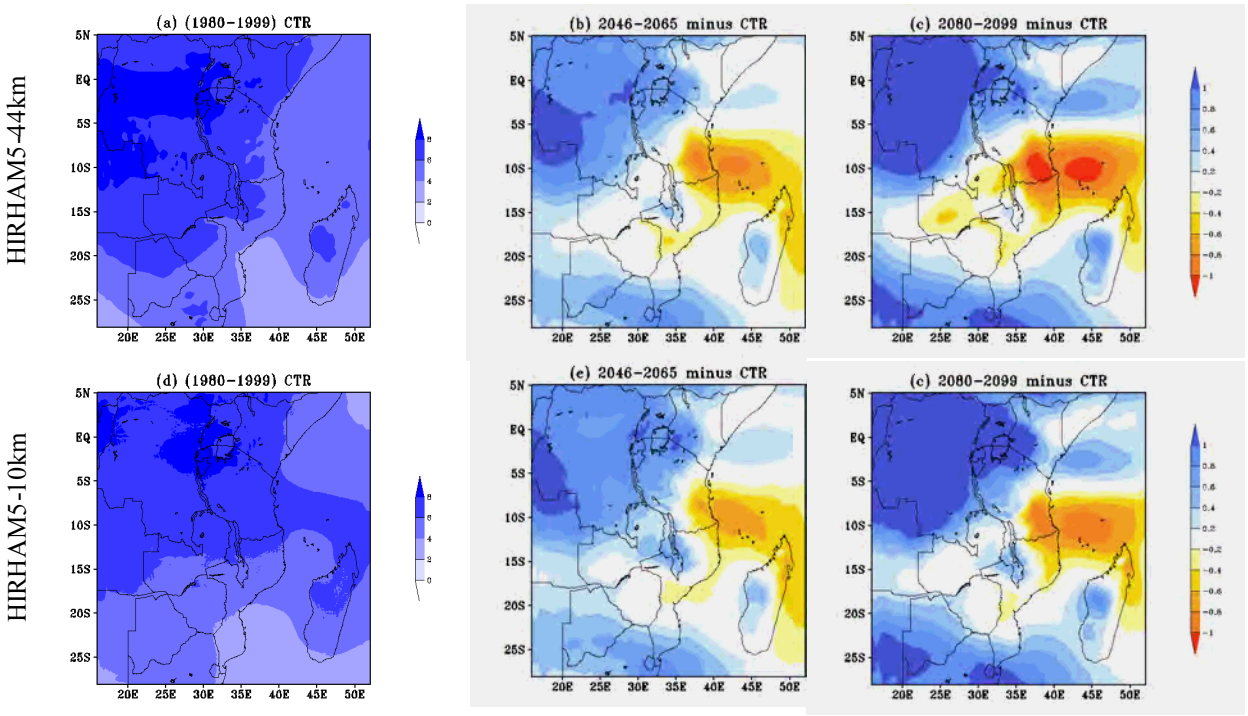

A3.8: Projected mean change of 700 hPa specific humidity (g/kg) in the wet season (OND) season) as simulated by HIRHAM5 at 50 km (first row) and 10 km (second row) for present-day climate (1980–1999, left column) and the differences to present-day climate for 2046-2065 (mid column) and 2080-2099 (right column).